DOCTOR OF PHILOSOPHY

Analysis of human germ lines genes for clinical applications

Alharbi, Ahmed

Award date:
2017

Awarding institution:
Bangor University

Link to publication

Analysis of human germ lines genes for clinical applications

PhD. Thesis

2017

Ahmed Mulfi Alharbi

Declaration and Consent

Details of the Work

I hereby agree to deposit the following item in the digital repository maintained by Bangor University and/or in any other repository authorized for use by Bangor University.

Author Name:

Title:

Supervisor/Department:

Funding body (if any):

Qualification/Degree obtained:

This item is a product of my own research endeavours and is covered by the agreement below in which the item is referred to as "the Work". It is identical in content to that deposited in the Library, subject to point 4 below.

Non-exclusive Rights

Rights granted to the digital repository through this agreement are entirely non-exclusive. I am free to publish the Work in its present version or future versions elsewhere.

I agree that Bangor University may electronically store, copy or translate the Work to any approved medium or format for the purpose of future preservation and accessibility. Bangor University is not under any obligation to reproduce or display the Work in the same formats or resolutions in which it was originally deposited.

Bangor University Digital Repository

I understand that work deposited in the digital repository will be accessible to a wide variety of people and institutions, including automated agents and search engines via the World Wide Web.

I understand that once the Work is deposited, the item and its metadata may be incorporated into public access catalogues or services, national databases of electronic theses and dissertations such as the British Library's EThOS or any service provided by the National Library of Wales.

I understand that the Work may be made available via the National Library of Wales Online Electronic Theses Service under the declared terms and conditions of use (http://www.llgc.org.uk/index.php?id=4676). I agree that as part of this service the National Library of Wales may electronically store, copy or convert the Work to any approved medium or format for the purpose of future preservation and accessibility. The National Library of Wales is not under any obligation to reproduce or display the Work in the same formats or resolutions in which it was originally deposited.

Statement 1:

This work has not previously been accepted in substance for any degree and is not being concurrently submitted in candidature for any degree unless as agreed by the University for approved dual awards.

Signed   (candidate)

Date

Statement 2:

This thesis is the result of my own investigations, except where otherwise stated. Where correction services have been used, the extent and nature of the correction is clearly marked in a footnote(s).

All other sources are acknowledged by footnotes and/or a bibliography.

Signed   (candidate)

Date

Statement 3:

I hereby give consent for my thesis, if accepted, to be available for photocopying, for inter-library loan and for electronic storage (subject to any constraints as defined in statement 4), and for the title and summary to be made available to outside organisations.

Signed   (candidate)

Date

NB: Candidates on whose behalf a bar on access has been approved by the Academic Registry should use the following version of **Statement 3:**

Statement 3 (bar):

I hereby give consent for my thesis, if accepted, to be available for photocopying, for inter-library loans and for electronic storage (subject to any constraints as defined in statement 4), after expiry of a bar on access.

Signed   (candidate)

Date

Statement 4:

Choose **one** of the following options

a) I agree to deposit an electronic copy of my thesis (the Work) in the Bangor University (BU) Institutional Digital Repository, the British Library ETHOS system, and/or in any other repository authorized for use by Bangor University and where necessary have gained the required permissions for the use of third party material.	
b) I agree to deposit an electronic copy of my thesis (the Work) in the Bangor University (BU) Institutional Digital Repository, the British Library ETHOS system, and/or in any other repository authorized for use by Bangor University when the approved **bar on access** has been lifted.	
c) I agree to submit my thesis (the Work) electronically via Bangor University's e-submission system, however I **opt-out** of the electronic deposit to the Bangor University (BU) Institutional Digital Repository, the British Library ETHOS system, and/or in any other repository authorized for use by Bangor University, due to lack of permissions for use of third party material.	

Options B should only be used if a bar on access has been approved by the University.

In addition to the above I also agree to the following:

1. That I am the author or have the authority of the author(s) to make this agreement and do hereby give Bangor University the right to make available the Work in the way described above.

2. That the electronic copy of the Work deposited in the digital repository and covered by this agreement, is identical in content to the paper copy of the Work deposited in the Bangor University Library, subject to point 4 below.

3. That I have exercised reasonable care to ensure that the Work is original and, to the best of my knowledge, does not breach any laws – including those relating to defamation, libel and copyright.

4. That I have, in instances where the intellectual property of other authors or copyright holders is included in the Work, and where appropriate, gained explicit permission for the inclusion of that material in the Work, and in the electronic form of the Work as accessed through the open access digital repository, *or* that I have identified and removed that material for which adequate and appropriate permission has not been obtained and which will be inaccessible via the digital repository.

5. That Bangor University does not hold any obligation to take legal action on behalf of the Depositor, or other rights holders, in the event of a breach of intellectual property rights, or any other right, in the material deposited.

6. That I will indemnify and keep indemnified Bangor University and the National Library of Wales from and against any loss, liability, claim or damage, including without limitation any related legal fees and court costs (on a full indemnity bases), related to any breach by myself of any term of this agreement.

Signature: …………………………………………………… Date : ……………………………

Abstract

Identification of cancer biomarkers it is essential for the diagnosis of cancer during the early stage of disease, which might increase the possibility of successful treatment and improve patient outcomes. The identification of new cancer-specific biomarkers for cancer diagnosis patient stratification is challenging, but they also provide therapeutic targets so they are of fundmental importance in addressing unmet clinical needs in oncology. Cancer/testis antigens (CTAs) genes possess unique features, as they encode proteins that are normally only present in the testis, placenta and ovary, and the expression of these genes has been associated with various types of malignant tumours. Therefore, cancer testis (CT) genes have exceptional clinical potential.

Here, a cohort of genes that were reported to be associated with aggressive lung tumours has been re-validated. Among these promising 26 genes, expression profiles for 10 genes were detected in normal lungs tissue as well in a panel of different normal tissues, and consequently these 10 genes were excluded as good candidates for lung cancer biomarkers. In addition, the 26 genes were screened in normal ovary tissues, as these genes may be useful as ovarian biomarkers, but the same 10 genes were also found to be expressed in normal ovarian tissue. The other remaining 16 genes could serve as ovarian biomarkers. In total, 156 genes known as CT genes and derived from different sources were investigated. TaqMan Low Density Array (TLDA) card analysis was used to re-validate this large group of genes in normal tissues and clinical samples from different patients. Out of 156 genes, 55 were expressed in different types of normal tissue other than testis tissue and central nervous system (CNS), and thus these genes were excluded as CT genes.

Brachyury is a transcription factor that has been reported to be a CTA and may represent a target for cancer treatment. New drugs that may target the cancer associated functions of Brachyury were examined to assess their efficacy and the potential for targeting CTAs. The effect of these drugs on a panel of cancer associated genes known to be specifically regulated by Brachyury was carried out. An evaluation of the drugs revealed that three of the drugs were effective in altering the proliferation rate of cancer cell line, with their action being Brachyury-specific, rather than due to general cytotoxicity.

Acknowledgments

The research work presented in this thesis was carried out at the Department of Biological Science, North West Cancer Research Institute at Bangor University.

First and foremost, I would like to thank my supervisor, Dr. Ramsay James McFarlane. It has been an honour to be his PhD student. I appreciate all his guidance, encouragement, motivation, support and advice during my research and throughout the writing of this thesis. Special thanks are due to Dr. Jane Wakeman for all her help and advice. Thanks to all members of the McFarlane & Wakeman laboratory for their unlimited support and their kind help and especially Dr. Natalia Gomez-Escobar and Dr. Ellen Vernon. Special thanks are also offered to Dr. Jana Jezkova for her support and to Dr. John Sammut, who obtained the tissue samples. Thanks to all my laboratory colleagues, previous and current, as they were always ready to offer any help that I needed. Moreover, I would like to thank the government of the Kingdom of Saudi Arabia for their funding of my Master's degree and PhD.

Finally, many thanks to my parents for being supportive, encouraging and standing alongside me since I was born. Thanks to my wife and my children, Fahad and Abdulrahman, for helping and encouraging me. My thanks also go to my brothers and sister for enormous support throughout the years.

Abbreviations

5-AZA-CdR	5-aza-2′-deoxycytidine
ACT	Adoptive cell therapy
AdCC	Adenoid cystic carcinoma cell
APC	Antigen presenting cell
ATM	Ataxia-telangiectasia mutated
BCA	Bicinchoninic acid
bp	Base pair(s)
BSA	Bovine serum albumin
BTB	Blood-testis barrier
CAR	Chimeric antigen receptor
cDNA	Complementary DNA
CEA	Carcinoembryonic antigen
CML	Chronic myeloid leukaemia
CT	Cancer testis
CTAs	Cancer testis antigens
CTL	Cytotoxic T lymphocytes
CTLA-4	Cytotoxic T-lymphocyte antigen 4
DCs	Dendritic cells (DCs)
DMSO	Dimethyl sulfoxide
DNMT	DNA methyltransferase
DNMTi	DNA methyltransferase inhibitor
DSBs	DNA double-strand breaks
DTC	Disseminated tumour cell
EBV	Epstein-Barr virus
ECM	Extra cellular matrix
EEC	Enteroendocrine
eEF2	Eukaryotic elongation factor 2 (*eEF2*)
EMT	Epithelial–mesenchymal transition
ESCs	Embryonic stem cells

FBS	Foetal bovine serum
GM-CSF	Granulocyte macrophage colony stimulating factor
HATs	Histone acetyltransferases
HCC	Hepatocellular carcinoma
HDACs	Histone deacetylases
HMTs	Histone methyltransferases
HPV	Human papillomaviruses
HSV	Herpes simplex virus
IF	Immunofluorescence
kDa	Kilodalton
LDS	Lithium dodecyl sulfate
mAbs	Monoclonal antibodies
MAPK	Mitogen-activated protein kinase
MBPs	Methyl-CpG-binding proteins (MBPs)
MHC	Histocompatibility complex
ml	Milliliter
MM	Malignant melanoma
M-PER	Mammalian protein extraction reagent
mRNA	Messenger RNA
NCBI	National Centre for Biotechnology Information
NHEJ	Non-homologous end-joining
NI	Negative control siRNA
NL	Non-tumour lung
NSCLC	Non-small cell lung cancer
NTC	No template controls
oligo-dT	Oligodeoxythymidylic acid
PBS	Phosphate buffered saline
PBST	Phosphate buffered saline-tween-20
PCR	Polymerase chain reaction
PD-1	Programmed death-1
PFA	Paraformaldehyde

PS	Placenta-specific
PSA	Prostate-specific antigen
qRT-PCR	Real time quantitative PCR
RB	Retinoblastoma-associated gene
RBP	RNA-binding protein
RNA	Ribonucleic acid
ROS	Reactive oxygen species (ROS)
RT-PCR	Reverse transcriptase PCR
SC	Synaptonemal complex (SC)
SDS	Sodium dodecyl sulphate
SDS-PAGE	Sodium Dodecyl Sulphate- Polyacrylamide Gel Electrophoresis
SEREX	Serological expression cloning
SFM	Serum-free medium
siRNA	Small interfering RNA
T5	Brachyury siRNA (T5)
TAA	Tumour–associated antigen
TAG-72	Tumour-associated glycoprotein 72
TB	Tuberculosis
TBE	Tris-borate-EDTA
T-cells	T-lymphocytes (T-cells)
TF	Transcription factors
TLDA	TaqMan Low Density Array
Tm	Melting temperature
TS	Testis-specific
TS/PS	Testis-specific/placenta-specific
TSGs	Tumour suppressor genes
VEGF-A	Vascular endothelial growth factor-A

Table of Contents

List of Figures

List of Tables

Chapter 1.0 Introduction

1.1 Cancer

Cancer is a serious disease and its prevalence is steadily increasing in many populations around the world. The estimated number of new diagnosed cases is 14.1 million, accounting for 8.2% of all deaths in 2012 worldwide. The cancer mortality rate is expected to increase with population growth, lifestyle changes and other factors known to increase the risk of cancer, such as viral infections (Torre *et al*., 2015). Cancer diagnosis is more prevalent in developed countries than in developing countries; for example, prostate, colorectal, female breast and lung cancers are less frequently diagnosed in developing countries than in developed countries (De Martel *et al*., 2012).

Obesity has been found to increase the risk of invasive cancer. In the United States (US), the cancer death rate of people who are overweight is estimated to be 120,400 per year (Gallagher and LeRoith, 2015). Smoking is the main factor known to cause lung cancer, and it accounts for approximately 80% of the lung cancer diagnosed in the United Kingdom (UK) every year (Parkin, 2011). Smoking is also associated with a variety of other cancers, including rectal, colon, uterine and cervical cancer, as well as the increased rate of death within the population (Secretan *et al*., 2009; Ordóñez-Mena *et al*., 2016) . Environmental factors, such as exposure to ultra-violet (UV) radiation and air pollution, also cause cancer. The mechanisms underlying these factors include genetics, but the effects that these factors have on cancer development in different tissues remain poorly understood (Giovannucci, 2015). Estimates of the number of new cases of cancer diagnosis and the number of deaths in 2016 in the US are shown in Table1.1.

Cancer arises when cells grow and proliferate without control. A combination of multiple genetic processes and epigenetic aberration lead to the initiation and formation of cancer from normal cells (Esteller, 2008; Macheret and Halazonetis, 2015). Cancer cells can invade other organs through the circulatory and/or lymphatic system. To invade other organs, cancer cells must first invade the surrounding tissue, leading to intravasation, the process by which cancer cells spread through the

Table 1.1 Estimated number of new cases and deaths from cancer in the US.
New cases of the most commonly diagnosed types of cancer in men and women in the US and the expected number of cancer deaths in 2016. Adapted from (Siegel *et al.,* 2016).

Estimated New Cases					
Males			**Females**		
Prostate	180,890	21%	Breast	246,660	29%
Lung & bronchus	117,920	14%	Lung & bronchus	106.470	13%
Colon & rectum	70,820	8%	Colon & rectum	63,670	8%
Urinary bladder	58,950	7%	Uterine corpus	60,050	7%
Melanoma of skin	46,870	6%	Thyroid	49,350	6%
Non-Hodgkin lymphoma	40,170	5%	Non-Hodgkin lymphoma	32,410	4%
Kidney & renal pelvis	39,650	5%	Melanoma of skin	29,510	3%
Oral cavity & pharynx	34,780	4%	Leukemia	26,050	3%
Leukemia	34.090	4%	Pancreas	25,400	3%
Liver & intrahepatic bile duct	28,410	3%	Kidney & renal pelvis	23,0505	3%
All Sites	**841,390**	**100%**	**All Sites**	**843,820**	**100%**

Estimated Death					
Males			**Females**		
Lung & bronchus	85,920	27%	Lung & bronchus	72,160	26%
Prostate	26,120	8%	Breast	40,450	14%
Colon & rectum	2,020	8%	Colon & rectum	23,170	8%
Pancreas	21,450	7%	Pancreas	20,330	7%
Liver & intrahepatic bile duct	18,280	6%	Ovary	14,240	5%
Leukemia	14,130	4%	Uterine corpus	10,470	5%
Esophagus	12,720	4%	Leukemia	10,270	4%
Urinary bladder	11,820	4%	Liver & intrahepatic bile duct	8,890	3%
Non-Hodgkin lymphoma	11,520	4%	Non-Hodgkin lymphoma	8,630	3%
Brain &other nervous system	9,440	3%	Brain &other nervous system	6,610	2%
All Sites	**314,290**	**100%**	**All Sites**	**281,400**	**100%**
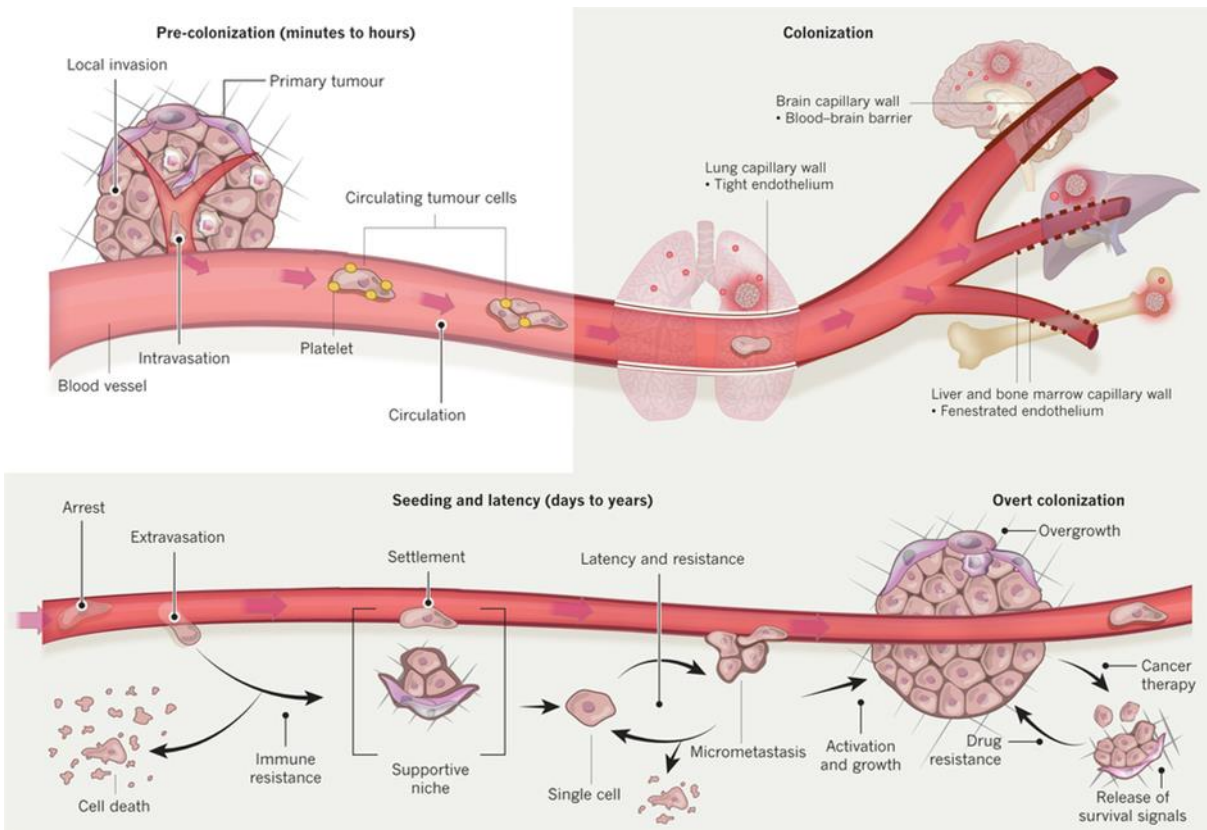
Figure 1.1 Stages of metastatic cancer.

Metastatic cancer starts with pre-colonisation leading to invasion by primary tumours. The cancer cells then enter the circulatory system as single cells and move to the lung via the blood, and then to other organs. Cancer cells in the blood enter the parenchyma of the organs and initiate colonisation. Cancer cells develop resistance to host tissue immunity. Cancer becomes active and then it overtakes the local tissue microenvironment. Adapted from (Massagué and Obenauf, 2016).

blood; they then move to the lungs and then to other organs. During extravasation, cancer cells escape the blood and colonise other tissues, resulting in metastasis. Cancer cells build resistance to the body's immune system and host tissue defence to ensure their survival. While many cancer cells do not manage to invade distant organs, disseminated tumour cells (DTCs) can colonise distant organs (Fukunaga-Kalabis *et al*., 2010; Massagué and Obenauf, 2016). The steps involved in metastasis are shown in Figure 1.1.

Cancer can be classified by the primary site of origin, such as lung cancer, prostate cancer or liver cancer, or by the type of tissue in which it originates. Epithelial carcinoma originates in the epithelial layer of cells. Other types of carcinoma include adenocarcinoma and squamous cell carcinoma. Adenocarcinoma is neoplasia of the epithelial tissue that develops in the body's mucus-secreting glands. It can spread throughout the body, invading many organs. Squamous cell carcinoma develops in the squamous epithelium (Perez-Moreno *et al*., 2012). Sarcoma develops in the connective tissue, and osteosarcoma is a cancerous tumour that develops in the bone. Myeloma, which originates in the plasma cells of bone marrow, is a type of blood cancer. Leukaemia originates in the white blood cells, and it can be distinguished from lymphoma, which develops in the lymphoid tissue. Finally, mixed cancers, such as mesodermal tumours, have both carcinomatous and sarcomatous components (Kunkel *et al*., 2012).

1.2   Hallmarks of cancer and tumour growth

In order for cancer to develop in humans, normal tissue must be transformed into malignant tissue. The hallmarks of cancer cell development include sustained proliferative signalling, evasion of the growth suppressor, resistance to apoptosis, the ability to sustain immortality through replication, sustained angiogenesis, the ability to enhance the invasion and metastasis. Furthermore, cancer cells can escape immune destruction, reprogram energy metabolism, initiate genomic instability and mutation and promote inflammation. (Figure 1.2) (Hanahan and Weinberg, 2011; Macheret and Halazonetis, 2015).
Cell growth and proliferation are processes that normal tissues control by releasing the signals that enhance cell growth and regulate the cell cycle. To deregulate proliferation signalling, cancer cells might stimulate normal cells by sending a signal that initiate the release of growth factor, which
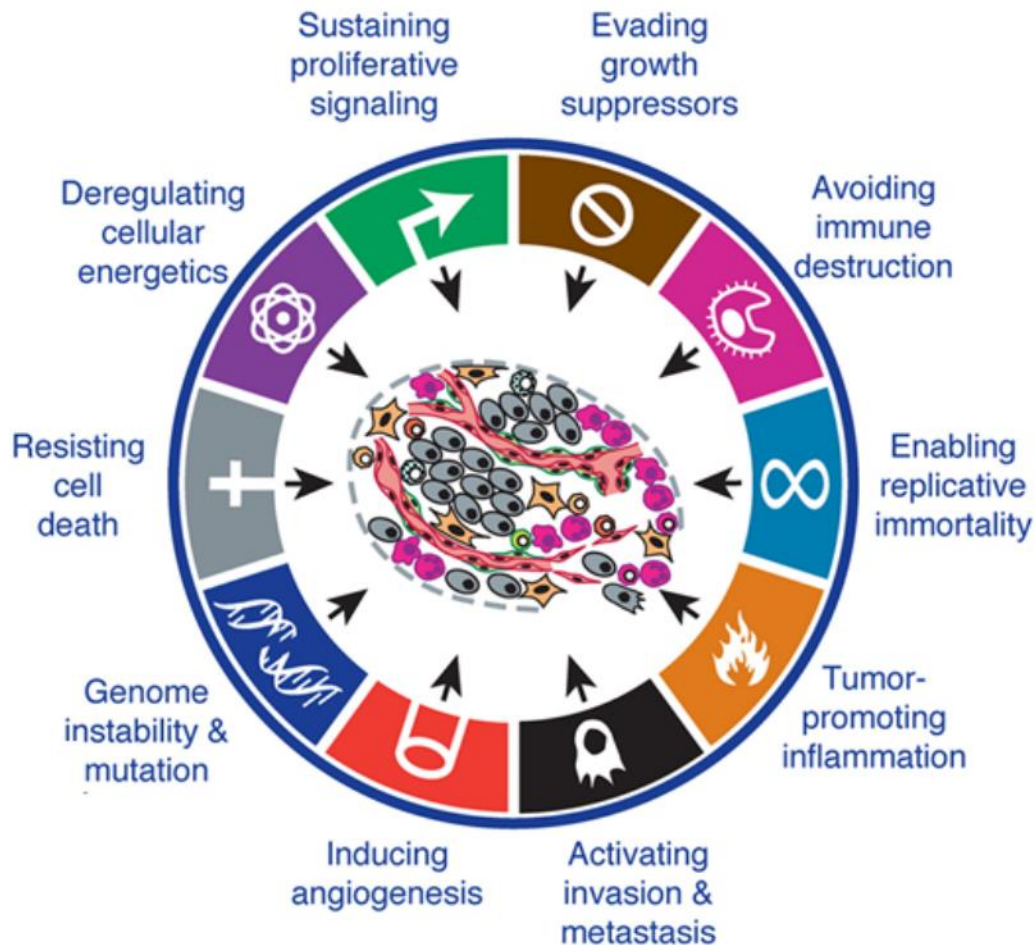
Figure 1.2 The six core hallmarks of cancer and the new hallmarks of cancer.
Hanahan and Weinberg (2011) reported that normal cells are able to transform into cancer cells by sustaining the proliferation signalling, evading the growth suppressor, resisting apoptosis, achieving immortality through replication, losing the angiogenesis function and invading and metastasising to the distant organ. In addition to these six core hallmarks of cancer, escaping immune system attack, changing the cells' energy requirements and metabolism, genomic instability and enhancing inflammation were added the list of the hallmarks of cancer. Adapted and modified from (Hanahan and Weinberg, 2011).

cancer cells need to survive(Fukunaga-Kalabis *et al*., 2011; Cheng *et al*., 2008; Bhowmick *et al*., 2004)

Tumour suppressors control cell proliferation and growth and eliminate the formation of cancer cells. Some types of tumour suppressors control cell proliferation and cell apoptosis. For example, tumour suppressor genes *RB* (retinoblastoma-associate) and *TP53* become inactive when they mutate; this impacts cell proliferation and apoptosis, which stimulates cell growth and increases proliferation. In normal cells, the tumour suppressor gene *TP53* is active to protect cells from becoming cancerous through DNA damage by removing the damaged cells. Thus, mutation in the *TP53* gene enables cancer cells to survive (Hanahan and Weinberg, 2011; Agathanggelou *et al*., 2005; Vogelstein *et al*., 2013).

Cancer cells are able to resist apoptosis, which protects normal cells from transforming into cancer cells. Thus, another hallmark of cancer is the ability to escape apoptotic control. By eliminating the function of the tumour protein p53 tumour suppressor, cancer cells avoid apoptotic control, which leads to the development of tumours (Hanahan and Weinberg, 2011). The cell apoptosis mechanism is regulated by the Bc12 family, and these protein regulators play an indirect role in the apoptotic program. The levels of pro-and anti-apoptotic Bc12 family members, such as Bax and Bak, are controlled by the upstream regulator signal that triggers Bax and Bak activity on the mitochondrial membrane. Bax and Bak enhance the change and disrupt the mitochondrial membrane, which results in the release of protein from the mitochondria, as well as proteins, such as cytochrome-c that bind to the protein known as apoptotic protease activating factor 1 (Apaf-1). The apoptosome complex then binds with procaspase-9 leading to active caspase-9, which is an initiator caspase that belongs to the cysteine proteases family that is involved in programmed cell death (Hanahan and Weinberg, 2011; Arya and White, 2015).

Cancer cells go through multiple divisions, whereas normal cells undergo cell division to produce the specific number of cells required for tissue homeostasis. Uncontrolled cell growth initiates the formation of macroscopic tumours. Telomeres function by protecting the ends of chromosomes in normal cells and they become shorter with each cell division. However, upregulation of the enzyme telomerase has been associated with malignant cells because that enzyme controls the

length of the chromosome maintaining replication potential and preventing the end of the chromosome from replicative degradation (Blasco, 2005; Shay and Wright, 2000).

Angiogenesis is the physiological process in which blood vessels are formed in the placenta or through which new blood vessels are formed from pre-existing vessels. Angiogenesis plays a key role in the development of tumours as it supplies cancer cells with the nutrients they need to increase their rate of growth. This depends on factors, such as vascular endothelial growth factor-A (VEGF-A), which regulate angiogenesis by controlling the activity of the endothelial cell receptors (Bergers and Hanahan, 2008). This hallmark of cancer plays a role in tumour metastasis. It induces the growth of cancer cells, provides them with all the components they need for metabolism and enables them to expel the products resulting from metabolism. Two steps are involved in the development of blood vessels: vasculogenesis, which generates the primary vascular system during embryogenesis, and angiogenesis, which is responsible for maintaining existing vessels. In adults, angiogenesis enables the body to produce new blood vessels (Polverini, 1995).

Tissue invasion and metastasis are also hallmarks of cancer. The invasion-metastasis cascade refers to the way in which the metastasis spreads to other organs after the cancer invades the tissue. This allows the cancer cells to migrate to a distant region and develop the microenvironments it needs to survive in the targeted tissue (Valastyan and Weinberg, 2011). To invade the host tissue, the surrounding extra cellular matrix (ECM) must be attacked, and then intravasation occurs in the blood vessels at the targeted site. This allows cancer cells to survive through the vasculature in the distant organ. After this step, the invading cancer cells extravasate to the parenchyma at the target site. Consequently, they are able to form micrometastases so they can survive in the microenvironments. In fact, the proliferation mechanism occurs in the metastasis phase, which eventually produces the macroscopic tumour (Fidler, 2003).

Recently, other features—such as genomic instability and mutations, inflammation, reprogramming of energy, and escaping from immune systems—have been described as the hallmarks of cancer (Negrini *et al*., 2010; Luo *et al*., 2009; Colotta *et al*., 2009).

A link between genomic instability and genetic mutations has been observed (Sousa *et al*., 2015). Mutations in DNA repair genes promote the development of cancer and genomic instability. Mutations in genes, such *TP53* and *ATM*, recruit and enhance oncogene-induced DNA replication stress (Negrini *et al*., 2010).

Inflammation contributes to tumour initiation and development by enhancing the spread of metastasis. Inflammation has been observed to stimulate tumour growth (Grivennikov *et al*., 2010). Chronic inflammation plays an important role in tumour formation because it has been identified as a probable cause of cancer (Mantovani *et al*., 2008). Chronic inflammation, as well as environmental elements, such as pollution, has been found to cause higher levels of mutations in somatic cells in comparison to mutations in germlines cells, which have been found to play a minor role in causing cancer (Karin, 2006; Mantovani *et al*., 2008; Aggarwal *et al*., 2009).

Cancer cells need energy to fuel rapid and uncontrolled tumour growth. Tumour cells must be able to modify their metabolic system (Liu *et al*., 2015). The metabolic changes that are directed and enhanced by the tumour are linked to the mutations that occur in *TP53*, such as dysregulation of lipid metabolism in the tumour that affects the cell processes, including growth and proliferation, and which induce glycolysis which is essential for energy production (Freed-Pastor *et al*., 2012; Liu *et al*., 2015).

Escaping from immune system attack has also been included in the list of the hallmarks of cancer. The fundamental role of the immune system is to monitor and protect the body from "foreign agents" that can attack and harm the cells. The immune system allows tumours to create their own immunogenicity. It protects tumours through a mechanism called immunoediting, which involves three important steps: elimination, equilibrium and escape from the immune system. Elimination is the mechanism that enables the immune system to destroy the tumour through innate and adaptive immunity (Mittal *et al*., 2014). If the tumour survives through the elimination phase, it could enter the equilibrium step and it could take years to grow. During this period, the tumour expands and becomes more resistant to the immune system (Koebel *et al*., 2007). When a tumour escapes from an immune attack, which is the final step in immunoediting, uncontrolled growth and proliferation occurs followed by metastasis (Mittal *et al*., 2014).

1.3   Dysfunction of tumour suppressor genes and oncogene promotion of tumourigenesis

In order to protect normal cells from becoming cancer cells, cells use checkpoint control to regulate and balance their activity. In healthy cells, genes, such as *TP53*, play a critical role in controlling the cell cycle checkpoint process. However, when these genes mutate they become dysfunctional and prompt tumourigenesis as well the genomic instability associated with the development of cancer (Warfel and El-Deiry, 2013; Macheret and Halazonetis, 2015).

1.3.1   Tumour suppressor genes (TSGs)

Tumour suppressor genes, known as anti-oncogenes, are genes that encode proteins that are essential to preventing cells from forming tumours; these proteins inhibit cellular growth or induce cellular apoptosis. A variety of tumour suppressors played roles in different types of cancers, such as *TP53*, which is called the guardian of the genome, and *RB* (retinoblastoma-associate) genes. Genetic mutation and DNA methylation lead to loss or inactivation of the function of these genes (Macheret and Halazonetis, 2015; Thoma *et al*., 2011). A two-hit hypothesis by Knudson (1971) explains the loss of tumour suppressor function. This model suggests that, in order to cause cancer, two alleles must lose their function (see Figure 1.3). For instance, mutations in *RB1* genes have been observed in various types of cancers, including lung, breast, and eye. In cell cycle processes, RB proteins act as the checkpoint that regulates the cellular entry into S-phase. In addition, the RB protein is associated with and regulates the function of transcription factors such as the E2F family, which are involved in the cell cycle regulation. Mutation may affect the binding of transcriptional factors E2F1 and E2F2 with dimerise protein (DP) complex in the RB pathway (Chen *et al*., 2009; Thoma *et al*., 2011).

Furthermore, the guardian of genome p53 protein also has a vital role, controlling and regulating various aspects of cellular progression, including cell cycle checkpoint, activation of the senescence, and the apoptotic program. Loss of function or mutation in the *TP53* gene has been reported in about half of human cancers (Muller *et al*., 2011). The role of *TP53* in cell maintenance and the factors that enhance the activation of *TP53* are shown in Figure 1.4.
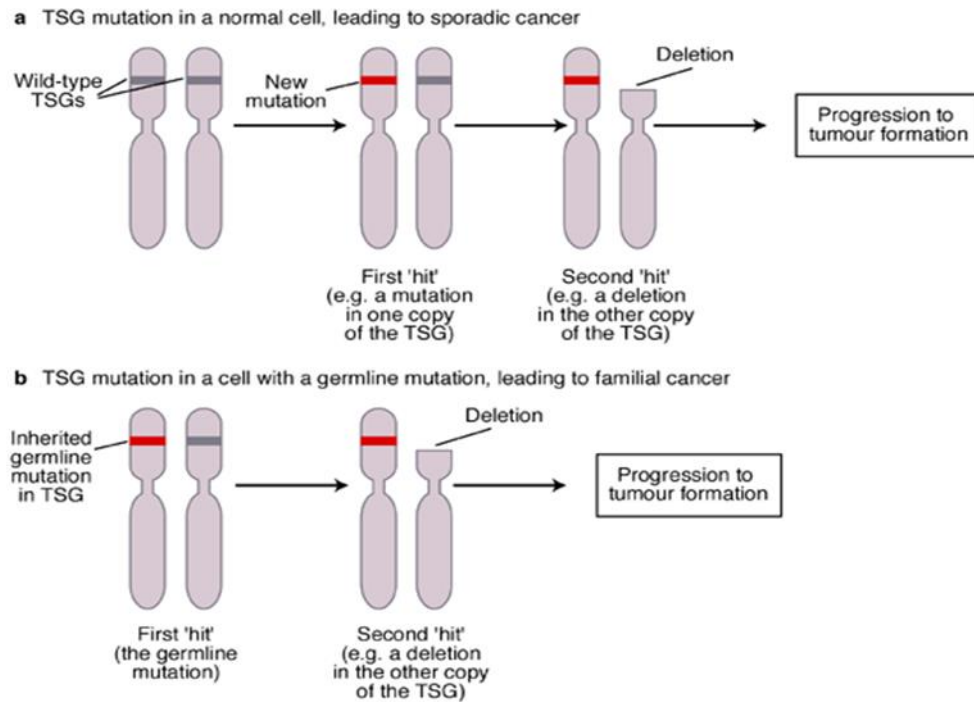
Figure 1.3 Two-hit hypothesis proposed by Knudsen for tumour suppressor genes and tumorigenesis.
(A) Each normal cell carries two copies of TSG; in cancer development, two different hits of mutations must occur. (B) Normal cells have one hit in TSG that is inherited in the germline; as a result, another hit is required to initiate the cancer. Adapted from expert review molecular medicine website 2001; http://www-ermm.cbcu.cam.ac.uk.
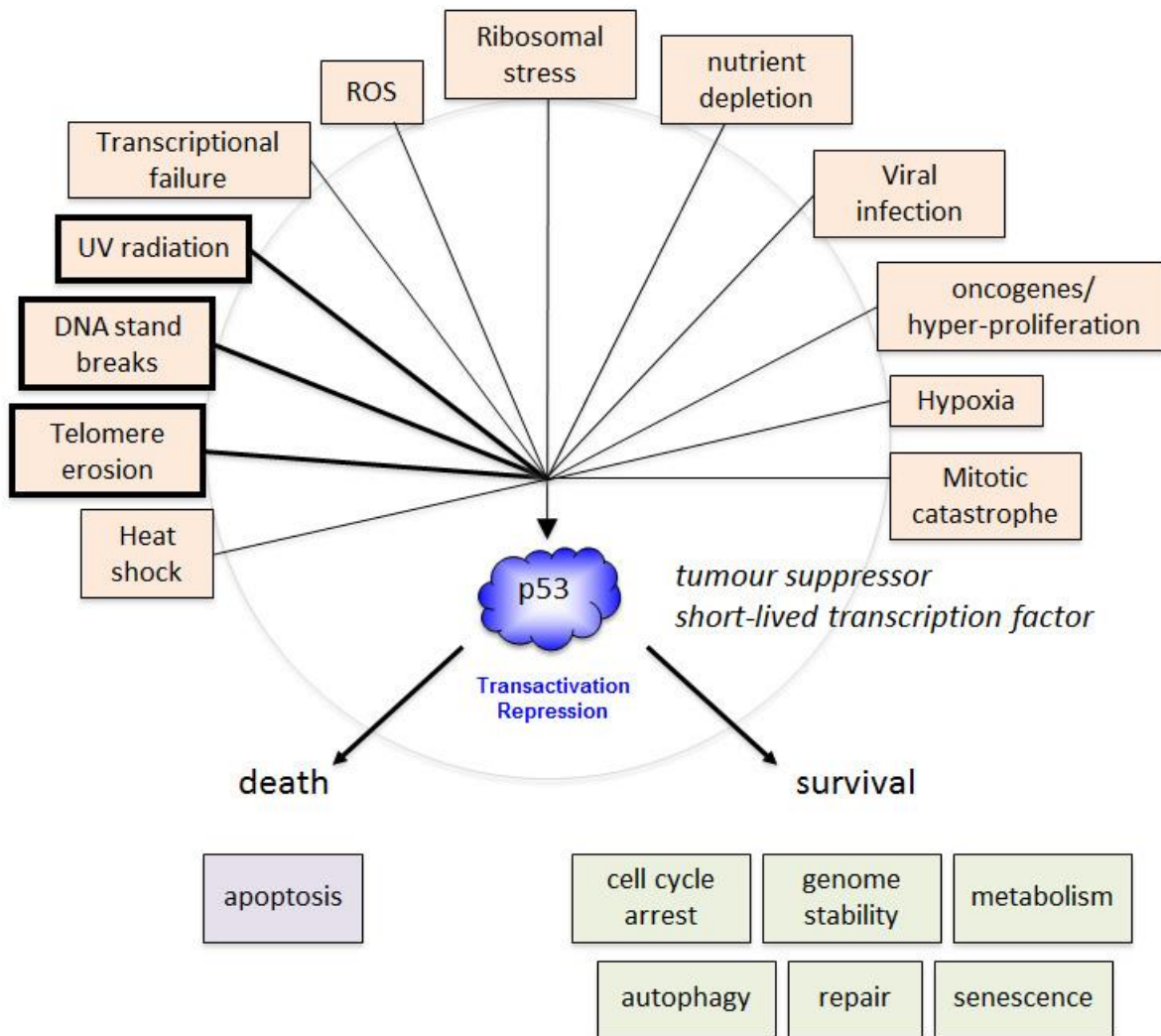
Figure 1.4 Elements that activate the function of *TP53*.
A variety of factors stimulate the activity of *TP53*. Thus, *TP53* responds to these factors to control the
cells and protect their biological function from dysfunction and from inducing tumour growth. Adapted
from (Loughery and Meek, 2013).

1.3.2   Oncogenes

Aberrations in the function of some genes, such as mutations or unregulated gene expression, are associated with transforming normal cells into cancer cells. These genes are known as oncogenes. The vast majority of oncogenes that have been observed to cause cancer are genes that have mutated, which leads to tumourigenesis. In proto-oncogenes, proteins that are encoded by a gene in normal cells are essential in cell processes, such as cell growth and proliferation. Three mechanisms are associated with dysregulating the function of proto-oncogenes: mutations, over-expression and translocation of chromosomes. For example, translocation between chromosome 9 and chromosome 22 occurs in chronic myeloid leukaemia (CML). In order to convert normal cells into cancer cells, proto-oncogenes must associate with other genes (oncogenes) or with the aberrant function of the tumour suppressor genes, as they are unable to cause the cancer on their own (Croce, 2008; Bagci and Kurtgöz, 2015). Human cancer that arises from an oncogene virus has been found to cause 10.8% of all cancers. Viral oncogenes play a role in the upregulation of proto-oncogenes by inserting their promoter into the DNA of the host, which leads to the activation of the transcription factor genes (Ranzani *et al.*, 2013; Bagci and Kurtgöz, 2015). Viral oncogenes have been found to change normal cells into cancer cells by the following mechanisms:

1. Destroying the signalling that is responsible for cell growth or controlling the cells via proteins that target the signalling mechanism in the host (Mesri *et al.*, 2014).

2. The loss of the DNA damage response (DDR), which in normal cells is considered to play a key role in preventing tumour growth by responding to any damage in the DNA and by promoting the DNA repair pathways. Genetic instability occurs in the host cells, so DDR allows the viruses to replicate within the host cells (McFadden ad Luftig, 2013; Weitzman and Weitzman, 2014).

3. Chronic hepatitis B (HBV) or hepatitis C (HCV) may lead to cirrhosis and hepatocellular carcinoma (HCC) following the progression of liver inflammation. In hepatitis, the inflammatory process associated with oxidative stress occurs by reactive oxygen species (ROS) (Arzumanyan *et al.*, 2013).

1.3.3   Genomic instability

The rate of change in the genome significantly increases in cancer cells, leading to genomic instability and mutation. In contrast, healthy cells have a low rate of genome instability (Negrini *et al*., 2010; Vogelstein *et al*., 2013). Mutations, chromosome variations or chromosomal instability (due to the loss of segregation) and a variety of genetic alterations lead to genome instability. Kinase ataxia-telangiectasia mutated (ATM) is a protein that has been found to play an important role in response to DNA double-strand breaks (DSBs), a type of DNA damage (Paull, 2015). Furthermore, ATM has been associated with the metabolic pathway. Recently, ATM has been found to maintain the balance of the redox cycle in cells (Shiloh, 2014; Boohaker and Xu, 2014; Guleria and Chandna, 2016; Shiloh and Ziv, 2013; Zhang *et al*., 2015). Mutations in other genes that have a critical role in DDR, such as *BRCA1*, *BRCA2* and *PALB2*, contribute to genome instability because the DNA repair pathway may not function properly. Ovarian cancer and breast cancer are examples of cancers with mutations in *BRCA1* and *BRCA2* genes, and both of these genes have been found to have a role in the development different types of cancers (Bucholtz and Demuth, 2013; Zhang *et al*., 2013; Khlifi *et al*., 2012; Karahalil *et al*., 2012; Yin *et al*., 2011; Negrini *et al*., 2010; Abbas *et al*., 2013; Aguilera and García-Muse, 2013; Easton, 1999).

1.4   Cancer biomarkers and antigen markers

Cancer biomarkers can reduce the risk of death by enabling early detection and treatment. Tissue, serum and other genetic biomarkers, such as DNA, RNA and enzymes, can indicate the presence of tumours (Wu and Qu, 2015; Mäbert *et al*., 2014). Cancer biomarkers can be used in a variety of ways to monitor a patient's response to treatment (e.g., mutations in the *KRAS* gene that cause colon cancer), identify the type of cancer and screen people who have a high risk of cancer, such as those with the *BRCA1* gene mutation that causes breast and ovarian cancers. Biomarkers can also be used to distinguish benign tumours from malignant tumours. Many types of cancer markers have been detected in the blood system, including in blood serum and plasma, while others have seen in tissues. Genetic biomarkers can be identified in the DNA that is obtained from blood or sputum (Perfézou *et al*., 2012; Henry and Hayes, 2012). Two types of cancer markers have been associated with cancer that is a specific marker that only functions in one type of cancer; in contrast, unspecific markers can be used to identify a variety of cancers (Freidlin and Korn, 2014;

Lindblom and Liljegren, 2000). Prostate-specific antigen (PSA) is an example of a well-known specific biomarker. PSA is a member of the kallikrein family. It functions as a biomarker for prostate cancer, and it is widely used to measure the level of cancer as well to screen patients and determine their response to treatment (LeBeau *et al*., 2009).

Another promising cancer biomarker may be useful when applied to lung cancer. Rousseaux and co-workers have revealed a sub-class of genes that are testis-specific/placenta-specific (TS/PS), and the aberrant expression of these genes has been associated with lung cancer in all stages but not in non-tumour lungs (NL). Patients with lung cancer were assigned to different groups depending on the number of genes expressed in the tumours. The researchers found that the expression of these genes indicated the aggressive tumour phenotype in patients who were in the advanced stages of cancer and were more likely to lead to quick relapses, metastasis, and poor survival outcomes. Thus, these genes may serve as biomarkers, as they are associated with poor prognoses (Rousseaux *et al*., 2013).

1.5   Categories of tumour–associated antigens (TAAs)

Tumour-associated antigens (TAAs) are aberrations of the proteins that arise from the cells within a tumour. They are able to active the immune system to produce anti-tumour antibodies. Importantly, this immune reactivity can be noticeable before the tumour is identified clinically (Chapman *et al*., 2007). Specific antibodies target TAAs, including the antigens that might detect cancer in its early stage. Vaccinations based on TAAs have mostly had poor response, until now, as the immune defence has been non-responsive to TAAs due to their self-tolerance, which leads to the dysfunction of cytotoxic T-lymphocytes (T-cells) that play an important role in inhibiting tumour growth by activating the antitumor immunity pathway (Menez-Jamet *et al*., 2016). In order to apply TAAs in immunotherapy, they must be expressed in the tumour but not in normal cells, they must be homogenous within stable tumours and they must be targeted by T-cells. A vaccination might be designed from studying the antigen found in the tumour (Chiang *et al*., 2015). Antigens that are expressed in the tumour have been classified as overexpressed antigens, oncoviral antigens, oncofetal antigens, differentiation antigens and cancer testis antigens (see Section 1.7 for more details). De novo antigens occur when a gene for protein is mutated.

1.5.1   Overexpressed antigens

Expression of this type of antigen has been observed in normal cells and cancer cells. In cancer cells, metabolism requires a high level of protein synthesis. In cancer cells, the regulation of translation occurs via different mechanisms, such as the eukaryotic elongation factor 2 (*eEF2*) gene, which is a key player in protein synthesis. By controlling *eEF2*, cells maintain the necessary level of protein. Overexpression of the eEF2 protein is associated with the vast majority of cancers, including oesophageal, pancreatic, lung, breast and prostate cancers. In addition, eEF2 enhances tumour growth as it plays a role in the cell cycle by accelerating the progression of G2 and M, thereby activating other proteins (Grzmil and Hemmings, 2012; Bilanges and Stokoe, 2007; Hizli *et al*., 2013; Oji *et al*., 2014).

1.5.2   Oncoviral antigens

It has been noted that certain types of oncoviruses, such as HBV, HCV, hepatitis E virus (HEV), Epstein-Barr virus (EBV) and human papillomaviruses (HPV), can cause cancer. For instance, HPV encoded proteins E6 and E7 play a role in the development of cancers, such as cervical carcinoma (Chen *et al*., 2016).

1.5.3   Oncofetal antigens

Oncofetal antigens are restrictedly expressed in the development of some cells, which enable them to initiate cancer. For instance, the carcinoembryonic antigen (CEA) has been associated with colorectal carcinoma and the tumour-associated glycoprotein 72 (TAG-72) antigen has been found to play a role in the development of prostate carcinoma (Butterfield, 2015; Liu *et al*., 2016).

1.5.4   Differentiation antigens

Differentiation antigens are encoded by genes that are expressed in specific tissues, including normal retinal and other types of tumours. Melanoma is an example of a type of cancer that is known to be associated with differentiation antigens. Proteins, such as gp75/TRP1, TRP2 and tyrosinase, have been found in healthy cells as well in cancer cells in malignant melanoma, and

this protein may serve as a target that enables the immune system to eradicate tumours (Vigneron, 2015).

1.6 Methods of cancer treatment

Unfortunately, some cancers are only diagnosed after it metastasis, which is characterised as the advanced stage of the disease. At that stage, the main objective of treatment is to minimise the growth or spread of the cancer. Depending on the type of cancer and the location of the tumour, several treatment options can be considered including chemotherapy, hormone therapy and surgery (Suri, 2006; Aly, 2012; Brown *et al*., 2015). Although these treatments have been effective in battling cancer, they might have side effects because they affect normal cells as well as cancer cells. It has been found that surgery might be an effective treatment for solid tumours because the procedure also removes normal tissue around the lesion. If a tumour has invaded and spread to the lymphatic system, it is highly likely that the tumour will recur even after it has been removed (Aly, 2012; Aris and Barrio, 2015). Radiation therapy is a clinical treatment that uses X-rays, gamma rays and charged particles to target cancer cells. However, it also impacts the normal tissue near the tumour tissue, which leads to major side effects that can affect a patient's quality of life, such as destroying the salivary glands. Moreover, patients that undergo radiation therapy are at a high risk of infection, osteoradionecrosis (bone death) and taste disorders (Aly, 2012; De Ryck *et al*., 2015).

Chemotherapeutic agents, such as doxorubicin and paclitaxel, are used to target cancer that has spread; however, it can also have a serious effect on quality of life, including fatigue, psychological effects, nausea, tiredness, sleep difficulties, an increase in the loss of the concentration, and vomiting (Carelle *et al*., 2002; Carr *et al*., 2014; Kober *et al*., 2016). The failure of chemotherapy might be due to the resistance that arises from the inclusion of different therapeutic elements, which leads to inhibiting the drugs' ability to fight their intended targets. This can change the drugs' efficacy, thereby enhancing cell death. In addition, chemotherapy can target normal cells in addition to cancer cells, because drugs often work to target dividing cells irrespective of their condition (Seguin *et al*., 2015; Rivera and Gomez, 2010).

The immune system can either fight against or allow the tumour to invade and grow because, depending on the immunoediting phase, the immune system can become tolerant of the tumour. Since the immune system is able to slow or eliminate the spread of the tumour, immunotherapy was developed. Examples of immunotherapy include: T-cell therapy, oncolytic virus, monoclonal antibodies and non-specific immunotherapies. Immunotherapy's aim in targeting cancer depends on the ability of the T-cells to destroy the cancer cells that stimulate the production of antigens (Aris and Barrio, 2015; thor Straten and Garrido, 2016).

Immunotherapy, which is associated with T-cells and B-cells, activates the immune system to recognise and response to the cancer cells and destroy them (thor Straten and Garrido, 2016; Pardoll, 2003; Page *et al*., 2015). Thus, immunotherapy enhances the immune system's ability to naturally eliminate the growth of cancer, thereby preventing the cancer from spreading to other organs (Melero *et al*., 2014).

As previously mentioned, T-cell therapy is an example of a type of immunotherapy that devastates the cancer cells that produce antigens, without impacting the normal tissue. T-cell therapy induces the immune system to recognise the tumour via a mechanism that causes cell modification, including T-cells that are genetically engineered (transduced) with a chimeric antigen receptor (CAR), which is able to recognise molecules, such as glycopeptides, which are present on the surface of cells in a variety of cancers. When T-cells are infused into the blood of cancer patients, they attack the cancer cells. This therapy has been administered to patients with blood cancer, and it has rapidly increased their response to treatment. However, T-cell therapy has not been shown to be as successful in treating solid tumours, and the reason for this is being currently being studied (Rosenberg and Restifo, 2015; Posey *et al*., 2016; Newick *et al*., 2016).

Another form of immunotherapy uses oncolytic viruses, which have been changed genetically to enhance the activity of the immune system. This leads to the production of antigens resulting from the replication of the virus inside the cancer cells. The virus will be selective to the cancer cells, but not the normal cells. This form of therapy, which uses viruses such as talimogene laherparepvec (IMLYGIC) and T-VEC, has been successful in treating melanoma. The genetic modification of these viruses was done by modify the herpes simplex virus (HSV) to replicate the

cancer cells, leading to the expression of granulocyte macrophage colony stimulating factor (GM-CSF) (Chiocca and Rabkin, 2014; Andtbacka *et al*., 2015).

As an immunotherapy, monoclonal antibodies (mAbs) have a major advantage in the treatment of cancers, including solid tumours, and the success of effect has been dramatically noticed. Changing cellular signalling enables mAbs to kill malignant cells. mAbs play a fundamental role in the host immune by repressing the growth of tumours because they eliminate or inhibit angiogenesis, which is required for tumour growth. In addition, they are able to control the immune system pathways, which are called immune checkpoints. Thus, they stimulate the immune system response (Weiner, 2015; Aris and Barrio, 2015). mAbs use a different mechanism in order to control and destroy cancer cells. For example, the overexpression of human epidermal growth factor receptor 2 (HER2) causes different types of cancer, including ovarian, breast, gastric and non-small cell lung cancer (NSCLC), but mAbs, such as Trastuzumab, can recognise the target and degrade cancer cells, but not normal cells; this effect has been clinically proven in malignant breast tissue as it binds to the HER2 (Weiner, 2015; de Goeij, *et al*. 2014).

In addition, the immune system checkpoint enables the immune system to response to the lesion by controlling the T-cell activity and repressing the tumour-specific T cells. The unregulated response from the T-cells may enable tumours to escape from the immune system attack. This occurs when the expression of signals from the tumour induce the ligand receptor to evade the attack. The signalling from the tumour could be blocked by targeting the signals that eliminate the T-cell activity, which is known as the checkpoint blockade. Consequently, T-cell activity will increase, the tumour will be targeted and the efficiency of the immune response pathways against the tumour will increase. Thus, the tumour can be sustained (Aris and Barrio, 2015; Weiner, 2015; Pardoll, 2012).

Expression of cytotoxic T-lymphocyte antigen 4 (CTLA-4), known as CD152, is crucial to negatively regulating T-cell function and regulating T-cell proliferation. CTLA4, and a variety of factors that negatively regulate T-cell function, is able to prevent T-cell activity from responding to immune tolerance, such as a low level of autoimmunity. Thus, CTLA-4 has a crucial function in immune tolerance. However, to maintain and sustain the tumour blocking this mechanism could induce the T-cell response. For example, Ipilimumab has been shown to block the CTLA4

function, and it is widely used to treat melanoma patients (Weiner, 2015; Topalian and Sharpe, 2014; Aris and Barrio, 2015; Peggs *et al*., 2006; Hodi *et al*., 2010). CTLA4 contributes to enhancing T-cell activity and targeting cancer cells by binding B7, which is present in the antigen presenting cells (APC), to T-cells through their receptor CD28. This disables CTLA4 because the expression of the T-cells against the cancer cells would increase in order to recognise and destroy the cancer cells. Binding CTLA4 to B7 has a higher binding affinity than CD28 to B7 (Peggs *et al*., 2009; Smyth *et al*., 2016).

Programmed death-1 (PD-1) is another type of immune checkpoint pathway that activates the expression of T-cells. PD-1 is a fundamental player in controlling T-cells because it maintains T-cell activity by driving the signalling to the T-cells. This is essential for T-cell functioning and T-cell response to foreign agents, but not for immune tolerance. The PD-1 pathway is different from the CTLA-4 pathway, as it has two ligands, PD-L1 and PD-L2. PD-1 is expressed in both T-cells and B cells, and it has been found in some types of human cancer, such as melanoma, kidney and lung cancers (Wang *et al*., 2014; Blank *et al*., 2006). PD-L2 was recently found to be expressed in T-cells in addition to other cells. In T-cells, the signalling response is controlled by the interactions between PD-1 and PD-L1 or PD-L2. To target the cancer cells, it is essential to block this binding. This has been applied clinically to various tumours with great success, such as by using Nivolumab, which blocks PD-1 from binding to its own ligands, thus enabling the T-cells to target cancer cells (Heinzerling *et al*., 2016; Wang *et al*., 2014).

1.7 Cancer Testis Antigens

Cancer testis antigens (CTAs) are proteins that are produced aberrantly in various types of tumours, and cancer testis (CT) genes encode these proteins. The normal expression of these genes occurs exclusively in male germline cells, ovaries and trophoblasts (Whitehurst, 2014). The expression of CTA genes in tumour cells varies, as some CTA genes are highly expressed in tumours, such as melanoma, non-small cell lung cancer and bladder cancer. CTA genes could express in prostate cancer and breast cancer (with a mediatory level of expression) or in colorectal cancer and kidney cancer, where they show a very low level of CTA gene expression (Scanlan *et al*., 2002; Scanlan *et al*., 2004). In the testis tissue, the immune system is prevented from targeting germ cells by inhibiting their response to the immune system. This is known as an

immunoprivileged site. This feature allows the testis to safeguard against microorganisms and control the immune response (Chen *et al*., 2016; Bhushan *et al*., 2016). The immunoprivileged site in the testis is controlled by a blood-testis barrier (BTB). Studies have found that the BTB is one of the tightest blood-tissue barriers. It forms the basal and the adluminal compartments of seminiferous tubules as a result of dividing the seminiferous epithelium into two parts. Sertoli cells function to create this barrier; they also enhance the process where germ cells create spermatozoa, they provide the nutrients and transfer substances that protect the lumen by controlling the type of molecules that move to the lumen, and they enhance immune tolerance (Li *et al*., 2016; Whitehurst, 2014; Kaur *et al*., 2014). In addition, germ cells do not present antigens on their surface due to the lack of expression of major histocompatibility complex (MHC), which serves as a target for immunotherapy (Morgan *et al*., 2013). In the early stage of germination, primary spermatocytes and spermatogonia reside in the basal compartment. Other events, such as the advanced stage of meiosis, leptotene and pachytene spermatocytes occur in the adluminal compartment (Stanton, 2016).

1.7.1   Identification of CTAs

The first identification of CTA genes was described by De *et al*. (1991). Melanoma antigen-1 (MAGE-A1) was the first CTA discovered by using the T-cell epitope cloning technique (De *et al*., 1991). Expression of *MAGE-1A* is restricted to the testis and placenta in normal tissue. In addition, *MAGE-1A* has been observed to be expressed in different types of cancer, not exclusively in melanoma (De Plaen *et al*., 1994; Zendman *et al*., 2003). This approach is widely used to identify other tumour antigens, such as BAGE and GAGE-1 as well as MAGE-A2 and MAGE-A3 (Boël *et al*., 1995; De Backer *et al*., 1999; Chomez *et al*., 2001; Gaugler *et al*., 1994). These antigens have the same features, and their presence is widely used in characterising various types of cancers, including ovarian cancer, breast cancer and lung cancer (Boon *et al*., 1997). Serological expression cloning (SEREX) is another technique that was invented by Pfreundschuh *et al*. (1997). This approach identified new tumour antigens and overcomes limitations imposed by only using the T-cell epitope approach. SEREX is based on the patient's antibodies and the immunological screening of tumour cDNA expression libraries (Sahin *et al*., 1995). They were able to recognise the antigen by using antibody repertoire isolated from a specific tumour; the antibody response could be detected by using SEREX. In the SEREX approach, cDNA expression libraries were

constructed from patient tumours, cloned to phage expression vector, and expressed in *Escherichia coli*. The recombinant protein produced was transferred and incubated with the serum from an autologous patient with a specific tumour. Cloning reactivity with a high titre of antibody present in patient serum can be recognised, and the nucleotide sequence from the cDNA can be determined. Applying this technique has led to identifying a number of novel CTAs, for example, synovial sarcoma/X breakpoint 2 (SSX-2) (Türeci *et al*., 1998), New York oesophageal squamous cell carcinoma 1 (NY-ESO-1) (Chen *et al*., 1997), synaptonemal complex protein 1 (SCP-1) (Türeci *et al*., 1998), cancer-associated gene-1 (CAGE-1) (Cho *et al*., 2002) and PAS domain containing 1 (PASD1) (Liggins *et al*., 2004).

Recent studies have revealed a new group of CT genes that might be prognostic biomarkers in patients with all stages of lung cancer due to their specific expression as testis and placenta. There is a correlation between the expression of these genes and aggressive tumours (Rousseaux *et al*., 2013). In addition, another CTA was discovered that might be used as a biomarker to investigate breast cancer metastasis (Maine *et al*., 2016). More than 200 CTAs have been identified and classified into different types of families. However, some CT genes express in different types of normal tissue at low levels, even though they express in the testis at a high level (Whitehurst, 2014).

1.7.2   Classification of CTAs

As previously noted, over 200 CTAs have been identified and classified, and the identification of new CTAs is currently underway. The expression of these genes, including other features and characterisations, is compiled in a database (http://www.cta.lncc.br) (Almeida *et al*., 2009; Hovey *et al*., 2015). The majority of CTA genes have been classified according to their expression because their function and their association with cancer development are poorly understood (Maine *et al*., 2016).

CTA genes are also classified based on their chromosomal location. X-encoded CTA genes are classified as X-CT genes whereas autosomal CTA genes are non-X-CT genes (Simpson *et al*., 2005; Doyle *et al*., 2010). Approximately 50% of CTA genes are found to be located on the X chromosome. Studies of the sequencing of human X chromosomes has found that about 10% from

genes located on X chromosome are members of the CTA gene family (Figure 1.5) (Simpson *et al*., 2005; Ross *et al*., 2005). The X-CT genes include a group of paralogue gene families, such as the *GAGE*, *PAGE*, and *XAGE* superfamily and the *MAGE* family (Ross *et al*., 2005; Mueller *et al*., 2008).

Expression of some genes in the X-CT group, including *MAGE-A3*, *MAGE-A8*, *MAGE-A10*, *XAGE2* and *XAGE3*, has been observed in the placenta and in the testis (Silva *et al*., 2007; Makise *et al*., 2016). Furthermore, in somatic tissue, including the testis and the placenta, a low expression of some CTA genes has been observed in comparison to the testis, where high expression of these genes occurs. The findings indicate that the level of mRNA is less than 1%. In contrast, the group of CTA genes that display a wide expansion of expression in mRNA should not be classified as CTA genes; those genes include *SPA17* and *JARID1B* (Caballero and Chen, 2009). The activation of CTA genes plays a fundamental role in malignancy, which might arise from the upregulation of the gametogenic program, which is considered to be inactive (Lifantseva *et al*., 2011; Whitehurst, 2014; Tarnowski *et al*., 2016).

Non-X-CT genes were also classified according to the chromosomal location of the gene. These genes are found on autosomes, and their expression is associated with the process of spermatogenesis, such as the stages of meiosis. In addition, these genes are different from the X-CT genes because they only have a single-copy (see Table 1.2) (Simpson *et al*., 2005). About 52% of CT genes are located on the X chromosome (Rajagopalan *et al*., 2011).

In addition, to the classification of CT genes based on their location on the X chromosome, the expression pattern of CT genes was classified into four categories: (A) testis restricted (their expression is exclusive to the testis, including more than one type of cancer tissue), (B) testis-brain restricted [including the testis, they were found to express in the central nervous system (CNS) and cancer tissue], (C) testis selective (they display a high level of expression in the testis in comparison to low level expression with two different types of normal tissues as well as cancer tissue) (Hofmann *et al*., 2008), and (D) testis brain selective (they are express in the testis as well as in the CNS, with no more than two different normal tissues, and in cancer tissue) (Feichtinger *et al*., 2012). Hofmann *et al*. (2008) found that, out of 153 CT genes, 83 genes were located on the
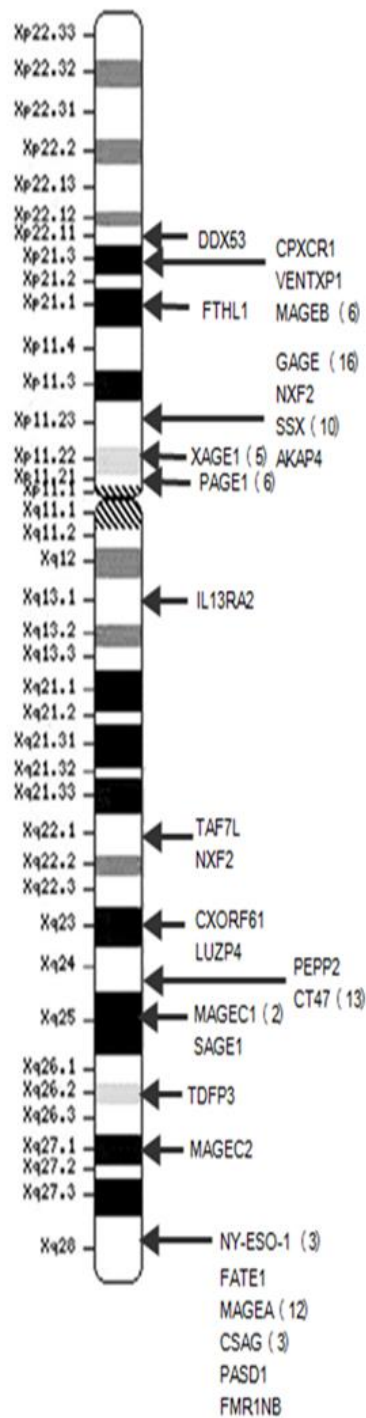
Figure 1.5 Localisation of the CTA genes on the X chromosome.
Many types of CTA genes families are located on the X chromosome.
Adapted from (Caballero and Chen, 2009).

Table 1.2 Some of the identified CTA genes families and their chromosomal location.
Adapted from (Fratta *et al*., 2011).

	CTA gene family	Number of genes	The location on the chromosome
	MAGE family		
X-CTA	*MAGE-A*	12	Xq28
	MAGE-B	6	Xp21.3
	MAGE-C	3	Xp26-27
	GAGE/PAGE/XAGE superfamily		
	GAGE-A	8	Xp11.23
	GAGE-B	8	Xp11.23
	PAGE	5	Xp11.23
	XAGE	5	Xp11.21–11.22
	SSX family		
	SSX	5	Xp11.2
	NY-ESO family		
	CTAG	3	Xq28
	Non-familial		
	CAGE	1	Xp22.11
	HOM-TES-85	1	Xq23
	SAGE	1	Xq26
Non-X CTA	*BAGE*	5	21p11.1
	BORIS	1	20q13.2
	CT9/3BRDT	1	1p22.1
	HAGE	1	6q12-13
	OY-TES-1	1	12p12-13
	SCP-1	1	1p12-p13
	SPO11	1	20q13.2-q13.3

X-CT and 70 genes were located on the autosomes. Genes were then classify into three categories depending on their expression and whether or not they were testis restricted (a total of 35 X-CT genes and four non-X-CT genes). Furthermore, 12 X-CT genes were testis brain restricted, whereas only two CT genes were non-X-CT. In the third category, testis selective, 36 genes were located on the X-CT and 64 genes were non-X-CT genes (Hofmann *et al*., 2008).

1.7.3   Expression of CTA genes in cancers

However, many CTA genes have been observed to be associated with various types of human cancers, but their function is poorly understood (Bode *et al*., 2014). Some CTA genes have high levels of expression with melanoma, ovarian cancer, and lung cancer tumours. Alternatively, some tumours display a low expression of CTA genes, including leukaemia, lymphomas, pancreatic cancers, colon cancer, and renal cancer (Scanlan *et al*., 2004; Hofmann *et al*., 2008). Tumours that show moderate levels of CTA genes expression, such as breast cancer, prostate cancer, and bladder cancer, are referred to as epithelial cancers. For example, expression of the *NY-ESO-1* gene was 52% in melanoma, 27% in non-small-cell lung carcinoma, and 35% in bladder cancer. In contrast, expression of the *NY-ESO-1* gene in colon cancer was 10% (Gure *et al*., 2005; Sharma *et al*., 2003; Goydos *et al*., 2001; Li *et al*., 2005).

In addition, the CTA genes appear to be co-expressed in some aggressive tumours in which the CTA genes expression is higher than in the primary tumour (Table 1.3) (Caballero and Chen, 2009). Also, high levels of expression of the CTA genes were correlated with higher grades of tumours. For instance, in high-grade bladder tumours (G3), expression of the NY-ESO-1 gene was 40%; however, expression in intermediate-grade bladder tumours (G2) was 23%, and no expression was observed in low grade (G1) tumours (Kurashige *et al*., 2001). Conversely, in various types of normal and cancerous tissues, CTA genes such as NY-ESO-1, SCP-1, and MAGE-A have been studied at the protein level to evaluate the proteins produced from cancerous tissues and to develop the antibody that is expressed against these genes (Caballero and Chen, 2009).

Recently, a large-scale study revealed sub-classes of genes identified as testis-specific and placenta-specific (TS/PS) that might serve as prognostic markers in certain types of tumours and be considered as cancer biomarkers because of their expression in testicular and placental tissues.

Table 1.3 Association of CTA protein presence including clinicopathologic features and prognoses. Adapted from (Caballero and Chen, 2009).

Tumour Type	Antigen	Association
Melanoma	MAGE-A1, MAGE-A2, MAGE-A3, MAGE-A4	Tumour thickness and metastasis
Non-small-cell lung cancer	MAGE-A1, MAGE-A3, MAGE-A4, MAGE-A10, MAGE-C1	High grade tumours, pathologic stage, and nodal as well as pleural invasion
Pancreatic cancer	MAGE-A3	Poor survival
Hepatocellular carcinoma	MAGE-C1	Reduced overall survival
Multiple myeloma	MAGE-A1, MAGE-A3, MAGE-A4, MAGE-C1	Stage and risk status of disease
Melanoma	NY-ESO-1	Thicker primary lesions and a higher frequency of metastatic disease

These genes are epigenetically silenced in normal tissues, and their expression is associated clinically with lung cancer patients with aggressive, metastasis prone tumours and poor prognoses (see Chapter 3 for more details) (Rousseaux *et al*., 2013).

A soma-to-germline transition may lead to the cancer development. For instance, the expression pattern of the human orthologues of the *Drosophila melanogaster* germline genes are shown their expression in brain tumour which indicate most of these genes are expressed in germline as well in a variety type of human cancers (Feichtinger *et al*., 2014). In *Drosophila melanogaster*, the activation of these germline genes has been found to play a crucial role in the process of oncogenesis (Janic *et al*., 2010) and the aberrant activation of these genes may have potential function in human cancers (Feichtinger *et al*., 2014). By inhibiting some of germline genes may contribute to repress the tumour development, which indicate the important functional role of these genes in tumorigenesis (Janic *et al*., 2010).

1.7.4   The functional role of CTA genes

CTA genes have been studied widely, but their roles in germline tissue and cancer development remain unclear. However, a variety of CTAs were reported that might be associated with human tumourigenesis, because the CTA genes are expressed in high levels in malignant tumours (Fratta *et al*., 2011). Importantly, CTA genes have been implicated in certain cell processes, including proliferation, movement, and drug resistance (Kim *et al*., 2013).

1.7.4.1 Role of CTAs in the germ line

CTA genes perform a fundamental role in the germline process, and examples of germline function are given below. During meiosis, certain CTA genes are required to achieve this process, such as SPO11, by generating double-strand breaks (DSBs) leading to crossover between the homologous chromosomes, which is essential in the exchange of genetic material (Lange *et al*., 2011). Sister chromatids are held together by subunits of cohesin proteins, such as CTAs, including SMC1β, RAD21L, and REC8, which are required for chromosome segregation (Garcia-Cruz *et al*., 2010). Furthermore, the presence of CTAs, such as the synaptonemal complex central element 1 (SYCE1), are important elements in the synaptonemal complex (SC) that occur during meiosis I

and play a role in enhancing association of the sister chromatid and stimulation of DSB repair. The synaptonemal complex protein 1 (SYCP1) is crucial to DSB repair, as is HORMAD1, which is a member of the synaptonemal complex; the loss of HORMAD1 was observed to affect the synapse, including the pairing of the homologous chromosomes (de Vries *et al*., 2005; Bolcun-Filas *et al*., 2009). Many CTAs are involved in the maintenance of sperm energy, such as SPATA19 and COX6B2, which are essential for packing the mitochondria to the sperm and enhancing the movement of sperm (Goldberg *et al*., 2010). Members of the CTA family, such as ADAM2, are involved in fertilization by enabling the interaction between the egg and sperm (Nishimura *et al*., 2004).

CTAs such as TDRD1 and PIWIL2 may be associated with the piwi-interacting RNAs, which are expressed exclusively in the germline function in spermatogenesis, thus leading to the silencing of the transposon in the events of spermatogenesis (Aravin *et al*., 2007; Kuramochi-Miyagawa *et al*., 2004). In addition, the CTA PIWIL2 may contribute to maintaining the level of p53 (Lu *et al*., 2012). Many CTAs that are classified as X-CT genes exhibit their expression during the stages of spermatogenesis (Figure 1.6) (Whitehurst, 2014).

1.7.4.2 CTAs and their role in tumour growth

Many CTAs have been observed to enhance the growth of cancer cells, and specific examples are given below. The downregulation of the *SSX* CTA genes in melanoma effects cell proliferation and genomic instability (Greve *et al*., 2015). SSX has been linked to signalling pathway activities involving the mitogen-activated protein kinase (MAPK), which is responsive to the extracellular signals that control processes such as proliferation. During tumour development, the aberrant SSX function may affect the activity of MAPK pathways (D'Arcy *et al*., 2014). Another CTA, CAGE, has been observed to induce the activity of cyclin D1 and E in the cell cycle, which leads to increased cell proliferation; as a result, CAGE may advance tumour development (Por *et al*., 2010). In addition, CAGE may promote the growth of tumours as it exhibits angiogenic potential (Kim *et al*., 2013).

Other CTAs have also been shown to function in cancer cells, such as the MAGE members including MAGE-A3 and MAGE-C2, which perform a critical role of regulating the *TP53* tumour suppressor gene (Yang *et al*., 2007). Inhibition of the function of these genes leads to acceleration of the p53 activity and increases the rate of apoptosis. These genes affect KAP1, which is known
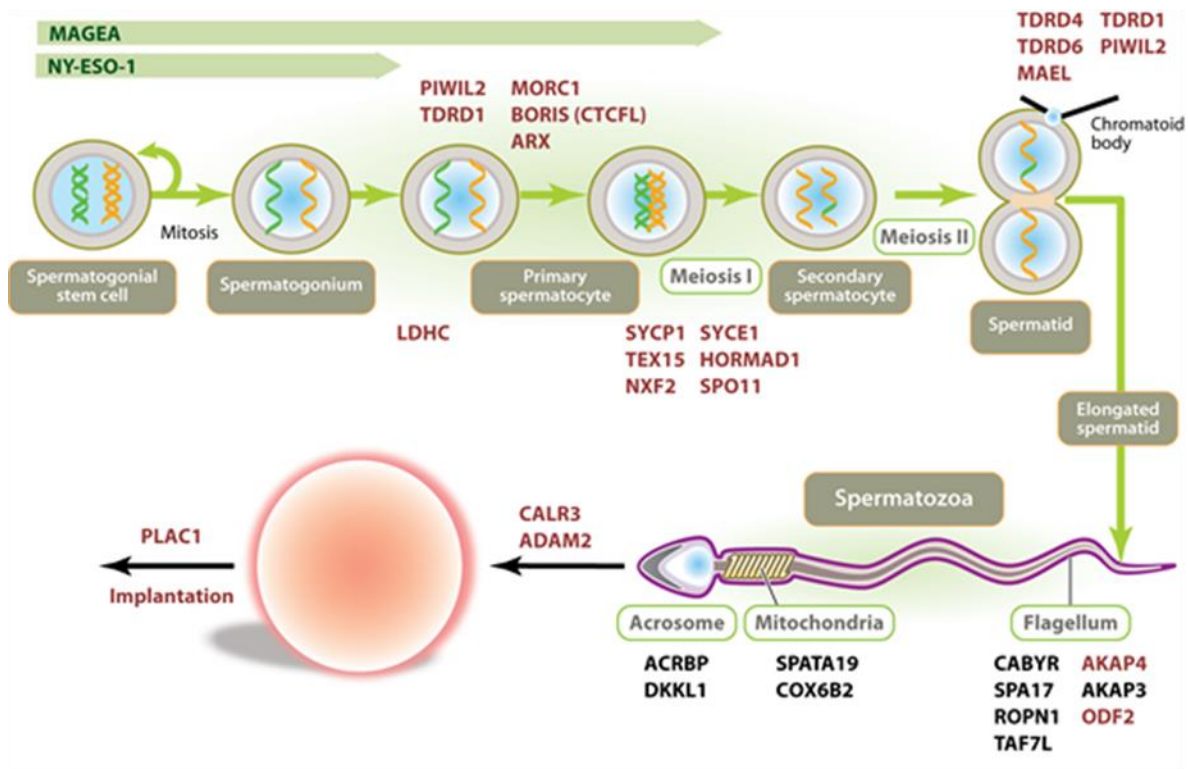
Figure 1.6 Roles of CTA genes that are implicated in the early stages of spermatogenesis.
Expression of X-linked CTAs, such as MAGEA1 and NY-ESO-1, have been found to occur during early spermatogenesis, demonstrating that these proteins are essential in the initial stages of spermatogenesis. In addtion, the proteins in a group of CTAs are cruical during fertilisation. CTAs also play an important role in promoting tumourigenic features. The red colour indicates CTA knockouts in these stages, which will defeat fertilisation, and the black colour represents the functional studies of these CTAs. Adapted from (Whitehurst, 2014).
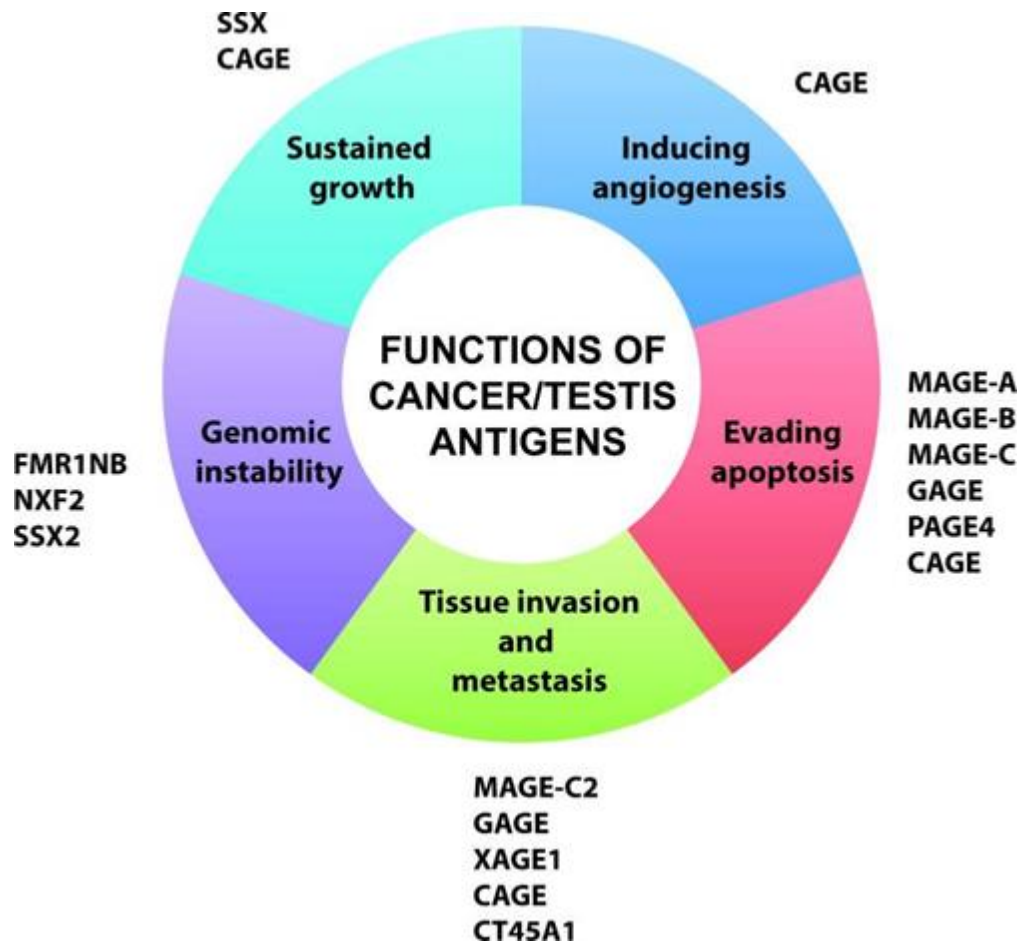
Figure 1.7 The oncogenic functions of CTAs.
Some CTAs have been implicated in cancer development. Hallmarks of cancer described by Hanahan and Weinberg require some aspect in order to cause the cancer. Studies have revealed that CTAs might be associated with these features or hallmarks of cancers, which suggests that their direct role is implicated in tumourigenesis. Adapted from (Gjerstorff *et al*., 2015).

as the corepressor of p53, by suppressing the interaction between p53 and KAP1. Thus, the expression of MAGE may prevent the cell from programming death, which leads to the development of cancer (Yang *et al*., 2007). Furthermore, certain CTAs, such as PAGE and GAGE, also protect different types of tumours from the apoptotic pathway (Kasuga *et al*., 2008; Cilensek *et al*., 2002) and the loss of the functional ability of PAGE4 to increase cell death and the growth of tumours (Zeng *et al*., 2011). Many CTAs are oncogenic and are associated with tumourigenesis; they are classified depending on their function (Figure 1.7) (Gjerstorff *et al*., 2015).

1.7.5   Epigenetic-regulated CTA expression

The term "epigenetic" refers to modifications that alter the phenotype but do not alter DNA sequencing. Epigenetic processes play a fundamental role in the regulation of gene expression, including normal cell development. Epigenetic aberrations can change gene function and initiate cancer by activating the oncogenes and/or silencing the tumour suppressors, or associating with the genetic mutation or deletion (Sandoval and Esteller, 2012). The expression of CTA genes in tumours that correlate positively with each other and their role in cancer may result in activation of a global epigenetic mechanism (Hackett *et al*., 2012). CTA expression is regulated by two types of epigenetics—DNA methylation and post-translational modifications of histone (Figure 1.8) (Fratta *et al*., 2011).

1.7.5.1 DNA methylation

DNA methylation is an epigenetic process that performs a crucial role in regulation of the silencing of gene expression and cellular differentiation (Hackett *et al*., 2012). In humans, DNA methylation has been found to occur in the cytosines at the sequence of the CpG dinucleotide. Much of the genomic DNA is CpG-poor and the DNA is heavily methylated, whereas a CpG island (CpG-rich region) is primarily unmethlyated and associated with gene promoter sites (Messerschmidt *et al*., 2014; Shen and Laird, 2013). The aberration of CpG-island methylation has been observed in tumours (Sharma *et al*., 2010).

The normal activation of CTA genes occurs by hypomethylation during spermatogenesis and methylation regulates their silencing in somatic tissues. (Fratta *et al*., 2011). The first evidence that

illustrated that DNA methylation can regulate the expression of CTA was provided by Weber *et al*. (1994), who found that the expression of the *MAGE-A1* gene in the human melanoma cell line was activated by treating the cells with DNA methyltransferase inhibitors (DNMTi), such as 5-aza-2′-deoxycytidine (5-AZA-CdR) (Weber *et al*., 1994). 5-AZA-CdR entraps the DNA methyltransferase (DNMT) enzyme in a covalent complex with DNA, leading to an increase in the progressive loss of DNA methylation during cell division. In cancer, these agents are capable of reversing the silencing of the epigenetic process and restoring the normal functions of cells (Zendman *et al*., 2003; Gjerstorff *et al*., 2015).

A high level activity of CTA genes is associated with the dehypomethylated promoter DNA (Karpf *et al*., 2004). Some examples include the *MAGE* (Weber *et al*., 1994; De Smet *et al*., 1996; De Smet *et al*., 1999), *LAGE-1* (Lethé *et al*., 1998; De Smet *et al*., 1999), *SSX-2* (dos Santos *et al*., 2000; Sigalotti *et al*., 2002), *NY-ESO-1,* and *GAGE* (Sigalotti *et al*., 2002) CT genes. Some CTA genes exhibit a low density of CpG dinucleotides; however, they are activated by the DNMT inhibitors, such as *SPANX* and *XAGE*. Conversely, several CTA genes are inhibited even in the presence of CpG dinucleotides (Zendman *et al*., 2003; Menendez *et al*., 2007).

1.7.5.2 Histone modifications

Histone modification appears to be crucial to the epigenetic regulation of the expression of CTA genes (Karpf, 2006; Sigalotti *et al*., 2007; Wischnewski *et al*., 2006). Histones are basic proteins consisting of nucleosomes and N-terminal tails that protrude from the nucleosome. The fundamental feature of the histone tail domain is posttranslational modification, such as acetylation, phosphorylation, methylation, and ubiquitination. These modifications are associated with essential biological functions, including transcription, DNA repair, replication, and condensation (Fratta *et al*., 2011; Strahl and Allis, 2000; Kouzarides, 2007). Enzymes are responsible for controlling the balance of histone modifications by adding the acetyl groups to lysine residues on histone, which is accomplished by histone acetyltransferases (HATs), and additional methyl groups to the N-terminal, which is catalysed by histone methyltransferases (HMTs). Conversely, removal of these groups is catalysed by histone deacetylases (HDACs) and histone demethylases (HDMs) (Gräff and Tsai, 2013). In mammalian cells, the G9a and G9a-like proteins (GLPs) are key elements of the H3K9 methyltransferase enzyme involved in gene regulation, which is generated by methylating H3 Lys 9 (Inagawa *et al*., 2013). The functional role
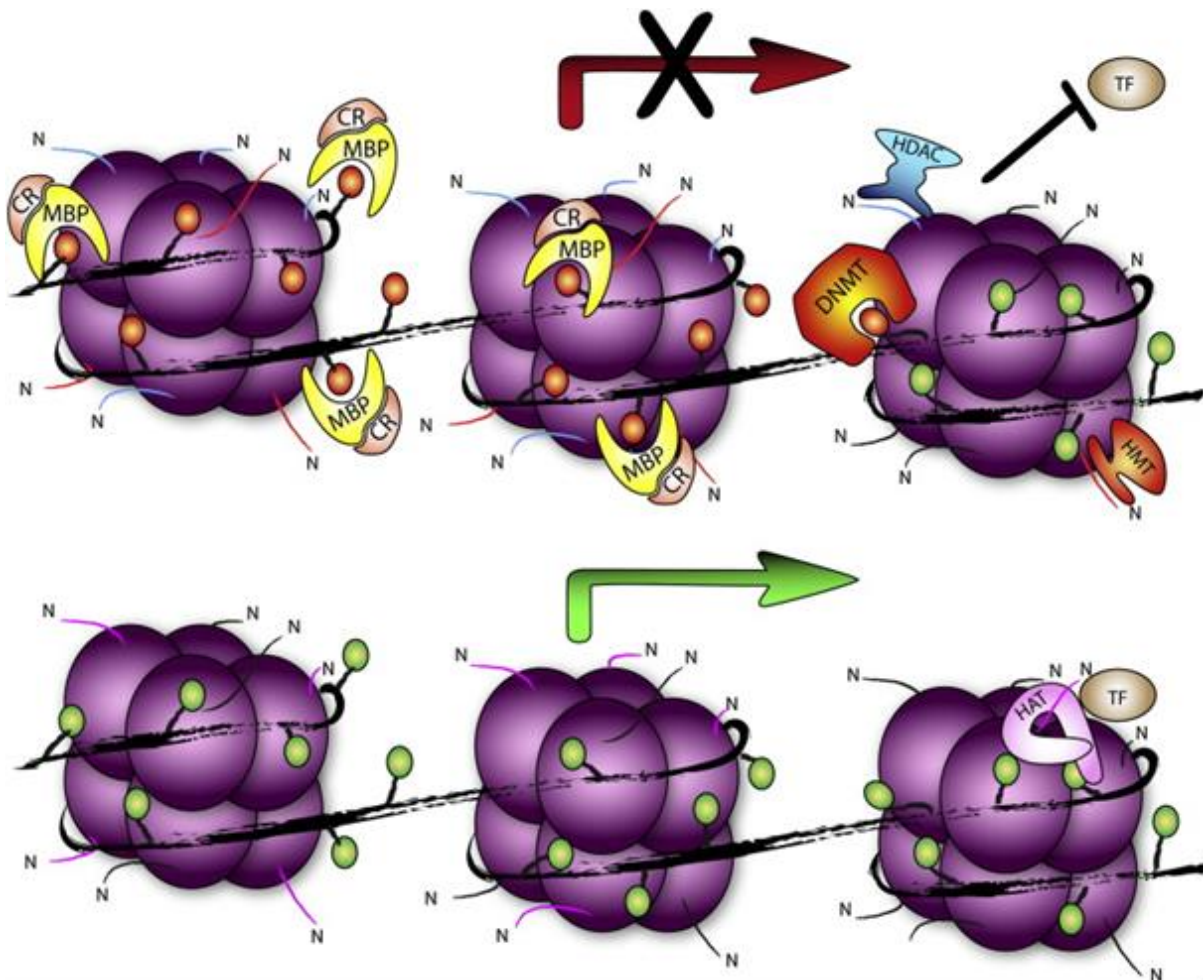
Figure 1.8 Epigenetic regulation of the expression of CTA genes.
The presence of methylated cytosines leads to transcriptionally inactive CTA genes (upper panel) surrounded by promoter regions (orange circles), which is performed and controlled by DNA methyltransferases (DNMT). Inhibition of CTA genetic activity may arise from the methylated recognition sequence that hinders the binding of transcription factors (TFs) or it may result from attachment of the methyl-CpG-binding proteins (MBPs) leading to inhibition of CTA gene expression by enhancing chromatin remodelling co-repressor complexes (CRs). The inhibition of chromatin is a consequence of the presence within the CRs of histone deacetylases (HDACs) that mediate deacetylation of histones (blue N-terminal tails) and histone methyltransferases (HMTs) and are responsible for the catalysis of histone methylation, represented by red N-terminal tails. As a result, chromatin becomes more condensed and inaccessible to the TFs. Thus, inhibition of the expression of CTAs (see red arrow) is a fundamental role of DNA methylation. The demethylated CTA promoters represented by green circles also play an important role by preventing the binding of MBPs and CRs. TFs and histone acetyltransferases (HATs) (represented by pink N-terminal tails) mediate acetylation of histones. The final outcome of these processes is transcriptional activation of the CTA genes (see green arrow). Adapted from (Fratta *et al*., 2011).

of histone methylation that controls silencing of the expression of CTA genes has been revealed. For example, in embryonic stem cells (ESCs), the knockout of HMT G9a and/or GLPs was shown to induce the expression of the *MAGE-A* gene (Tachibana *et al*., 2002; Tachibana *et al*., 2005). However, in human colon cancer cells, the knockdown of G9a and/or GLPs decreased the methylation of H3K9 globally, including the promoter of the CTA genes, even though they did not enhance the expression of the CTA genes (Link *et al*., 2009).

1.7.6   Therapeutic potential of CTA

1.7.6.1 CTA targets for cancer immunotherapy

Due to their unique features, CTAs could be promising targets for immunotherapy in various types of human cancers. As previously discussed, CTAs are expressed in different types of tumours but not in normal tissues, except the testis, which is an immune-privileged site. In addition, the blood-testis barrier (BTB) and the lack of MHC class I molecules that are present on the surface of germ cells. These features prevent the immune system from attacking the CTA proteins, which are non-self-structures (Gjerstorff *et al*., 2015; Fratta *et al*., 2011). The spontaneous humoral and cellular immune reactions have been shown to occur in many CTAs. NY-ESO-1 is one of the best-known immunogenic CTAs that enhances the spontaneous humoral- and cell-mediated immune reactions in a high proportion of patients with positive NY-ESO-1-expressing tumours (Akers *et al*., 2010; Gjerstorff *et al*., 2015). The NY-ESO-1 antibody was detected in a variety of cancers, such as thyroid cancers, 36% (Maio *et al*., 2003), lung cancers, 4%−12.5% (Stockert *et al*., 1998; Scanlan *et al*., 2001), melanoma, 10% (Stockert *et al*., 1998), oesophageal cancers, 13% (Scanlan *et al*., 2001), and bladder cancer, 12.5% (Kurashige *et al*., 2001).

1.7.6.2 CTA vaccine therapy

Vaccination therapy with CTA molecules is an ideal targeted-approach for cancer treatment. Several clinical trials currently target CTA vaccine therapy, particularly the MAGE-A3 and NY-ESO-1 CTAs for the vaccination of patients with prostate, lung, ovarian, and melanoma cancers (Fratta *et al*., 2011; Gjerstorff *et al*., 2015; Domae *et al*., 2014).

Application of a combination of the CTA characteristics, including immunogenic peptides from selected CTAs and identification the respective MHC class I antigen restrictions, represents a preliminary basis for a CTA-based immunotherapeutic approach that uses the CTA peptides as vaccination agents for cancer patients. For instance, the peptides that derive from MAGE-A3 could be used to treat a patient with a tumour that expresses specific antigens. In clinical trials that applied MAGE-A3 to melanoma patients, seven of 25 patients experienced dramatically enhanced sustained tumour regressions and three patients showed fully successful responses (Marchand *et al*., 1999; Gjerstorff *et al*., 2015; Weon and Potts, 2015).

Despite the positive outcomes observed during the vaccination treatment with MAGE-A3, specific cytotoxic T lymphocytes (CTL) were not detected even in patients that demonstrated a positive response (Marchand *et al*., 1999).

In addition, MAGE-A peptides were used with vaccines comprised of peptide-loaded monocyte-derived dendritic cells (DCs). For example, patients with metastatic melanoma were treated by using DCs along with MCH class II restricted antigens, including tyrosinase, gp100, and melan-A peptides; patients were also treated with MCH class I antigens that were specific to the MAGE-A1 and MAGE-A3 peptides. Two patients out of 16 exhibited complete tumour responses (Nesrua *et al*., 1998). In clinical trials, proteins including MAGE-A3 and NY-ESO-1 are being tested as anticancer vaccines (Marchand *et al*., 2003; Krishnadas *et al*., 2015).

1.7.7   Clinical application of CTA genes

Vaccines such as Gardasil and Cervarix are administered to prevent the development of cancer as a result of infection by the human papillomavirus (HPV), which may be responsible for the initiation and development of cervical cancer and have efficiently been used to immunize against HPV infection (Tagliamonte *et al*., 2014; Lehtinen and Dillner, 2013; Herrero *et al*., 2015). However, to date, a vaccine targeting tumour-associated antigens has not been successfully developed for the treatment of cancer, because the immune system exhibits self-tolerance to the tumour-associated antigens (TAA) (Menez-Jamet *et al*., 2016). In existing cancers, the therapeutic vaccine is essential to control or eliminate the cancer by stimulation of the natural immune system response to attack invaders (Palucka and Banchereau, 2013).

Immunotherapy targets cancer by applying two different strategies. One strategy involves the use of passive immunotherapy, such as adoptive cell therapy and monoclonal antibodies. A second strategy—known as active immunotherapy—uses vaccines to stimulate the immune system response.

1.7.7.1 Adoptive cell therapy (ACT)

The principle of using an adoptive immunotherapy approach for treating patients by isolation of T-lymphocyte cells using genetic engineering expands the benefits of using these cells *in vitro* to enhance the expression of selective tumour antigens. Subsequently, infusion therapy is used to re-infuse these cells into the patient. The two primary sources of cells for ACT are the peripheral blood of the patient and the tumour (Rosenberg and Restifo, 2015; Varela-Rohena *et al*., 2008). The aim of this technique is to control or eliminate the malignant cells. The primary success of this approach is that ACT targets the specific tumour antigen without harming normal cells (Rosenberg and Restifo, 2015). Hunder *et al*. (2008) described the successful application of using this approach; they were able to treat patients with metastatic melanomas by using autologous CD4+ T cells targeting the NY-ESO-1. After expanding these cells *in vitro*, they were infused into the patient's blood. Two months after the cells were infused into the patient, scanning the patient revealed no signs of pulmonary or nodal tumours; after two years, the patient was free of cancer (Hunder *et al*., 2008).

1.7.7.2 Active immunotherapy

In a variety of tumours, many studies have detected the humoral immune response to CTAs. For example, in breast cancer, various types of antibodies were expressed against the SCP-1, SSX-2, CTSP, and NY-ESO-1 CTAs. In multiple myelomas, antibodies against the NY-ESO-1, SSX2, and MAGE-A3 CTAs are also produced and have been developed. In addition, a cancer vaccine trial in patients with melanoma who received the MAG-A3 or NYESO-1, demonstrated the regression of tumour nodules. Also, the immune response was found to occur in greater proportion in patients vaccinated with NY-ESO-1 as compared to MAGE-A3. For NYESO-1, more than 34 trails have been conducted by applying the NY-ESO-1 peptide, the protein, and the pox-NY-ESO-1. Jonathan Cebon provided the most sufficient evidence resulting in positive outcomes by using

the vaccine NY-ESO-1 Protein/ISCOMATRIX®. CTAs are directed therapies that may eliminate the risk of melanoma and promote immune system adaptations (Caballero and Chen, 2009; Old, 2008).

1.8 Project aims

In this project, we aim to (1) validate a new cohort of CTA genes that have been reported to be associated with aggressive tumours and may serve as potential targets / biomarkers (Rousseaux *et al*., 2013), (2) evaluate the expression pattern of genes that have been identified as CTA genes by using novel computational tools, and (3) screen drugs that have been developed *in silico* for targeting a CTA-like factor, Brachyury.

The specific goals of this project are:

1. To validate a sub-group of CTA genes reported to be associated with aggressive lung tumours. The validation of these genes will be accomplished by using RNA isolated from normal and cancerous human lung tissues, and from normal and cancerous ovarian tissues.

2. To characterise the expression pattern of genes that are known to be cancer biomarkers. Their ON/OFF expression will be evaluated using a TLDA array, which aims to assess their utility as clinical biomarkers

3. To screen drugs that are designed *in silico* to target the *Brachyury* gene product. The SW480 cancer cell line will be treated with 19 newly developed drugs and qRT-PCR will be used to analyse the efficacy of these drugs by monitoring cell survival and gene expression profiling.

Chapter 2.0 Materials and Methods

2.1 The source of human cell lines

The embryonal carcinoma NTERA-2 (clone D1) cell line was a kind gift from Prof. P.W. Andrews (University of Sheffield) and the ovarian cancer cell line (A2780) was gifted by Prof. P. Workman (Cancer Research UK Centre for Cancer Therapeutics, Surrey, UK). The purchased cell lines were 1231N1, COLO800, COLO857, G-361, HCT116, HT29, LoVo, MCF-7, MM127, SW480 and T84 from the European Collection of Cell Cultures (ECACC). The ovarian adenocarcinoma cell lines PEO14 and TO14 were obtained from Cancer Research Technology Ltd. The lung cancer line H460 and breast cancer cell lines MDA-MB-453, k562, Jurkat and KBM-7 were obtained from the American Type Culture Collection (ATCC). Cancer cell lines were tested routinely using the LGC Standards Cell Line Authentication service.

2.2 Cell culture and growth maintenance

Cancer cell lines were cultured and maintained in humidified incubators at 37°C in a 5% CO_2 atmosphere and in 10% CO_2 for cell proliferation. Cell lines were proliferated in media supplemented with foetal bovine serum (FBS) (Invitrogen, Catalogue number; 10270, Lot 41Q6208K). The LookOut® Mycoplasma PCR Detection kit (Sigma Aldrich; MP0035) was used according to the manufacturer's protocol to check the cancer cell lines for mycoplasma contamination. The growth media, description of each cell line and condition of the cell lines are listed in Table 2.1.

Table 2.1 Description of the human cancer cell lines used and their growth conditions.

Cell line	Description	Media of growth	CO_2
K562	Caucasian chronic myelogenous leukaemia	Roswell Park Memorial Institute 1640 medium (RPMI 1640) + GLUTAMAX™ (Invitrogen, 61870) supplemented with10% FBS	5%
Jurkat	T cell leukemia		
COLO800	Human melanoma		
COLO857	Human melanoma		
H460	Large cell lung carcinoma		
G-361	Human Caucasian malignant melanoma	McCoy's 5A medium + GLUTAMAX™ (Invitrogen, 36600) with10% Foetal Bovine Serum	5%
HCT116	Human colon carcinoma		
HT29	Human Caucasian colon adenocarcinoma		
KBM-7	Myeloid leukemia	IMDM(1X)+GLUTAMAX™(Invitrogen,31980) with10% FBS and 25 mM HEPES	5%
HEP-G2	Hepatocellular carcinoma	Dubeco's modified Eagle's medium (DMEM) + GLATAMAXTM (Invitrogen; 61965) + 10% FBS	5%
SW480	Human colon adenocarcinoma		
1231N1	Human brain astrocytoma		
HeLa	Human cervical cancer cell		
NTERA-2	Human Caucasian pluripotent embryonal carcinoma		10%
(clone D1)			
A2780	Human ovarian carcinoma	DMEM + GLATAMAXTM + 10% FBS and 1xNEAA (non-essential amino acids)	5%
MCF-7	Human Caucasian breast adenocarcinoma		

PEO14	Ovarian Adenocarcinoma, peritoneal ascites	RPMI 1640 + GLUTAMAX™ + with10% FBS and 2 mM sodium pyruvate	**5%**
T84	Human colon carcinoma	Ham's F12 + DMEM (1:1) + GLUTAMAXTM (Invitrogen; 31331) + 10% FBS	**5%**
LoVo	Human colon adenocarcinoma	Ham's F12 + 2mM Glutamine + 10% Foetal Bovine Serum (FBS).	**5%**
MDA-MB-453	Human breast carcinoma	Leibovitz's (L-15) medium + GLUTAMAXTM (Invitrogen; 31415) + 10% FBS	0%

2.3 Preparation of cell stocks

Confluent cells were washed with 1X PBS (Invitrogen; 14190-094) and trypsinised with 1X trypsin-EDTA (Invitrogen, 1370163). The cells were then counted with either an automatic cell counter or a haemocytometer, followed by centrifugation at 1,500 ×g for 5 minutes. The pellet was resuspended in a freezing medium containing dimethyl sulfoxide (DMSO) (Sigma-Aldrich; D8418) and FBS (1:9). The cryotube was used to transfer and store the cells at −80°C for short-term storage or in liquid nitrogen for long-term storage.

2.4 Thawing cells from frozen stock

Cells in vials were removed from liquid nitrogen or the -80°C freezer, placed in a 37°C water bath and swirled gently until nearly 80% of the cells were thawed. The vial was wiped with 70% ethanol before opening and its contents were added slowly to a 15 ml Falcon tube containing 5 ml pre-warmed culture medium. This mixture was centrifuged for 5 minutes at 1,500 ×g to pellet the cells and the supernatant was removed. The cells were resuspended in 10 ml culture medium and transferred into T25 flasks, which were then placed in a 37°C incubator with the required CO_2 concentration. After 24 hours, the medium was gently replaced and culturing continued at 37°C in a CO_2 atmosphere.

2.5 Optimisation of the cell seeding density in 24-well plate tissue culture

The cells used in this study were seeded in 24 well plates (Costar; 3524) to optimise the initial cell seeding density for cell growth. The cell growth rate for each cell line was monitored by light microscopy, as each cell line has specific growth conditions. The average number of seeding cells is shown in Table 2.2.

Table 2.2 Average number of seeding cells in 24-well plates.

Cells names	Seeding density per well (number of cells
1. HepG2	$3x10^4$
2. SW480	$2x10^4$
3. HCT116	
4. NTERA2	
5. MCF-7	
6. G-361	
7. A2780	
8. H460	$1.5x10^4$
9. Jurkat	
10. K562	
11. KBM-7	$1x10^4$
12. HeLa	$2.5 x10^4$
13. PEO14	
14. T84	
15. LoVo	
16. 1231N1	
17. COLO800	
18. HEK-293	$4 x10^4$

2.6 Treatment of cells with different drugs

The cells were seeded in 24-well tissue culture plates as shown in Table 2.2. The drugs were 19 Brachyury drugs designed by the Cardiff University Group. The cancer cells were treated in 24-well plates with these 19 drugs from well 1 to 19 (100 µM of a 10 mM drug stock), DMSO was added as a vehicle control to the cells in well 20 and the last 4 wells contained only cells. Depending on the cell seeding density, culture medium was added to each well to give a final volume of 500 µl. The plate was then placed in an incubator at 37°C at an appropriate CO_2 level for 72 hours. Cell proliferation was then determined by light microscopy and the drug effect was noted by comparing the cells in each well to those in the wells that were free of drugs and DMSO.

2.7 RNA extraction from cell culture

The RNeasy Plus Mini Kit (Qiagen, Catalogue number, 74104) was used according to the manufacturer's instructions. Briefly, total RNA was isolated from all the cancer cell lines used in this study (Table 2.1). Cells were collected by centrifugation at 1,500 ×g for 5 minutes and the cell pellets were washed with PBS (Invitrogen; 14190-094). The RLT Plus Lysis buffer was used to resuspend the cell pellets; the amount of added buffer depended on the cell numbers counted with a haemocytometer slide or by an automated cell counter (BioRad). Cells at a density of 5×10^6 cells/ml were resuspended in 350 µl RLT plus; cells with a density of 5×10^6 to 5×10^7 cells/ml were resuspended in 600 µl. The lysates were homogenised using a QIAshredder spin column (Qiagen, Catalogue number; 97654) and DNA genomic was removed with the gDNA Eliminator spin column provided with the kit. A NanoDrop (ND_1000) spectrophotometer was used to measure the RNA concentration.

2.8 Synthesising of complementary DNA (cDNA)

Total RNA was isolated from the human cancer cell lines selected for this study. A range of human tissues with normal RNA was purchased from Clontech (Catalogue number; 636643), while cancer tissue and cancer cell lines were supplied from Clontech and Ambion. The RNA tissue types purchased from Origen, Amsbio and Ambion are listed in Table 2.3. According to the manufacturer's instructions, RNA was used to synthesise cDNA using the SuperScript III First Strand Synthesis Kit for RT-PCR (Invitrogen; 18080-051). Oligo-dT primer was used to transcribe

1 µg of the RNA into single-strand cDNA. The cDNA was then diluted 1:8 and its quality was checked, using *ACTB* primers as controls in the PCR.

Table 2.3 List of human RNA tissue from Origen, Amsbio and Ambion.

Lung Normal	Catalogue number	Ovary normal	Catalogue number
1	Amsbio,R1234159-50	1	Origene,CR560119
2	Amsbio,R1234152-50	2	Origene,CR560293
3	Amsbio,HR-601	3	Origene,CR560512
4	Ambion,636643	4	Ambion,636643
5	Origene,CR562777	5	Origene,CR560727

RNA from human cancer tissue supplied from Origene.			
Lung cancer	**Catalogue number**	**Ovary cancer**	**Catalogue number**
1. **ADC1**	CR560634	1. **OSPA1**	CR560272
2. **SCC1**	CR562036	2. **ADC1**	CR562471
3. **ADC2**	CR560308	3. **ADC2**	CR560815
4. **ADC3**	CR560064	4. **OCCA**	CR561515
5. **SCC2**	CR561521	5. **OSPA2**	CR561357
6. **ADC4**	CR561858	6. **OSPA3**	CR559223
7. **ADC5**	CR562426	7. **ADC3**	CR566319
8. **ADC6**	CR561625	8. **OSPA4**	CR560992
Melanoma		**Colon**	
MM 1	CR562857	Colitis	CR561525
MM 2	CR562901		
Recurrent melanoma	CR559628		

2.9   Reverse transcription PCR (RT-PCR)

Sequences of each gene were obtained from National Center for Biotechnology Information (NCBI; http://www.ncbi.nlm.nih.gov) database and each specific primers were designed to span more than one intron where possible. Primers were designed using the Oligonucleotide Properties Calculator (http://biotools.nubic.northwestern.edu/OligoCalc.html) and Primer 3 software (available at http://primer3.ut.ee/).

A 1µl volume of diluted cDNA template was used for PCR in 12.5 µl of BioMix^{TM} Red (Bioline; BIO-25006) and 0.5 µl of each of the forward and reverse primer; DNase/RNase –free water was added to a final volume of 25 µl. The samples were amplified using a Techne TC-312 thermal cycle at 96°C for 5 minutes, followed by 40 cycles of denaturing at 96°C for 30 seconds. The annealing temperatures for each specific primer used for RT-PCR are shown in Table 2.4. Annealing was conducted for 30 seconds and extension at 72°C for 30 seconds, followed by a final extension step at 72°C for 5 minutes. A total volume of 10 µl from the master mix reaction was run on a 1% agarose gel stained with ethidium bromide (Sigma-Aldrich; 46067) or the DNA/RNA dye, peqGREEN (PEQLAB - Life Science, 37-5010) (see Section 2.10).

2.10 Preparation of agarose gel electrophoresis

The 1% agarose gel was prepared from a mixture of 900 ml of distilled water and 100 ml of 10x TBE buffer. A 150 ml volume of this 1x TBE was added to 1.5g agarose gel powder (Melford, catalogue number; 9012-36-6) and mixed. The solution was then carefully heated in the microwave until completely melted (approximately 2–3 minutes), cooled to about 50–60°C and then 1.5 µl ethidium bromide or peqGREEN was added. The solution was poured into a tray containing a sample comb and allowed to set at room temperature. The PCR products were determined using 5 µl of a 50 bp Hyper Ladder (Bioline, H2-415208).

Table 2.4 Primer sequences and their expected sizes used in RT-PCR.

Gene	Primer	Primer Sequence	Tm (°C)	Product size (bp)
ACTB	F1	5'- AGAAAATCTGGCACCACACC-3'	58	553
	R1	5'- AGGAAGGAAGGCTGGAAGAG-3'		
	F2	5'-TGCTATCCCTGTACGCCTCT-3'	58	675
	R2	5'-CGTCATACTCCTGCTTGCTG-3'		
BTG4	F	5'-CCTCATCAGACGTTTCCTC-3'	57.5	162
	R	5'-CCACATTCTTTTTGCGGGGGA-3'		
C12orf37	F	5'-CAACTCCTTCATTAGGCATATTCC-3'	58	330
	R	5'-TTCAACATACTACTGGAAGTCC-3'		
C10orf82	F	5'-ATGACATGAACCACTGTG -3'	56	310
	R	5'- TCCTTGTAGCAGTTTTTGGCCA -3'		
EBI3	F	5'-CCTGCAGTGGAAGGAAAGG-3'	58.5	324
	R	5'-GCTCTGTTATGAAAGGCACG-3'		
HIST1H3C	F	5'-GGCGTGAAGAAACCTCATCGCT-3'	60	281
	R	5'-GCCAGCTGGATATCTTTGGGC-3'		
Hs.601545	F	5'- GCTACTTGCTGTGTGACCTG-3'	58	298
	R	5'-CTGTTTGGCATCCCAGCT -3'		
ISM2	F	5'-TACCCCTAACCCTGATAACCAG-3'	60	530
	R	5'-AGGTGTCCTTGTCCTCAGTGC -3'		
KIAA1257	F	5'-GGCCTTCCCTGTGAATATGG-3'	59.5	339
	R	5'-GTGTTCCAGAGCCTCAAGG-3'		
LGALS14	F	5'-TGTGCAAGTACTGGGGCTG-3'	59.5	467
	R	5'-CACTCTGGTCAGGGAGATATCTC-3'		
NBPF4	F	5'-GCAGCACCTTGTCCTCATTGG-3'	58.5	509
	R	5'-CTCTGCGCTCTCAGCATGCGGG -3'		

2.11 RT-PCR purification

The desired fragments of the PCR products were purified from a 1% agarose gel stained with ethidium bromide or peqGREEN. A sterile blade was carefully used to cut the fragment, which was then used with a purification kit (Roche Applied Science; 11732676001 or Geneclean MP;111102400) according to the manufacturer's instructors.

The DNA fragments were then sent to Eurofins MWG for sequencing. This step was done using a Mix 25seq Kit from Eurofins. A tube containing 1 ng/µl of the PCR products (150-300 bp), 5 ng/µl of the PCR products (300-1000 bp) and 10 ng/µl of the PCR products larger than 1000 bp, together with specific forward or reverse sequencing primers, were reacted at room temperature. The sequencing results for each gene were blasted and aligned against the expected sequence of the PCR product using the NCBI Basic Local Alignment Search Tool.

2.12 Real time quantitative PCR (qRT-PCR)

RNA was isolated from confluent cell cultures (Section 2.7) and the RNA concentration and quality were tested using the NanoDrop instrument. The SuperScript III First Strand synthesis kit was used to synthesise cDNA from 1 µg of total RNA. This process was done according to the manufacturer's instructions and the resulting cDNA was diluted 8-fold. The quality of cDNA was tested with *ACTB*, which also confirmed that the reverse transcription was successful.

2.12.1 TaqMan Low Density Array (TLDA) card

The TaqMan array containing genes and their endogenous control genes used in this study, shown in Table 2.5, was purchased from Thermo Fisher Scientific. The real-time PCR was conducted on the lab bench in 1.5 ml microcentrifuge tubes. A volume of cDNA equal to 110 µl was mixed with TaqMan® Universal Master Mix II and with UNG (Applied Biosystems™, Catalogue number 4440038; Lot1403028) equal to the volume of cDNA when the reagent reached room temperature. From the mixture, 100 µl of the desired specific PCR reaction was dispensed to fill the reservoir of the card. The TaqMan card was inserted into the card holder and centrifuged for 1 minute at 1,000 ×g in a Sorvall® Legend T centrifuge (Heraeus™ rotor 75006445). The card was sealed by positioning the sealer (Life Technologies sealer device) and inserting the card into it. The sealed

card was removed from the sealer using scissors and the fill reservoirs were trimmed from the card.

The Applied Biosystems 7900HT Fast Real-Time PCR System was used according to manufacturer's standard thermal cycling conditions (initial steps at $50°C$ for 2 minutes, $94.5°C$ for 10 minutes, 40 cycles of $97.0°C$ for 30 seconds, and $59.7°C$ for 1 minute). The SDS file that corresponded to the assay card was placed in the instrument tray and the run was started. Expression Suite Software Version 1.03 from Life Technologies was used to analyse the results.

Table 2.5 Genes used in the TLDA card and amplified by 7900HT Real-Time PCR.

Gene	Assay Name	Gene	Assay Name
ACTL9	Hs00742102_s1	*CHEK2*	Hs00200485_ml
ACTRT1	Hs00536564_s1	*CPXCR1*	Hs00263695_s1
ADAD1	Hs00330122_ml	*CST8*	Hs00193978_ml
ADAM2	Hs00155182_ml	*CTAGE1*	Hs00535737_s1
AKAP3	Hs00179042_ml	*CXorf27*	Hs01589213_s1
ARMC3	Hs00330456_ml	*CYLC1*	Hs03005816_ml
ASB17	Hs00404173_ml	*CYLC2*	Hs00915767_ml
ATAD2	Hs00204205_ml	*DAZL*	Hs00154706_ml
BOLL	Hs00263613_ml	*DDX4*	Hs00987125_ml
BRDT	Hs00976114_ml	*DDX53*	Hs00704566_s1
C12orf50	Hs00541362_ml	*DKKL1*	Hs01011550_g1
C16orf46	Hs00329971_ml	*DNAJC5G*	Hs00543504_ml
C16orf78	Hs00906699_ml	*DUSP21*	Hs00254403_s1
C17orf98	Hs01373054_ml	*EQTN*	Hs00294888_ml
C19orf45	Hs00380981_ml	*FABP9*	Hs00908573_ml
C19orf67	Hs01098206_ml	*FAM170A*	Hs00766182_ml
C1orf65	Hs00541426_s1	*FAM71B*	Hs00330949_ml
C20orf195	Hs00225281_ml	*FKBP6*	Hs00975708_ml
C20orf201	Hs00905447_g1	*FTMT*	Hs00893202_s1
C2orf70	Hs01375040_ml	*GK2*	Hs01087041_s1
C3orf22	Hs00381841_ml	*GPAT2*	Hs00418637_g1
C4orf17	Hs00259777_ml	*HMGB4*	Hs00536849_s1
C5orf47	Hs01585417_ml	*HORMAD1*	Hs00611993_ml
C8orf74	Hs00416912_ml	*HORMAD2*	Hs00381066_ml
CAGE1	Hs00379721_ml	*IL31*	Hs01098710_ml
CAPZA3	Hs00264539_s1	*IQCF1*	Hs00380884_ml
CASC5	Hs00538241_ml	*IQCF3*	Hs00378831_ml
CATSPER1	Hs00364950_ml	*KLF17*	Hs00703004_s1
CATSPERD	Hs00735890_ml	*LEMD1*	Hs01073236_ml
CCDC110	Hs00380240_ml	*LINC00615*	Hs00332472_ml
CCDC113	Hs00204293_ml	*LRRC6*	Hs00917168_ml
CCDC116	Hs04190030_ml	*LUZP4*	Hs00212609_ml
CCDC38	Hs00403640_ml	*LYZL6*	Hs00220795_ml
CCDC79	Hs00543366_ml	*MAEL*	Hs00262601_ml
CCER1	Hs00541466_s1	*MAGEA12*	Hs00855175_s1
CEP290	Hs00228353_ml	*MAGEA1*	Hs00607097_ml
CEP55	Hs01070181_ml	*MAGEA2*	Hs01650773_ml
CEP72	Hs00986151_ml	*MAGEA4*	Hs00751150_s1

Gene	Assay Name	Gene	Assay Name
MAGEA9;MAGEA9B	Hs00245619_s1	*SPAG4*	Hs00162127_m1
MAGEB3	Hs00267135_s1	*SPAG9*	Hs00187715_m1
MAGEB4	Hs00267142_s1	*SPANXE;SPANXC*	Hs04224960_gH
MBD3L1	Hs00376997_s1	*SPATA19*	Hs00545367_m1
MND1	Hs00259549_m1	*SPO11*	Hs00173288_m1
MRE11A	Hs00967443_m1	*SPZ1*	Hs00261454_s1
NANOS2	Hs02384758_s1	*SSX5*	Hs00820186_m1
NBPF6	Hs00823768_m1	*STK31*	Hs00230012_m1
NLRP4	Hs00370499_m1	*STRA8*	Hs00699316_m1
NOL4	Hs00269457_m1	*SYCE1*	Hs00365683_m1
NR6A1	Hs00265966_m1	*SYCP1*	Hs00172654_m1
NT5C1B	Hs00403674_m1	*SYCP3*	Hs00538146_m1
NUTM1	Hs01395191_m1	*SYNGR4*	Hs00202872_m1
NXF2B;NXF2	Hs00903817_mH	*TBC1D21*	Hs00907160_m1
ODF3	Hs00560560_m1	*TCFL5*	Hs00232444_m1
ODF4	Hs00537806_m1	*TCTE3*	Hs00601792_m1
OIP5	Hs00299079_m1	*TDRD12*	Hs01370702_m1
OTOA	Hs01043543_m1	*TDRD1*	Hs00229805_m1
PAPOLB	Hs00252346_s1	*TDRD5*	Hs00543012_m1
PBK	Hs00218544_m1	*TEPP*	Hs01383912_m1
PBX4	Hs00257935_m1	*TEX101*	Hs00758335_m1
PDHA2	Hs01043024_s1	*TEX14*	Hs00258708_m1
PFN3	Hs00907971_s1	*TEX15*	Hs00229744_m1
PIWIL2	Hs00216263_m1	*TEX19*	Hs00401475_m1
PLAC1	Hs00222307_m1	*TEX33*	Hs00418081_m1
PLD6	Hs00381651_m1	*TGIF2*	Hs00904994_g1
PPP3R2	Hs00330865_s1	*TGIF2LX*	Hs00536782_s1
PRDM9	Hs00360639_m1	*TMEFF1*	Hs00902905_m1
PRPS1L1	Hs00741943_s1	*TRIM42*	Hs00403661_m1
PRSS54	Hs00399820_m1	*TRIML1*	Hs00385739_m1
PTPN20A	Hs00417254_m1	*TRIP13*	Hs01020073_m1
RAD21L1	Hs00416293_m1	*TSSK1B*	Hs03044235_s1
RANBP17	Hs00224684_m1	*TSSK6*	Hs00230713_m1
RBM44	Hs01374444_m1	*TTK*	Hs01009870_m1
RNF17	Hs00229787_m1	*TULP2*	Hs00163252_m1
RQCD1	Hs00193762_m1	*ZCCHC13*	Hs00743101_s1
SCP2D1	Hs00708917_s1	*ZSWIM2*	Hs00381578_m1
SEPT12	Hs00332566_m1	*18S*	Hs99999901_s1
SHCBP1L	Hs01102289_m1	*GAPDH*	Hs02758991_g1
SMC1B	Hs00933203_m1	*RPS13*	Hs01011487_g1
SPACA3	Hs00420105_m1		

2.12.2 SYBR Green Real-Time PCR Master

The Go Taq qPCR Master mix Kit (Promega; A6002) was used according to the manufacturer's instructions to prepare the reaction mixture. In brief, a total of 20 µl containing 1.5 µl cDNA and 2 µl of each forward and reverse sequencing primer was added to a Hard-Shell® 96-well plate (Bio-Rad; 9655) or 0.2 ml a 96-well PCR microplate for ABI.el (StarLab,15304). Reactions were run in triplicate for each sample in a Bio-Rad CFX instrument. The genes of interest were amplified by pre-denaturation at 95°C for 3 minutes, then 40 cycles at 95°C for 10 seconds. After annealing at 60°C for 30 seconds, the final step was 95°C for 10 seconds. The melting curve analysis was obtained after completion of the 40 cycles. The results were analysed using Bio-Rad CFX Manager Software (version 2). QuantiTect Primer Assays (Qiagen) and designed qPCR primers were used in this study, as shown in Tables 2.6 and 2.7.

Table 2.6 Quantitative real-time PCR assays used in this study.

Gene	Primer Assays	Catalogue number
Brachyury	Hs_T_1_SG QuantiTect Primer Assay	QT00062314
CCNE1	Hs_ CCNE1_1_SG QuantiTect Primer Assay	QT00041986
CROT	Hs_CROT_1_SG QuantiTect Primer Assay	QT00021112
IGFBP3	Hs_IGFBP3_1_SG QuantiTect Primer Assay	QT00072737
MEST	Hs_MEST _1_SG QuantiTect Primer Assay	QT00048426
MFN2	Hs_MFN2 _1_SG QuantiTect Primer Assay	QT00057589
MSH2	Hs_MSH2_1_SG QuantiTect Primer Assay	QT00032466
MTHFD2	Hs_MTHFD2_1_SG QuantiTect Primer Assay	QT00081592
SFRP5	Hs_SFRP5_2_SG QuantiTect Primer Assay	QT01008182
GAPDH	Hs_GAPDH _1_SG QuantiTect Primer Assay	QT00079247
HSP90AB1	Hs_ HSP90AB1 _1_SG QuantiTect Primer Assay	QT01002624
Tubulin	Hs_ TUBA1C _1_SG QuantiTect Primer Assay	QT00062720

Table 2.7 Designed primers for genes of interests used in real-time PCR.

Gene	Primer	Primer Sequence	Tm (°C)	Product size (bp)
Brachyury (TV1)	F	5'-GTGACAGGTACCCAACCCTG-3'	55	97
	R	5'-GGTGAGTTGTCAGAATAGGTTGGA-3'		
Brachyury (TV2)	F	5'-ACCTGGGTACTCCCAATCCTA-3'	55	79
	R	5'- GCTGGACCAATTGTCATGGG-3'		
BTG4	F	5'-GCCTCATCAGACGTTTCCTC-3'	58.5	125
	R	5'-CACTTAGGATGCTTCTGCG-3'		
C10orf82	F	5'-CTGCCAAGGAATGTCCAAGGA-3'	60.3	134
	R	5'-TGACAGGTTTCAGTTTCGGGG -3'		
C12orf37	F	5'-ATGGGATGCTTTGATTGCTC-3'	55	143
	R	5'-AGAGATGTGAGGCTGGCAGT-3'		
CCDC83	F	5'-AATCCTCGTCATCTGCTGCT-3'	58.5	90
	R	5'-TCCAGCAGCTTGGGTAAGATA-3'		
CPA5	F	5'-CAGCACCAACAGCTTCAGTT-3'	59	76
	R	5'-CATTACAAAGTTGTCAATCCAGCTA-3'		
DPEP3	F	5'-CCTGGACAGGCTTAGAGACG-3'	58.5	72
	R	5'-TCCTGGGACTGGCATGAG-3'		
EBI3	F	5'-CCTGCAGTGGAAGGAAAGG-3'	58.5	100
	R	5'-AGGGTCCAGGAGCAATCC-3'		
FLJ43944	F	5'-ACCTCTGGAGTCTCCTGAAG-3'	60	110
	R	5'-GAAACTCTTGCTGGACTG-3'		
HIST1H3C	F	5'-CGCAGGTCGGTTTTGAAGTCC-3'	58	120
	R	5'-AATAGCGCACAGATTGGTGTC-3'		
Hs.601545	F	5'-CTGCTACTTGCTGTGTGACCT-3'	60	116
	R	5'-AGATGAGCAGAATGAAGTTC-3'		
ISM2	F	5'-ACTCGGCCCTGTGGCTAT-3'	60	87
	R	5'-GGTGTCCTTGTCCTCAGTGC-3'		
KIAA1257	F	5'-GACGATTCTTGGACGATTCAA-3'	56	86
	R	5'-AATTCCTTGATCTCCATCATGC-3'		
LGALS14	F	5'-TCACTTTTGTCAAGGACCCAC-3'	58.4	211
	R	5'-TTGTGACGCACATAGATGCAC-3'		

LOC441601	F	5'-GCCAAAGCAGACACACTCAC-3'	58.5	95
	R	5'-ACAATGTTCACCATTTTCAACTGT-3'		
MAGEB6	F	5'-TGAGCCTGAAAAGTGCTGTC-3'	52	93
	R	5'-TGTGGGTAGGAAGACTAGGAAGG-3'		
NBPF4	F	5'-CATGCTGAGAGCGCAGAG-3'	58	62
	R	5'-TTTCATCCTGCCATCCTTTG-3'		
OR7E156P	F	5'-GGTACCAGCCGTCGGCAGATTTGA-3'	58	87
	R	5'-GAACCTTAGGACCCACCTGGA-3'		
PIWIL1	F	5'-AGAGGTTACCAGACCAGAATGG-3'	60	77
	R	5'-GTGTGGGAGAAACACTACCACTT-3'		
RBM46	F	5'-GGAAATTTGGCGGTCCTC-3'	56	70
	R	5'-CCTACAAAAACTTCACAGCCTCT-3'		
RFX4	F	5'-CATCACCAAGCAAACCCTTT-3'	57	117
	R	5'-GACTCGATGGGAGACTGCTC-3'		
ROPN1	F	5'-CCAAAGTGGATGGGGAGAT-3'	56	89
	R	5'-GATTATACCATCAGGGCCAATTA-3'		
TKTL2	F	5'-ACGACCGGTTCATCCTCTC-3'	58.5	61
	R	5'- TCCACCCAAGCAGCATAGA-3'		
TPTE	F	5'-AGGCACCTGCGAAAGAAAG-3'	58.5	85
	R	5'-CGTGCTAACACACTTTCACTGAT-3'		
TPTE2P2	F	5'-CAGAAGCAGTCTGGCTTTCA-3'	56	98
	R	5'-TGTCATCGGTGTCTCTATCAATG-3'		
TUBA3C	F	5'- CGGAGGAGCTCAACATGC-3'	58	82
	R	5'-AGTTCCCAGCAGGCATTG-3'		
VCY	F	5'-GGCCAAGGAGACAGGAAAG-3'	57	80
	R	5'-CGGCCACCTTGGTAGTCTT-3'		

2.13 Western blot analysis

2.13.1 Protein extraction from whole cell culture

Whole cell extracts were made from confluent cell cultures by washing with 1X cold PBS, followed by trypsin treatment to harvest the cells. Up to 10 ml of media specific for each cell culture were then added to deactivate the trypsin. The cell pellets were obtained by centrifugation at 5,000×g for 5 minutes at 4°C. The M-PER Mammalian Extraction Reagent (Thermo; 78503) was used to resuspend the cells pellets by adding 10 μl to each 1 mg of cell pellet after the pellets were weighed. Total protein (supernatant) was separated from cell debris (pellet) after centrifugation for 15 minutes at 14,000×g.

The protein concentration was measured using the Pierce™ BCA Protein Assay Kit (Thermo; 23227) according to the manufacturer's protocol. NuPAGE® LDS Sample Buffer (4X) (Invitrogen; NP0007) and NuPAGE® Sample Reducing Agent (10X) (Invitrogen; NP0004) in volumes of 4X and 2X, respectively, were added to each sample (approximately 20 μg). The solution was mixed by pipetting, heated at 70°C for 10 minutes and then placed on ice for 5 minutes.

2.13.2 Cell fractionation

Protein fractionation was achieved by adding protease inhibitor to the lysates, followed by separation of cytoplasmic and nuclear fractions by using a Thermo 78835 instrument according to the manufacturer's protocol. Briefly, ice-cold CER I (depending on the cell pellet) was added to the pellet collected after centrifugation and the tube was vortexed at the high setting for 15 seconds to resuspend the cells completely. The tube was then incubated for 10 minutes, followed by addition of ice-cold CERII, vortexing for 5 seconds at the high setting, and incubating for 1 minute. The protein concentrations in the cytoplasmic and nuclear fractions were then determined using the BCA protein Assay. A heating block was used at 70°C for 10 minutes to heat the fractions, with vortexing every 2 minutes. The samples were then loaded in equal amounts onto SDS-PAGE gels.

2.13.3 Human cancer lysates used in western blotting

All the human cancer lysates used in this study are shown in Table 2.8

Table 2.8 Human cancer lysates used in western bolting.

Cell Lysates	Organ
1. A2780	Ovary
2. PEO14	
3. HeLa	Cervical
4. MCF-7	Breast
5. MDA-MB-453	
6. H460	Lung
7. COLO800	Melanoma
8. G-361	
9. Jurkat	Leukemia
10. K562	
11. KBM-7	
12. HCT116	Colon
13. T84	
14. SW480	
15. LoVo	
16. NTERA2	Embryonal carcinoma
17. 1231N1	Astrocytoma

2.13.4 SDS-PAGE gel and western blotting

The electrophoresis tank contained 1X MOPS SDS Running Buffer (Invitrogen; NP0001). The protein lysate samples (approximately 20 µg) were loaded onto a NuPAGE® 4-12% Bis-Tris gel (Invitrogen; NP0322) and run for 2 hours at 100 V, together with 3 µl of the Precision plus protein standard (Bio-Rad; 161-0377) to determine the molecular weights of the proteins. The proteins were transferred to an Immobilon-P PVDF membrane (Millipore; IPVH00010) by first placing the gel into 100% methanol for activation and then transferring at 400 mA for about 2–3 hours. Alternatively, a Bio-Rad Trans-Blot® Turbo™ Transfer Starter System was used. Briefly, the

transfer was prepared by adding 200 ml of 5X transfer buffer, 600 ml of distilled water and ethanol in a total volume of 1L and carried out according to manufacturer's instruction. Nonspecific binding was blocked by treating the membrane with 5% non-fat dry milk (1X PBS + 0.5% Tween-20, Sigma-Aldrich; P1379) with shaking for 1 hour at room temperature. The membrane was then incubated overnight with the recommended primary antibody concentration in a cold room at 4°C on the shaker. The membrane was then washed three times for 10 minutes with 1X PBST and 0.5% Tween. The membrane was then incubated with the secondary antibody at room temperature for 1 hour with shaking. The concentrations of primary and secondary antibodies are listed in Table 2.9. After incubation with the secondary antibody, the membrane was washed three times for 10 minutes in 1X PBST and 0.5% Tween. The proteins were detected using Enhanced chemiluminescence (ECL; Thermo Scientific; 34087) and the protein bands were then visualised using X-Ray films (Thermo Scientific; 34091)

Table 2.9 Primary and secondary antibody dilutions used in western blotting.

Primary antibody					
Antibody	**Cat. No.**	**Source**	**Host**	**Clonality**	**Dilution**
Anti-Brachyury	AF2085	R&D systems	Goat	Polyclonal	1/500
Anti-GAPDH	sc-365062	Santa-Cruz	Mouse	Monoclonal	1/2000
Anti-Lamin B1	ab16048	Abcam	Rabbit	Polyclonal	1/1000
Anti-α-Tubulin	T6074	Sigma	Mouse	Monoclonal	1/8000
Secondary antibody					
Antibody	**Cat. No.**	**Source**	**Host**	**Reactivity**	**Dilution**
Goat Anti-Rabbit IgG	ab97051	Abcam	Rabbit	Goat	1/25000
Anti-rabbit IgG	7074	Cell Signaling	Goat	Rabbit	1/3000
Anti-mouse IgG	7076	Cell signaling	Horse	Mouse	1/3000

2.14 *Brachyury* gene knockdown using small interfering RNA (siRNA)

2.14.1 *Brachyury* treatment with siRNA

In a 6-well plate (Corning® Costar® cell culture plates; 3516), 1.5×10^5 cells were seeded in each well containing complete medium and incubated under the specific growth conditions. The transfection was prepared for each well by adding 6 μl of Hiperfect Transfection Reagent (1ml)

(Qiagen; 301705) and 0.6 µl of a 10 µM siRNA of the gene of interest to an Eppendorf tube containing 100 µl serum-free medium (SFM). The mixture was mixed by vortexing and then incubated at room temperature for 15 minutes. The mixture was then added dropwise to each well and the plate was gently shaken. The negative control siRNA and *Brachyury* siRNA are listed in Table 2.10. After 24 hours, a second treatment (2 hits) of siRNA was given, followed by a third treatment (3 hits) after 48 hours. Cells were collected after 72 hours by adding 400 µl trypsin to each well and 600 µl of medium with serum.

2.14.2 Treatment with Brachyury drugs

Cells were seeded at 1.5×10^5 cells in each well in a 6-well plate and 100 or 10 µM of 19 Brachyury drugs (designed by the Cardiff University group) or DMSO were added to each well containing media with serum. Each drug treatment used a whole 6-well plate for both concentrations including DMSO. After 72 hours, the cells were harvested and used to perform either RNA extraction or blot analysis.

Table 2.10 The siRNA used in gene knockdown.

Gene	siRNAName	Source	Cat.No.	Target Sequence
Brachyury	Hs_T_5	Qiagen	SI00738255	5'-GAGGATGTTTCCGGTGCTGAA-3'
Negative control	AllStars Negative Control siRNA	Qiagen	1027280	

2.15 Cell proliferation assay

Cell were seeded in 96-well cell culture plates (Corning® 96 Well Solid White Flat TC-Treated Microplate; 3917) by adding 80 µl medium containing serum and cells to each well. Cells were counted and the optimal number of seeding density cells was prepared in Falcon tube and then medium was added for a total of 10 ml. Using a multi-channel pipette, 80 µl from the mixture was dispensed into each well, followed by 20 µl from each of the 19 mixtures containing 1µl of 10 µM and 100 µM of 10 mM drug and 19 µl medium. This dilution was repeated three times for each drug (three wells for each drug). The DMSO control was prepared by mixing 3 µl of DMSO with 57 µl of medium for a total of 60 µl. The positive control consisted of 6 µl NP-40 Surfact-Amps™ Detergent Solution (Thermo;28324B) mixed with 54 µl of medium; 20 µl of the mixture was then added to the plate. A 100 µl volume of medium was used for the luminescence background. The siRNA study was run in 96-well plates by adding 0.3µl siRNA, 0.3µl of Hiperfect (Qiagen, SI04133521) and medium for a total 20 µl volume. The mixture was then incubated at room temperature for 5 minutes and then added to each well (three wells were prepared for untreated, negative control and siRNA assays). The plate was then placed in a cell culture incubator at 37°C in CO_2 for 72 hours. The MT Cell Viability Substrate (Promega; G7913) was prepared by diluting the MT Cell Viability Substrate and NanoLuc^R Enzyme at 37°C in cell culture medium according to the manufacturer's instructions to prepare a 2X concentration of each reagent. After vortexing, an equal volume of 2X Real Time–Glo^{TM} reagent was added to the cells. The cells were incubated for 1 hour in an incubator. A plate-reading luminometer was used to measure the luminescence. Cell treatments with siRNA and the negative control consisted of 3 treatments (3 hits).

2.16 Growth curve analysis

Cells were seeded in 10 plates from a 6-well plate cell culture at equal cell densities for each cell type and the plates was placed in an incubator at 37°C in CO_2 for 24 hours. The mixture was prepared at room temperature by adding 0.6 µl of 10 µM siRNA of the gene of interest to 6 µl of Hiperfect transfection medium in a tube containing 100 µl serum-free medium (SFM). Also, cells were treated with 10 µM of a10 mM Brachyury drugs and DMSO. The mixture was vortexed and let stand at room temperature for 15 minutes. Treated and negative control cells were prepared as per the siRNA-treated cells. The first treatment was given to all 8 plates, which were then incubated

for 24 hours. The cells were trypsinised and three wells per each condition were counted using a Bio-Rad TC10 automated cell counter. The other plate was given a second treatment and the medium was changed. This process was done daily until day 8.

2.17 Immunofluorescence staining of human cancer cells

Cells were seeded at 1×10^5 cells per well on glass coverslips in 24-well cell culture plates (Costar; 3524) containing 1 ml medium and placed in incubator at 37°C in 5% CO_2 until they reached 70–80% confluency. The cells were then fixed with 4% paraformaldehyde (PFA) (Thermo; 28908) in PBS. Nonspecific binding was blocked and the membranes were permeabilised by incubating the cells on a shaker for 1 hour at room temperature in 5% FBS/0.3% Triton™ X-100/1X PBS. The cells were then incubated overnight with primary antibodies (Table 2.11) diluted in 1%BSA/0.3% Triton™ X-100/1X PBS and the cells were washed three times with 1X PBS for 5 minutes each time. The cells were then incubated with the secondary antibodies (Table 2.11) diluted in 1% BSA/0.3% Triton™ X-100/1X PBS for 2 hours at room temperature in the dark, followed by washing three times with 1X PBS for 5 minutes each time. Coverslips were mounted with Prolong® Gold Antifade Reagent with DAPI (Cell Signalling; 8961) and the staining was viewed with a ZEISS LSM 710 confocal microscope and ZEN software (Zeiss).

For staining, tissue sections on slides were deparaffinised by washing three times in xylene at room temperature and dehydrated by washing two times in different concentrations of alcohol (100%, 70%) for 10 minutes. The slides were then rinsed with distilled water twice for 5 minutes. Antigen retrieval was conducted by heat-induced epitope retrieval by boiling the slides in 10 mM sodium citrate buffer pH 6.0 for 10 minutes. The slides were then incubated at room temperature until cool down. Blocking and staining with antibody were conducted as described in Section 2.17.

Table 2.11 Primary and secondary antibodies used in IF staining.

Primary	Cat. No.	Source	Host	Clonality	Dilution
Anti-Brachyury	ab140661	Abcam	Mouse	Monoclonal	1:200
MSH2	2017S	Cell signaling	Rabbit	Monoclonal	1:200
Secondary	**Cat. No.**	**Source**	**Host**	**Reactivity**	**Dilution**
Anti-mouse IgG (H+L)	A11029	Life Technologies	Goat	Mouse	1:500
Anti-rabbit IgG (H+L)	A11034	Life Technologies	Goat	Rabbit	1:500

Chapter 3.0 Quantitative analysis of the expression of germline genes employing in cancer stratification

3.1 Introduction

Identification of new candidate biomarkers is a major challenge for the development of cancer diagnoses and prognoses technologies (Feichtinger *et al*., 2012). The CTA/germline class of genes is normally expressed exclusively in the adult testis (see Section 1.7). However, the expression of these genes has been observed widely in various types of cancers (Simpson *et al*., 2005: Whitehurst, 2014) (see Section 1.7). Meiosis is a type of cell division that is key to exchanging and re-arranging genetic material. The function of some of germline genes has been revealed to contribute to and maintain germline-specific processes including spermatogenesis. Additionally, meiotic cell division drives reductional chromosome segregation and activation of these genes in somatic cells may affect genomic stability and promote tumourigenesis (McFarlane *et al*., 2015; Nielsen and Gjerstorff, 2016). Studies have associated the expression of some CTA genes and their activity in tumours with poor prognoses; however, the functional role of these genes and their correlation with cancer is poorly understood (for example, Rousseaux *et al*., 2013; Rosa *et al*., 2012). Meiosis-specific genes are a large group of genes considered to be a rich source of CTA genes (see Section 1.7). The blood-testis barrier provides an immunological feature which protects the CTAs produced in normal cells by eliciting an immune response generated by the human immune system; however, when these proteins are produced in cancer cells they are not recognised by the immune system (Cheng and Mruk, 2012; Whitehurst, 2014). Due to this unique feature, CTAs are promising targets that can be applied clinically, including their use as cancer biomarkers, in the development of vaccines, and as immunotherapeutic targets (Fratta *et al*., 2011; Whitehurst, 2014).

In this study, different approaches were applied for discovering new cancer testis CTA gene biomarkers. Based on silencing of these genes in normal somatic tissues, many CTA genes have been targeted for identification as biomarkers using different methods. Recently, a large group of genes was identified, the expression of which can potentially serve as prognostic markers in cancer. Briefly, Rousseaux and co-worker (2013) have applied an *in silico* approach to identify

CTA genes that can be used in patient stratification. They identified 439 testis/germline-restricted and 67 placenta-restricted tissue-specific genes 506 genes in total. Subsequently, from the transcriptomic data, a total of 1,776 solid human cancers isolated from 14 various types of cancer were characterized in which many of these 506 genes were expressed aberrantly in all types of selected tumours, including genes that were promising sources of cancer biomarkers. Expression of these genes were subjected to further investigation by microarray and qRT-PCR analyses to determine the possibility of applying them as lung cancer biomarkers, because they are testis- and placenta-specific (TS/PS). They examined a number of patients (293) who had aggressive lung cancer in addition to a group of patients (152) who indicated early-stage cancer. Activation of the TS/PS genes was observed in all 293 patients having all grades of lung cancer as well as in the 152 patients exhibiting low grades of cancer. These genes are not expressed or are rarely expressed in non-tumourous lung (NL) tissues. Consequently, 26 TS/PS genes were identified and their aberrant activation was correlated with aggressive types of lung cancers. Patients with lung cancer were divided into three groups: group P1 (in which none of the 26 genes were detected), group P2 (in which 1 or 2 of the 26 genes were expressed in the tumours), and group P3 (in which 3 or more of the 26 genes were expressed in the tumour) (Figure 3.1) (Rousseaux *et al*., 2013). They then carried out Kaplan-Meier survival analysis on each group, finding that the P1 profile was associated with good prognoses, the P3 profile with poor metastasis-prone outcomes, and the P2 profile had an intermediate profile.

The aims of this current study was to re-validate these 26 genes as potential candidates by using qRT-PCR and to confirm whether they can be applied as biomarkers for lung and ovarian cancers.
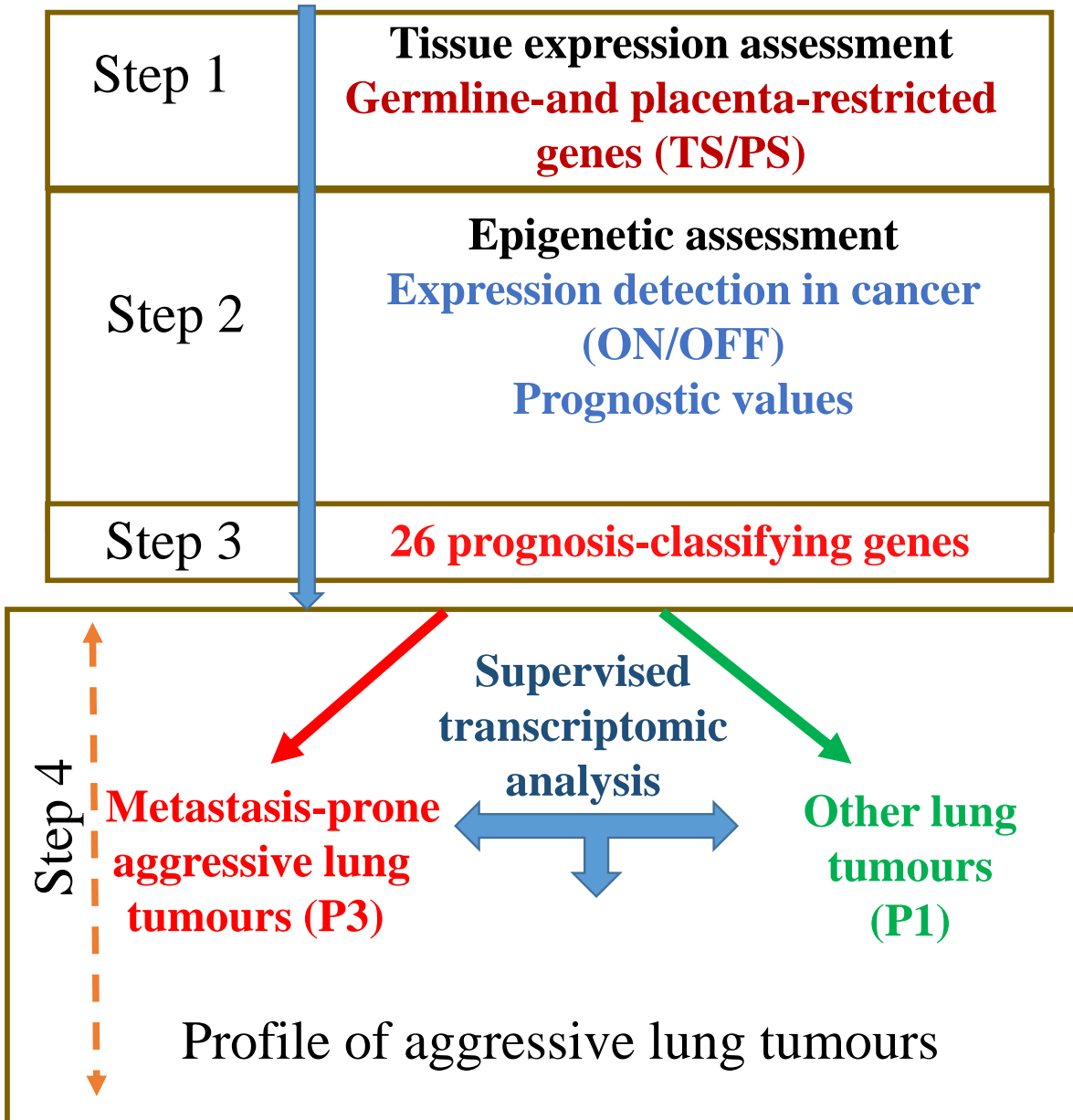
Figure 3.1. Steps used to identify expression of specific genes in aggressive lung tumours. Adapted from (Rousseaux *et al.*, 2013).

3.2 Results

3.2.1 Validation of a group of CTA genes as a potential CT antigens in lung tumours and ovarian cancer

26 TS/PS genes were identified, and the aberrant activation of these genes was correlated with lung cancer incidence, and they were investigated as potential lung cancer biomarkers (Rousseaux *et al*., 2013); these genes are listed in Table 3.1. Here, qRT-PCR with SYBR green detection was used to analyse the expression of these 26 genes in total RNA from normal and cancerous human adult lung and ovarian tissues, using RNA from testicular tissues as a positive control. The normal RNA tissue samples were purchased from Amsbio, Ambion, and Origene, whereas the cancer samples were purchased from Origene. RNA was used for the synthesis of cDNA, and RT-PCR was used to assess the quality of cDNA with the expression of the *ACTB* gene serving as a positive control for the cDNA (Figure 3.2). Sequences of the qRT-PCR primer designed for the 26 genes used in this study was selected from Rousseaux *et al*. (2013). In addition to investigating the expression of these genes in normal and cancerous lung tissues, qRT-PCR was used to screen the expression of these genes in different normal and cancerous ovarian tissues. Based on the qRT-PCR analyses, some of the 26 genes were identified that displayed expression in normal tissues which is in contrast to the findings of Rousseaux *et al*. (2013), although a number of the genes tested were validated. However, before the genes expressed in normal tissue were excluded as CT gene candidates, further investigation was performed using RT-PCR to screen for their expression profiles in a range of normal tissues (n = 21), then, the PCR products of these genes were sequenced to ensure identification of the correct expression of these genes in normal tissues (see below).
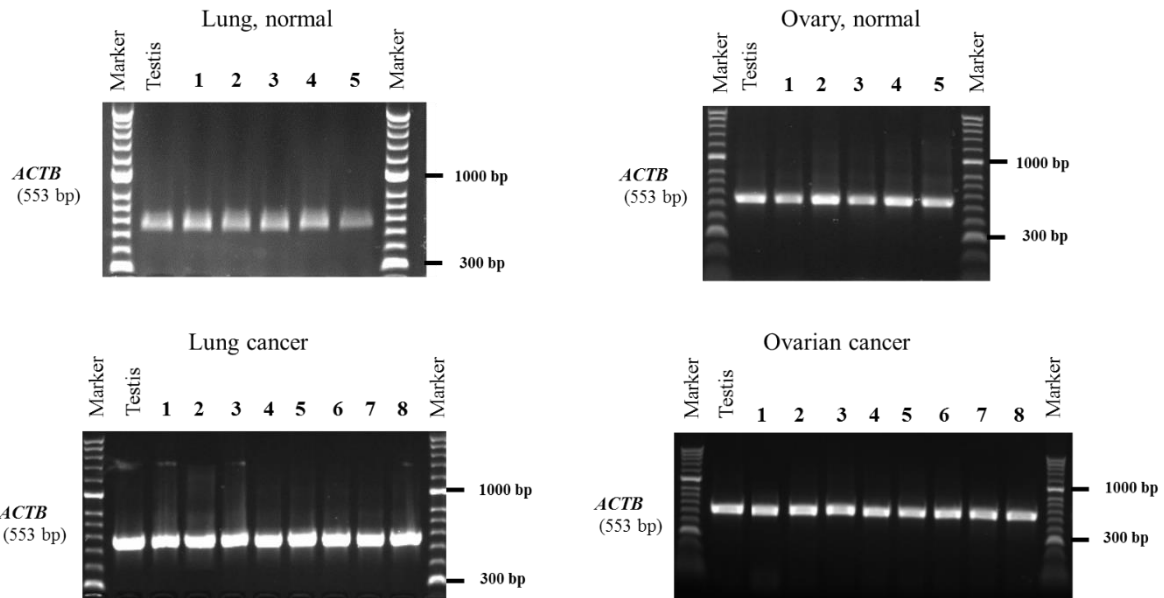
Figure 3.2. RT-PCR analysis of the *ACTB* gene in normal and cancerous human tissues.
Agarose gels showing the expression profile of *ACTB* as a positive control for cDNA samples generated from normal lung and ovarian tissues, and cancerous lung and ovarian tissues. The expected size of the PCR products of *ACTB* on agarose gel is 553 bp. The RNA analyses of normal lung and ovarian tissues (n = 5) and cancerous lung and ovarian tissues (n = 8) are depicted. Lane numbers indicate independent samples.

3.2.1.1 Analysis of the expression profiles of selected genes in normal lung tissues

The qRT-PCR procedure was performed to analyse the expression of 26 genes (Table3.1).

Table 3.1 Expression profiles of 26 genes in normal and cancerous tissues determined by qRT-PCR analysis.

1- *PIWIL1*	**10-** *BTG4*	**19-** *LGALS14*
2- *ROPN1*	**11-** *TKTL2*	**20-** *EBI3*
3- *TUBA3C*	**12-** *TPTE2P2*	**21-** *HIST1H3C*
4- *DPEP3*	**13-** *CCDC83*	**22-** *C12orf37*
5- *VCY*	**14-** *LOC441601*	**23-** *NBPF4*
6- *CPA5*	**15-** *RFX4*	**24-** *KIAA1257*
7- *MAGEB6*	**16-** *FLJ43944*	**25-** *ISM2*
8- *RBM46*	**17-** *OR7E156P*	**26-** *C10orf82*
9- *TPTE*	**18-** *Hs.601545*	

Five different normal lung tissues and one testicular tissue, were examined to validate whether these genes might be good CT gene candidates (Figure 3.3). *GAPDH* and *TUBA1C* were the RT-qPCR control genes. The no template controls (NTC) and no RT were used with each experiment; their analyses exhibited no amplification, which indicated no contamination with genomic DNA.

The qRT-PCR analyses primarily revealed high expression levels in testicular tissues for most genes and no expression in normal lung tissues for selected genes (Figure 3.3 A–F). *PIWIL1*, *ROPN1*, and *TUBA3C* (Figure 3.3 A), *DPEP3*, *VCY*, and *CPA5* (Figure 3.3 B), *MAGEB6*, *RBM46*, and *TPTE* (Figure 3.3 C), *TKTL2* and *TPTE2P2* (Figure 3.3 D), *CCDC83*, *LOC441601,* and *RFX4* (Figure 3.3 E), and *FLJ43944* and *OR7E156P* (Figure 3.3 F) were highly expressed in testicular tissue, but exhibited no measurable expression in normal lung tissues. The *BTG4* gene was dismissed as a CT gene because it's expression profile was detected at low levels in normal lung tissues (Figure 3.3 D). The expression of the genes shown in (Figure 3.3 A–F) were further analysed using different lung cancer tissues (see Section 3.2.1.2).

 Figure 3.3 G–I depicts other genes of the original 26 that displayed expression in normal lung samples as well as testicular tissues. Some of these genes showed significantly higher expression in normal lung tissues compared to testicular tissue. The expression profile of *Hs.601545* was significantly lower in testicular tissue compared to the expression of this gene in normal lung tissues, and the expression of *LGALS14* was greater in lung tissue sample 1 than in testicular tissue

(Figure 3.3 G). Another gene, *EBI3*, was detectably expressed in all normal lung tissues at very high levels, particularly in normal lung tissue samples 1, 4, and 5 compared to testicular tissue (Figure 3.3 G). Also, *HIST1H3C*, *C12orf37*, and *NBPF4* (Figure 3.3 H) exhibited expression profiles in normal lung tissues, such as the expression of *HIST1H3C* in lung tissue samples 3 and 4 compared with the level of expression for *C12orf37* in lung tissue samples 3 and 4. *KIAA1257*, *ISM2*, and *C10orf82* (Figure 3.3 I) were also expressed in testicular tissues as well as in normal lung tissue samples. Because 10 of the 26 genes were expressed in normal lung tissue samples, they were dismissed as bona fide CT gene and were not subjected to screening against human lung cancer tissues.

Standard RT-PCR primers were designed for the 10 genes identified as having expression in healthy lung tissue (*BTG4*, *Hs.601545*, *LGALS14*, *EBI3*, *HIST1H3C*, *C12orf37*, *NBPF4*, *KIAA1257*, *ISM2*, and *C10orf82*) and RT-PCR was performed for additional investigation of the expression of these genes in a panel of 21 normal tissues, including lung and testicular tissues. This analysis demonstrated that these genes were expressed in an extensive range of normal tissues (Figure 3.4). A selection of RT-PCR products were DNA-sequenced, and all bands matched the expressed gene (Table 3.2).
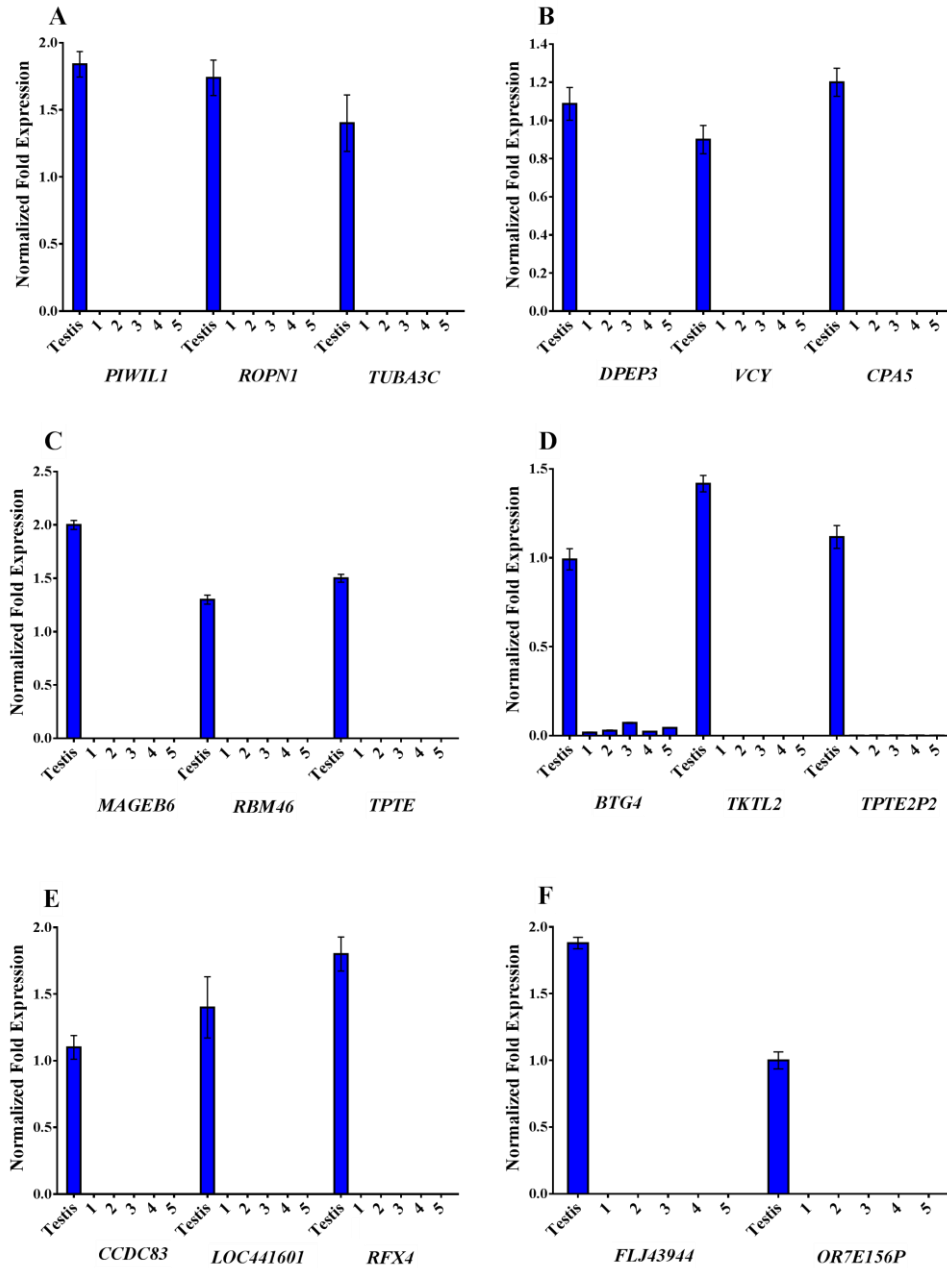
Figure 3.3. Real-time quantitative RT-PCR analyses of the expression levels of selected genes in normal human lung tissues.
cDNA was generated from normal human total RNA prepared from testicular and five lung tissues. Results were normalized by using two endogenous reference genes (*GAPDH* and *TUBA1C*) and the relative fold-change was computed by the ΔΔCt method. Error bars represent the standard error of the mean for triplicate replications. Bar charts illustrate the expression of different genes in testicular and five normal lung tissues as follows: (A) *PIWIL1*, *ROPN1,* and *TUBA3C*; (B) *DPEP3*, *VCY,* and *CPA5*; (C) *MAGEB6*, *RBM46,* and *TPTE*; (D) *BTG4*, *TKTL2,* and *TPTE2P2;* (E) *CCDC83*, *LOC441601,* and *RFX4* (F) *FLJ43944* and *OR7E156P*.
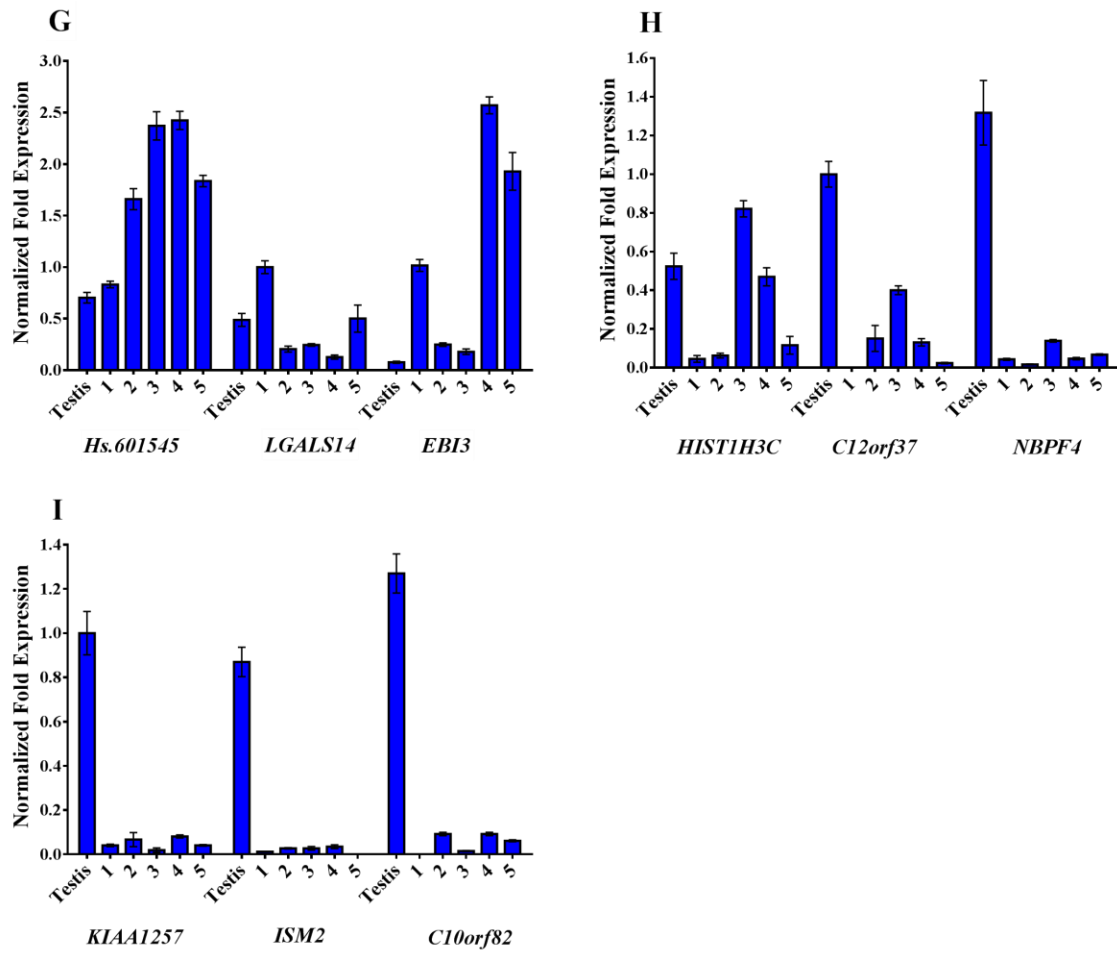
Figure 3.3 (continue**d).**
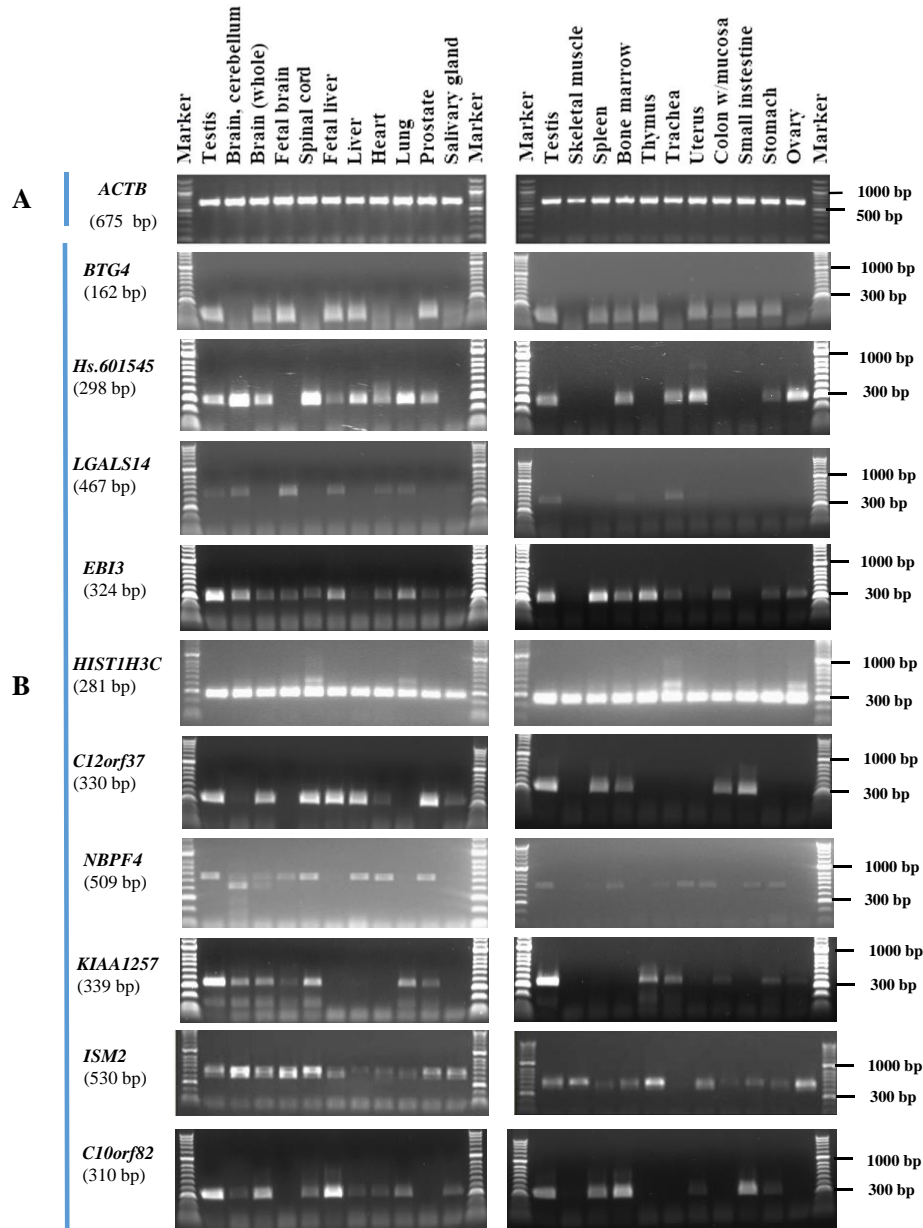
Figure 3.4 RT-PCR analyses of the expression of dismissed genes in a range of normal human tissues.
Agarose gels showing the expression profiles of 10 genes in 21 normal human tissues. The total RNA from different tissues was isolated and used to generate cDNA samples. (A) *ACTB* expression served as a positive control for the normal tissue samples. (B) Expression profiles of dismissed genes exhibited in normal tissues. The numbers in parentheses indicate the expected size of each gene.

Table 3.2 Summary of the DNA sequencing results of dismissed genes using RT-PCR to validate expression of these genes in a range of normal tissues.

Gene Name	Primer	Sequenced in normal tissues	Sequencing Identity %
BTG4	Forward	Testis Prostate	99% 99%
Hs.601545	Forward	Testis Brain, cerebellum	100% 99%
LGALS14	Forward	Testis Brain, cerebellum	100% 99%
EBI	Forward	Testis Brain, cerebellum	100% 99 %
HIST1H3C	Forward	Testis Fetal brain	100% 99%
C12orf37	Forward	Testis prostate	100% 99%
NBPF4	Forward	Testis Spinal cord	100% 99%
KIAA1257	Forward	Testis Lung	100% 100%
ISM2	Forward	Testis Spinal cord	100% 99%
C10orf82	Forward	Testis Fetal liver	100% 99%

3.2.1.2 Analyses of the expression profiles of candidate genes in lung cancer tissues

Based on qRT-PCR analysis of the expression of 26 genes in normal lung and testicular tissues (see Section 3.2.1.1), 16 genes out of 26 were observed to exhibit high levels of expression in testicular tissue with no detectable expression in other normal tissues. The candidate genes are: *PIWIL1*, *ROPN1*, *TUBA3C*, *DPEP3*, *VCY*, *CPA5*, *MAGEB6*, *RBM46*, *TPTE*, *OR7E156P*, *TKTL2*, *TPTE2P2*, *CCDC83*, *LOC441601*, *RFX4*, and *FLJ43944*. cDNA was synthesized from the RNA of eight human lung cancer samples, which were obtained from Origene. The *ACTB* gene was used to assess the quality of the cDNA (Figure 3.2). All cancer samples were collected from patients with metastatic disease (Table 2.3). The two endogenous control genes used in expression analysis were *GAPDH* and *TUBA1C*.

Figure 3.5 shows the expression of these genes in testicular tissues compared to lung cancer samples. *PIWIL1* (Figure 3.5 A) showed no expression in lung cancer samples 4, 6, 7, and 8 (lung adenocarcinoma) or in sample 5 (squamous cell carcinoma), whereas *PIWIL1* was detected in lung cancer sample 1 (bronchioloalveolar adenocarcinoma), lung cancer sample 2 (squamous cell carcinoma), and lung cancer sample 3 (lung adenocarcinoma). Expression of *ROPN1* (Figure 3.5 A) was observed in six lung cancer samples. *TUBA3C* (Figure 3.5A) was expressed in five lung cancer samples. *DPEP3* was detectable in two lung cancer samples, and *VCY* was expressed in most of the lung cancer tissues (Figure 3.5 B). *CPA5* (Figure 3.5 B) showed no detectable levels of expression in lung cancer tissues. *MAGEB6* (Figure 3.5 C) was expressed in some of the lung cancer samples. *RBM46* (Figure 3.5 C) exhibited detectable expression in all lung cancer tissues except lung cancer sample 8. The expression of *TPTE* was detectable in lung cancer samples 1, 2, and 6 but the expression of *TPTE* was undetectable in other lung cancer samples (Figure 3.5 C). *OR7E156P* was expressed in one lung cancer sample, and expression of *TKTL2* and *TPTE2P2* was exhibited in three lung cancer samples although the expression of these three genes in other lung cancer samples was undetectable (Figure 3.5 D). *CCDC83* (Figure 3.5 E) was expressed only in one lung cancer sample. In other cancer samples, *CCDC83* exhibited no detectable expression. *LOC441601* and *RFX4* were each expressed in four lung cancer samples (Figure 3.5 E); *LOC441601* was expressed in lung cancer samples 3, 6, 7, and 8, whereas *RFX4* was observed to have expression in lung cancer samples 1, 2, 6, and 7. *FLJ43944* exhibited detectable expression in all eight lung cancer samples (Figure 3.5 E).
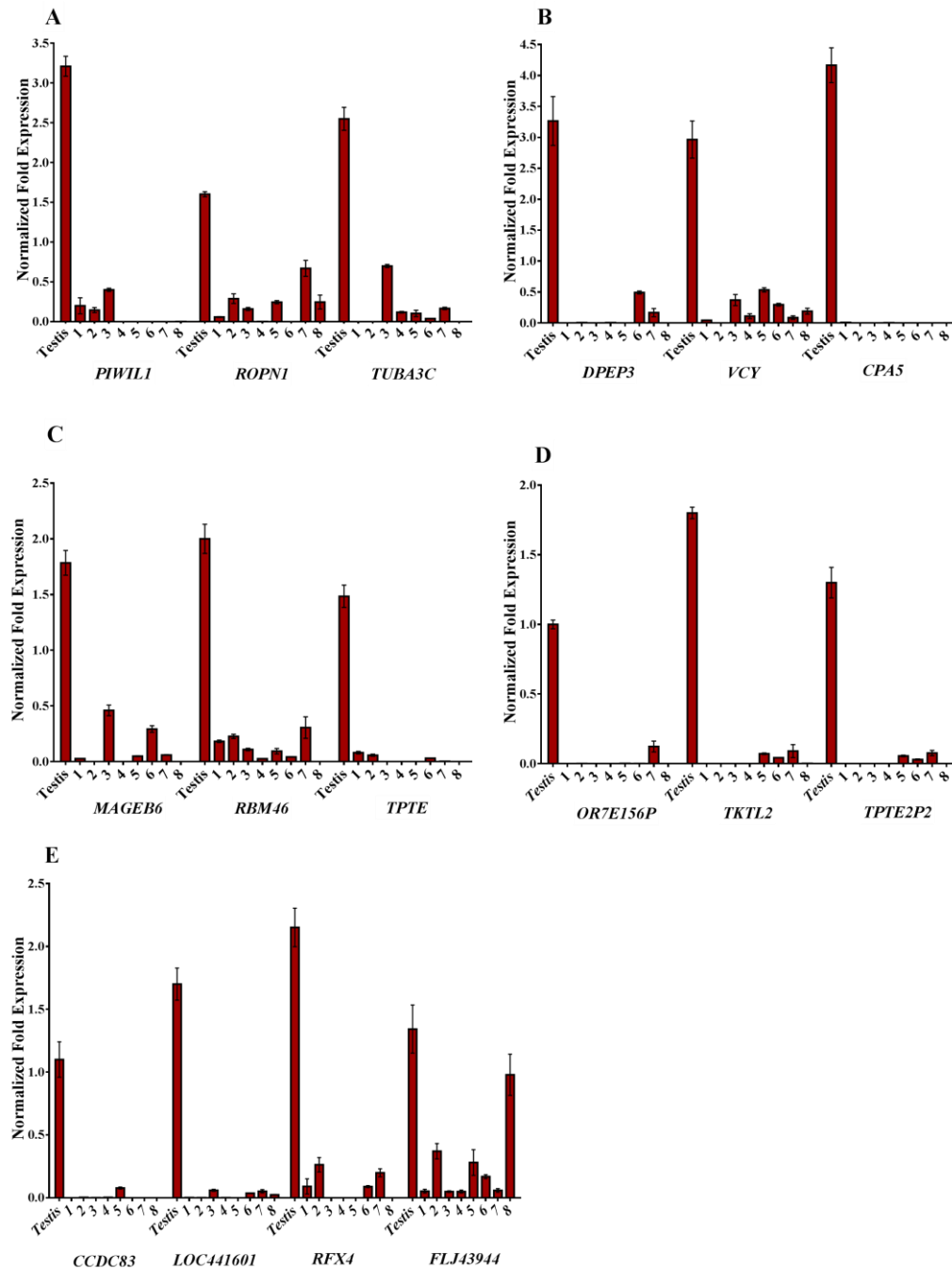
Figure 3.5 qRT-PCR analyses of the expression levels of genes in lung cancer and normal testicular tissue.
cDNA was generated from human total RNA prepared from normal testicular tissue and different lung cancer tumours from different patients: (1) bronchioloalveolar adenocarcinoma; (2) and (5) squamous cell carcinoma; and (3), (4), (6), (7), and (8) lung adenocarcinoma. Data were normalized by using two endogenous reference genes (*GAPDH* and *TUBA1C*). The relative fold-change was computed by using the ΔΔCt method. The error bars represent the standard error of the mean for three replications. Bar charts illustrate the expression of different genes in normal testicular tissue and eight lung cancer samples.

3.2.1.3 Analyses of the expression profiles of the 26 genes in normal ovarian tissues

The expression profiles of the 26 genes were validated by qRT-PCR analyses of RNA extracted from five normal human ovarian tissues. The quality of cDNA was assessed relative to the *ACTB* gene and compared to the accepted size in each tissue (Figure 3.2). Two genes, *GAPDH* and *TUBA1C*, were used as qRT-PCR controls. The qRT-PCR screening of normal ovarian tissues was compared to testicular tissue. *PIWIL1*, *ROPN1,* and *TUBA3C* (Figure 3.6 A), *DPEP3*, *VCY*, and *CPA5* (Figure 3.6 B), *MAGEB6*, *RBM46*, and *TPTE* (Figure 3.6 C), *TKTL2* and *TPTE2P2* (Figure 3.6 D), *CCDC83*, *LOC441601,* and *RFX4* (Figure 3.6 E), and *FLJ43944* and *OR7E156P* (Figure 3.6 F) were highly expressed in testicular tissue, but exhibited no measurable expression in normal ovarian tissues. However, the screening of *BTG4* revealed that it was expressed in all the normal ovarian tissues as well as in the testicular tissue (Figure 3.6 D). Therefore, *BTG4* was excluded from further investigation.

The expression patterns of nine other genes, *Hs.601545*, *LGALS14*, *EBI3*, *HIST1H3C*, *C12orf37*, *NBPF4*, *KIAA1257*, *ISM2*, and *C10orf82,* in different normal ovarian and testicular tissues are shown in Figure 3.6 G–I. Interestingly, investigation of these genes revealed that *Hs.601545* and *EBI3* (Figure 3.6 G) were more highly expressed in most normal ovarian tissues compared to the testicular tissue. Six of these genes, *Hs.601545*, *EBI3*, *HIST1H3C*, *C12orf37*, *NBPF4*, and *ISM2,* were expressed in all five ovarian tissues tested, whereas each of the three genes, *LGALS14*, *KIAA1257*, and *C10orf82,*were expressed in ovarian tissue samples 1–4 but were not expressed in ovarian tissue sample 5. The expression profile of *Hs.601545* was highly expressed in most of the normal ovarian tissue samples. Validation of the expression of *LGALS14* was determined to be expressed at higher levels than in the testicular tissue by the normal ovarian tissue sample 3, or at detectable levels of expression for normal ovarian samples 1, 2, and 4 (Figure 3.6 G). *EBI3* was most highly expressed in ovarian tissue samples 2 and 3. *HIST1H3C* was more highly expressed in normal ovarian tissue samples 2 and 3, *C12orf37* in normal ovarian tissue samples 1, 2, and 3, and *NBPF4* in normal ovarian tissue sample 3 (Figure 3.6 H). *KIAA1257* and *C10orf82* were more highly expressed in normal ovarian tissue samples 2 and 3, whereas the expression profile of *ISM2* was more highly expressed in the normal ovarian tissues samples 3 and 4 (Figure 3.6 I).

Based on Figure 3.6 G–I, 10 genes that were expressed in normal ovarian tissues (*BTG4*, *Hs.601545*, *LGALS14*, *EBI3*, *HIST1H3C*, *C12orf37*, *NBPF4*, *KIAA1257*, *ISM2,* and *C10orf82*)

were dismissed as candidates. No detectable expression was observed for 16 genes in normal ovarian tissues (Figure 3.6). These were the same 16 genes that exhibited no expression in normal lung tissues. Consequently, further investigation of these genes was performed by qRT-PCR with various types of ovarian cancer tissues (Section 3.2.1.4).
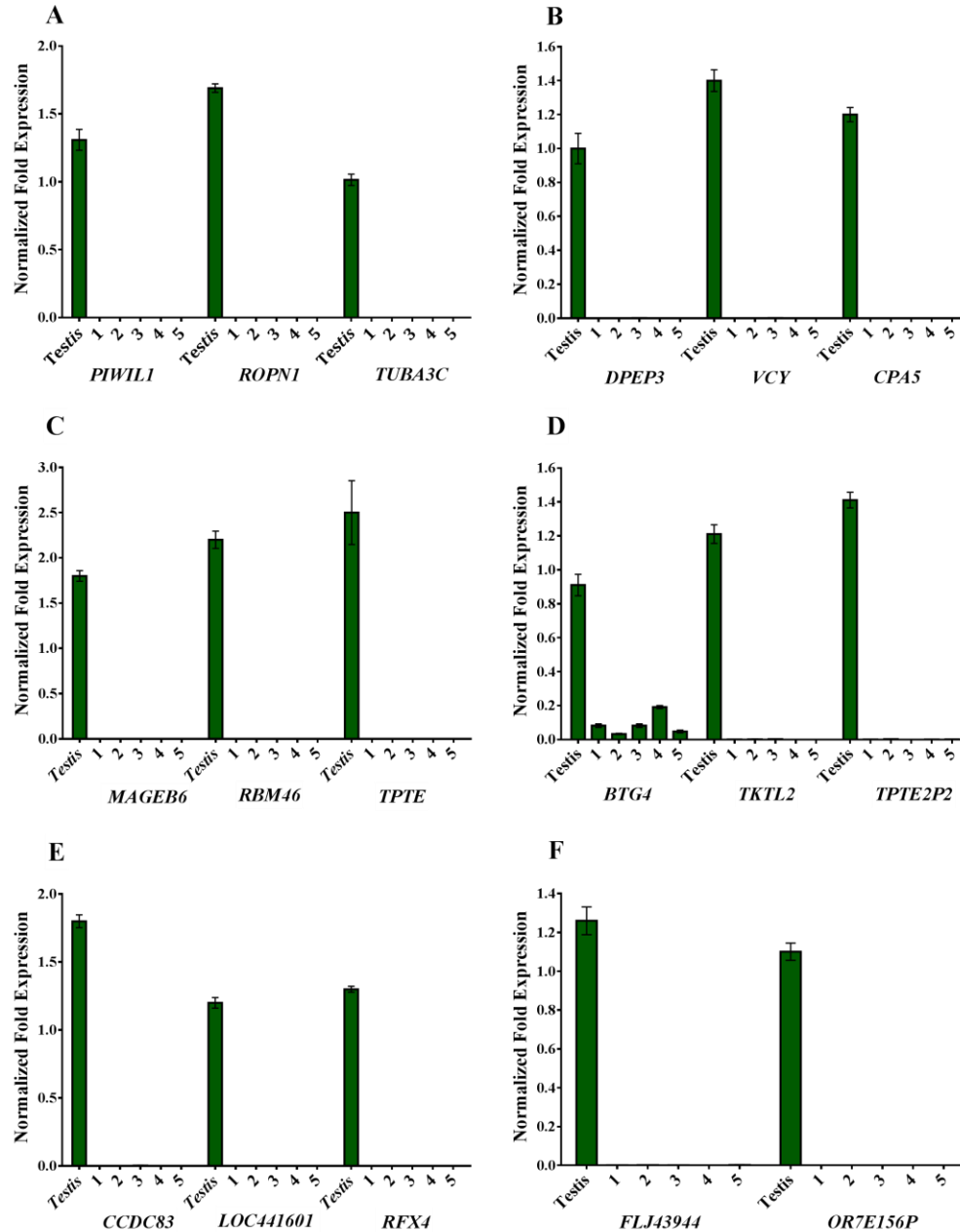
Figure 3.6 qRT-PCR analyses of the expression levels of genes in normal human ovarian tissues.
cDNA was generated from normal human total RNA prepared from testicular tissue and five ovarian tissues. Results were normalized by using two endogenous reference genes (*GAPDH* and *TUBA1C*) and the relative fold-change was computed by the ΔΔCt method. Error bars represent the standard error of the mean for triplicate replications. Bar charts illustrate the expression of different genes in normal testicular and five normal ovarian tissues as follows: (A) *PIWIL1*, *ROPN1,* and *TUBA3C*; (B) *DPEP3*, *VCY,* and *CPA5*; (C) *MAGEB6*, *RBM46,* and *TPTE*; (D) *BTG4*, *TKTL2,* and *TPTE2P2*; (E) *CCDC83*, *LOC441601,* and *RFX4*; and (F) *FLJ43944* and *OR7E156P*.

G

H

I
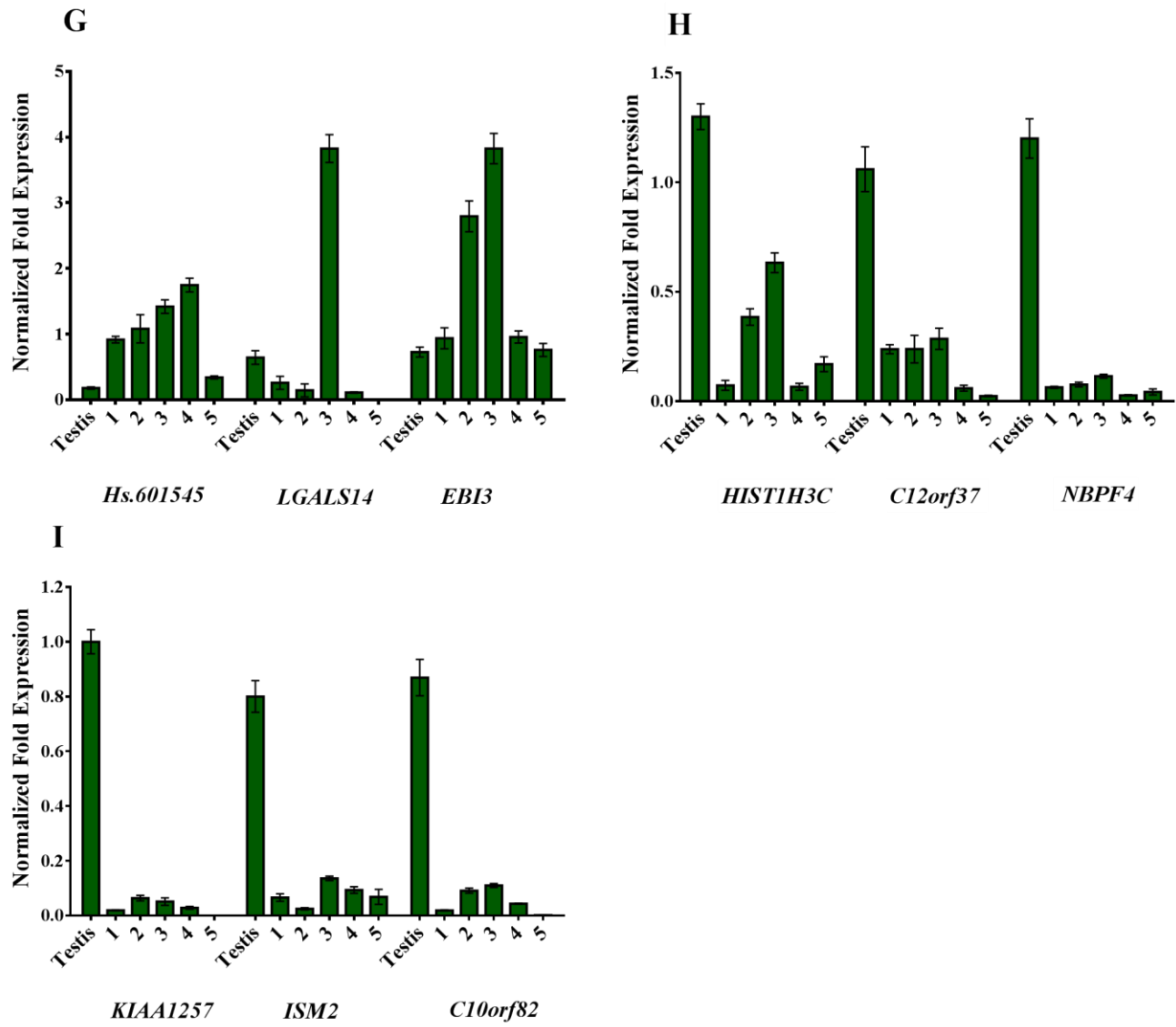
Figure 3.6 (continue**d).**

3.2.1.4 Analyses of the expression profiles of candidate genes in ovarian cancer tissues

Of the 26 genes investigated, 16 genes were considered good candidates (Figure 3.6). The expression of these genes was investigated with 8 ovarian cancer tissues using qRT-PCR. RNA from various human types of ovarian cancer was obtained from patients with metastases (Origene; for more detail see Table 2.3). cDNA was generated; subsequently, the *ACTB* gene was used as a positive control to compare with ovarian cancer cDNA (see Figure 3.2). *GAPDH* and *TUBA1C* served as controls genes for qRT-PCR.

The expression of these candidate CT genes in ovarian cancer and normal testicular tissues presented various levels of expression, with higher levels demonstrated in normal testicular tissue than in ovarian cancer tissues (Figure 3.7). *PIWIL1*, *ROPN1,* and *TUBA3C* were highly expressed in testicular tissue. *PIWIL1* expression was detected in most ovarian cancer samples except for ovarian cancer sample 3 (ovarian adenocarcinoma). For example, *PIWIL1* was observed with detectable expression in ovarian cancer sample 1 (ovarian serous papillary adenocarcinoma [OSPA]), ovarian cancer sample 2 (ovarian adenocarcinoma), ovarian cancer sample 4 (ovarian clear cell adenocarcinoma [OCCA]), ovarian cancer sample 5, ovarian cancer sample 6 (OSPA), ovarian cancer sample 7 (ovarian adenocarcinoma), and ovarian cancer sample 8 (OSPA) (Figure 3.7A). The expression of *ROPN1* and *TUBA3C* were also detected, such as the expression of *ROPN1* in ovarian cancer samples 4. *TUBA3C* was also expressed in five ovarian cancer tissues with detected expression (Figure 3.7A). *DPEP3*, *VCY,* and *CPA5* were expressed in various types of ovarian cancer tissues demonstrating high expression such as the expression of *DPEP3* in ovarian cancer samples 2 and 4 (Figure 3.7 B). *VCY* and *CPA5* were also expressed in ovarian cancer tissues. *VCY* was expressed in all ovarian cancer samples except sample 8. *CPA5* was expressed in two ovarian cancer samples with undetectable expression of *CPA5* in other ovarian cancer samples (Figure 3.7 B). The expression of other genes such as *MAGEB6*, *RBM46*, and *TPTE* were also observed in some ovarian cancer tissues (Figure 3.7 C). *OR7E156P*, *TKTL2,* and *TPTE2P2* were each expressed in at least two of the types of ovarian cancer tested. *OR7E156P* was expressed in two samples but demonstrated no expression in the other cancer samples. The expression of *TKTL2* and *TPTE2P2* each demonstrated detectable expression in four ovarian cancer types (Figure 3.7 D). Groups of genes including *CCDC83*, *LOC441601*, *RFX4,* and *FLJ43944* were also expressed highly in normal testicular tissue and in selected cancer samples.

FLJ43944 was expressed in all ovarian cancer samples, whereas *CCDC83* was expressed only in ovarian cancer sample 5, but it exhibited an undetectable expression in other ovarian cancer samples. *RFX4* and *LOC441601* each exhibited expression in four ovarian cancer samples (Figure 3.7 E).
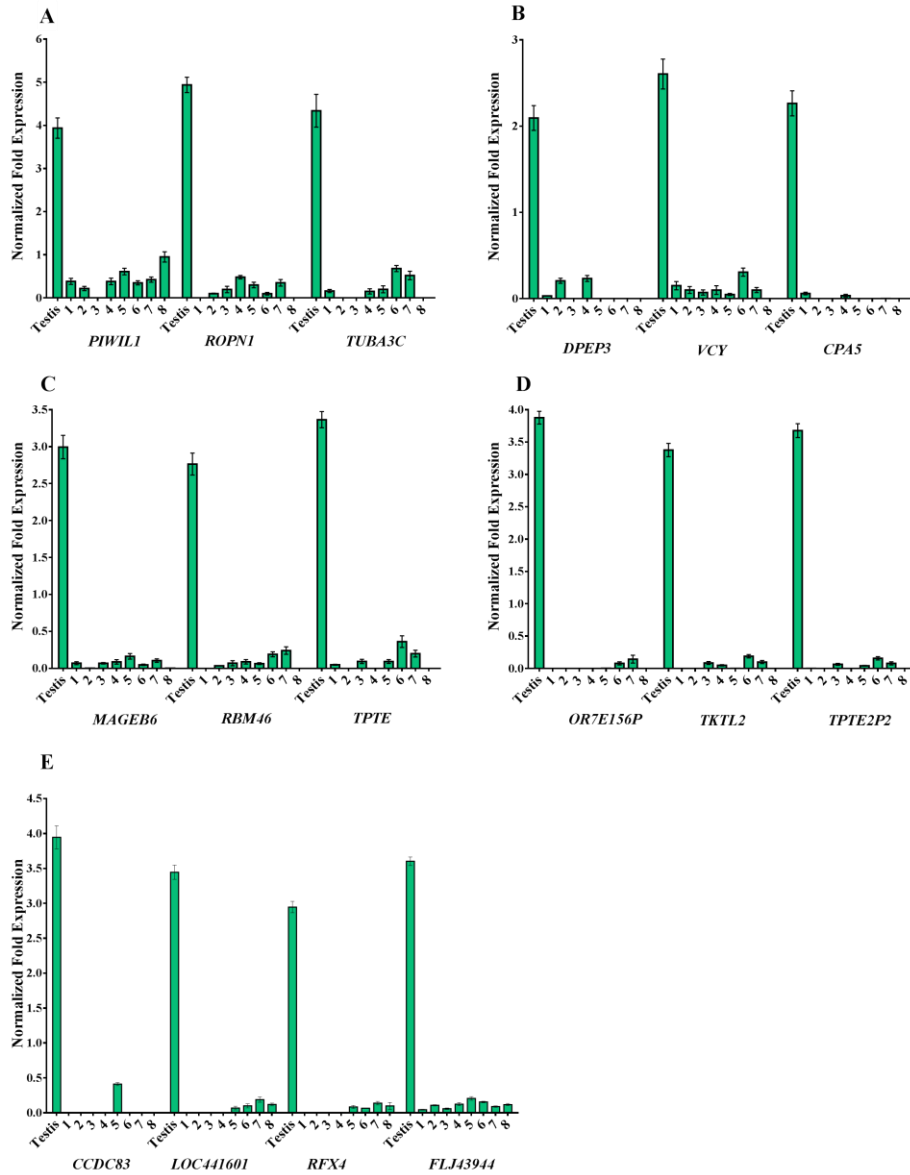
Figure 3.7 qRT-PCR analyses of the expression levels of genes in ovarian tumours and normal testicular tissues.
RNA was isolated from human total RNA prepared from normal testicular tissue and various ovarian cancer tumours: (1), (5), (6), and (8) ovarian serous papillary adenocarcinoma (OSPA); (2), (3), and (7) ovarian adenocarcinoma; and (4) ovarian clear cell adenocarcinoma (OCCA). Results were normalized using two endogenous reference genes (*GAPDH* and *TUBA1C*) the relative fold-change was computed by using the ΔΔCt method. The error bars represent the standard error of the mean for three replications. Bar charts showing the expression of different genes in normal testicular tissue and eight ovarian cancer samples.

3.3 Discussion

Metastasis is responsible for the death of approximately 90% of patients with solid tumours. To date, the mechanism of metastasis is insufficiently understood. The metastasised cells have specific features that allow them to disseminate from the original affected site to other organs in the human body (McGuire *et al*., 2015; Gupta and Massagué, 2006; Chanvorachote *et al*., 2016). Cancer is often diagnosed and treated when the cancer cells begin to metastasise (Aly, 2012; Suri, 2006). Tumour-associated antigens (TAAs) are proteins produced by mutations and alterations that occur in gene expression profiles (see Section 1.5). The identification and characterisation of TAAs that serve as cancer biomarkers and/or targets are key challenges in the development of immunotherapeutic strategies that target tumours (Krishnadas *et al*., 2013). Among various types of tumour antigens, the CTAs provide the most promising targets for human cancer therapies due to the specific unique feature by which their genes expression is restricted to normal testicular tissues and to cancer cells (Greve *et al*., 2014; Chen *et al*., 2009).

Rousseaux and co-workers (2013) have identified and reported 26 CT/ germline genes that could potentially serve as lung cancer biomarkers. *In silico* tools were used, including EST and the Transcriptomic database to identify these TS/PS genes. Further microarray and qRT-PCR analyses were applied to investigate these 26 genes as potential biomarkers in lung cancer. These genes were screened in 293 lung samples from patients presenting different stages of cancer (Rousseaux *et al*., 2013) (see Section 3.1 for more details).

In this study, qRT-PCR analyses were used to validate the expression profile of these 26 genes in normal and cancerous lung tissues and compared with normal testicular tissues. Additionally, these genes were validated with normal and cancerous ovarian tissues, to explore their potential as biomarkers for ovarian cancer. Based on the same qRT-PCR primer sequencing as used the previous study (Rousseaux *et al*., 2013), 10 of the 26 genes were determined to display an expression profile in normal lung and ovarian tissues. The expression of these genes 10 genes was detected using Ct value threshold of 38 determined by negative control (see summary grid in Figure 3.8 C and 3.9 C). RT-PCR intron-spanning primers were designed for each of these 10 genes, and further validation for these 10 genes was conducted by RT-PCR in 21 normal tissues.

RT-PCR analyses revealed the existence of expression profiles for 10 genes in multiple types of normal tissues. Thus, these 10 genes (*BTG4*, *Hs.601545*, *LGALS14*, *EBI3*, *HIST1H3C*, *C12orf37*, *NBPF4*, *KIAA1257*, *ISM2,* and *C10orf82*) may not be considered as CT genes. Based on this current analysis some of these genes, such as the histone cluster 1 H3 family member C gene (*HIST1H3C*), exhibit expression in all normal tissues, or others, such as the Epstein-Barr virus induced 3 gene (*EBI3*) and the isthmin 2 gene (*ISM2*), were expressed in most normal tissues. Additionally, 7 of these 10 genes *BTG4*, *Hs.601545*, *LGALS14*, *C12orf37*, *NBPF4*, *KIAA1257*, and *C10orf82* that exhibited their expression in different types of normal tissues were screened by RT-PCR (Figure 3.4). DNA sequencing confirmed the cDNA of these 10 specific genes (see sequencing summary Table 3.2). Consequently, these 10 genes were dismissed as poor candidates for CT genes. Expression of these 10 genes was reported to be testis- and placenta-specific; Rousseaux *et al*. (2013) used qRT-PCR analyses to identify the expression of these genes. The reason for this distinct inter study difference is unclear, but it might simply be the case that our current study was more stringent in setting a threshold for negative expression in normal tissue.

However, another study demonstrated *EBI3* as a potential biomarker in lung cancer due to its expression in lung cancer but not in normal tissue (Nishino *et al*., 2011). Northern blot analysis was used to evaluate the expression of *EBI3* in 16 normal human tissues—heart, brain, placenta, lung, liver, skeletal muscle, kidney, pancreas, spleen, thymus, prostate, testis, ovary, colon, leukocyte, and small intestine—and this method indicated it appeared to only be expressed in the placenta. At the protein level, *EBI3* was not observed in normal tissues, such as the kidney, liver, heart and lung (Nishino *et al*., 2011). In addition, RT-PCR was used to analyse the expression of *EBI3* in normal cell lines such as HEK-293 and normal bronchial epithelial cells (Beas-2B), and the expression of *EBI3* was not detected (Long *et al*., 2013). In our results, *EBI3* was determined to be expressed in five normal lung and ovarian tissues by using qRT-PCR (see summary grid in Figure 3.8 C and 3.9 C), and in 17 normal tissues using RT-PCR and sequencing results combined that confirmed the identities of the genes (Figure 3.4).

In this study, *HIST1H3C* was determined to be expressed in five normal lung and ovarian tissues by using qRT-PCR; also, the expression profile of *HIST1H3C* was detected by RT-PCR with strong bands in 21 normal human tissues, such as liver, skeletal muscle, lung, kidney, thymus, prostate, and spleen. Therefore, *HIST1H3C* was excluded from further analysis in cancerous

tissues and was not considered to be a CT gene candidate. However, *HIST1H3C* is one of the 26 genes that were reported as promising biomarkers in lung cancer, and the aberrant activation of this gene was detected previously in lung cancer tissue using qRT-PCR (Rousseaux *et al*., 2013). *HIST1H3C,* which is member of the H3 family, plays an important role in regulating transcriptional processes; dysfunction of this process can affect the function of gene transcription causing diseases, including lung diseases (Barnes *et al*., 2005; Huang *et al*., 2003). Recently, in cases of pulmonary tuberculosis (TB), which increases the risk of lung cancer, *HIST1H3C* was found to be upregulated and can serve as biomarker in patients with TB (Qin *et al*., 2016).

B-Cell translocation Gene 4 (*BTG4*), also known as *PC3B*, belongs to the BTG family that has been characterised as cell cycle regulators (Winkler, 2010). The loss of function in *BTG4* can lead to chronic lymphocytic leukaemia (CLL) (Auer *et al*., 2005); also, *BTG4* in patients with gastric cancer may be a prognostic biomarker (Dong *et al*., 2009). In the present study, qRT-PCR was used to assess the expression of *BTG4* in normal lung and ovarian tissues, and *BTG4* was also screened in an expanded panel of 21 normal tissues by RT-PCR. qRT-PCR demonstrated that the expression of *BTG4* was detected in five normal lung and ovarian tissues (see summary grid in Figure 3.8 C and 3.9 C). Also, RT-PCR analyses exhibited the expression of *BTG4* in multiple types of normal tissues—brain (whole), fetal brain, liver, prostate, spleen, bone marrow, and stomach (see Figure 3.4). The expression of *BTG4* was richly expressed in ovarian and testicular tissues in humans and mice (Hou *et al*., 2013). By using qRT-PCR, another study determined the expression of *BTG4* as well in testicular and ovarian tissues among a small number of normal tissues tested that also included uterine, kidney, spleen, and muscle tissues (Yu *et al*., 2016).

Lectin, galactoside-binding, soluble, 14 (*LGALS14*), also known as *PPL13*, belongs to the family of multifunctional lectin genes, which is essential for cellular processes, such as immunomodulation, cell signalling, neuroprotection, and angiogenesis (Guardia *et al*., 2014). Expression of *LGALS14* was detected in placental tissue, but it was either not detected or detected at low levels in other normal tissues—brain, heart, liver, lung, skeletal muscle, kidney, and pancreas—using the northern blot technique (Yang *et al*., 2002). However, in this study, *LGALS14* was expressed in five normal lung tissues and in four normal ovarian tissues by qRT-PCR (see summary grid in Figure 3.8 C and 3.9 C). Furthermore, RT-PCR was performed to investigate the expression of *LGALS14* in 21 normal tissues and its expression was demonstrated in multiple types

of normal tissues—brain, fetal brain, fetal liver, heart, lung, and trachea—and was also faintly detected in tissues from the salivary gland and bone marrow.

qRT-PCR was performed to determine the expression of these genes in ovarian cancer and whether these genes also can be potential biomarkers in ovarian cancer. These 16 genes were screened with one normal testicular tissue and five normal ovarian tissues that derived from different sources. Thus, all these genes were detected in testicular tissue, but they were not observed in all normal ovarian tissues (see summary grid in Figure 3.9 B). Consequently, these genes were further analysed by qRT-PCR with various types of lung and ovarian cancer tissues (see summary grid in Figure 3.10 B and 3.11 B). In a previous study, qRT-PCR was performed to screen for the expression of piwi like RNA-mediated gene silencing1 (*PIWIL1*) in 20 normal human tissues, including testicular tissue, and *PIWIL1* was determined to be highly expressed in testicular tissue, but it was not expressed or barely detected in other tissues (Sugimoto *et al*., 2007). In the present study, the expression profile of *PIWIL1* was detected in testicular tissue at a high level but it was not expressed in five other normal tissues, including lung and ovarian tissues (see summary grid in Figure 3.8 B and 3.9 B). In addition, *PIWIL1* was expressed in lung cancer samples by qRT-PCR (see summary grid in Figure 3.10 B). Also, *PIWIL1* was observed in various types of ovarian cancer tissues (see summary grid in Figure 3.11 B). A recent study revealed the expression of *PIWIL1* in a group of patients with lung cancer, whereas in normal lung tissues *PIWIL1* was not expressed (Navarro *et al*., 2015). *PIWIL1* was found to be upregulated in some tumours, including cervical cancer (Liu *et al*., 2010), breast cancer (Wang *et al*., 2013), and glioma (Wang *et al*., 2014). Another study demonstrated that the expression of *PIWIL1* was significantly higher in ovarian cancer than in normal ovarian tissue by RT-PCR (Lim *et al*., 2014).The important function of the piwi family is their key role in stem cell self-renewal, controlling RNA silencing, and regulating translation (Lingel and Sattler, 2005).

TUBA3C and *DPEP3* are also known as CT genes, because they are exclusively expressed in testicular tissue but not in other somatic tissues (Djureinovic *et al*., 2016). However, in patients with lung tumours, these genes exhibited an expression profile in squamous carcinoma and adenocarcinoma tissues (Djureinovic *et al*., 2016). In this study *TUBA3C* and *DPEP3* were expressed in different types of lung and ovarian cancer tissues. Tubulin, alpha 3c (*TUBA3C*) belongs to the tubulin superfamily, which encode proteins considered to be key elements of the

microtubule components (Mikelsaar *et al*., 2012). It was expressed in various types of lung cancer, including lung cancer samples 3, 4, 5, 6, and 7. Also, *TUBA3C* was observed in different human ovarian cancer tissues, such as ovarian tissue samples 1, 4, 5, 6, and 7, in this research (see summary grid in Figure 3.10 B and 3.11 B). Dipeptidase 3 (*DPEP3*) is required for proteolysis, and it is associated with cancer metastasis (Pierce *et al*., 2008). In our results, using qRT-PCR, *DPEP3* was detected in lung and ovarian cancer tissues; *DPEP3* was expressed in lung cancer samples 6 and 7 and in ovarian cancer samples 1, 2, and 4 (see summary grid in Figure 3.10 B and 3.11 B).

The expression of melanoma-associated antigen B6 (*MAGEB6*), also included in the panel of normal tissues investigated in this research, was determined by qRT-PCR not to be expressed in these normal tissues, except in the testicular tissue. By using qRT-PCR, *MAGEB6* was screened in tumour samples and was detected in a lung carcinoma (Lucas *et al*., 2000). Also, a previous study demonstrated that *MAGEB6* was highly expressed in lung adenocarcinoma (Tsai *et al*., 2007). In this study, qRT-PCR was performed to determine the expression of *MAGEB6* in different types of lung and ovarian cancer tissues. In lung cancer samples 1, 3, 5, 6, and 7, *MAGEB6* was observed at detectable levels, and in most of the ovarian cancer samples *MAGEB6* was expressed, except in ovarian cancer tissue samples 2 and 8 (see summary grid in Figure 3.10 B and 3.11 B).

		Chromosome	Testis	Lung normal 1	2	3	4	5
A	*ACTB*	7	■	■	■	■	■	■
B	*PIWIL1*	12	■					
	ROPN1	3	■					
	TUBA3C	13	■					
	DPEP3	16	■					
	VCY	X	■					
	CPA5	7	■					
	MAGEB6	X	■					
	RBM46	4	■					
	TPTE	21	■					
	TKTL2	4	■					
	TPTE2P2	13	■					
	CCDC83	11	■					
	LOC441601	11	■					
	RFX4	12	■					
	FLJ43944	17	■					
	OR7E156P	13	■					
C	*BTG4*	11	■	■	■	■	■	■
	Hs.601545	14	■	■	■	■	■	■
	LGALS14	19	■	■	■	■	■	■
	EBI3	19	■	■	■	■	■	■
	HIST1H3C	6	■	■	■	■	■	■
	C12orf37	12	■		■	■	■	■
	NBPF4	1	■	■	■	■	■	■
	KIAA1257	3	■	■	■	■	■	■
	ISM2	14	■	■	■	■	■	
	C10orf82	10	■		■	■	■	■

Figure 3.8 Summary of qRT-PCR results for the expression profiles of 26 genes in normal testicular and lung tissues obtained from different sources.
The rows represent the expression patterns of genes (left), while columns numbered 1–5 represent normal lung tissues from different sources. (A) The expression profile of the *ACTB* gene for the quality of cDNA; (B) The expression patterns of 16 genes previously identified as good CT gene biomarkers; (C) The expression patterns of 10 genes verified in five different normal lung tissues; therefore, this group of genes was dismissed as CTA genes. The blue cells in each column represent the positive expression of the gene, whereas empty cells represent undetectable expression or a Ct level greater than 38 as determined by qRT-PCR.

	Gene	Chromosome	Testis	Ovary normal 1	2	3	4	5
A	ACTB	7	■	■	■	■	■	■
B	PIWIL1	12	■					
	ROPN1	3	■					
	TUBA3C	13	■					
	DPEP3	16	■					
	VCY	X	■					
	CPA5	7	■					
	MAGEB6	X	■					
	RBM46	4	■					
	TPTE	21	■					
	TKTL2	4	■					
	TPTE2P2	13	■					
	CCDC83	11	■					
	LOC441601	11	■					
	RFX4	12	■					
	FLJ43944	17	■					
	OR7E156P	13	■					
C	BTG4	11	■	■	■	■	■	■
	Hs.601545	14	■	■	■	■	■	■
	LGALS14	19	■	■	■	■	■	
	EBI3	19	■	■	■	■	■	■
	HIST1H3C	6	■	■	■	■	■	■
	C12orf37	12	■	■	■	■	■	■
	NBPF4	1	■	■	■	■	■	■
	KIAA1257	3	■	■	■	■	■	
	ISM2	14	■	■	■	■	■	■
	C10orf82	10	■	■	■	■	■	

Figure 3.9 Summary of qRT-PCR results for the expression profiles of 26 genes in normal testicular and ovarian tissues obtained from different sources.
The rows represent the expression patterns of genes (left), while the columns numbered 1–5 represent the normal ovarian tissues from different sources. (A) The expression profile of the *ACTB* gene for the quality of cDNA; (B) The expression patterns of 16 genes previously identified as good CT gene biomarkers; (C) The expression patterns of 10 genes verified in five different normal ovarian tissues; therefore, this group of genes was dismissed as CTA genes. The blue cells in each column represent the positive expression of the gene, whereas empty cells represent undetectable expression or a Ct level greater than 38 as determined by qRT-PCR.

	Gene	Chromosome	Testis	Lung cancer 1	2	3	4	5	6	7	8
A	ACTB	7	■	■	■	■	■	■	■	■	■
B	PIWIL1	12	■	■	■	■					
	ROPN1	3	■	■	■	■		■		■	■
	TUBA3C	13	■			■	■	■	■	■	
	DPEP3	16	■			■			■		
	VCY	X	■	■		■	■	■	■	■	■
	CPA5	7	■								
	MAGEB6	X	■			■		■	■	■	■
	RBM46	4	■		■	■	■	■	■		
	TPTE	21	■					■	■		■
	TKTL2	4	■					■	■		
	TPTE2P2	13	■					■	■		
	CCDC83	11	■					■			
	LOC441601	11	■			■			■	■	■
	RFX4	12	■	■	■			■	■		
	FLJ43944	17	■	■		■	■	■		■	■
	OR7E156P	13	■							■	

Figure 3.10 Summary of qRT-PCR results for the expression profiles of 16 genes in normal testicular tissue and eight lung cancer tissues obtained from different sources.
The rows represent the expression patterns of genes (left), while the columns numbered 1–8 represent the lung cancer tissues as follows: (1) bronchioloalveolar adenocarcinoma; (2) and (5) squamous cell carcinoma; and (3), (4), (6), (7), and (8) lung adenocarcinoma. (A) The expression profile of the *ACTB* gene for the quality of cDNA; (B) The expression patterns of candidate genes in different lung cancer tissues. The blue cells in each column represent the positive expression of the gene, whereas empty cells represent undetectable expression or a Ct value greater than 38 as determined by qRT-PCR.

Gene	Chromosome	Testis	1	2	3	4	5	6	7	8
A										
ACTB	7	■	■	■	■	■	■	■	■	■
PIWIL1	12	■	■	■		■	■	■	■	■
ROPN1	3	■		■	■	■	■	■	■	
TUBA3C	13	■	■		■	■	■	■	■	
DPEP3	16	■	■		■	■				
VCY	X	■	■	■	■	■	■	■	■	
CPA5	7	■	■			■				
MAGEB6	X	■			■	■	■	■	■	■
B										
RBM46	4	■		■	■	■	■	■	■	■
TPTE	21	■	■		■		■	■	■	■
TKTL2	4	■			■	■		■	■	■
TPTE2P2	13	■			■		■		■	■
CCDC83	11	■					■		■	■
LOC441601	11	■					■	■	■	■
RFX4	12	■					■	■	■	■
FLJ43944	17	■	■	■	■	■	■			■
OR7E156P	13	■						■	■	

Figure 3.11 Summary of qRT-PCR results for the expression profiles of 16 genes in normal testicular tissue and eight ovarian cancer tissues obtained from different sources.
The rows represent the expression patterns of genes (left), while the columns numbered 1–8 represent the ovarian cancer tissues as follows: (1), (5), (6), and (8) ovarian serous papillary adenocarcinoma (OSPA); (2), (3), and (7) ovarian adenocarcinoma; and (4) ovarian clear cell adenocarcinoma (OCCA). (A) The expression profile of the *ACTB* gene for the quality of cDNA. (B) The expression patterns of candidate genes in different ovarian cancer tissues. The blue cells in each column represent the positive expression of the gene, whereas empty cells represent undetectable expression or a Ct value greater than 38 as determined by qRT-PCR.

3.4 Conclusion

Here, we validated the expression of 26 genes that were previously identified as CTA genes and were reported to serve as potential biomarkers in lung cancer, because their expression was linked with aggressive lung tumours. Out of 26 genes, we confirmed the expression of 16 genes as specific CTA genes, because their expression profiles were detected in normal testicular tissue but not in various normal lung tissue samples. These 16 genes were also expressed in various lung cancer tissues that were obtained from different patients with metastases, which indicates that these genes can serve as cancer biomarkers. In addition, we demonstrated the expression of 16 genes in normal ovarian tissues from different sources and demonstrated that the expression of these genes was found only in testicular tissue. In different ovarian cancer tissues, we analysed the expression of these genes by qRT-PCR, because these genes can be used as biomarkers in ovarian cancer and potential targets in development of vaccines or diagnostics. However, further investigation is still needed with a larger group of samples to confirm our findings. Finally, in this study, 10 genes were excluded, whereas the Rousseaux et al. (2013) study defined these genes as CTA candidates. The explanation for incorrectly reporting these genes as CTA genes might be the choice of the cut-off they used in qPCR or the low-level expression of these genes because they applied qRT-PCR with 40 cycles. It would be of great value to investigate whether the restricted 16 genes we validated could be used for patient stratification in the absence of the expression data for the 10 genes excluded here. This could help to reduce the number of genes to profile in the development of prognostic/ stratification technologies based on profiling of expression of small cohorts of genes.

Chapter 4.0 Validating an extensive cohort of CTA genes derived from different sources using TaqMan Low Density Array Cards

4.1 Introduction

Cancer is defined as uncontrolled cell proliferation with heterogeneity in cell morphology, phenotype and function. Some factors, such as epigenetic alteration, genetic mutation and metabolic changes, are known to affect the heterogeneity of tumours (Hirohashi *et al*., 2016; Massagué and Obenauf, 2016). Tumour heterogeneity plays a fundamental role in enabling the survival and proliferation of cancer cells (Xue *et al*., 2016). Cancer-specific biomarkers can be employed to diagnose cancer at an early stage, predict the future course of the disease and determine an effective treatment. Thus, the identification and development of cancer biomarkers has become important, as they can be useful to predict and assess the responses of patients with aggressive tumours to treatment (Patel and Ahmed, 2015; Bailey *et al*., 2014). Cancer/testis antigens (CTAs) are biomarkers that provide therapeutic targets for specific tumours, for example, the expression of the CTA genes *LIN28B*, *TSPY10* and *C12orf54* in non-small-cell lung cancer (NSCLC) (Djureinovic *et al*., 2016). Recently, the aberrant expression of CTA genes, including *AURKC*, *TEX101* and *DAZ1*, in breast cancer tumours and cell lines was reported (Mobasheri *et al*., 2015). An extensive cohort of CTA genes was identified by applying novel computational tools (for example, see Rousseaux *et al*., 2013; Hofmann *et al*., 2008; Feichtinger *et al*., 2012). In addition, a bioinformatics pipeline was developed to identify new potential CTA genes based on the expressed sequence tag (EST) and microarray data (Feichtinger *et al*., 2012a; 2012b; Feichtinger *et al*., 2014). The bioinformatics pipeline was based on a study that revealed genes in mice with specific associations to the development of meiotic spermatocytes (Chalmel *et al*., 2007). In total, 744 of these genes were predicted to have meiosis-associated features and may play a fundamental role in the meiotic process (Chalmel *et al*., 2007). From these mouse genes, a subset of 408 genes were identified as human orthologues (Feichtinger *et al*., 2012b) (Figure 4.1). The expression of these human orthologue genes was investigated to reveal genes with non-meiotic

features, which show their activity in mitosis, using MitoCheck analysis (http://www.mitocheck.org). Of the 408 genes, 33 were mitotically expressed; thus, 375 genes remained as human meiosis candidates. These genes were further analysed after filtration by applying two previous bioinformatics methods: the microarray analysis from ArrayExpress and GEO data (http://www.cancerma.org.uk/) and analysis based on the ESTs identified using Unigene database tools (http://www.cancerest.org.uk/) (Feichtinger *et al*., 2012a; 2012b; Feichtinger *et al*., 2014). ESTs are sequences that consist of nucleotide lengths from 200–500 that are clustered and counted following the reading of a single pass of the nucleotide sequence (Adams *et al*., 1991). The EST method has been determined to be effective for the identification and characterisation of new candidates of CTA genes (Bettoni *et al*., 2009; Hofmann *et al*., 2008; Kim *et al*., 2007). In total, 375 candidate genes were analysed using the EST method to assess their expression in normal tissues but not in the germline or central nervous system (CNS). Then, a cancer EST library was used to target the genes that demonstrated expression in specific tissues, including testis and CNS tissues. Consequently, 177 potential candidate genes were identified, and based on their expression profile according to the EST method, they were classified into four different classes. The first class (Group 1) consisted of nine cancer/testis-restricted genes. The second class (Group 2) was comprised of 75 genes found exclusively in testis tissues. The third class (Group 3) exhibited their expression in normal testis/CNS-restricted tissues, including cancer, consisting of 21 genes. The fourth class (Group 4) of 72 genes was classified as testis/CNS-restricted (Feichtinger *et al*., 2012a; Feichtinger *et al*., 2014; Sammut *et al*., 2014). As aforementioned, different approaches were utilised, leading to the identification of an extensive cohort of specific candidate genes that may serve as cancer biomarkers. Therefore, the aim of this chapter is to analyse the expression pattern of genes that are known to be CTA genes selected from five sources (see Section 4.2). Using TaqMan Low Density Array (TLDA) cards, 156 CTA genes that may serve as potential clinical biomarkers from different sources, along with their ON/OFF expression, were evaluated and classified. The ultimate aim being to determine whether expression of these genes can ultimately be applied to the development of tools for precision medicine.
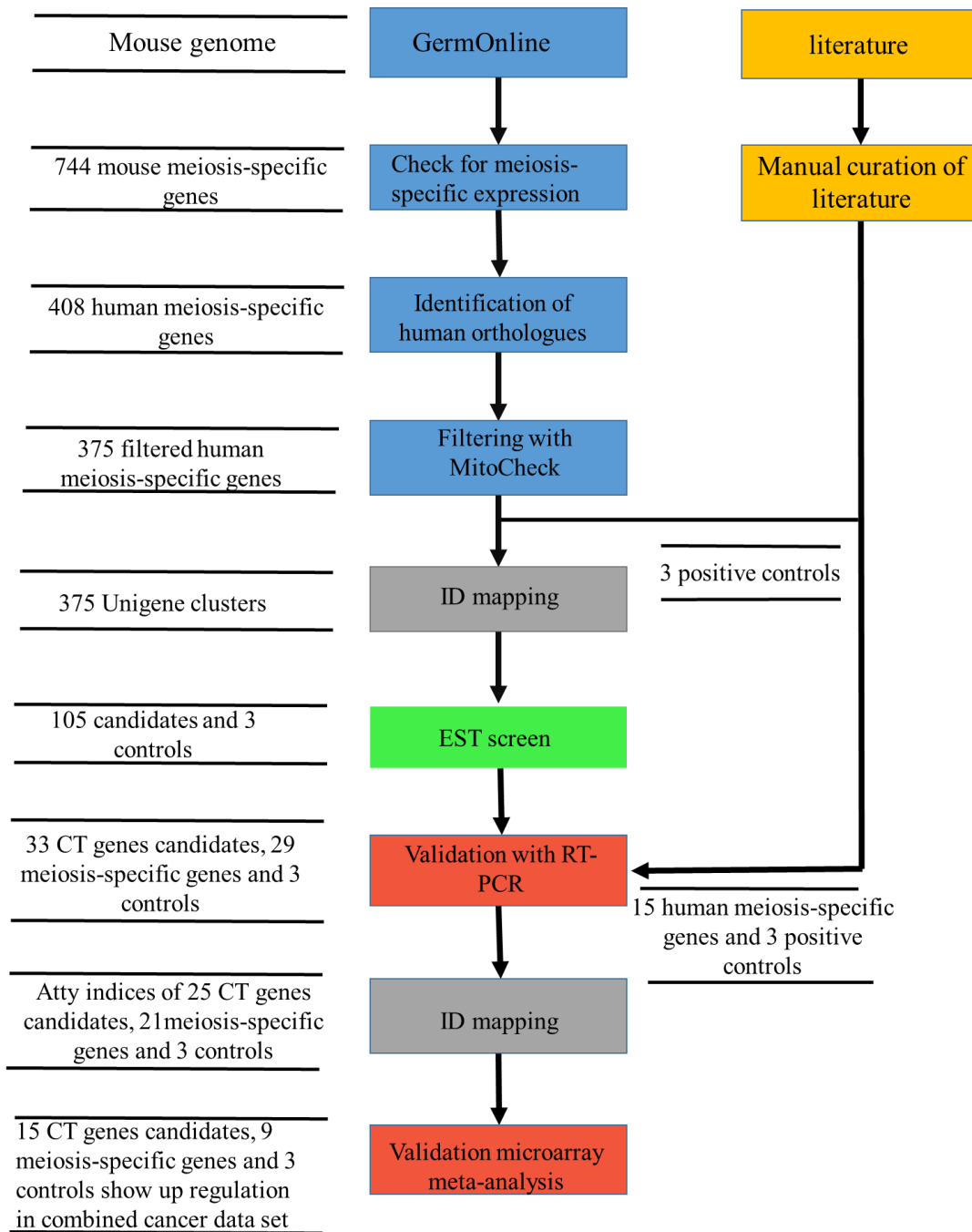
Figure 4.1 Schematic flow diagram that illustrates the application of bioinformatics methods to identify novel CTA gene candidates.
In mice, 744 meiosis-specific genes and 408 human orthologue genes were identified. Of the 408 human orthologue genes, 33 were excluded; the remaining 375 genes are human meiosis-specific genes. The three genes that served as controls, *MAGE-C1*, *SSX2* and *GAGE1*, were fed into the EST analysis pipeline. A total of 105 genes was returned, which were further analysed using RT-PCR validation/microarray meta-analysis. Adapted from (Feichtinger *et al.*, 2012a).

4.2 Results

Based on the different sources used, the expression patterns of known meiosis-specific genes in certain tissues, such as testis and placenta tissues, were explored. Accordingly, multiple CTA genes were selected, and their expression patterns (ON or OFF) were investigated and classified by qRT-PCR using the TLDA cards embedded with three endogenous control genes: *18S*, *GAPDH* and *RPS13*. The Applied Biosystems 7900HT Fast Real-Time PCR System was used, and the relative quantities were obtained from the Expression Suite Software by calculating the ΔΔCt method. The cut-off for the Ct value was chosen to be ≤ 32, as recommended by the TaqMan programme, meaning that genes with Ct values greater than 32 were excluded from further analyses. The value of the cut-off was set at 32, because, when using the cards with a cut-off value greater than 32, the number of copies in each well are reduced, thereby affecting the accuracy and reproducibly of detecting a given amount of the target. Further, a small reaction volume of cDNA was used in the card, approximately 1 µL. In addition, the TLDA cards were designed to target genes in single runs (i.e., not in triplicates). To re-validate these genes using this high throughput system, 34 RNA samples derived from normal human tissues, including the testis, were extracted. Normal RNA panels were obtained from Clontech, Ambion, Amsbio and Origene, including those from the normal colon tissues adjacent to the tumourous tissues. cDNA was generated, and the RT-PCR for the *ACTB* gene was used to check the RNA quality (Figure 4.2A). The RNA was extracted from various types of human cancer tissues and cell lines obtained from different organs (Figure 4.2B) (Ambion and Origene, see Section 2.8, details of RNA that was extracted from cancerous colon samples, in CD Appendix A). Each gene was classified according to its expression pattern; in total, 156 genes that were identified as potential biomarkers were collected from 5 different sources: (1) the human orthologue genes of the meiosis-specific genes in mice (Feichtinger *et al*., 2012), (2) the large-scale genes expressed in testis and placenta tissues (Rousseaux *et al*., 2013), (3) the human orthologue genes of the *Drosophila* germline (Feichtinger *et al*., 2014; Janic *et al*., 2010), (4) the list of CTA genes compiled using the CT database (Almeida *et al*., 2009) and (5) other groups of genes characterised as CTA genes (Hofmann *et al*., 2008) (Source of genes, in CD Appendix B).

A
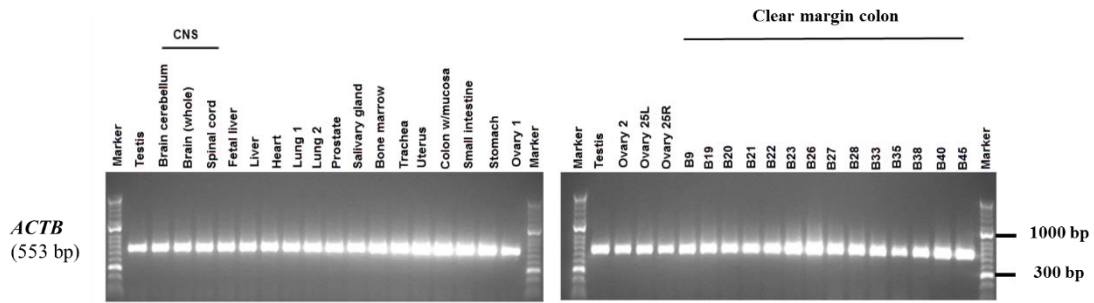
B
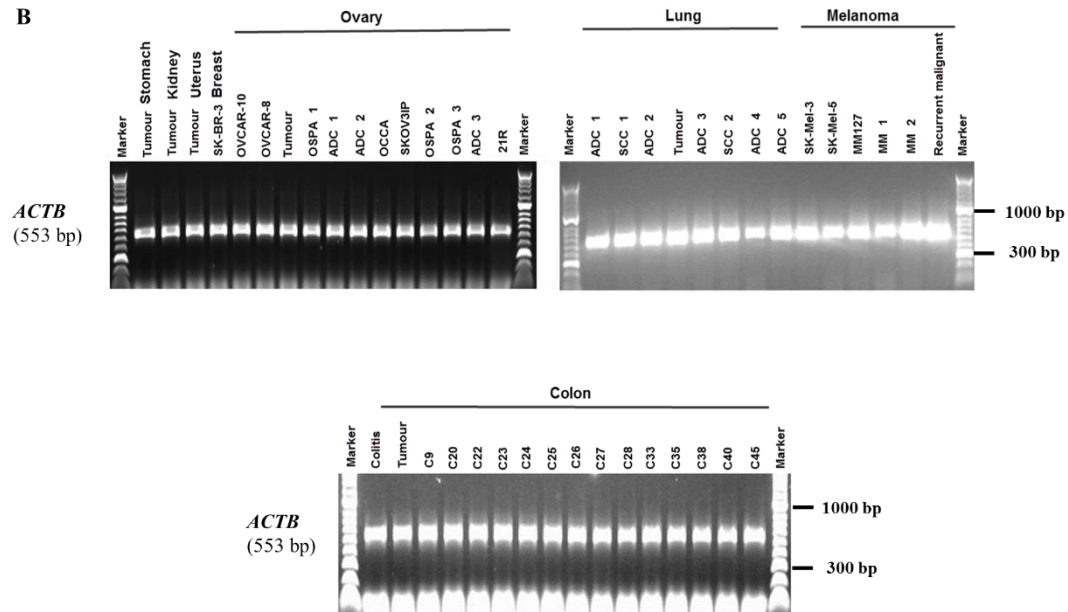
Figure 4.2 Analysis of the expression of *ACTB* gene by RT-PCR in normal tissues and cancer samples.
RNA was extracted from different normal human tissues as well as cancer tissues and cell lines. The *ACTB* gene was used to assess the quality of cDNA as a positive control. (A) Expression of *ACTB* gene in the panels of normal tissues with normal colon-adjacent tumours. (B) *ACTB* expression served as positive control in different type of cancer tissues and cell lines. The expected size of the PCR products of *ACTB* on agarose gel is 553 bp.

4.2.1   Testis-restricted genes

TLDA cards was used to investigate the expression profile of these genes within testicular tissues and multiple normal tissues selected from different sources of organs. The cohort of the selected genes exhibited that their expression was highly restricted to testis tissues. Based on the TLDA card analysis, 67 of 156 genes were classified as testis-restricted genes due to the exclusive expression of these genes in testis tissues (Figure 4.3). Consequently, the further analysis of these genes was performed in a panel of cancer cell lines and cancer sample tissues to reveal whether they could be used as potential CTA genes. Out of these 67 genes, 43 genes were shown to be restricted to the testis with no detectable expression in other cancer samples, including *ACTRT1*, *ASB17*, *BOLL*, *CTAGE1*, *IQCF3*, *ODF3*, *SHCBP1L*, *SPO11* and *TSSK6*. Further, 24 genes were found to exhibit expressions in the different types of cancer panels. Some were shown to be expressed in one cancer sample, including the testis, such as *ACTL9*, *C17orf98*, *C19orf67*, *CATSPERD*, *FKBP6*, *LYZL6* and *NT5C1B*. The genes that were expressed in only two cancer samples included *LUZP4*, *ODF4*, *PFN3* and *SPZ1*. Those that were expressed in three cancer samples included *CAPZA3*, *MAGEA9*, *MAGEA9B* and *MBD3L1*. *KLF17* and *STRA8* were expressed in four cancer samples. *TGIF2LX* or *C1orf65* were expressed in five and six cancer samples, respectively. *MAGEA1* and *MAGEA4* were expressed in eight cancer samples, whereas *MAGEA2* was expressed in nine cancer samples. Other genes were expressed in an even greater number of various types of cancer samples. For example, *TEX19* expression was detected in 11 types of cancer samples, while *PLAC1* expression was detected in 13 cancer samples (Figure 4.4).

	Gene name	Chromosome	Normal tissues — CNS: Testis, Brain cerebellum, Brain (whole), Spinal cord, Fetal liver, Liver, Heart, Lung 1, Lung 2, Prostate, Salivary gland, Bone marrow, Trachea, Uterus, Colon w/mucosa, Small intestine, Stomach, Ovary 1, Ovary 2, Ovary 25L, Ovary 25 R; Clear margin colon: B9, B19, B20, B21, B22, B23, B26, B27, B28, B33, B35, B38, B40, B45
A	*ACTB*	7	(all cells positive / blue)
B	*ACTL9*	19	- (Ovary 25 R)
	ACTRT1	x	- (Ovary 2)
	ASB17	1	- (Ovary 2)
	BOLL	2	- (Ovary 25L)
	C16orf78	16	- (Ovary 25L)
	C17orf98	17	- (Ovary 2)
	C19orf45	19	- (Ovary 2)
	C19orf67	19	- (Ovary 2)
	C1orf65	1	- (Ovary 25L)
	C3orf22	3	- (Ovary 25L)
	C4orf17	4	- (Ovary 25L)
	C5orf47	5	- (Ovary 25L)
	C8orf74	8	- (Ovary 25L)
	CAGE1	6	- (Ovary 25L)
	CAPZA3	12	- (Ovary 25L)
	CATSPERD	19	- (Ovary 1)
	CCDC38	12	- (Ovary 25L)
	CCER1	12	- (Ovary 25L)
	CPXCR1	x	- (Ovary 25L)
	CST8	20	- (Ovary 25L)
	CTAGE1	18	- (Ovary 25L)
	CYLC1	x	- (Ovary 25L)
	CYLC2	9	- (Ovary 25L)
	FABP9	8	- (Ovary 1)
	FAM170A	5	- (Ovary 1)
	FAM71B	5	- (Ovary 25L)
	FKBP6	7	- (Ovary 25L)
	FTMT	5	- (Ovary 1)
	HORMAD1	1	- (Ovary 25L)
	IL31	12	- (Ovary 1)
	IQCF3	3	- (Ovary 25L)
	KLF17	1	- (Ovary 25L)
	LEMD1	1	- (Ovary 25L)
	LINC00615	12	- (Ovary 25L)

Figure 4.3 TLDA card analysis results for the expression profiles of 67 genes in different normal tissues classified as testis-restricted genes.

The rows indicate the gene expression patterns, and the columns represent the range of normal human tissues examined. (A) The quality of cDNA was assessed by the *ACTB* gene. (B) The expression patterns of 67 genes were selected from various sources and classified as testis-restricted genes. Three genes were used as controls: *18S*, *GAPDH* and *RPS13*. A dash (-) in a cell indicates that the expression of this gene was not tested in the normal tissue samples. Positive gene expression (Ct ≤ 32) is represented by blue cells, whereas empty cells signify that undetectable expression was obtained by qRT-PCR.

	Gene name	Chromosome	Normal tissues																				Clear margin colon													
			Testis	Brain cerebellum	Brain (whole)	Spinal cord	Fetal liver	Liver	Heart	Lung 1	Lung 2	Prostate	Salivary gland	Bone marrow	Trachea	Uterus	Colon w/mucosa	Small intestine	Stomach	Ovary 1	Ovary 2	Ovary 25L	Ovary 25 R	B9	B19	B20	B21	B22	B23	B26	B27	B28	B33	B35	B38	B40	B45
A	*ACTB*	7	■	■	■	■	■	■	■	■	■	■	■	■	■	■	■	■	■	■	■	■	■	■	■	■	■	■	■	■	■	■	■	■	■	■	■	■
	LUZP4	x																							-													
	LYZL6	17																							-													
	MAGEA1	x																						-														
	MAGEA2	x																						-														
	MAGEA4	x																						-														
	MAGEA9;MAGEA9B	x																						-														
	MAGEB3	x																							-													
	MAGEB4	x																							-													
	MBD3L1	19																							-													
	NT5C1B	2																							-													
	ODF3	11																							-													
	ODF4	17																							-													
	PDHA2	4																							-													
	PFN3	5																						-														
B	*PLAC1*	x																						-														
	PRDM9	5																						-														
	PRPS1L1	7																							-													
	SCP2D1	20																							-													
	SHCBP1L	1																						-														
	SPO11	20																							-													
	SPZ1	5																							-													
	SSX5	x																							-													
	STRA8	7																						-														
	TBC1D21	15																							-													
	TCTE3	6																						-														
	TEPP	16																						-														
	TEX19	17																							-													
	TGIF2LX	x																							-													
	TRIM42	3																						-														
	TSSK6	19																							-													
	ZCCHC13	x																							-													
	ZSWIM2	2																						-														

Figure 4.3 (continued).

Figure 4.4 (A) — Gene *ACTB* (Chromosome 7): the quality-control row is positive (blue) across all cancer cells/tissues columns.

Gene name	Chr	Sto	Kid	Ute	Bre	OVCAR-10	OVCAR-8	Ov Tumour	OSPA 1	ADC 1	ADC 2	OCCA	SKOV3IP	OSPA 2	OSPA 3	ADC 3	21R	Lu ADC 1	SCC 1	ADC 2	Lu Tumour	ADC 3	SCC 2	ADC 4	ADC 5	SK-Mel-3	SK-Mel-5	MM127	MM 1	MM 2	Rec. malig.	Colitis	Co Tumour	C9	C20	C22	C23	C24	C25	C26	C27	C28	C33	C35	C38	C40	C45
ACTB (A)	7	■	■	■	■	■	■	■	■	■	■	■	■	■	■	■	■	■	■	■	■	■	■	■	■	■	■	■	■	■	■	■	■	■	■	■	■	■	■	■	■	■	■	■	■	■	■
ACTL9	19	-	-	-	-	-	-	-	-								■	-	-							-																						
ACTRT1	x									-	-	-	-										-	-				-	-	-															-		-
ASB17	1									-	-	-	-										-	-				-	-	-															-		-
BOLL	2	-	-	-	-	-	-	-	-									-	-							-																						
C16orf78	16	-	-	-	-	-	-	-	-									-	-							-																						
C17orf98	17									-	-	-	-										-	-				-	-	-								■		-						-		-
C19orf45	19									-	-	-	-										-	-				-	-	-										-						-		-
C19orf67	19									-	-	-	-										-	-				-	-	-								■		-						-		-
C1orf65	1	-	-	-	-	-	-	-	-			■	■				■	-	-				■			-					■	■																
C3orf22	3	-	-	-	-	-	-	-	-									-	-							-																						
C4orf17	4	-	-	-	-	-	-	-	-									-	-							-																						
C5orf47	5	-	-	-	-	-	-	-	-									-	-							-																						
C8orf74	8	-	-	-	-	-	-	-										-	-							-																						
CAGE1	6	-	-	-	-	-	-	-	-									-	-							-																						
CAPZA3	12	-	-	-	-	-	-	-	-									-	-				■			-			■	■																		-
CATSPERD	19								-	-	-	-	■									-	-				-	-	-																-		
CCDC38	12	-	-	-	-	-	-	-	-									-	-							-																						
CCER1	12	-	-	-	-	-	-	-	-									-	-							-																						
CPXCR1	x	-	-	-	-	-	-	-	-									-	-							-																						
CST8	20	-	-	-	-	-	-	-	-									-	-							-																						
CTAGE1	18	-	-	-	-	-	-	-	-									-	-							-																						
CYLC1	x	-	-	-	-	-	-	-	-									-	-							-																						
CYLC2	9	-	-	-	-	-	-	-	-									-	-							-																						
FABP9	8								-	-	-	-										-	-				-	-	-								-	-	-							-		-
FAM170A	5								-	-	-	-										-	-				-	-	-								-	-	-							-		-
FAM71B	5	-	-	-	-	-	-	-	-									-	-							-																						
FKBP6	7	-	-	-	-	-	-	-	-									-	-										■																			
FTMT	5								-	-	-	-										-	-				-	-	-								-	-	-							-		-
HORMAD1	1	-	-	-	-	-	-	-	-									-	-							-																						
IL31	12								-	-	-	-										-	-				-	-	-								-	-	-							-		-
IQCF3	3	-	-	-	-	-	-	-	-									-	-							-																						
KLF17	1	-	-	-	-	-	-	-	-									-	-							-		■	■	■												■						
LEMD1	1	-	-	-	-	-	-	-	-									-	-							-																						
LINC00615	12								-	-	-	-										-	-				-	-	-								-	-	-							-		-

Figure 4.4 TLDA card analysis results for the expression profiles of 67 genes in a range of human cancer tissues and cell lines.

The rows indicate the gene expression patterns, and the columns represent the range of human cancer tissues and cell lines examined. (A) The quality of cDNA was assessed by the *ACTB* gene. (B) The expression patterns of 67 genes in cancer samples were selected from various sources and classified as testis-restricted genes. Three genes were used as controls: *18S*, *GAPDH* and *RPS13*. A dash (-) in a cell indicates that the expression of the gene was not tested in the cancer tissue samples. Positive gene expression (Ct ≤ 32) is represented by blue cells, whereas empty cells signify that undetectable expression was obtained by qRT-PCR.

Cancer cells/tissues

| Gene name | Chromosome | Stomach Tumour | Kidney Tumour | Uterus Tumour | Breast SK-BR-3 | Ovary OVCAR-10 | Ovary OVCAR-8 | Ovary Tumour | Ovary OSPA 1 | Ovary ADC 1 | Ovary ADC 2 | Ovary OCCA | Ovary SKOV3IP | Ovary OSPA 2 | Ovary OSPA 3 | Ovary ADC 3 | Ovary 21R | Lung ADC 1 | Lung SCC 1 | Lung ADC 2 | Lung Tumour | Lung ADC 3 | Lung SCC 2 | Lung ADC 4 | Lung ADC 5 | Melanoma SK-Mel-3 | Melanoma SK-Mel-5 | Melanoma MM127 | Melanoma MM 1 | Melanoma MM 2 | Melanoma Recurrent malignant | Colitis | Colon Tumour | Colon C9 | Colon C20 | Colon C22 | Colon C23 | Colon C24 | Colon C25 | Colon C26 | Colon C27 | Colon C28 | Colon C33 | Colon C35 | Colon C38 | Colon C40 | Colon C45 |

A
- ACTB — 7
- LUZP4 — x
- LYZL6 — 17

B
- MAGEA1 — x
- MAGEA2 — x
- MAGEA4 — x
- MAGEA9;MAGEA9B — x
- MAGEB3 — x
- MAGEB4 — x
- MBD3L1 — 19
- NT5C1B — 2
- ODF3 — 11
- ODF4 — 17
- PDHA2 — 4
- PFN3 — 5
- PLAC1 — x
- PRDM9 — 5
- PRPS1L1 — 7
- SCP2D1 — 20
- SHCBP1L — 1
- SPO11 — 20
- SPZ1 — 5
- SSX5 — x
- STRA8 — 7
- TBC1D21 — 15
- TCTE3 — 6
- TEPP — 16
- TEX19 — 17
- TGIF2LX — x
- TRIM42 — 3
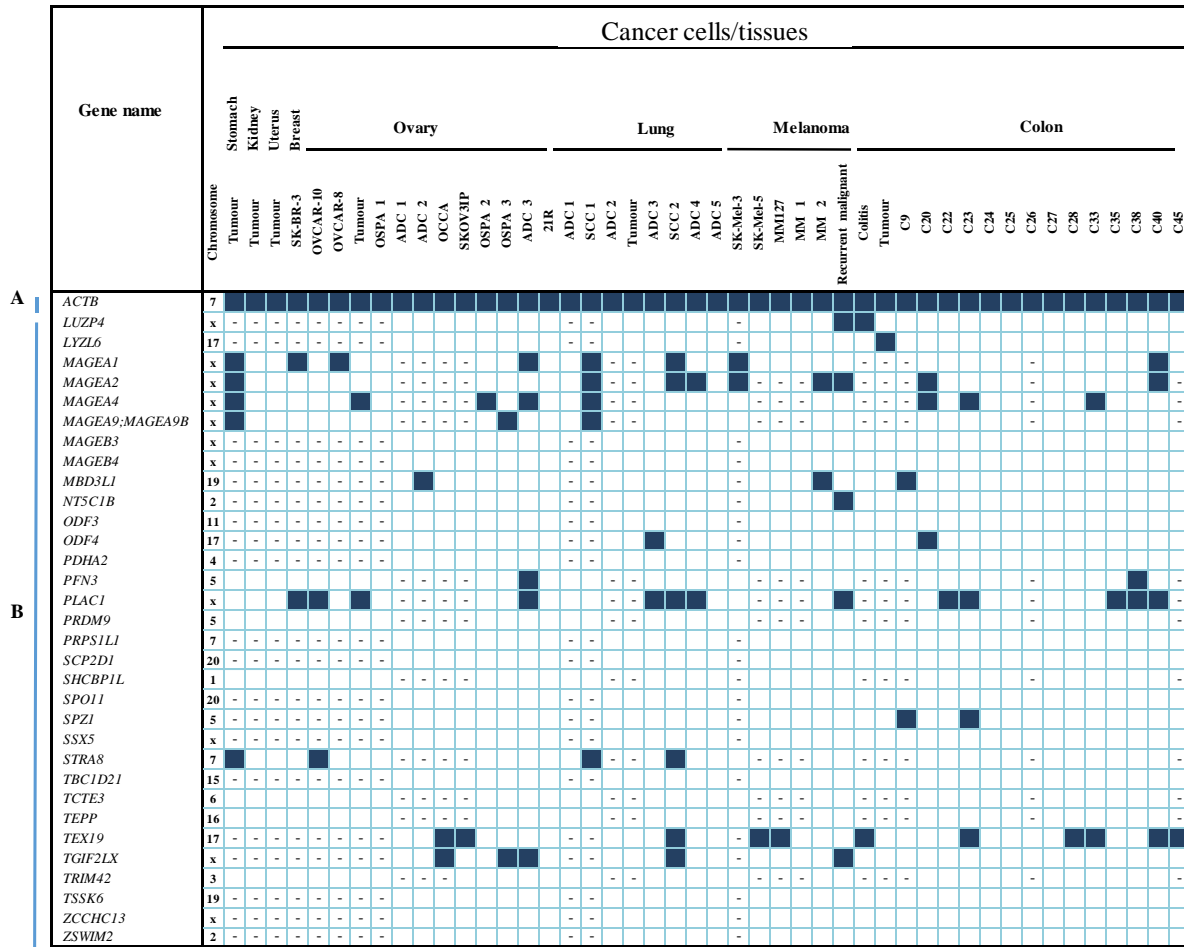- TSSK6 — 19
- ZCCHC13 — x
- ZSWIM2 — 2

Figure 4.4 (continued).

4.2.2   Testis/CNS-restricted genes

The TLDA card analysis revealed that the 9 of 156 genes were expressed in CNS and in testis tissues. Due to their limited expression, these genes— including *C12orf50*, *DNAJC5G*, *EQTN*, *HORMAD2*, *MAGEA12*, *NANOS2*, *PPP3R2*, *RAD21L1* and *SYCP1*—were classified as testis/CNS-restricted. *C12orf50* and *NANOS2* were expressed in the brain cerebellum and *DNAJC5G* was expressed in whole brain tissues. *EQTN*, *HORMAD2* and *RAD21L1* were observed in two types of CNS tissues: the brain cerebellum and the spinal cord (Figure 4.5).

These genes were further analysed in various human cancer tissues and cell lines to determine whether they may be potential CTA genes. These genes were found to be expressed in cancer samples in addition to their exclusive expression in testicular and CNS tissues. Three genes displayed expression in one cancer sample: *C12orf50* and *EQTN* were found in the malignant melanoma sample (MM1), whereas *PPP3R2* was found in the ovarian cancer sample (21R). *HORMAD2* was expressed in the ovarian adenocarcinoma sample (ADC2) and in the lung adenocarcinoma sample (ADC3). The expression of *MAGEA12* was found in nine types of cancer samples, including stomach tumour, breast cancer cell line (SK-BR-3), ovarian cancer cell line (OVCAR-8), lung cancer, squamous cell carcinoma (SCC1), human melanoma cell line (SK-Mel-3), malignant melanoma (MM2), recurrent malignant melanoma and colon cancer samples 20 and 40. In contrast, some genes in the cancer samples tested in the current study showed no detectable expression, including *DNAJC5G*, *NANOS2*, *RAD21L1* and *SYCP1*. However, these genes may be expressed in different types of cancer samples not used in the present study; therefore, these genes were not excluded as promising candidate genes (Figure 4.6).

Gene name	Chromosome	Testis	Brain cerebellum	Brain (whole)	Spinal cord	Fetal liver	liver	Heart	Lung 1	liver	Lung 2	Prostate	Salivary gland	Bone marrow	Trachea	Uterus	Colon w/mucosa	Small intestine	Stomach	Ovary 1	Ovary 2	Ovary 25L	Ovary 25 R	B9	B19	B20	B21	B22	B23	B26	B27	B28	B33	B35	B38	B40	B45
ACTB (A)	7	■	■	■	■	■	■	■	■	■	■	■	■	■	■	■	■	■	■	■	■	■	■	■	■	■	■	■	■	■	■	■	■	■	■	■	■
C12orf50 (B)	12	■																						-														
DNAJC5G	2	■		■																				-														
EQTN	9	■			■																			-														
HORMAD2	22	■			■																			-														
MAGEA12	x	■	■	■																				-														
NANOS2	19	■		■	■																			-														
PPP3R2	9	■			■																			-														
RAD21L1	20	■		■																				-														
SYCP1	1	■	■	■	■																			-														

Figure 4.5 Expression patterns of nine genes in different normal tissues were classified as testis/CNS-restricted genes by using the TLDA card method.
The gene expression patterns are represented by rows and columns for various types of normal human tissues. (A) The quality of cDNA was assessed by the *ACTB* gene. (B) The expression patterns of nine genes in normal samples were selected from various sources and classified as testis/CNS-restricted genes. Three genes were used as controls: *18S*, *GAPDH* and *RPS13*. A dash (-) in a cell indicates that the expression of the gene was not tested in the normal tissue samples. Positive gene expression (Ct ≤ 32) is represented by blue cells, whereas empty cells signify that negative expression was determined by qRT-PCR.

Gene name	Chromosome	Stomach Tumour	Kidney Tumour	Uterus Tumour	Breast SK-BR-3	Ovary OVCAR-10	Ovary OVCAR-8	Ovary Tumour	Ovary OSPA 1	Ovary ADC 1	Ovary ADC 2	Ovary OCCA	Ovary SKOV3IP	Ovary OSPA 2	Ovary OSPA 3	Ovary ADC 3	Ovary 21R	Lung ADC 1	Lung SCC 1	Lung ADC 2	Lung Tumour	Lung ADC 3	Lung SCC 2	Lung ADC 4	Lung ADC 5	Melanoma SK-Mel-3	Melanoma SK-Mel-5	Melanoma MM127	Melanoma MM 1	Melanoma MM 2	Melanoma Recurrent malignant	Colon Colitis Tumour	Colon C9	Colon C20	Colon C22	Colon C23	Colon C24	Colon C25	Colon C26	Colon C27	Colon C28	Colon C33	Colon C35	Colon C38	Colon C40	Colon C45
A																																														
ACTB	7	■	■	■	■	■	■	■	■	■	■	■	■	■	■	■	■	■	■	■	■	■	■	■	■	■	■	■	■	■	■	■	■	■	■	■	■	■	■	■	■	■	■	■	■	■
B																																														
C12orf50	12	-	-	-	-	-	-	-										-	-							-			■																	
DNAJC5G	2	-	-	-	-	-	-	-										-	-							-																				
EQTN	9	-	-	-	-	-	-	-										-	-							-			■																	
HORMAD2	22	-	-	-	-	-	-	-			■							-	-			■				-																				
MAGEA12	x	■			■		■				-	-	-	-					■	-	-					■	-	-		■	■	-	-	-		■						-				■	-
NANOS2	19	-	-	-	-	-	-	-										-	-							-																				
PPP3R2	9	-	-	-	-	-	-	-									■	-	-							-																				
RAD21L1	20								-	-	-	-												-	-				-	-						-	-	-						-		-
SYCP1	1	-	-	-	-	-	-	-										-	-							-																				
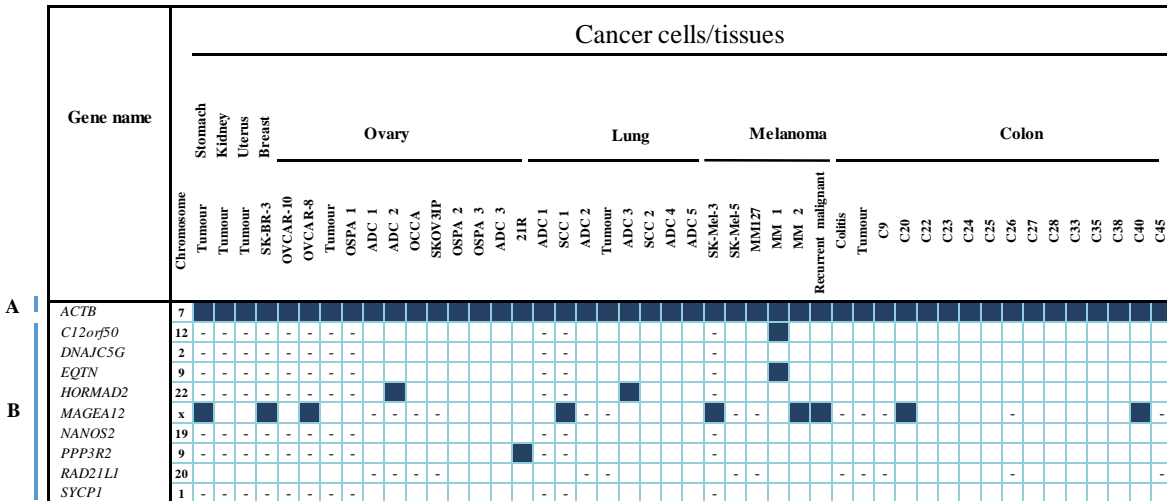
Figure 4.6 Expression patterns of nine genes in a range of cancer tissues and cell lines using the TLDA card method.

The gene expression patterns are represented by rows and columns for various types of human cancer cell lines and tissues. (A) The quality of cDNA was assessed by the *ACTB* gene. (B) The expression patterns of nine genes in cancer samples were selected from various sources and classified as testis/CNS-restricted genes. Three genes were used as controls: *18S*, *GAPDH* and *RPS13*. A dash (-) in a cell indicates that the expression of the gene was not tested in the cancer samples. Positive gene expression (Ct ≤ 32) is represented by blue cells, whereas empty cells signify that negative expression was determined by qRT-PCR.

4.2.3   Testis-selective genes

Of the 156 genes that were re-validated using the TLDA cards, only 11 genes—*ADAD1*, *ADAM2*, *BRDT*, *C20orf195*, *CXorf27*, *NUTM1*, *RBM44*, *RNF17*, *SMC1B*, *TEX101* and *TEX33*—were classified as testis-selective genes. *ADAM2*, *NUTM1* and *TEX33* exhibited expression in only one normal tissue as well as in testicular tissue; *ADAM2* was expressed in prostate tissue, *NUTM1* was expressed in a normal colon sample obtained as histologically clear margin adjacent to colonic tumour (B27) and *TEX33* expression was detected in normal lung tissue 2. *ADAD1* and *BRDT* were expressed in normal ovarian samples, i.e., the ovary 25L (left) and the ovary 25R (right). *C20orf195*, *CXorf27* and *TEX101* were exclusively expressed in two clear margin normal colon samples and testicular tissues. In contrast, the expression of other genes, including *RBM44*, *RNF17* and *SMC1B*, was detected in different normal tissues. For instance, *RBM44* was expressed in normal lung tissue 2 and normal colon tissue B22, whereas *RNF17* was observed in the colon w/mucosa tissue and in the ovary 25L sample. *SMC1B* was also expressed in two normal tissues— the fetal liver and normal colon tissue B26 (Figure 4.7).

These genes were further investigated in various human cancer samples. The expression profiles of some of these genes were observed in one cancer sample, such as the expression of *CXorf27* in the human melanoma cell line (SK-Mel-3); *NUTM1* expression was also observed only in colon cancer sample 38 (C38), and *RBM44* showed expression in the stomach tumour sample. Other genes demonstrated expression in two cancer samples: *ADAM2* was expressed in the colon tumour and colon cancer sample (C22), and *TEX101* was observed in the colon cancer sample (C28 and C45). *BRDT* was expressed in the lung cancer samples, including lung sample ADC 2 and ADC 5. The expression of *C20orf195* and *SMC1B* was observed in seven and nine cancer samples, respectively. The expression of these two genes was observed to be preferentially expressed in the ovarian cancer cells tested. In contrast, *ADAD1*, *RNF17* and *TEX33* exhibited no detectable expression in all of the cancer samples (Figure 4.8).
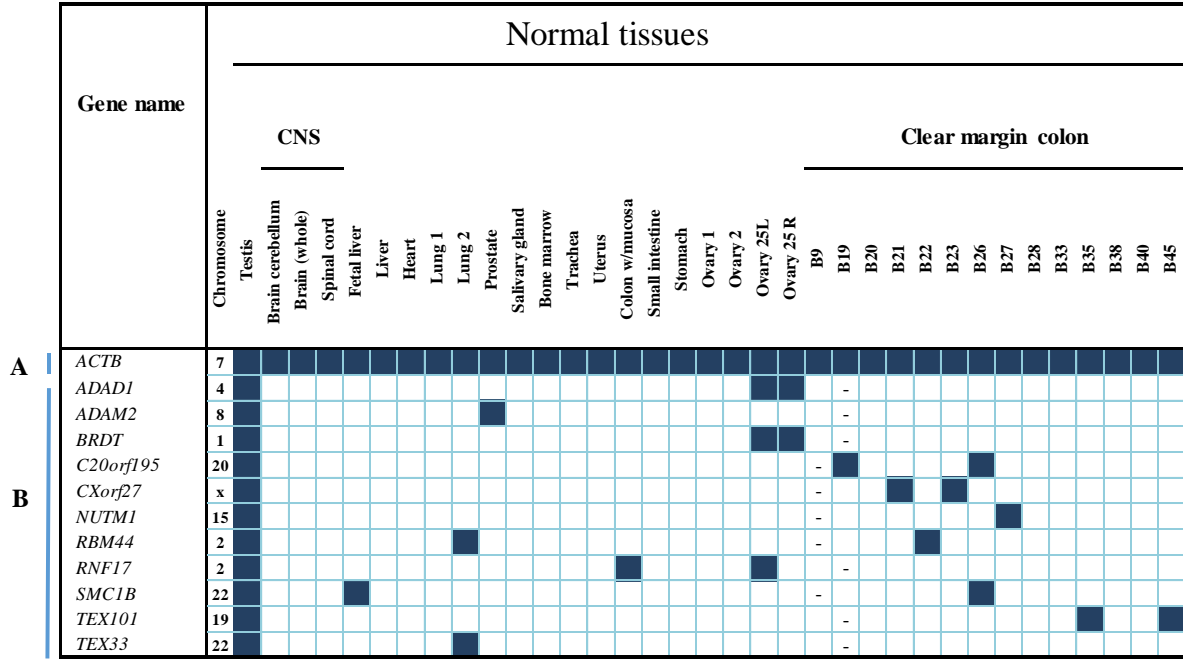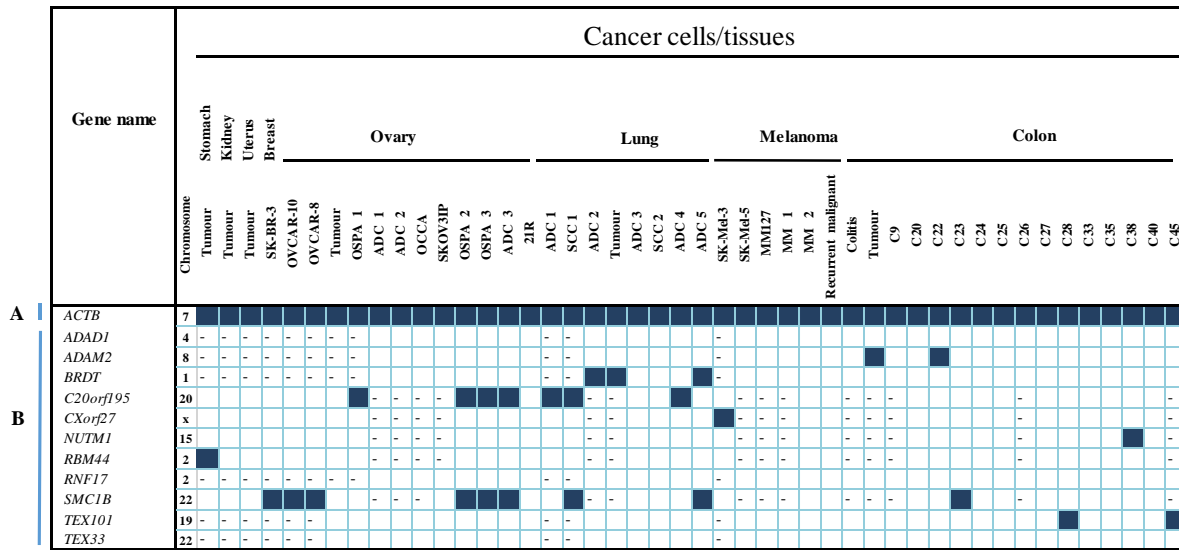
Gene name	Chromosome	Testis	Brain cerebellum	Brain (whole)	Spinal cord	Fetal liver	Liver	Heart	Lung 1	Lung 2	Prostate	Salivary gland	Bone marrow	Trachea	Uterus	Colon w/mucosa	Small intestine	Stomach	Ovary 1	Ovary 2	Ovary 25L	Ovary 25 R	B9	B19	B20	B21	B22	B23	B26	B27	B28	B33	B35	B38	B40	B45
(A) *ACTB*	7	■	■	■	■	■	■	■	■	■	■	■	■	■	■	■	■	■	■	■	■	■	■	■	■	■	■	■	■	■	■	■	■	■	■	■
(B) *ADAD1*	4	■																			■	■	-													
ADAM2	8	■									■												-													
BRDT	1	■																			■	■	-													
C20orf195	20	■																					-	■						■						
CXorf27	x	■																					-			■		■			■					
NUTM1	15	■																					-							■						
RBM44	2	■								■													-					■								
RNF17	2	■														■						■	-													
SMC1B	22	■			■																		-									■				
TEX101	19	■																					-											■		■
TEX33	22	■								■													-													

Figure 4.7 TLDA card analysis results for expression profiles of 11 genes in different sources of normal human tissues classified as testis-selective genes.
The rows indicate the gene expression patterns and the columns represent the panels of normal human tissues obtained from various sources that were examined. (A) The quality of cDNA was assessed by the *ACTB* gene. (B) The expression patterns of 11 genes in normal samples were selected from various sources and classified as testis-selective genes. Three genes were used as controls: *18S*, *GAPDH*, and *RPS13*. A dash (-) in a cell indicates that the expression of this gene was not tested in the normal tissue samples. Positive gene expression (Ct ≤ 32) is represented by cells with blue colour, whereas empty cells signify that undetectable expression was obtained by qRT-PCR.

Gene name	Chromosome
A *ACTB*	7
B *ADAD1*	4
ADAM2	8
BRDT	1
C20orf195	20
CXorf27	x
NUTM1	15
RBM44	2
RNF17	2
SMC1B	22
TEX101	19
TEX33	22

Cancer cells/tissues columns: Stomach (Tumour), Kidney (Tumour), Uterus (Tumour), Breast (SK-BR-3); Ovary (OVCAR-10, OVCAR-8, Tumour, OSPA 1, ADC 1, ADC 2, OCCA, SKOV3IP, OSPA 2, OSPA 3, ADC 3, 21R); Lung (ADC 1, SCC 1, ADC 2, Tumour, ADC 3, SCC 2, ADC 4, ADC 5); Melanoma (SK-Mel-3, SK-Mel-5, MM127, MM 1, MM 2, Recurrent malignant); Colon (Colitis, Tumour, C9, C20, C22, C23, C24, C25, C26, C27, C28, C33, C35, C38, C40, C45).

Figure 4.8 Expression patterns of 11 genes in a range of cancer tissues and cell lines using the TLDA card method.

The gene expression patterns are represented by rows and columns for various types of human cancer cell lines and tissues. (A) The quality of cDNA was assessed by the *ACTB* gene. (B) The expression patterns of 11 genes in cancer samples were selected from various sources and classified as testis-selective genes. Three genes were used as controls: *18S*, *GAPDH* and *RPS13*. A dash (-) in a cell indicates that the expression of this gene was not examined in the cancer samples. Positive gene expression (Ct ≤ 32) is represented by blue cells, whereas empty cells signify that negative expression was determined by qRT-PCR.

4.2.4   Testis/CNS-selective genes

Based on the classification of CT genes, 14 of the 156 genes re-validated in the current study demonstrated some limited expression in normal somatic tissues other than testis and CNS tissues, including *DDX4*, *DDX53*, *GK2*, *HMGB4*, *IQCF1*, *NLRP4*, *NXF2B*, *NXF2*, *OTOA*, *PAPOLB*, *PRSS54*, *SEPT12*, *SPATA19* and *SYCP3*. Of these 14 genes, 6 genes were expressed in one normal somatic non-testicular and CNS tissues , *DDX53* expression was observed in the prostate sample, *GK2* in the normal colon sample B21, *PRSS54* in the colon w/mucosa sample, *SEPT12* in the normal colon sample B40, *SPATA19* in the normal colon sample B35 and *SYCP3* in the ovarian sample (25L). The other genes examined by the TLDA method— *DDX4*, *HMGB4*, *IQCF1*, *NLRP4*, *NXF2B*, *NXF2*, *OTOA* and *PAPOLB*—were only expressed in two normal somatic tissues non- testicular or CNS tissues (Figure 4.9).

The TLDA card analysis was performed using different types of cancer samples to assess the expression of this class of genes in order to determine if they were promising candidates. In the cancer samples tested here, six genes—*DDX4*, *GK2*, *IQCF1*, *NLRP4*, *PRSS54* and *SYCP3*—were expressed in one cancer sample, whereas the genes *DDX53*, *HMGB4* and *PAPOLB* were expressed in two cancer samples. The genes *NXF2B*, *NXF2* and *SEPT12* were detected in more than four cancer samples. No evidence of *SPATA19* and *OTOA* expression was detected in any cancer samples tested here; however, these two genes were not dismissed because they may be expressed in other types of cancer cell samples. Interestingly, *GK2* and *HMGB4* were expressed exclusively in human melanoma samples; *GK2* was observed in the MM2 sample, and *HMGB4* was found in the MM2 and recurrent malignant samples, which may indicate that they are potential CTA genes for human melanoma (Figure 4.10).

Gene name	Chromosome
ACTB	7
DDX4	5
DDX53	x
GK2	4
HMGB4	1
IQCF1	3
NLRP4	19
NXF2B;NXF2	x
OTOA	16
PAPOLB	7
PRSS54	16
SEPT12	16
SPATA19	11
SYCP3	12

Column groups (Normal tissues): CNS (Testis, Brain cerebellum, Brain (whole), Spinal cord), Fetal liver, Liver, Heart, Lung 1, Lung 2, Prostate, Salivary gland, Bone marrow, Trachea, Uterus, Colon w/mucosa, Small intestine, Stomach, Ovary 1, Ovary 2, Ovary 25L, Ovary 25 R; Clear margin colon (B9, B19, B20, B21, B22, B23, B26, B27, B28, B33, B35, B38, B40, B45).

Figure 4.9 TLDA card analysis results for the expression profiles of 14 genes in different sources of normal human tissues classified as testis/CNS-selective genes.
The rows indicate the gene expression patterns, and the columns represent panels of normal human tissues obtained from various sources. (A) The quality of cDNA was assessed by the *ACTB* gene. (B) The expression patterns of 14 genes in normal samples were selected from various sources and classified as testis/CNS-selective genes. Three genes were used as controls: *18S*, *GAPDH* and *RPS13*. A dash (-) in a cell indicates that the expression of the gene was not tested in the normal tissue samples. Positive gene expression (Ct ≤ 32) is represented by blue cells, whereas empty cells signify that undetectable expression was obtained by qRT-PCR.

Figure 4.10 Expression patterns of 14 genes in a range of cancer tissues and cell lines using the TLDA card method.

The gene expression patterns are represented by rows and columns for various types of human cancer cell lines and tissues obtained from different sources. (A) The quality of cDNA was assessed by the *ACTB* gene. (B) The expression patterns of 14 genes in cancer samples were selected from various sources and classified as testis/CNS-selective genes. Three genes were used as controls: *18S*, *GAPDH* and *RPS13*. A dash (-) in a cell indicates that the expression of this gene was not examined in the cancer sample. Positive gene expression (Ct ≤ 32) is represented by blue cells, whereas empty cells signify that negative expression was determined by qRT-PCR.

4.2.5   Expression of dismissed genes

An extensive cohort of genes that were reported as CTA candidates was screened based on the TLDA method, which was used to analyse the expression profiles of the genes. In total, 55 genes were found to be expressed in multiple types of normal somatic tissues rather than in testicular tissues and CNS. This large group of genes was excluded at this stage and was not subjected to further investigation in cancer samples. Some of these genes, including *RANBP17*, *RQCD1*, *SPAG9* and *TGIF2*, exhibited expression in all the normal tissues used in this study. The genes *ATAD2*, *CCDC113*, *CEP72*, *CHEK2*, *GPAT2*, *LRRC6*, *MRE11A*, *OIP5*, *PBX4*, *PLD6*, *PTPN20A*, *RANBP17*, *SPAG4*, *SPAG9*, *TCFL5* and *TRIP13* exhibited extensive expression patterns in most of the normal tissues. In the 34 normal tissues examined in the TLDA card analysis, multiple genes were observed to have detectable expression in various types of non-testicular and CNS tissues. For instance, *ARMC3*, *DAZL*, *DKKL1*, *SPACA3*, *SPANXE, SPANXC* and *TMEFF1* were expressed in six normal tissues. The expression of *C20orf201*, *DUSP21* and *TEX15* was observed in five normal tissues. *CCDC79*, *TDRD12* and *TEX14* were expressed in eight normal tissues, whereas *C16orf46* and *NOL4* were expressed in nine normal tissues. *MAEL*, *NBPF6* and *SYNGR4* were tested and demonstrated expression in 10 normal tissues other than CNS and testicular tissues (Figure 4.11).

Normal tissues

CNS

Clear margin colon

Gene name	Chromosome	Testis	Brain cerebellum	Brain (whole)	Spinal cord	Fetal liver	Liver	Heart	Lung 1	Lung 2	Prostate	Salivary gland	Bone marrow	Trachea	Uterus	Colon w/mucosa	Small intestine	Stomach	Ovary 1	Ovary 2	Ovary 25L	Ovary 25 R	B9	B19	B20	B21	B22	B23	B26	B27	B28	B33	B35	B38	B40	B45

A

ACTB	7
AKAP3	12
ARMC3	10
ATAD2	8
C16orf46	16
C20orf201	20
C2orf70	2
CASC5	15
CATSPER1	11
CCDC110	4

B

CCDC113	16
CCDC116	22
CCDC79	16
CEP290	12
CEP55	10
CEP72	5
CHEK2	22
DAZL	3
DKKL1	19
DUSP21	x
GPAT2	2
LRRC6	8
MAEL	1
MND1	4
MRE11A	11
NBPF6	1
NOL4	18
NR6A1	9
OIP5	15

Figure 4.11 TLDA card analysis results for the expression profiles of 55 genes in normal tissues that were dismissed as CT gene candidates.
Based on the TLDA card analysis, 55 genes were excluded from further investigation with the cancer samples. The rows indicate the gene expression patterns, and the columns represent the range of normal human tissues. (A) The quality of cDNA was assessed by the *ACTB* gene. (B) The 55 genes selected from various sources were dismissed as CT genes. Three genes were used as controls: *18S*, *GAPDH* and *RPS13*. A dash (-) in a cell indicates that the expression of the gene was not tested in the normal tissue samples. Positive gene expression (Ct ≤ 32) is represented by blue cells, whereas empty cells signify that undetectable expression was obtained by qRT-PCR.

Gene name	Chromosome	Normal tissues — CNS (Testis, Brain cerebellum, Brain (whole), Spinal cord, Fetal liver, Liver, Heart, Lung 1, Lung 2, Prostate, Salivary gland, Bone marrow, Trachea, Uterus, Colon w/mucosa, Small intestine, Stomach, Ovary 1, Ovary 2, Ovary 25L, Ovary 25 R)	Clear margin colon (B9, B19, B20, B21, B22, B23, B26, B27, B28, B33, B35, B38, B40, B45)
ACTB	7		
PBK	8		
PBX4	19		
PIWIL2	8		
PLD6	17		
PTPN20A	10		
RANBP17	5		
RQCD1	2		
SPACA3	17		
SPAG4	20		
SPAG9	17		
SPANXE;SPANXC	X		
STK31	7		
SYNGR4	19		
TCFL5	20		
TDRD12	19		
TDRD1	10		
TDRD5	1		
TEX14	17		
TEX15	8		
TGIF2	20		
TMEFF1	9		
TRIML1	4		
TRIP13	5		
TSSK1B	5		
TTK	6		
TULP2	19		

A
B

Figure 4.11 (continued).

4.3 Discussion

The clinical features of CTAs are attractive for the exploration of the potential functions of these specific genes and their possible role leading to the transformation of normal cells to neoplastic cells (Suri *et al*., 2015; Kim *et al*., 2013; Fratta *et al*., 2011; Kalejs and Erenpreisa, 2005; Simpson *et al*., 2005). The expression of CT genes has been observed to be correlated with poor patients prognoses, such as in lung cancer (Rousseaux *et al*., 2013; Maine *et al*., 2016), colorectal cancer (CRC) (Molania *et al*., 2014; Choi and Chang, 2012), breast cancer, ovarian cancer, osteosarcoma, neuroblastoma (Dyrskjøt *et al*., 2012; Partheen *et al*., 2008) and aggressive head and neck tumours (Dyrskjøt *et al*., 2012; Laban *et al*., 2014). Due to the unique features of CT genes that contribute to the rise of malignant tumours (Suri *et al*., 2015), these germline genes have been employed as biomarkers in various types of cancer using different approaches to identify new candidate genes (Feichtinger *et al*., 2012a; Sammut *et al*., 2014). Based on their expression, these genes have been classified into four different categories: testis-restricted, testis/brain-restricted, testis-selective (Hofmann *et al.,* 2008) and testis/brain-selective (Feichtinger *et al*., 2012a) (Figure 4.12).

Many genes have been reported to be CT genes; however, some of these genes should not be included in the list of promising genes that are present in the CT database; the expression of these genes should be re-validated. Thus, in this current research, the expression patterns of a group of 156 genes were re-evaluated against normal and cancerous tissue samples, including testicular tissues. The TLDA card method was used to analyse the expression of these genes in samples to test and classify these genes. In total, 156 CT genes were selected from five different sources that have been considered to characterise these genes as CT genes. The five primary sources of these collected genes are: (a) genes that appear to be expressed in specific germline tissue, e.g., the testis/placenta (Rousseaux *et al*., 2013), (b) the human orthologue germline in *Drosophila* that are oncogenic in brain tumours (Feichtinger *et al*., 2014; Janic *et al*., 2010), (c) human orthologues of mouse-specific genes (Feichtinger *et al*., 2012a), (d) the CT database that contains cancer testis genes (Almeida *et al*., 2009), and (e) other cohorts of CT genes that were identified (Hofmann *et al*., 2008) (Figure 4.12).
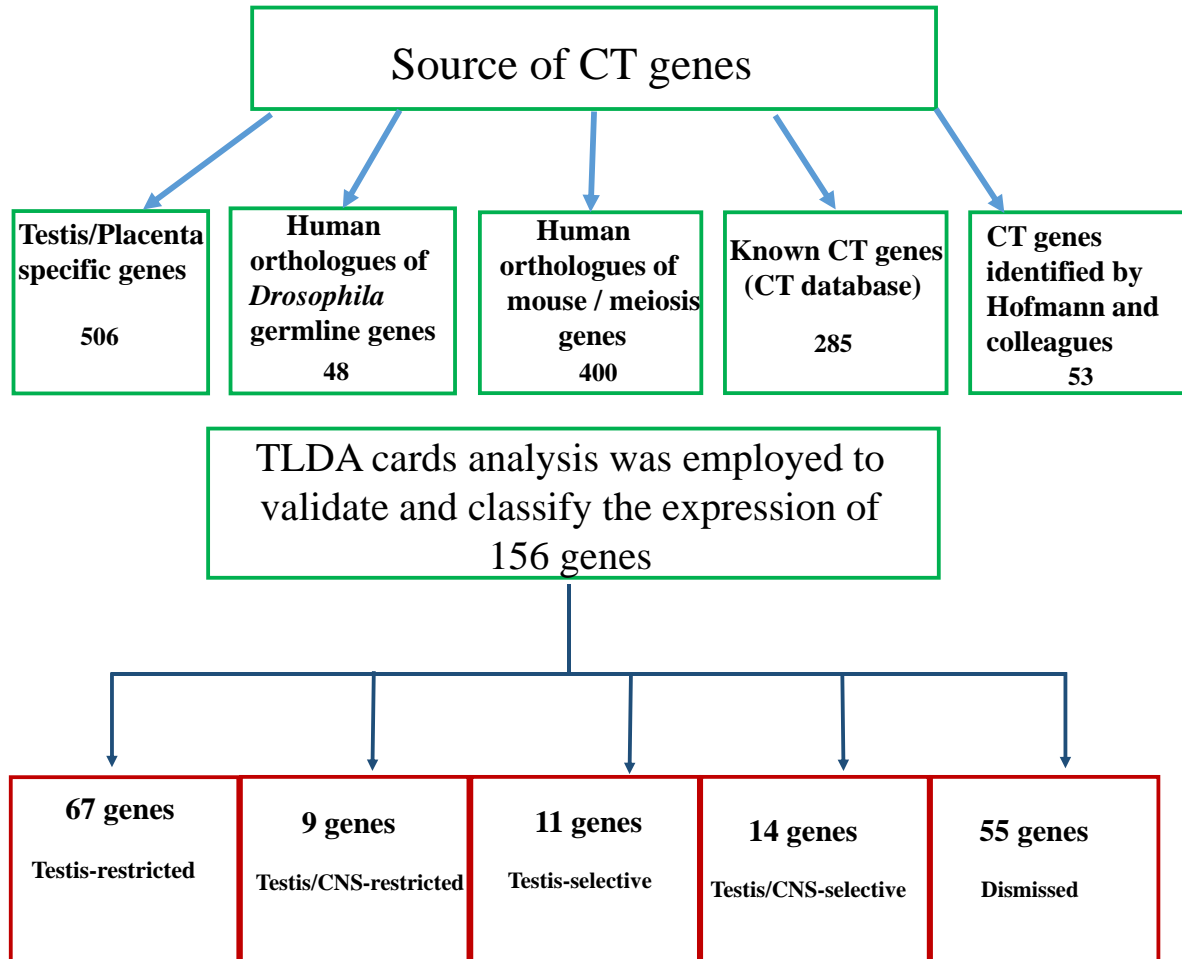
Figure 4.12 Summary of the validation process for 156 selected genes, including their sources and classification based on TLDA cards. There are overlap between these five different sources**.**

The investigation of the expression profiles of these target genes using an ON/OFF benchmark was based on strict criteria of threshold values, which were applied in this study. qRT-PCR was performed to determine whether the cohort of genes reported as potential targets might serve as clinical biomarkers. Previous studies have identified certain groups of CT genes as promising candidates; however, our results demonstrated that the profiles of the selected genes that exhibited expression in normal tissues were inappropriately assigned a CT gene classification. Consequently, these genes were dismissed from further examination in the cancer samples.

4.3.1   Expression of testis-restricted genes

The investigation of the expression of genes revealed 67 genes that demonstrated expression exclusively in testicular tissues among the different types of normal tissues obtained from different sources. Based on the TLDA card analysis, these 67 genes could be potential clinical biomarkers for various types of cancer. According to the classification of CT genes, this cohort of genes was classified as testis-restricted genes. This category includes a large group of genes, such as *BOLL*, *CTAGE1*, and *ODF3*, that are expressed in testicular tissue but not in normal tissues, as well as in all cancer samples examined, whereas other genes were expressed in testicular tissue and in cancer samples, such as *LUZP4*, *MBD3L1*, and *PLAC1*.

BOLL, also known as *BOULE* or *BOULE-LIKE*, is one of the genes that has been demonstrated to play an essential role as an oncogenic driver in the *Drosophila* germline (Janic *et al*., 2010). The human orthologues of this germline gene have been identified as CT genes (Feichtinger, *et al*., 2014). *BOULE* is a member of the *DAZ* gene family known as meiotic genes, which regulate the cell cycle process. The loss of the BOULE protein has been found to affect elements that are essential to perform meiosis. In patients with meiotic arrest, the BOULE protein has been observed to exhibit a low level of expression (Luetjens *et al*., 2004; González *et al*., 2016). The expression level of *BOULE* can be employed to investigate the testicular function and successful treatment of spermatozoa; therefore, it could be applied as a marker for meiotic progression (González *et al*., 2016; Ahmadivand *et al*., 2016). In the current study, TLDA card analysis was performed to validate the expression of *BOULE* genes with different types of normal tissues derived from various sources, including testis tissues. Based on our results, the expression of *BOULE* was demonstrated to be restricted to the testis and was not found in the other normal tissues examined

(Figure 4.3). Therefore, *BOULE* was further investigated with a range of cancer tissues and cell lines to assess whether this gene may serve as a clinical biomarker in some types of cancer. Interestingly, *BOULE* expression was not detected in any of the tumour tissues or cell lines tested, which indicates that this gene could be applied as a biomarker in some cancer samples that were not studied here (Figure 4.4). Our findings are consistent with the literature, which has reported *BOULE* to be a promising CT gene.

Cutaneous T-cell lymphoma-associated antigen 1 (*CTAGE1*) has been identified to exhibit CT gene features when expressed in germline tissues (Almeida *et al*., 2009; Hofmann *et al*., 2008; Rousseaux *et al*., 2013). The expression analysis of *CTAGE1* by RT-PCR revealed that *CTAGE1* was exclusively expressed in testis and tumour tissues, including in the head and neck as well as in breast carcinoma, melanoma and colon carcinoma. Therefore, *CTAGE1* is a potential target for immunotherapy (Koch *et al*., 2003). The up-regulation of *CTAGE1* has been associated with aggressive tumours and poor prognostics, such as in patients with glioma, compared to the expression of *CTAGE1* in normal brain tissues (Akiyama *et al*., 2014). In addition, the expression of *CTAGE1* has been observed in patients with cutaneous T-cell lymphoma (Litvinov *et al*., 2014; Liggins *et al*., 2010). Here, the expression of *CTAGE1* was subjected to validation against a large panel of normal tissues; the TLDA card analysis method was used. *CTAGE1* was expressed solely in the testis tissues rather than in the normal tissues tested (Figure 4.3). Thus, this gene may be a good CT candidate. Therefore, the *CTAGE1* gene was further analysed with various types of tumour tissues and cell lines; however, *CTAGE1* was not detected in any of the cancer samples (Figure 4.4). However, according to the CT gene classification, *CTAGE1* gene was considered to be one of the genes that can be applied as a predictive biomarker in patients with aggressive tumours.

 The outer dense fibres of sperm tails 3 (*ODF3*) are among the genes that have been identified to be CT genes through different approaches (Almeida *et al*., 2009; Feichtinger *et al*., 2012a). *ODF3* belong to the family that encodes the protein that is essential for the development of the sperm tail and protects the sperm tail during the epididymal transition (Kierszenbaum, 2002; Lindemann and Lesich, 2016). Aberration in the expression of *ODF3* has been reported in various types of cancer, such as basal cell carcinoma (Ghafouri-Fard and Modarressi, 2012). Northern blot and western blot analyses were used to investigate the expression of *ODF3* in normal mouse tissues, and *ODF3*

was expressed in testis tissues but not in any of the nine normal tissues examined (i.e., the brain, heart, intestine, kidney, liver, lung, muscle, ovary and spleen tissues) (Carvalho *et al.*, 2002). In the present study, the expression of *ODF3* was validated with a panel of normal tissues, and *ODF3* was found to be expressed in testis tissues without any detected expression in the normal tissues examined (Figure 4.3). The expression of *ODF3* was investigated with other types of cancer panels, including cancer tissues and cell lines derived from various sources; however, *ODF3* was not expressed in any of the cancer samples tested, which may indicate the expression of *ODF3* could appear in types of cancer not included in our cancer panels. *ODF3* could be a potential target for certain types of tumours (Figure 4.4).

Leucine zipper protein 4 (*LUZP4*) has been identified as a CT/germline gene (Almeida *et al.*, 2009; Feichtinger *et al.*, 2012a; Rousseaux *et al.*, 2013). The function of *LUZP4* is poorly understood; it has been suggested that *LUZP4* may be associated with mRNA processes, including mRNA export. The up-regulation of *LUZP4* has been noticed in a wide range of tumours, including melanoma and breast cancer (Viphakone *et al.*, 2015; de Anda-Jáuregui *et al.*, 2016). The functional role of *LUZP4* in cancer may be as an oncogenic driver, as it is capable of enhancing tumour proliferation (Viphakone *et al.*, 2015). Another study has revealed that, in the multiple myeloma cell line, *LUZP4* was upregulated, whereas the knockdown of *LUZP4* was correlated with reducing the formation of multiple myeloma, which might be employed as a potential clinical biomarker for this type of tumour (Wen *et al.*, 2014). RT-PCR analysis was used to investigate the expression of *LUZP4* in normal and cancerous human tissues. The expression profile of *LUZP4* was found only in testicular tissues among the normal tissues tested, including colon, skeletal muscle, breast, kidney, tonsil, ovary, brain and peripheral blood mononuclear cell tissues. *LUZP4* was widely expressed in melanoma, colorectal carcinoma, teratocarcinoma, lung cancer, glioma and ovarian cancer (Tureci *et al.*, 2002). The expression of *LUZP4* was validated in this study in different types of normal and caner samples and cell lines. *LUZP4* exhibited undetectable expression within the range of all normal tissues, except testis (Figure 4.3). To address whether this gene could be a potential therapeutic target, *LUZP4* was further analysed with various types of cancer tissues and cell lines. Among the panel of cancer samples tested, the expression of *LUZP4* was demonstrated in two cancer tissues: recurrent malignant melanoma and colitis colon (Figure 4.4). Based on the TLDA card analysis method, *LUZP4* was demonstrated to be a CT gene

that was only expressed in the testis tissues. Our findings are supported by Tureci et al. (2002). The up-regulation of this gene could be useful as a cancer biomarker.

The methyl-CpG-binding domain protein 3-like 1 (*MBD3L1*) gene is a CT gene that has been demonstrated previously to be a specific germline tissue (Feichtinger *et al*., 2012a; Rousseaux *et al*., 2013). *MBD3L1* was highly expressed in testis compared to other normal tissues, such as pancreas tissues, and the role of this gene is to encode protein involved in the regulation of gene transcription and repression by methylation processes(Jiang*et al*., 2004; Rauch and Pfeifer, 2005; Albalat *et al*.,2012). The MBD3L1 protein creates complexes with a high affinity for methylated DNA and may target tumour suppressor genes, which inhibit the activation of this gene in the development of tumours (Rauch *et al.*, 2006; Riebler *et al*., 2014). TLDA card analysis was employed to validate the expression pattern of *MBD3L1* in 34 normal human tissues, including testis tissue, and was expressed in testis tissue without any detectable expression in the other normal samples tested (Figure 4.3). In this study, *MBD3L1* was further analysed with multiple cancer samples, and *MBD3L1* was expressed in three different types of tumourous tissues: ovarian cancer (ADC 2), melanoma (MM 2) and colon cancer (C9) (Figure 4.4). Feichtinger et al. (2012a) demonstrated the expression of *MBD3L1* in an ovarian cancer cell line. More knowledge of the functional role of *MBD3L1* in cancer development and its direct effect on tumour suppressor genes will require further investigation. Due to the expression of this gene, it can be characterised as a promising CT gene.

Placenta-specific1 (*PLAC1*) has also been characterised as a CT gene that may function as a biomarker for some cancers, such as epithelial ovarian cancer (Almeida *et al*., 2009; Tchabo *et al*., 2009). *PLAC1*, which is a trophoblast gene, has been observed in the placenta at high levels, whereas it was detected in low levels in testis tissue. During placenta development, *PLAC1* is acquired in order to complete normal growth, and the loss of *PLAC1* is correlated with placenta (Fant *et al*., 2010; Jackman *et al*., 2012; Muto *et al*., 2016). The aberrant expression of *PLAC1* has been implicated in several types of tumours, including colon, liver, endometrial, breast, gastric and lung cancers in addition to human cancer cell lines. Therefore, *PLAC1* has been reported to be a potential therapeutic target (Yuan *et al*., 2015; Liu *et al*., 2014; Liu *et al*., 2012; Kumara *et al*., 2012). A deficiency of *PLAC1* during pregnancy can result in death (Muto *et al*., 2016). Mutations in tumour suppressor genes, such as *TP53*, have been implicated in the up-regulated expression of

PLAC1 in most cancer cell lines by effecting the promoter of this gene, which led to the loss of promoter suppression in somatic tissues (Chen *et al*., 2013; Pichiorri *et al*., 2010). RT-PCR analysis was applied to validate the expression of *PLAC1* in normal human tissues, and its expression was demonstrated in two placenta samples among nine tissue samples (i.e., adrenal gland, bone marrow, cerebellum, brain, fetal liver, fetal brain, heart, prostate and testis) (Tchabo *et al*., 2009). Another study revealed that *PLAC1* was observed with measurable expression in the testis, brain cerebellum and placenta among 20 normal tissues that were screened by qRT-PCR (Wang *et al*., 2014). Previously, *PLAC1* was identified as a CT gene. In the current work, the expression of *PLAC1* was investigated using the TLDA card analysis method with 34 normal tissues obtained from various sources. *PLAC1* was expressed in testis but exhibited undetectable expression in all of the normal tissues used (Figure 4.3). The expression of *PLAC1* was further studied in various cancer sample tissues and cell lines; it was expressed in multiple cancer tissues, including ovarian cancer (ADC3) and lung cancer tissues (ADC3, SCC2 and ADC4) and in two cell lines (SK-BR-3 and OVCAR-10) (Figure 4.4). Our results confirm that *PLAC1* is an important biomarker for different types of cancer.

4.3.2   Expression of testis/CNS-restricted genes

An evaluation of the expression of this cohort of genes re-validated that 9 of the 156 genes tested were exclusively expressed in the testis and CNS tissues; therefore, these genes were classified as testis/CNS-restricted genes (Figure 4.5). One of the genes belonging to this category—equatorin (*EQTN*), also termed chromosome 9 open reading frame 11 (*C9orf11*)—has been identified as a novel CT gene (Feichtinger *et al*., 2012a; Rousseaux *et al*., 2013). Northern blot hybridisation was employed to determine the expression of *C9orf11* in normal human tissues, and it was observed to have a high level of expression in the testis tissue in a panel of normal tissues, including heart, kidney, pituitary gland, placenta, amygdala, jejunum, salivary gland and thymus tissues, in which it exhibited minor expression (Ruiz *et al*., 2000). *C9orf11* has been postulated to have multiple transcriptional variants, such as those missing exons 7 and 8 in testis. *C9orf11* may be involved in the mechanism that leads to the creation of the membrane organelles during the process of spermatogenesis that are known as acrosomes (Li *et al*., 2006; Ito *et al*., 2014). In human lung cancer, the chromosome region (9p21) in which *C9orf11* is located was found to be deleted, such that aggressive tumour behaviour with poor NSCLC prognoses are associated with the loss of this

gene on chromosome 9p (Kang *et al*., 2010), chronic lymphocyte leukaemia (Baltiþ *et al*., 2008), colorectal cancer (Leary *et al*., 2008) and breast cancer(Baltiþ *et al*., 2008; da Cunha *et al*., 2013). In this study, the expression profile of *C9orf11* was investigated in a panel of normal human tissues, including testis, by the TLDA analysis method. *C9orf11* was expressed in the testis and CNS tissues (i.e., the brain cerebellum and spinal cord) but not in any of the 34 normal tissues that were examined (Figure 4.5). Consequently, *C9orf11* was defined and characterised as a testis/CNS-restricted gene, and *C9orf11* was further analysed in human cancer tissues and cell lines. Among these cancer samples, the expression profile of *C9orf11* was detected only in one cancer tissue (MM1) (Figure 4.6). However, *C9orf11* may be expressed in different types of tumours not used in the current study. Our findings confirm that *C9orf11* is one of the large group of CT genes and that it can be applied as a clinical immunotherapeutic target for cancer tumours, including melanoma.

4.3.3   Expression of testis-selective genes

A group of selected genes were expressed in testicular tissues and in a limited number of somatic tissues. Based on the TLDA card analysis, 11 of 156 genes were validated and classified as testis-selective genes because they presented in one or two normal tissues, including the testis (Figure 4.7). These 11 genes could be considered as biomarkers that might be useful for some types of tumours. One such example is the structural maintenance of chromosome 1B (*SMC1β*), a meiosis-specific gene that encodes the subunits of the cohesin SMC1β protein, which is essential for holding sister chromatids together, chromosome synapsis and preventing the rearrangement of telomeres (Mannini *et al*., 2015; Biswas *et al*., 2013; Daniel *et al*., 2014). *SMC1β* has been identified as having CT gene features and may play an important role leading to chromosome instability in tumours (Feichtinger *et al*., 2012a; Strunnikov, 2013). A deficiency of SMC1β has been found to cause infertility in mice (Mannini *et al*., 2015). Recently, *SMC1β* was identified to be mutated in some cancers, such as in urothelial bladder cancer (Balbás-Martínez *et al*., 2013). and in the early stages of cancer, polymorphisms in *SMC1β* were located in the microRNA binding site of this gene capable of associating with these cancers, including head and neck cancers (Zhang *et al*., 2010) and oropharyngeal cancer (De Ruyck *et al*., 2014). This indicates the key role of *SMC1β*, as any mutation that occurs will affect its function and enhance the transformation of normal cells to cancerous cells (Mannini *et al*., 2015). In the present study, the expression profile

of *SMC1β* was analysed and validated against 34 normal human tissues using the TLDA card method. *SMC1β* exhibited expression in the testis and in two normal tissues— fetal liver and normal colon sample B26—among the samples examined (Figure 4.7). In the panel of cancerous tissues and cell lines, *SMC1β* was further investigated to assess whether it could function as a good CT gene and be considered a biomarker to be applied in the diagnoses and prognoses of some cancers. Among these cancer samples and cell lines, *SMC1β* presented with measurable expression in six cancer tissues, including ovarian cancer [ovarian serous papillary adenocarcinoma (OSPA 2, OSPA 3), and ADC 3] lung cancer (SCC1 and ADC5), colon cancer sample 23 and three cancer cell lines (SK-BR-3, OVCAR-10 and OVCAR-8) (Figure 4.8). Our findings based on the TLDA card analysis confirm that SMC*1β* could be an excellent biomarker for various types of cancer because it is unexpressed in normal tissues and may be oncogenic with potential targets for cancer treatment.

4.3.4   Expression of testis/CNS-selective genes

Among the large cohort of genes examined, 14 genes revealed expression profiles in no more than two normal tissues rather than testis/CNS tissues as members of the class of genes denoted testis/CNS-selective genes (Figure 4.9). Spermatogenesis-associated 19 (*SPATA19*) has been identified and characterised as a germline gene (Almeida *et al*., 2009; Rousseaux *et al*., 2013). *SPATA19* is a novel gene that regulates spermatogenesis in testis; therefore, as a spermatogenesis-associated gene, the dysfunction of this gene may contribute to infertility (Miyamoto *et al*., 2003; Nourashrafeddin *et al*., 2014b). *SPATA19* encodes protein that might be involved in biological functions including development and differentiation (Suzuki-Toyota *et al*., 2007) as well as cell reproduction (Wang *et al*., 2012). In tumours, *SPATA19* may play an essential role that enables the growth of tumour cells that have acquired excessive energy, as it is implicated in the maintenance of mitochondria (Ghafouri-Fard *et al*., 2010; Nourashrafeddin *et al*., 2014a). The aberrant activation of *SPATA19* has been associated with aggressive tumours in patients with prostate cancer and basal cell carcinoma (Ghafouri-Fard *et al*., 2010). In the current work, *SPATA19* was re-validated using a large panel of normal human tissues, including testis, and *SPATA19* demonstrated expression in the testis, CNS and normal colon sample B35 (Figure 4.9). Thus, *SPATA19* was subjected to further analyses with a range of cancer tissues and cell lines. Even though *SPATA19* was not observed in any of these cancer samples, *SPATA19* is considered

a CT genes that may show expression in other cancer tissues not covered in this work. Further, *SPATA19* may be a potential biomarker for cancer immunotherapy (Figure 4.10).

4.3.5   Expression of dismissed genes

The source and expression profiles of other CT genes were selected, analysed and validated. *ATAD2*, *CEP55*, *SPAG9*, *TGIF2*, *TRIP13* and *TCFL5* were expressed in all or most of the normal tissues tested. *CCDC79*, *DAZL*, *STK31*, *SPANXE*, *SPANXC* and *SYNGR4* were detected in some normal tissues (Figure 4.11).

In the ATPase family, the AAA domain-containing 2 (*ATAD2*) a CT gene that belongs to the cohort of genes included in the CT database (Almeida *et al*., 2009). This gene has been found to be an essential element to control cell functions, including proliferation, differentiation and apoptosis (Wu *et al*., 2014b). The aberrant activation of *ATAD2* genes has been detected in various types of cancer, including lung cancer, breast cancer, large β-cell lymphoma and hepatocellular carcinoma (Hsia *et al*., 2010; Wu *et al*., 2014a) and expression is linked to poor prognosis (for example, see Caron *et al*., 2010; Kalashnikova *et al*., 2010; Hwang *et al*., 2015; Luo *et al*., 2015; Zhang *et al*., 2015; Hou *et al*., 2016). Based on the TLDA method used in this study, the expression profile of *ATAD2* was extensively exhibited in the normal tissue samples that were tested. Among the 34 normal tissues examined, *ATAD2* was detected in all the samples except in the heart and in the salivary gland. According to our findings, this gene should be re-validated and potentially excluded as a CT gene (Figure 4.11).

The centrosome protein 55 (*CEP55*) gene, also known as the *C10orf3* gene, was identified as a CT gene in the CT database (Almeida *et al*., 2009). During the cell cycle, *CEP55* may play a fundamental role due to the localisation of this gene in the centrosome; recently, the up-regulation of this gene has been noted in several types of tumours, including breast cancer (Wang *et al*., 2016), colon carcinoma (Sakai *et al*., 2006) and gastric specimens (Tao *et al*., 2014). The overexpression of *CEP55* has been associated with aggressive tumours and poor prognoses (Jeffery *et al*., 2016). According to Hofmann's CT gene classification (2008), other studies have identified *CEP55* and classified as a testis-selective gene (Shiraishi *et al*., 2011). In contrast, in this study, re-validating the expression of *CEP55* with multiple normal tissue samples revealed

that *CEP55* was detected in most of the tested samples, such as the fetal liver, lung 2, bone marrow, colon w/ mucosa, small intestine, stomach and normal colon B19 and B20 samples (Figure 4.11).

The sperm-associated antigen 9 (*SPAG9*) gene, also known as the *CT89* gene, was reported to be a CT gene, and it has been classified as a testis-selective gene (Almeida *et al*., 2009; Hofmann *et al*., 2008). Recently, the role of *SPAG9* in cancer cells has been described to enhance cell proliferation and invasion. *SPAG9* is a cancer biomarker because it is expressed in various types of tumours (Xie *et al*., 2014; Li *et al*., 2014). RT-PCR was performed to investigate the expression of *SPAG9* in a cohort of patients with lung cancer, and *SPAG9* was highly expressed in lung cancer tissues, whereas it showed a low level of expression in adjacent lung sample tissues; therefore, it may serve as a potential marker for lung cancer (Ren *et al*., 2016). Further, *SPAG9* has been reported to be a CT gene that can detect tumours in their early stages, such as in cervical cancer, ovarian and breast cancer (Garg *et al*., 2007; Garg *et al*., 2009; Kanojia *et al*., 2009), as well as in endometrial cancer (Baser *et al*., 2013). The fusion between *SPAG9* and *JAK2* has been associated with acute lymphoblastic leukaemia and poor outcomes (Kawamura *et al*., 2015). The validation of the expression profile of *SPAG9* in this study revealed that *SPAG9* was observed in 34 normal sample tissues, such as the liver, lung 1 and 2, prostate, salivary gland, bone marrow, trachea, uterus, colon w/mucosa and normal colon sample B20 (Figure 4.11). Our findings based on the TLDA method and a stringent threshold indicate that *SPAG9* is not considered to be a promising gene.

The TGFB-induced factor homeobox 2 (*TGIF2*) gene is a CT gene that has been identified as a human orthologue of the *Drosophila* germline gene. The overexpression of this gene has been observed to occur in brain tumours (Feichtinger *et al*., 2014; Janic *et al*., 2010). *TGIF2* has been suggested to have an important function as a transcription factor due to its presence in the nucleus (Imoto *et al*., 2000; Rashvand *et al*., 2013). *TGIF2* is highly expressed in some human cancer tissues, including the kidney, testis, heart and ovarian cancers (Hu *et al*., 2011; Jin *et al*., 2005). Further, the up-regulation of *TGIF2* expression might be used as a biomarker in some cancers, such as rectal cancer (Lips *et al*., 2008). Recently, *TGIF2* has been observed to target microRNAs and to contribute to the metastasis of diseases, such as bone metastases (Coleman, 2012; Ell and Kang, 2012). Our analyses demonstrated that the expression of *TGIF2* was widely detected in all the types of normal human tissues tested, including fetal liver, liver, heart, lung 1 and 2, salivary

gland, bone marrow, trachea, uterus, colon /mucosa, small intestine, stomach and ovary tissues (Figure 4.11). The expression profiles of *TGIF2* in normal tissues in the current study indicate that this gene, among others, should be excluded as specific germline genes.

The thyroid hormone receptor interactor 13 (*TRIP13*) gene, which encode protein and is a member of a family that is responsible for the regulation of cell functions. Studies have proposed that the TRIP13 protein may have a role in NHEJ, because some NHEJ proteins bind with *TRIP13* (Ding *et al*., 2006; Banerjee *et al*., 2014). In aggressive tumours, *TRIP13* was overexpressed, such as in head and neck tumours (Banerjee *et al*., 2014). In patients with prostate cancer, *TRIP13* can be applied as a biomarker (Larkin *et al*., 2012). The overexpression of *TRIP13* in human cancer cell lines stimulates cell proliferation and invasion (Banerjee *et al*., 2014). The *TRIP13* gene has been implicated in the mitotic checkpoint-silencing mechanism, which may enhance chromosome instability and may affect chromosome segregation (Wang *et al*., 2014). In the current work, *TRIP13* was expressed in 32 of the 34 normal human tissues examined, with the exception of the heart and the salivary gland, which indicates that *TRIP13* cannot be a CT gene (Figure 4.11).

In a previous study, the transcription factor-like 5 (*TCFL5*) gene has been demonstrated to be a CT gene with restricted expression in germline tissues (Siep *et al*., 2004). *TCFL5* has been reported to be overexpressed in some forms of epithelial cancer, such as in prostate, colon and breast cancer (Carvalho *et al*., 2009; Dardousis *et al*., 2007). The TCFL5 protein may contribute to cell proliferation or differentiation; also, *TCFL5* was observed to be associated with cancer development (Dardousis *et al*., 2007). A western blot analysis was conducted to assess the expression of the TCFL5 protein in mice. TCFL5 was only found in testicular tissue but not in other normal lysate tissues that were tested, including heart, brain, spleen, lung, liver, stomach muscle, and kidney (Shi *et al*., 2013). The role of *TCFL5* in chromosome instability has been demonstrated to enhance the progression of cancer. In addition, *TCFL5* may serve as a potential clinical biomarker in some tumours, such as colorectal tumours (Carvalho *et al*., 2009), and indicates poor prognostic signs in patients with acute lymphoblastic leukaemia (Silveira *et al*., 2013). In this study, the expression profiles of *TCFL5* were detected in all the normal tissues tested except in the normal colon sample B45. For example, *TCFL5* was expressed in fetal liver, liver, lung 1, salivary gland, bone marrow, trachea, uterus, colon w/mucosa and small intestine samples. Our findings suggest that the expression of *TCFL5* may not be restricted to germline tissues.

Therefore, *TCFL5* should be excluded from the list of CT gene candidates, as its profile was expressed in multiple normal tissues derived from different sources.

CCDC79, also known as the telomere repeat binding bouquet formation protein 1 (*TERB1*), was selected for testing because it has been identified as a germline gene (Feichtinger *et al*., 2012a; Rousseaux *et al*., 2013). Recently, the expression profile of *CCDC79* was found to occur preferentially in the testis. In meiotic processes, *CCDC79* encodes the protein required for telomere interaction and/or movement. The loss of CCDC79 may affect the efficiency of SMC1B, which leads to the instability of telomeres during the meiotic process (Daniel *et al*., 2014). Based on TLDA analysis, *CCDC79* was observed in eight normal somatic tissues—non-testis or CNS— including liver, lung 2, bone marrow and normal colon samples B20, B22, B33, B38 and B45. According to the CT gene categories, *CCDC79* was excluded from consideration as a good candidate at this stage (Figure 4.11).

Another gene is deleted in azoospermia-like (*DAZL*). The overexpression of this gene has been observed to be associated with brain tumours in the *Drosophila* germline, which indicates the important role of this gene, as it is implicated in oncogenesis in *Drosophila* (Janic *et al*., 2010). As a human orthologue of the *Drosophila* germline, it has been identified as an excellent cancer biomarker, as this gene is expressed in a variety of human cancers (Feichtinger *et al*., 2014), and it also has been reported to be a germline gene (Rousseaux *et al*., 2013). *DAZL* plays a critical role in germ cell development, as it encodes the RNA-binding protein (RBP) that is involved in germline processes, including germline differentiation and regulation (Smorag *et al*., 2014; Panula *et al*., 2016). A loss of *DAZL* will affect germ cells, which leads to cell apoptosis and affects the structure of chromatin (Schrans-Stassen *et al*., 2001; Lin and Page, 2005). The overexpression of *DAZL* has been demonstrated in various types of breast cancer cell lines and tumours by qRT-PCR (Mobasheri *et al*., 2015). DAZL was studied at the protein level and was detected only in testicular tissue obtained from adult humans and was not found in the prostate and testis that were derived from patients with Sertoli cells only (Ruggiu *et al*., 2000). Another study performed using northern blot analysis to assess the expression of *DAZL* within normal tissues demonstrated that *DAZL* appeared to be expressed only in the testis and not in other somatic tissues; however, a limited number of normal tissues was tested (Yen *et al*., 1996). In the current study, the *DAZL* gene was expressed in some normal human tissues including bone marrow, small intestine, and ovary 25L

and 25R and normal colon B20 and B23 samples. Therefore, *DAZL* was dismissed at this stage for further analysis with cancer cells and might be excluded as a CT gene candidate (Figure 4.11).

Serine/threonine kinase 31 (*STK31*) is another gene that has been characterised as a CT gene, as it is restrictedly expressed in germline tissues (Rousseaux *et al*., 2013). A previous study of human colorectal cancer cell lines and tissues revealed that the overexpression of *STK31* may contribute to human cancers; *STK31* was highly expressed compared to the normal tissues obtained from the same patient when qRT-PCR was applied (Kuo *et al*., 2014). In the testis tissue, the level of *STK31* was lower in patients who had immature germlines, whereas the level of *STK31* in normal men was highly expressed (Lin *et al*., 2006). The function of *STK31* remains unclear; however, *STK31* may affect the mitotic progression that leads to cell apoptosis. Also, STK31 contributes to the regulation of the cell cycle, as it is localised in the centrosome (Kuo *et al*., 2014). In colon cancer cells, the knockdown of STK31 was found to suppress tumourigenicity (Fok *et al*., 2012). In addition, *STK31* was found to be mutated in melanoma, which may permit its consideration as a potential target for melanoma treatment (Xia *et al*., 2014). According to this study, which performed by TLDA card analysis, the expression of *STK31* was observed among some normal tissues, such as fetal liver, lung 2, prostate and ovary 1, ovary 25L and 25R. Also, *STK31* was extensively expressed in the normal colon tissues adjacent to tumours, including B19, B20, B21 and B22. Our analytical results indicate that S*TK31* cannot be applied as a novel CT gene; however, that may result from the strategy used regarding the stringent cut-off threshold (Figure 4.11).

4.4 Conclusion

An extensive cohort of genes has been reported to be potential novel CT genes and the unique features that might make them useful as potential biomarkers in various types of cancer and as therapeutic targets in cancer immunotherapy was investigated. Their expression was validated and classified to determine their promise. A total of 156 CT genes were selected from 5 sources, and the research addressed whether these genes could be utilised as clinical biomarkers for cancer. These genes were validated with a range of normal human tissues and cancer samples and cell lines with a TLDA card analysis. Out of the 156 genes, 101 were confirmed to be CT genes. Subsequently, these candidate genes were classified depending on their expression behaviour as

follows: 67 testis-restricted genes that were expressed only in the testis; 9 testis/CNS-restricted genes that were expressed in the testis and CNS tissues but not in other normal tissues; 11 testis-selective genes that were expressed in the testis and in no more than two somatic tissues and 14 testis-CNS-selective genes. Some genes showed no expression among the cancer sample panels tested; however, these genes were considered candidates and were classified because they might be derived as cancer biomarkers in cancer sample types that were not covered in this study, such as *ASB17*, *BOLL*, *DNAJC5G* and *RNF17*. A group of 55 genes was dismissed as CT genes, as they demonstrated expression in various types of the normal and testicular tissues that were examined. Further investigation of the 101 genes confirmed to be CT genes is needed to determine whether they could be used clinically as predictive biomarkers. The exclusion of 55 genes was based on their expression profiles by applying the TLDA card analysis method with a stringent cut-off value.

Chapter 5.0 Treating Brachyury expressing cells with newly developed drugs

5.1 Introduction

The *Brachyury* (*T*) gene is a transcriptional factor belonging to the T-box family (Kispert and Herrmann, 1993; Edwards *et al.*, 1996; Naiche *et al.*, 2005). All these genes are characterised as having a conserved sequence-specific, DNA-binding T-box domain. The family of T-box genes is essential during embryo development in vertebrates due to its vital roles in the control of cell fate decisions, in the characterisation of body plans and in differentiation, as well as other organogenesis processes (Showell *et al.*, 2004;Wilson and Conlon, 2002; Papaioannou, 2014). The T-box family consists of five subfamilies: T, Tbx1, Tbx2, Tbx6 and Tbr1 (Naiche *et al.*, 2005) (Figure 5.1). Mutations of the *Brachyury* gene have resulted in the development of short tails in mice (Dobrovolskaia-Zavadskaia, 1927). In heterozygous mouse embryos, mutations affecting *Brachyury* have led to severe axial development and presacral vertebrae defects, whereas mutations targeting homozygous embryos caused embryos to die in about 10 days as defects in the primitive streak, the notochord is absent with abnormality in allantois (Gluecksohn-Schoenheimer, 1944; Papaioannou, 2001). Studies on gastrulation have revealed the critical role of the *Brachyury* gene in the development of the notochord, neural tube, and mesoderm (Pennimpede *et al.*, 2012; Satoh *et al.*, 2012) and it has also been described as contributing to cell movement (Nibu *et al.*, 2013). The *Brachyury* gene has been classified as a novel transcriptional factor with specific sequencing, localised in chromosome 6q27 (Edwards *et al.*, 1996). In some mammals, mutations affecting the *Brachyury* gene lead to outcomes and phenotypes similar to those occurring in mouse mutations; for example, mutations in the *Brachyury* gene were found to affect the tail length in some breeds of dogs (Hytonen *et al.*, 2009) as well as result in short tails in Manx cats (Buckingham *et al.*, 2013). This gene is implicated in human chordoma and inherited notochord tumours (Yang *et al.*, 2009, Pillay *et al.*, 2012; Nibu *et al.*, 2013). The *Brachyury* gene, therefore, is considered a good candidate for investigating phenotypical changes in the spinal cord and vertebral column of vertebrates (Kromik *et al.*, 2015). Overexpression of the *Brachyury* gene has been reported in various type of human tumours, including hemangioblastomas (Barresi *et al.*,

2012; Barresi *et al*., 2014) and non-small cell lung and breast carcinomas (Boyerinas *et al*., 2013). Its overexpression has also been detected in small intestine, stomach, kidney, uterus, bladder, ovary and testis tumours (Palena *et al*., 2007), other cancer cell lines derived from the colon (Palena *et al*., 2007; Kilic *et al*., 2011) and prostate carcinoma (Palena *et al*., 2007; Pinto *et al*., 2014). Expression of the *Brachyury* gene has not been observed in most normal tissues examined, other than testis which suggests it is a CTA gene and is a potential target for immunotherapy (Palena *et al*., 2007). However, it has been recently reported to define a sub-group of enteroendocrine cells in normal human colon crypts, so it might not be a highly restricted CTA gene (Jezkova *et al*., 2016). In aggressive tumours, such as those found in colorectal cancer (CRC), the expression of the *Brachyury* gene was found to be associated with poor prognoses, thus it might be useful to apply this gene as a biomarker for CRC (Kilic *et al*., 2011), gastrointestinal stromal tumours (Pinto *et al*., 2016) and in cases of poor clinical outcomes in patients with lung cancer (Shimamatsu *et al*., 2016).

The *Brachyury* gene, therefore, is a promising target as a CTA cancer biomarker drug target as it is implicated in several types of tumours. The aim of this chapter is to investigate the efficacy of newly developed drugs designed *in silico* to target the Brachyury. Briefly, in collaboration with the Drug Screening Platform at Cardiff University, we designed 19 drugs that might target the cancer-associated function of Brachyury in cells. These 19 drugs were selected *in silico* from among 6 million compounds; they were then tested on an SW480 cancer cell line that was treated with the drugs and subsequently subjected to qRT-PCR for analysis of the gene expression profiles. To determine whether expression of Brachyury target genes was altered. Currently, no human T domain Brachyury protein crystal structures are available, therefore, as a template, a homology model was built using the crystal structure of the T domain from *Xenopus laevis* Brachyury bound to DNA. The structure of the new model was investigated using a site finder tool in order to find potential binding sites for small molecule inhibitors. Selected amino acid areas (as potential binding sites) were used to screen the ZINC library of commercially available compounds containing around 6 million small molecules. A screening tool was used in order to quickly screen for the compounds capable of occupying the selected site. After visual inspection, the 19 best small molecules were ultimately selected, purchased and tested.
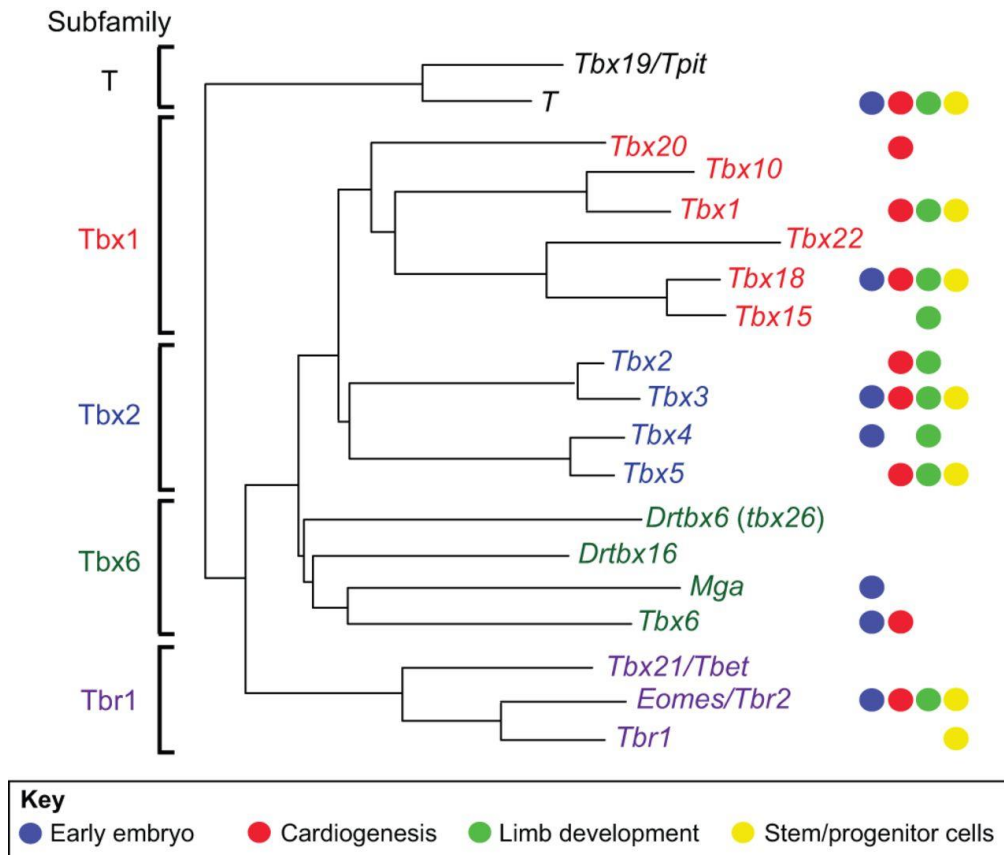
Figure 5.1 Phylogenetic tree of the T-box gene family of vertebrates.
The five subfamilies of genes are shown on the left; the colours of the circles on the right refer to their gene contribution. All these genes are present in humans and mice, except for *Drtbx6* and *Drtbx16*, which are zebrafish genes and are not found in mammals. Adapted from (Naiche *et al*., 2005).

5.2 Result

5.2.1 Investigating the efficacy of potential anti Brachyury drugs in a colorectal cancer cell line

To determine the efficacy of the 19 specific drugs, a Brachyury-positive CRC cell line, SW480, was treated with two different concentrations (10 μM and 100 μM) of each of the drugs, as well as dimethyl sulfoxide (DMSO) as a solute control. The knockdown of Brachyury in SW480 was performed using siRNA (T5) targeting *Brachyury*; the negative control siRNA (NI) was also used to treat SW480. SW480 cells were treated with one hit of the drugs and DMSO, while the (T5) and (NI) were treated with three hits. RNA was extracted after 72 hours for both concentrations of the drugs and DMSO, as well as for the (T5) and (NI). Then, cDNA was made and a positive control *ACTB* gene was used to determine the quality of the cDNA (Figure 5.2).

To monitor the efficiency of the Brachyury knockdown (T5) and the 19 drugs that were transfected with the SW480 cell line, qRT-PCR was applied with three control genes, *GAPDH*, *HSP90AB1* and *TUBA1C*. In a previous study, RNA-seq was performed to determine effects of *Brachyury* knockdown (T5) in the SW480 cells (Jezkova *et al.*, 2014) and, from the resulting data, some genes selected as their expression was associated with the depletion of Brachyury through the demonstration of up- or down-regulation. The expression profiles of these selected genes were compared to the RNA-seq results to determine whether the qRT-PCR analysis results were consistent with expression of the genes in RNA-seq (Table 5.1).

Table 5.1 Genes selected from the RNA-seq analysis data for Brachyury depletion in the SW480 cell line.

Down-regulated genes			
Gene	**Name**	**Function**	**Reference**
MFN2	Mitofusin 2	Required in mitochondrial processes such as mitochondrial fusion.	(Santel and Fuller, 2001; De Brito and Scorrano, 2008; Legros *et al*., 2002)
MSH2	Mut S homolog 2	DNA mismatch repair gene; an encoded protein that repairs any errors during the cell replication process that occurs in the S phase.	(Lagerstedt-Robinson *et al*., 2007; Zlatanou *et al*., 2011; Martín-López and Fishel, 2013; Dowty *et al*., 2013)
MEST	Mesoderm specific transcript	Might be involved in controlling the growth of adipocytes as well as lipid accumulation.	(Takahashi *et al*., 2005; Kamei *et al*., 2007; Nikonova *et al*., 2008; Jung *et al*., 2010; Karbiener *et al*., 2015)
CCNE1	Cyclin E1	Utilised during the cell cycle to control the G1 to S phase transition.	(Caldon and Musgrove, 2010; Hwang and Clurman, 2005; Satyanarayana and Kaldis, 2009)
MTHFD2	Methylene tetrahydrofolate dehydrogenase (NAD+ dependent), methenyltetrahydrofolate cyclohydrolase	A mitochondrial enzyme that participates in metabolic processes and is up-regulated in cancer.	(Pike *et al*., 2010; Nilsson *et al*., 2014)
Up-regulated genes			
CROT	Carnitine O-octanoyltransferase	Plays an important role in the metabolism of fatty acids.	(Le Borgne *et al*., 2011; Davalos *et al*., 2011; Gerin *et al*., 2010)
IGFBP3	Insulin-like growth factor binding protein 3	Induces mitosis and prevents cell apoptosis.	(Mohan and Baylink, 2002; Firth and Baxter, 2002; Hormones and Group, 2010)
SFRP5	Secreted frizzled-related protein 5	Tumour suppressor of Wnt antagonists.	(Veeck *et al*., 2008; Ouchi *et al*., 2010; Shenoy *et al*., 2015)

A

10 µM Drug

B

100 µM Drug
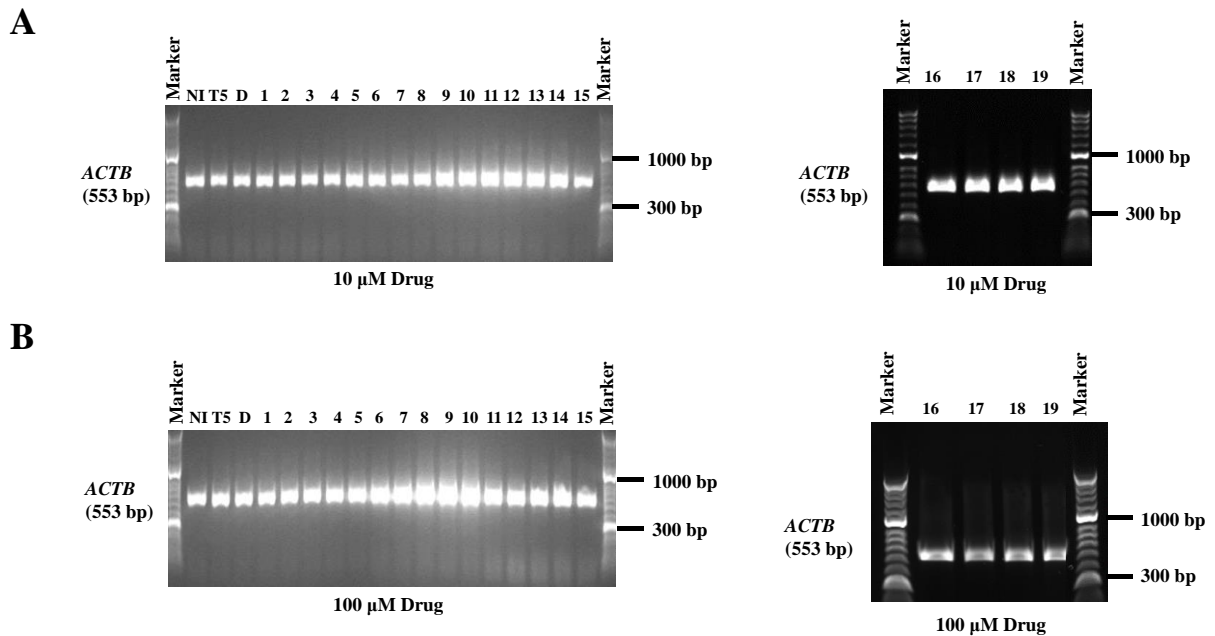
Figure 5.2 RT-PCR analysis of *ACTB* genes in an SW480 cell line treated with two different concentrations of potential anti-Brachyury drugs.
Agarose gel shows the expression profile of the positive control gene *ACTB* to monitor the quality of cDNA that was derived from the negative control siRNA (NI), *Brachyury* siRNA (T5), DMSO and 19 drugs, 72 hours after transfection with the SW480 cell line. (A) The drugs at a concentration of 10 µM. (B) The drugs at a concentration of 100 µM. The size of the actin PCR product positive control on the gel is 553 bp.

5.2.1.1 *Brachyury* gene expression

To address whether these 19 new drugs targeting Brachyury gene can affect expression of the *Brachyury* gene, including (T5), in SW480 cell, a *Brachyury* expressing cell line, was treated with the drugs. We conducted qRT-PCR to assess the expression levels of the *Brachyury* gene with the drugs at two different concentrations. The analysis revealed a significant reduction of *Brachyury* transcripts (T5) compared to (NI) in the SW480 cells. Among the drugs used for treatment at a concentration of 10 μM, only drugs 3 and 18 affected the transcript levels of the *Brachyury* gene, whereas other drugs, such as 2, 5, 7 and 10, showed up-regulation of the *Brachyury* transcripts (Figure 5.3A).

The *Brachyury* gene transcript level was down-regulated by some of the drugs at the 100 μM concentration. Interestingly, *Brachyury* exhibited down-regulated expression with drug 3 at both concentrations. Other drugs, such as 5, 12 and 14, that targeted this gene appeared to down-regulate *Brachyury* transcript levels compared to DMSO. Drugs that up-regulated the levels of *Brachyury* transcripts included 9, 10 and 13 (Figure 5.3 B).

5.2.1.2 Transcript analysis of down-regulated genes

Selected genes from the RNA-seq data (*MFN2*, *MSH2*, *MEST*, *CCNE1* and *MTHFD2*) appeared to be down-regulated with the *Brachyury* knockdown that was performed in the SW480 cells (Jezkova *et al*., 2014). The transcript levels of these genes were analysed to determine whether these transcripts were depleted following drug treatment in a similar fashion to the *Brachyury* siRNA treatment.

 MFN2 was down-regulated with (T5), which is consistent with the RNA-seq results (Jezkova *et al*., 2014). The transcript levels for *MFN2* were down-regulated with some of the drugs, such as drug 1, compared to DMSO. Up-regulation of *MFN2* transcripts was detected with some of the drugs, including 7, 8 and 13 (Figure 5.4 A). The transcript levels for *MFN2* were examined in the SW480 cell line that was treated with the drugs at the 100 μM concentration. Some of the drugs, including drug 1, down-regulated the transcripts of this gene, at this concentration. Some drugs, such as 7, 11, 16, 18 and 19 down-regulated transcripts, whereas *MFN2* transcripts level up-

regulated with drugs 3, 8, 15 and 17. However, drug 3 showed significantly up-regulated of *MFN2* transcripts compared to the other drugs (Figure 5.4 B).

Figure 5.5 demonstrates the expression of another gene among those selected to be down-regulated with the knockdown of *Brachyury*. The qRT-PCR analysis showed that the transcript profile of *MSH2* was down-regulated in SW480 cells treated with (T5) (Figure 5.5A and B). qRT-PCR analysis demonstrated that the transcripts of *MSH2* in (T5) were consistent with the RNA-seq results. *MSH2* exhibited down-regulated transcripts with drugs 3, 11 and 12 at a concentration of 10 μM, however, drug 3 had greater efficacy with regard to transcript levels than drugs 11and 12 at this concentration. Drugs 2 and 8 most significantly affected the up-regulation of *MSH2* transcripts (Figure 5.5A). Transcript levels of *MSH2* in SW480 cells treated with both concentrations of the drugs revealed that some of them inhibited down-regulation, such as drug 3, as well as drugs 1, 13 and 15, but with less efficiency, whereas up-regulated of *MSH2* transcripts was detected with drugs 2, 6, 7 and 19 (Figure 5.5 B).

Another gene was selected from the RNA-seq whose down-regulated transcript levels was found to be associated with knockdown of the *Brachyury* gene. In order to investigate the transcript levels of the *MEST* gene, qRT-PCR was performed. Transcript levels for this gene was observed in (T5), which was consistent with the RNA-seq data analysis results, and confirmed with both concentrations of the drugs (Figure 5.6A and B). The transcript pattern for *MEST* was investigated with the 19 drugs to assess their efficacy according to which drugs are able to up- or down-regulate transcript levels of the gene. In the SW480 cell line treated with the 19 drugs at the 10 μM concentration, the expression profile of *MEST* was affected most effectively by drugs 3, 14 and 15 as well as other drugs, such as drug 4, however, these drugs' abilities to target and down-regulate transcript levels of *MEST* was observed to be less effective. The transcripts from *MEST* were up-regulated with some of the tested drugs, including 7 and 18 (Figure 5.6 A). Other experiments that were performed in the SW480 cells with drugs at a concentration of 100 μM revealed that the drugs down-regulated the *MEST* transcript levels. Interestingly, drug 3 at both concentrations was the most promising drug in down-regulating the transcripts of *MEST*. Other drugs that showed down-regulated transcripts of *MEST* included 7, 12 and 16, which had greater efficacy than drugs 6, 11, 14 and 18. In contrast, some drugs, such as drug 2, up-regulated the level of *MEST* transcripts (Figure 5.6 B).

The *CCNE1* gene was among the genes that appeared to be down-regulated as a result of *Brachyury* gene knockdown. The transcripts levels of *CCNE1* was consistent with the results of the RNA-seq that was carried out previously (Jezkova *et al*., 2014) and that indicated the important function of the *Brachyury* gene which affected other genes. *CCNE1* was expressed in drug-treated SW480 cells and down-regulation of transcripts from this gene was observed with drugs at a concentration of 10 μM, including 3, 4 and 9, which were more effective than others. Drugs 5, 8 and 14 demonstrated efficacy, however, less so than drugs 3, 4 and 9. *CCNE1* was observed to have up-regulated transcript levels with drugs 6, 7, 13, 16 and 18 (Figure 5.7A). Transcript levels from the *CCNE1* gene were analysed with these drugs at the 100 μM concentration to investigate whether different conditions could affect the transcript levels of the gene, which is essential for determining the drugs' efficacies. Drug 3 was detected at the two concentrations, which may indicate that it was the most effective among the drugs that down-regulated the gene transcript levels. Furthermore, among the 19 drugs, 6, 7, 11, 12, 16 and 18 were observed to down-regulate the levels of *CCNE1* transcripts, whereas other drugs, such as 8 and 10, showed their effectiveness by up-regulating *CCNE1* transcripts (Figure 5.7B).

MTHFD2 exhibited down-regulated transcript levels associated with knockdown of the *Brachyury* gene in SW480 cells. qRT-PCR analysis was used to assess the transcripts from this gene in a large group of drugs as well as in (T5). RNA-seq analysis demonstrated that transcripts of *MTHFD2* were down-regulated with *Brachyury* knockdown, and qRT-PCR analysis confirmed the result. Then, the transcript levels of *MTHFD2* were investigated with the 19 drugs at the two concentrations to determine the drugs' efficacies on the target genes. Transcript levels from the *MTHFD2* gene was detected in the SW480 cells treated with the 19 drugs. *MTHFD2* transcripts were reduced at a concentration of 10 μM, specifically with drugs 6, 7 and 11, whereas most of the drugs demonstrated significant transcript up-regulation, as observed with drug 3 (Figure 5.8A). The efficacies of drugs that target transcript levels were investigated at the 100 μM concentrations in the SW480 cells. The transcript profile of *MTHFD2* was found to be down-regulated with some drugs, such as drug 2 and drug 6. At both concentrations, drug 3 up-regulated the transcripts from *MTHFD2* (Figure 5.8 B).
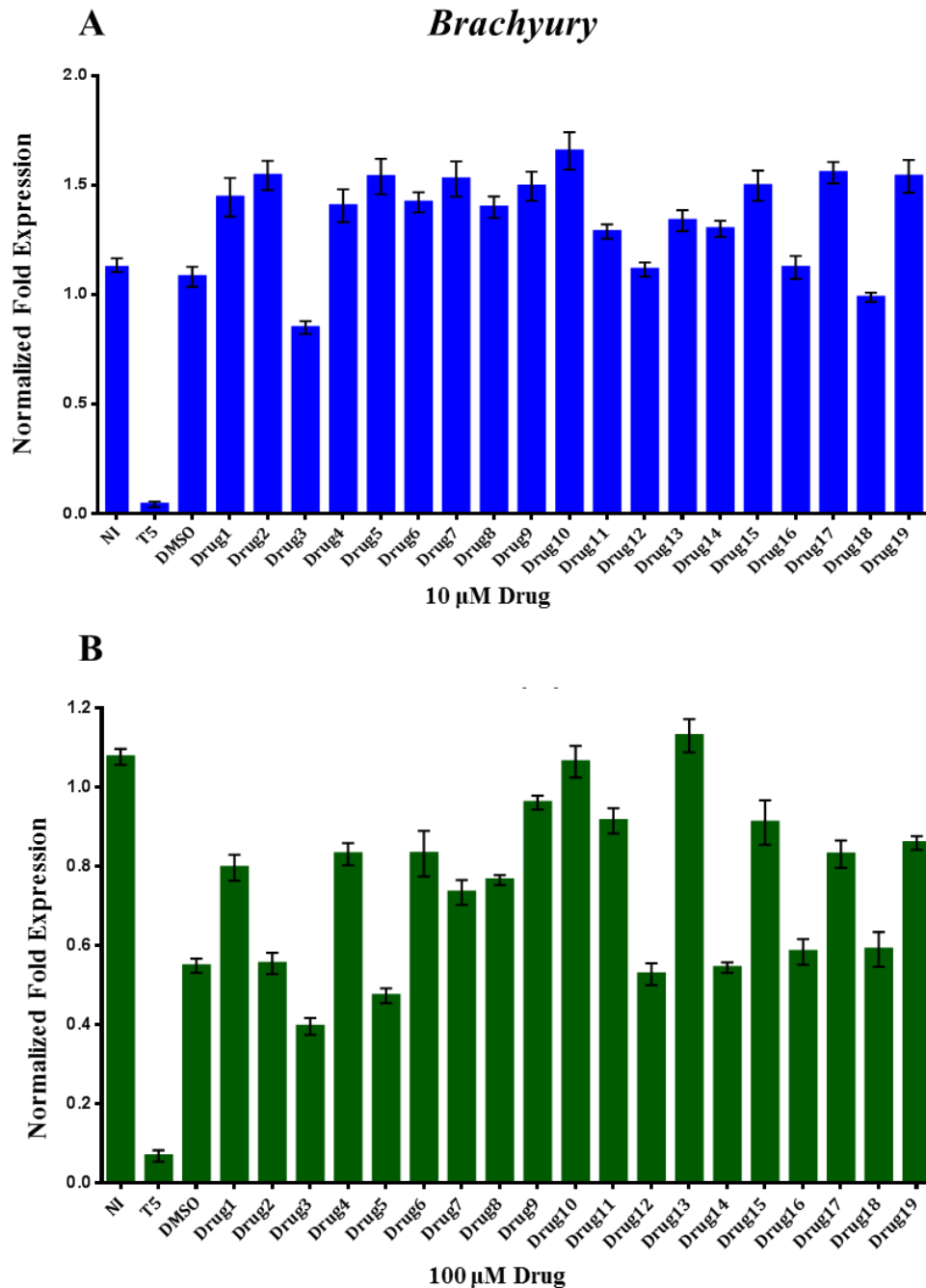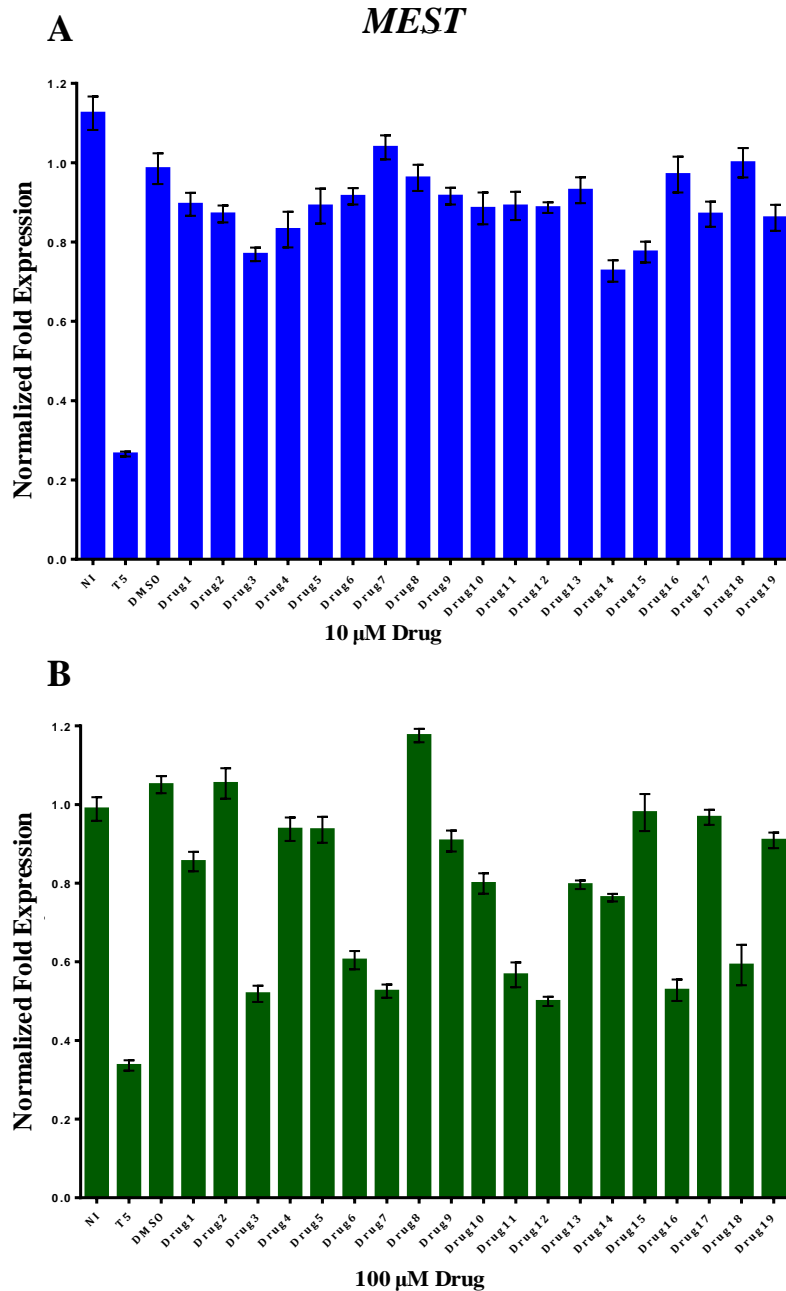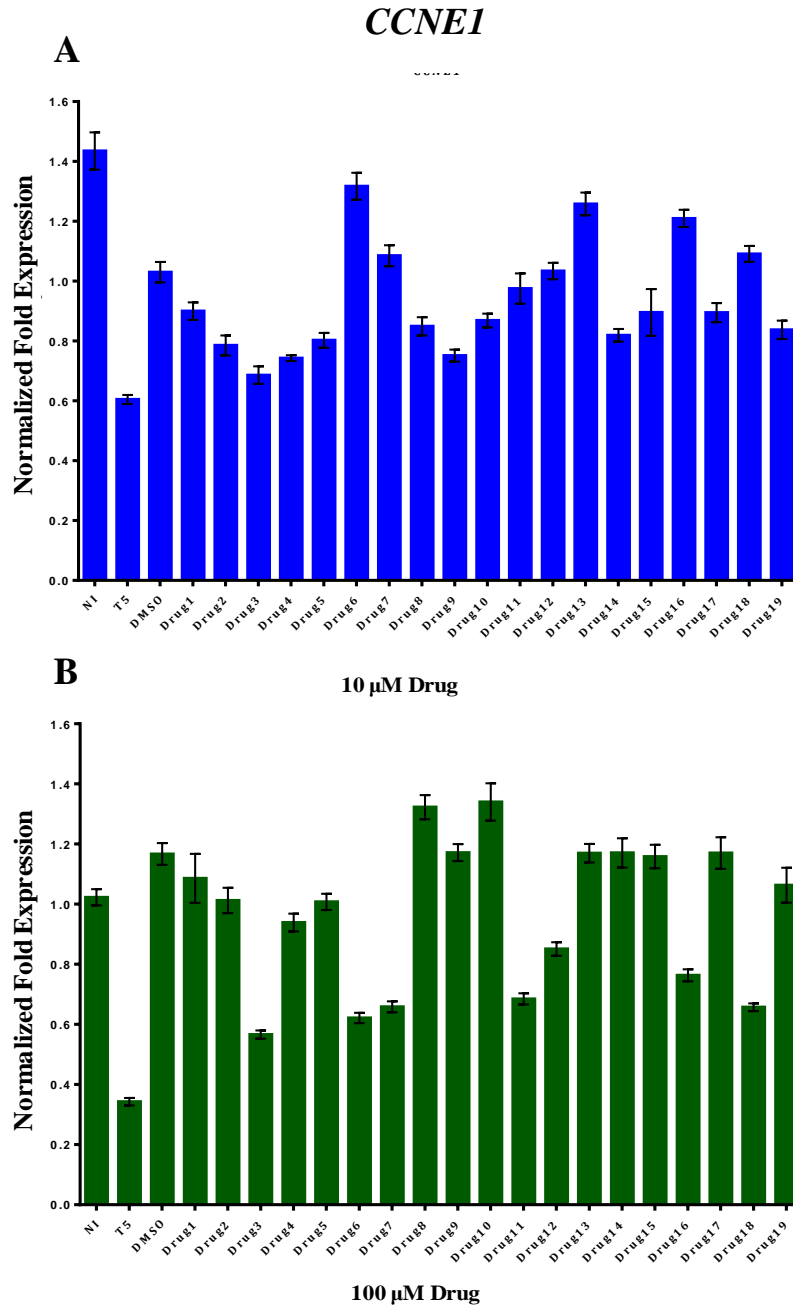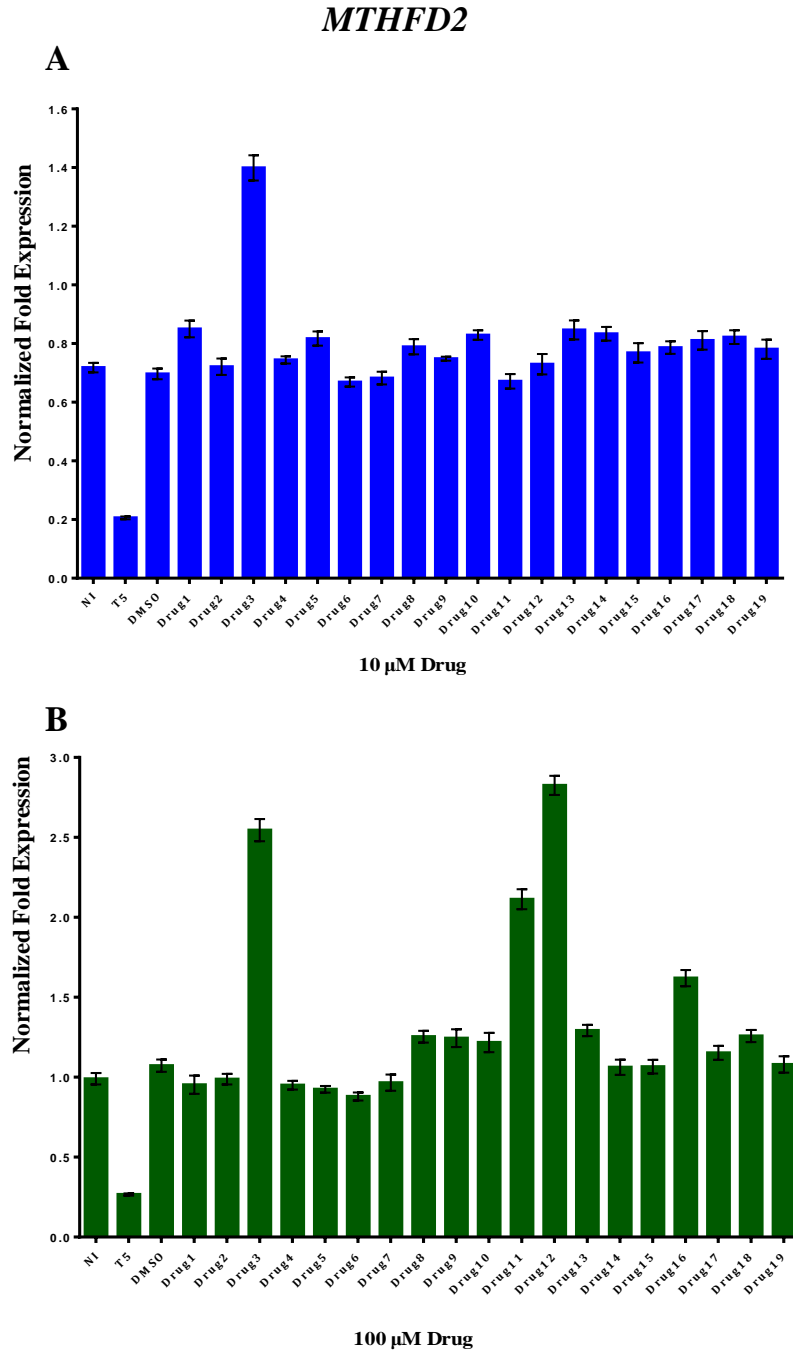
Figure 5.3 Transcript levels of the *Brachyury* mRNA in SW480 cells treated with the two drug concentrations.

Analysis of transcript levels in SW480 cells transfected with negative control siRNA (NI), *Brachyury* siRNA (T5), the 19 drugs and DMSO to assess the efficacies of the drugs. (A) SW480 cells treated with the 19 drugs at a concentration of 10 μM. (B) SW480 cells treated with the 19 drugs at a concentration of 100 μM. The results were normalized using three endogenous reference genes (*GAPDH*, *HSP90AB1* and *TUBA1C*) and the relative fold-change was computed using the ΔΔCt method. Error bars represent the standard error of the mean for triplicate replication.

MFN2

A

B
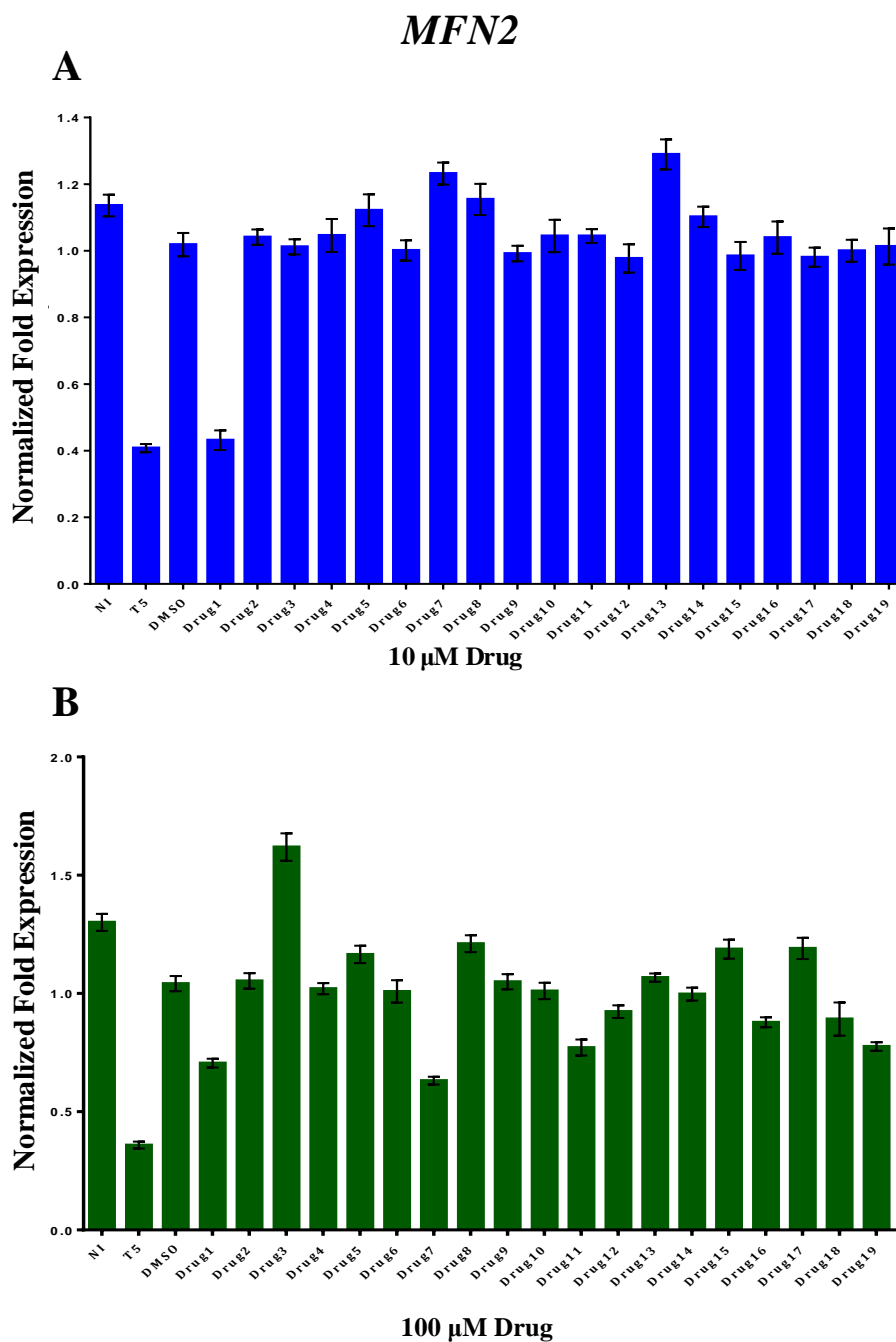
Figure 5.4 Transcript levels of the *MFN2* mRNA in SW480 cells treated with the two drug concentrations.

Analysis of transcript levels in SW480 cells transfected with negative control siRNA (NI), *Brachyury* siRNA (T5), the 19 drugs and DMSO to assess the efficacies of the drugs. (A) SW480 cells treated with the 19 drugs at a concentration of 10 µM. (B) SW480 cells treated with the 19 drugs at a concentration of 100 µM. The results were normalized using three endogenous reference genes (*GAPDH*, *HSP90AB1* and *TUBA1C*) and the relative fold-change was computed using the ΔΔCt method. Error bars represent the standard error of the mean for triplicate replications.
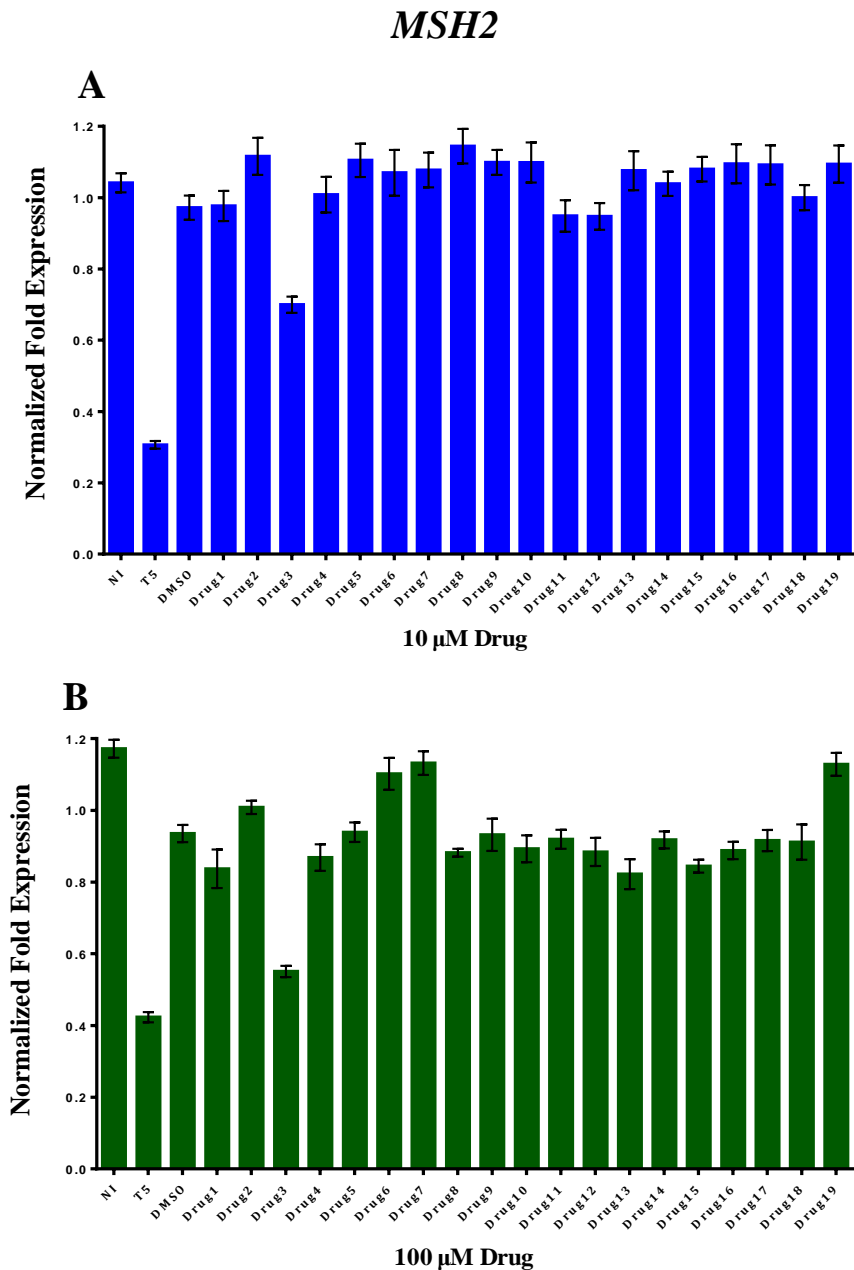
MSH2

Figure 5.5 Transcript levels of the *MSH2* mRNA in SW480 cells treated with the two drug concentrations.
Analysis of transcript levels in SW480 cells transfected with negative control siRNA (NI), *Brachyury* siRNA (T5), the 19 drugs and DMSO to assess the efficacies of the drugs. (A) SW480 cells treated with the 19 drugs at a concentration of 10 μM. (B) SW480 cells treated with the19 drugs at a concentration of 100 μM. The results were normalized using three endogenous reference genes (*GAPDH*, *HSP90AB1* and *TUBA1C*) and the relative fold-change was computed using the ΔΔCt method. Error bars represent the standard error of the mean for triplicate replications.

Figure 5.6 Transcript levels of *MEST* mRNA in SW480 cells treated with the two drug concentrations.

Analysis of transcript levels in SW480 cells transfected with negative control siRNA (NI), *Brachyury* siRNA (T5), the 19 drugs and DMSO to assess the efficacies of the drugs. (A) SW480 cells treated with the 19 drugs at a concentration of 10 μM. (B) SW480 cells treated with the 19 drugs at a concentration of 100 μM. The results were normalized using three endogenous reference genes (*GAPDH*, *HSP90AB1* and *TUBA1C*) and the relative fold-change was computed using the ΔΔCt method. Error bars represent the standard error of the mean for triplicate replications.

Figure 5.7 Transcript levels of the *CCNE1* mRNA in SW480 cells treated with the two drug concentrations.

Analysis of transcript levels in SW480 cells transfected with negative control siRNA (NI), *Brachyury* siRNA (T5), the 19 drugs and DMSO to assess the efficacies of the drugs. (A) SW480 cells treated with the 19 drugs at a concentration of 10 μM. (B) SW480 cells treated with the 19 drugs at a concentration of 100 μM. The results were normalized using three endogenous reference genes (*GAPDH*, *HSP90AB1* and *TUBA1C*) and the relative fold-change was computed using the ΔΔCt method. Error bars represent the standard error of the mean for triplicate replications.

MTHFD2

A

10 μM Drug

B

100 μM Drug

 Figure 5.8 Transcript levels of the *MTHFD2* mRNA in SW480 cells treated with the two drug concentrations.
Analysis of transcript levels in SW480 cells transfected with negative control siRNA (NI), *Brachyury* siRNA (T5), the 19 drugs and DMSO to assess the efficacies of the drugs. (A) SW480 cells treated with the 19 drugs at a concentration of 10 μM. (B) SW480 cells treated with the 19 drugs at a concentration of 100 μM. The results were normalized using three endogenous reference genes (*GAPDH*, *HSP90AB1* and *TUBA1C*) and the relative fold-change was computed using the ΔΔCt method. Error bars represent the standard error of the mean for triplicate replications.

5.2.1.3 Analysis of up-regulated gene transcripts

Other genes that exhibited up-regulated transcripts were the *CROT*, *IGFBP3* and *SFRP5* genes, which were selected from the RNA-seq results after the *Brachyury* gene was knocked down (Jezkova *et al*., 2014). To address whether these selected genes were expressed, as the RNA-seq analysis showed up-regulation of these genes after *Brachyury* was down-regulated by (T5), qRT-PCR analysis was applied; the transcript levels of these three genes were consistent with the results of the RNA-seq data analysis.

Two concentrations of the 19 drugs, as well as DMSO, were prepared and the transcript levels of *CROT* were investigated. In SW480 cells transfected with (T5), the transcript profile of *CROT* was consistent with the RNA-seq result. It was observed that drugs 2, 4, 8 and 19 at the 10 μM concentration affected the transcript levels for this gene. Up-regulation of *CROT* transcripts was detected with drugs 6, 7, 16 and 18 (Figure 5.9A). The transcript levels of *CROT* were also investigated in these drugs at the 100 μM concentration. Drug 3 was the most effective drug in the reduction of *CROT* mRNA levels. Other drugs, such as 18, had less efficacy than drug 3. Another group of these drugs that up-regulated transcripts from *CROT* included drugs 7, 8, 9, 10 and 13, which indicates that these drugs have similar *CROT* transcript profiles in (T5) (Figure 5.9B).

To screen the transcripts of *IGFBP3* in a colon cancer cell line, SW480 cells were treated with the 19 drugs at the two concentrations and (T5) revealed that the transcript levels of this gene were significantly upregulated, which was consistent with the RNA-seq analysis result. qRT-PCR analysis was carried out and the drugs tested at a concentration of 10 μM demonstrated down-regulatory effects on transcripts. Interestingly, several drugs, such as 1, 2, 4, 5, 8-10 and 13-15, were found to act as down-regulators of *IGFBP3*, whereas others, such as 6, 12 and 16, acted like (T5) by up-regulating gene transcripts (Figure 5.10A). In a similar experiment at a concentration of 100 μM, down-regulated transcripts of *IGFBP3* was observed with drugs 3, 12 and 18-19. Some drugs, such as 6 and 7, affected transcript levels but with less efficacy. Drugs 10, 13 and 17 were associated with up-regulation of *IGFBP3* transcript levels (Figure 5.10B).

Transcripts from the *SFRP5* gene were also investigated using different drugs at two concentrations to treat the SW480 cells. As the RNA-seq analysis demonstrated, transcripts of *SFRP5* gene appeared to be up-regulated with the knockdown of the *Brachyury* gene. qRT-PCR

analysis was applied to address whether this gene would act in a manner that was consistent with the RNA-seq finding. It is worth noting that the transcripts of *SFRP5* were significantly up-regulated with (T5). In addition, drugs 1, 4, 10 and 14 at the 10 µM concentration showed efficacy in down-regulating of *SFRP5* transcripts; drugs 2, 5, 8-9 and 13 were also able to down-regulate *SFRP5* transcripts but with less efficacy than 1, 4, 10 and 14. The up-regulation of *SFRP5* transcripts was observed, for example, in drugs 6, 11-12, 16 and 18 (Figure 5.11A). SW480 cells that were treated with the 19 drugs at a concentration of 100 µM exhibited down-regulation of *SFRP5* transcripts with drugs 3, 12 and 18. In contrast, drugs 7 and 13 were found to up-regulate of *SFRP5* transcript levels in SW480 cells (Figure 5.11B).

5.2.2   The effect of drugs on SW480 cell viability/proliferation

To determine the efficacies of the drugs and their effectiveness at targeting the proliferation of human SW480 cancer cells, the cells were treated with the 19 drugs at different concentration and SW480 cells were also transfected with (T5) in 96-well plates. After 72 hours, SW480 cell proliferation was measured using a plate- reading luminometer. These measurements showed that the numbers of cells reduced or increased according to the different drugs. Some drugs were able to effect the cell numbers after treatment when SW480 was administered at a concentration of 10 µM (such as drugs 3, 7 and 18); other drugs were observed as reducing cell numbers but were less efficient than drugs 3, 7 and 18 including drugs 11, 12 and 14. In contrast, drugs such as 1, 5 and 15 showed their ability to increase cell proliferation (Figure. 5.12 A); treatment SW480 with drugs at a concentration of 100 µM revealed the efficacy of these drugs. For example, drugs 3, 7, 11, 12 and 18 reduce cell numbers. Drugs 15, 16 and 17 appeared to increase the proliferation of cells (Figure 5.12B). Interestingly, some drugs, such as 3 and 18, were consistent with the qRT-PCR analysis in their effects on cell proliferation (Figure 5.3).
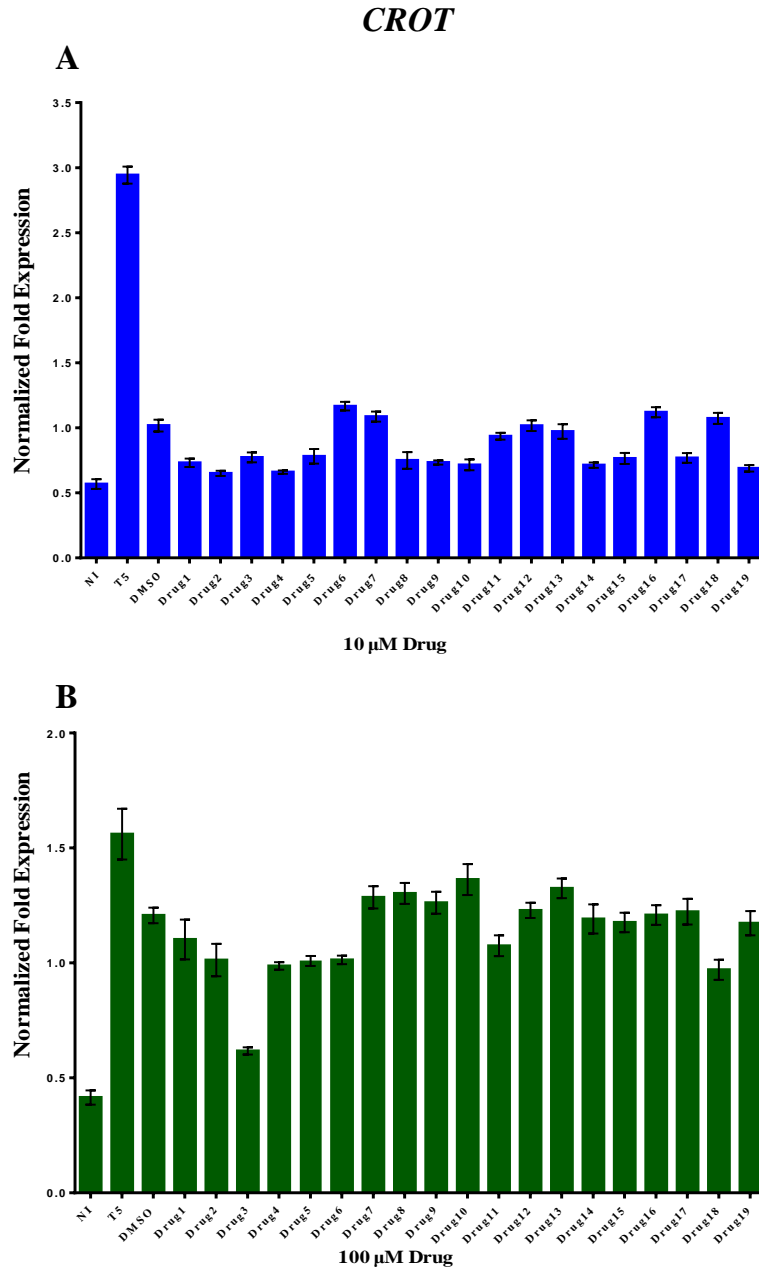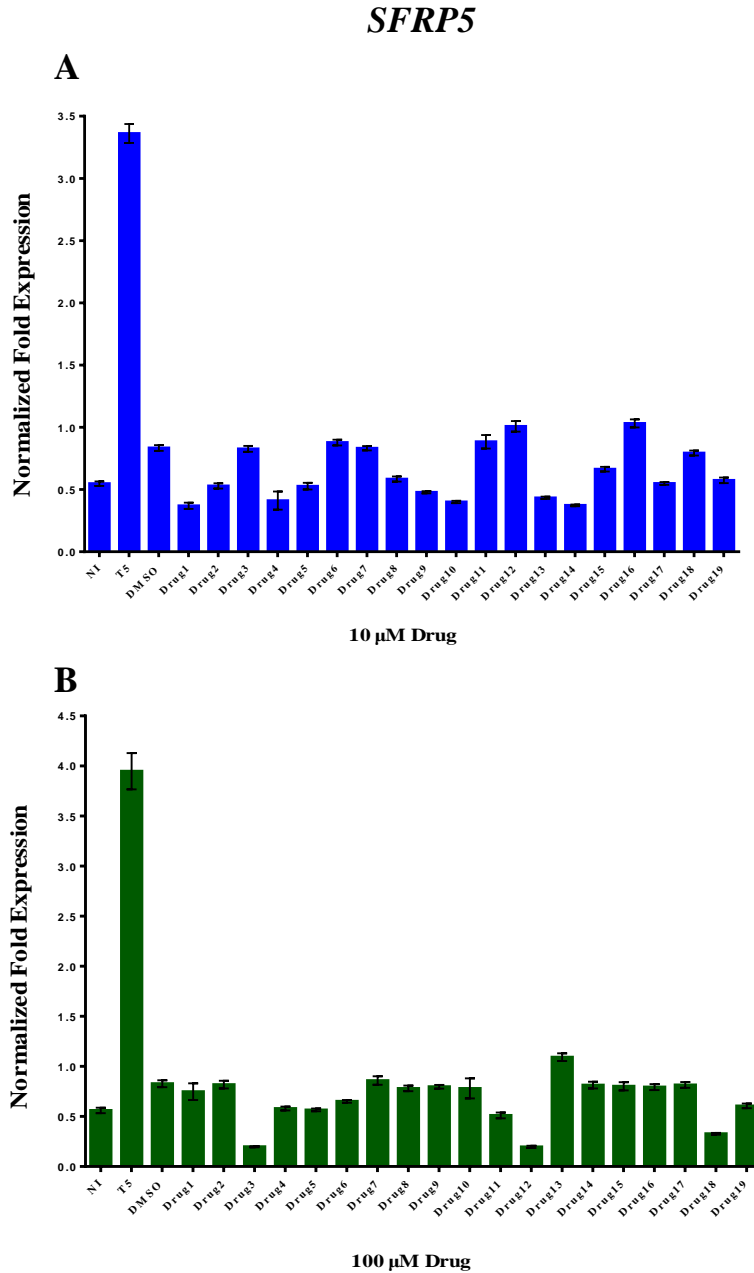
CROT

Figure 5.9 Transcript analysis of the *CROT* gene in SW480 cells treated with the two drug concentrations.
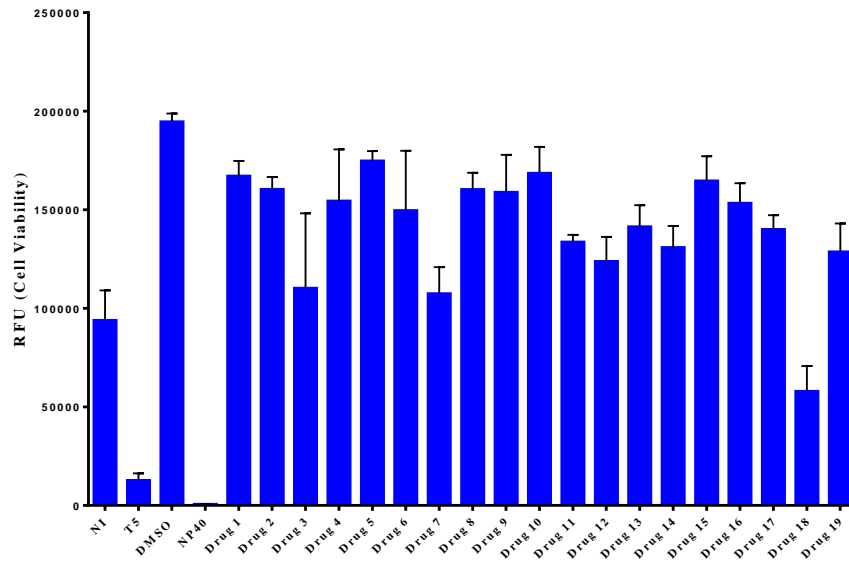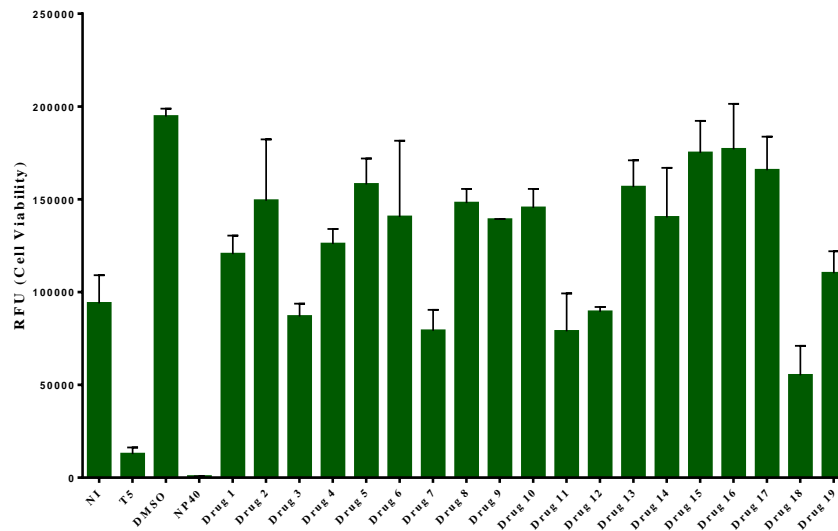Analysis of transcript levels in SW480 cells transfected with negative control siRNA (NI), *Brachyury* siRNA (T5), the 19 drugs and DMSO to assess the efficacies of the drugs. (A) SW480 cells treated with the 19 drugs at a concentration of 10 µM. (B) SW480 cells treated with the 19 drugs at a concentration of 100 µM. The results were normalized using three endogenous reference genes (*GAPDH*, *HSP90AB1* and *TUBA1C*) and the relative fold-change was computed using the ΔΔCt method. Error bars represent the standard error of the mean for triplicate replications.
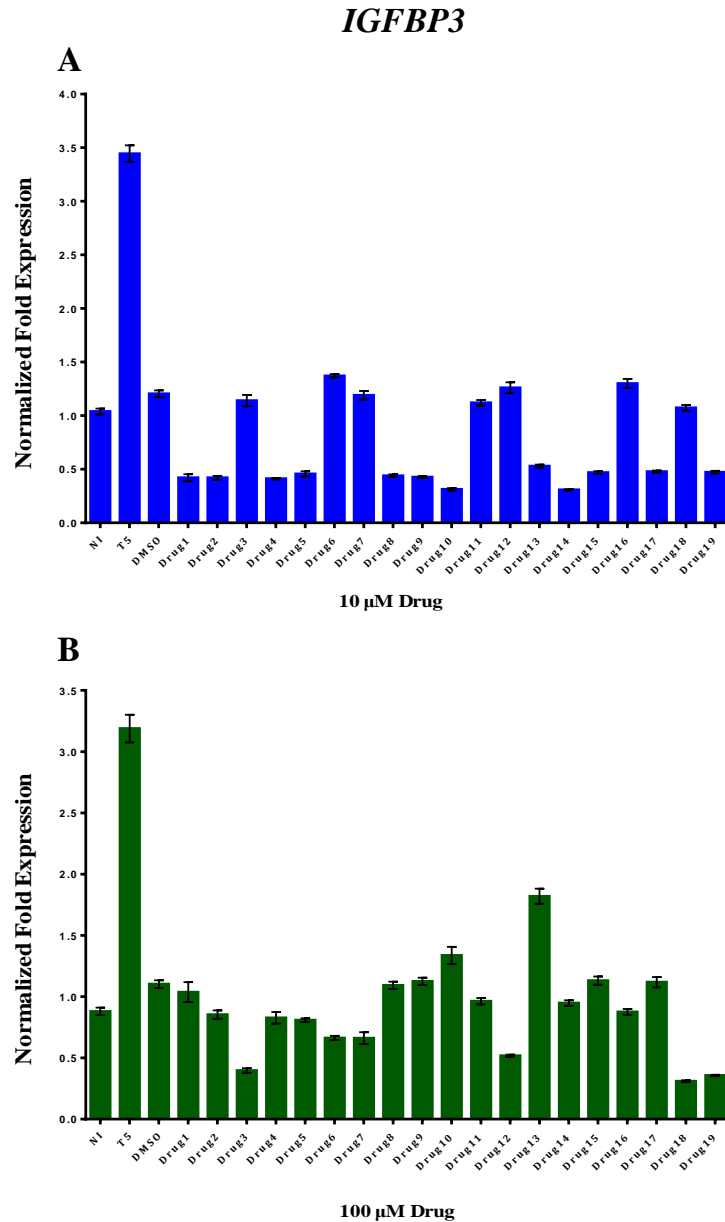
IGFBP3

Figure 5.10 Transcript analysis of the *IGFBP3* gene in SW480 cells treated with the two drug concentrations.
Analysis of transcript levels in SW480 cells transfected with negative control siRNA (NI), *Brachyury* siRNA (T5), the 19 drugs and DMSO to assess the efficacies of the drugs. (A) SW480 cells treated with the 19 drugs at a concentration of 10 μM. (B) SW480 cells treated with the 19 drugs at a concentration of 100 μM. The results were normalized using three endogenous reference genes (*GAPDH*, *HSP90AB1* and *TUBA1C*) and the relative fold-change was computed using the ΔΔCt method. Error bars represent the standard error of the mean for triplicate replications.

SFRP5

Figure 5.11 Transcript analysis of the *SFRP5* gene in the SW480 cell line treated with the two drug concentrations.

Analysis of transcript levels in the SW480 cells that were transfected with negative control siRNA (NI), *Brachyury* siRNA (T5), the 19 drugs and DMSO to assess the efficacies of the drugs. (A) SW480 cells treated with the 19 drugs at a concentration of 10 μM. (B) SW480 cells treated with the 19 drugs at a concentration of 100 μM. The results were normalized using three endogenous reference genes (*GAPDH*, *HSP90AB1* and *TUBA1C*) and the relative fold-change was computed using the ΔΔCt method. Error bars represent the standard error of the mean for triplicate replications.

A

10 µM Drug

B

100 µM Drug

Figure 5.12 Measurement of the proliferation of SW480 cells in response to potential anti-Brachyury drugs

SW480 cells were transfected with negative control siRNA (NI), *Brachyury* siRNA (T5), DMSO, NP40 and 19 drugs targeting Brachyury. After 72 hours, the cell viability SW480 cells were measured using a plate-reading luminometer to investigate the efficacies of the drugs. (A) SW480 cells treated with the 19 drugs at a concentration of 10 µM. (B) SW480 cells treated with the 19 drugs at a concentration of 100 µM.

5.2.3   Analysis of Brachyury protein in SW480 cells following drug treatment

Western blot analysis was performed to confirm the Brachyury knockdown observed by qRT-PCR (Figure 5.3). To reduce background and non-specific binding, the concentration of the antibody was optimized during the western blot procedure. Goat polyclonal antibody from an R&D system (AF2085) was used and the Brachyury protein was detected in SW480 cells with two bands with approximate sizes of 50 kDa and 43 kDa, which correspond to the Brachyury variants (splice variants TV1 and TV2). Based on western blot analysis, Brachyury knockdown was confirmed at the protein level and the SW480 cells were treated with some of the drugs. Then, western blot analysis was performed in order to investigate the influence of the drugs on Brachyury protein levels. The protein was detected at the expected sizes of 50 kDa and 43 kDa. Based on this result, band intensities in some drugs, including 3 and 18, appeared to be reduced compared to the control, which is consistent with the cell viability results (Figure 5.12). This indicates that the selected drugs appeared to down-regulate Brachyury at the protein level (Figure 5.13). Although this is only a quantitative analysis, the reductions are quite apparent.

5.2.4   Detection of the Brachyury protein in human cancer cell lines and cellular localisation of Brachyury in SW480 cells

Western blot analysis was used to investigate Brachyury at the protein level among different types of cancer cell lines. Cancer cell line lysates were prepared from 17 cancer cell lines; A2780, PEO14, HeLa, MCF-7, MD-MB-453, H460, COLO800, G-361, Jurkat, K562, KBM-7, HCT116, T84, SW480, LoVo, NTERA2 and 1231N1. The aim was to identify cell lines that were Brachyury positive, which might respond to the drugs, and those that were negative, so should not respond to the drugs if they are specific to Brachyury .The detection of the Brachyury protein was performed using goat polyclonal antibody from an R&D system (AF2085) that detected the protein with two band sizes of approximately 50 KDa and 43 KDa. Anti-GAPDH served as a positive control. Brachyury protein was detected with strong bands in all of the cancer cell lines, except K562, which showed a faint band (Figure 5.14A).

The cellular localisation of Brachyury was studied in the SW480 cancer cell line. The positive nuclear control was Lamin B, and α-Tubulin served as the cytoplasmic control. Brachyury was observed with a strong band in the cytoplasmic fraction and a small amount of Brachyury was

found in the nuclear fraction through the application of western blot analysis (Figure 5.14 B). The rabbit polyclonal antibody from Abcam (ab20680) was used and only one band of approximately 50 KDa was detected which have indicated one variant of Brachyury.
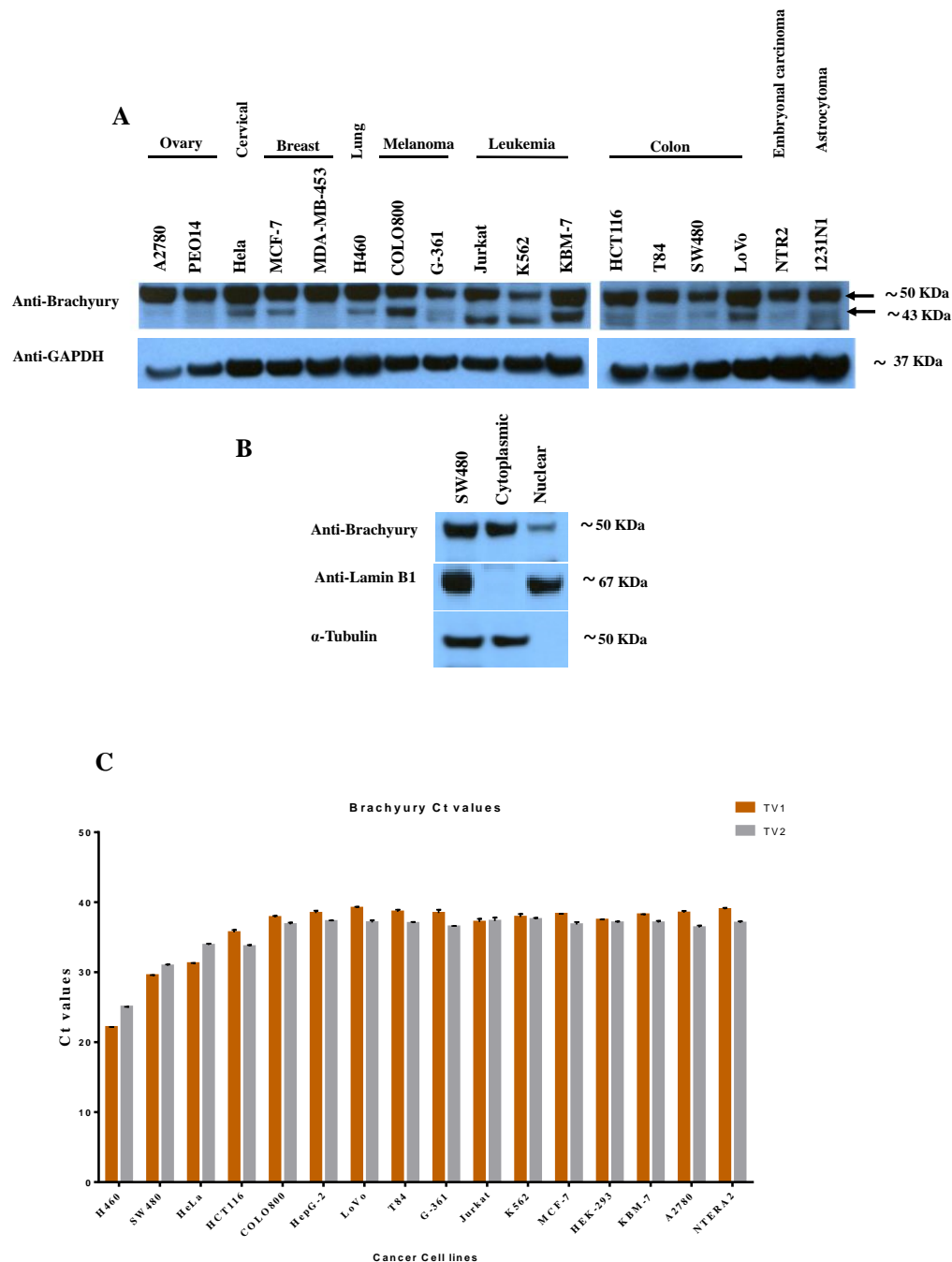
qRT-PCR was applied to investigate the expression of the *Brachyury* splice variants TV1 and TV2 in various types of cancer cell lines. Expression of TV1 and TV2 was detected with Ct values below 38, which were determined by negative controls. TV2 was detected within all cancer cell lines examined with Ct equalling less than 38, such as in H460 and SW480. Conversely, TV1 exhibited a Ct value greater than 38 with some cancer cell lines, such as LoVo and NTERA2 (Figure 5.14 C).
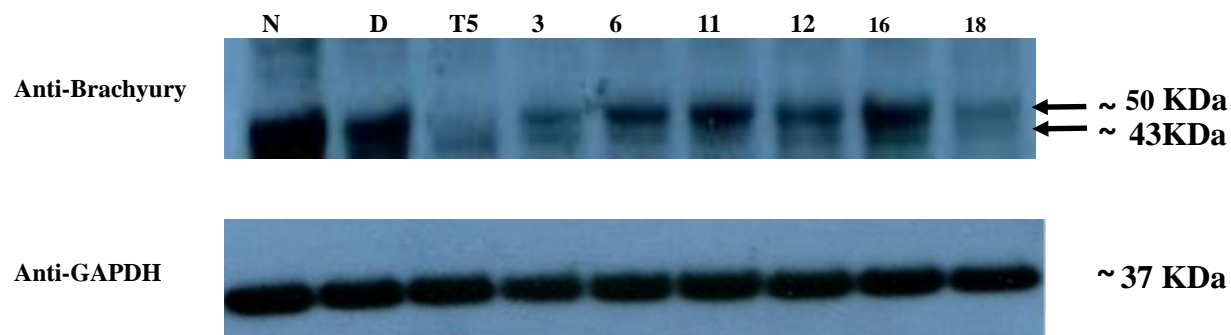
Figure 5.14 Western blot analysis of Brachyury in various cancer cell lines and cellular localisation of Brachyury in SW480 cells.
(A) Brachyury was detected in 17 cancer cell lines with the use of goat polyclonal antibody from an R&D system (AF2085). GAPDH served as the positive control. (B) The cellular localisation of Brachyury was determined in SW480 cells using rabbit polyclonal antibody from Abcam (ab20680). Lamin B1 served as the nuclear control, and α-Tubulin served as the cytoplasmic control. (C) qRT-PCR showing the Ct values of TV1 and TV2 in different cancer cell lines.The results were normalized using three endogenous reference genes (*GAPDH*, *HSP90AB1* and *TUBA1C*) and the relative fold-change was computed using the ΔΔCt method. Error bars represent the standard error of the mean for triplicate replication.

5.2.5   Determination of the localisation of Brachyury in SW480 cells and human tissue by immunofluorescence analysis

To determine the subcellular localisation of Brachyury in CRC cells, indirect immunofluorescence (IF) was carried out in the SW480 cells. The mouse monoclonal anti-Brachyury that was obtained from Abcam (ab140661) was used for the IF. Brachyury was shown to have strong localisation in the cytoplasm and weak localisation in the nuclei of the SW480 cells (Figure 5.15); this result was consistent with the findings from the western blot analysis (Figure 5.14B).

IF was carried out on patient-derived CRC material to determine the localisation pattern of Brachyury and MSH2 proteins encoded by a gene that was selected from the top 50 most differentially expressed genes as identified by analysis of the RNA-seq results following Brachyury knockdown in SW480 cells (Jezkova *et al*., 2014). The localisation of Brachyury and MSH2 was studied to investigate whether there is an association between these two genes in tissues. This could potentially be disrupted by drugs action, so could provide another assay to assess the action of potential anti-Brachyury drugs.

Brachyury mouse monoclonal antibody from Abcam (ab140661) was used in this study and the MSH2 antibody was a rabbit monoclonal antibody (Cell Signaling Technology, 2017S). Histologically normal and colon cancer tissues were derived from CRC patients (Figure 5.17-5.24). Brachyury staining in normal colon tissue seemed to be strong in the cytoplasm of enteroendocrine (EEC) cells, whereas it was weak in the cytoplasm of epithelial cells. MSH2 was detected by IF in the nuclei of epithelial cells (Figure 5.17). In colon cancer tissues, Brachyury was sometimes detected in the cytoplasm; in some samples, MSH2 was not detected in the cytoplasm or nucleus at all, as shown in Figure 5.18. Brachyury was present in all of the colon cancer samples, which indicates the important connection between Brachyury and cancer. The staining patterns for both proteins are summarized in Table 5.2.
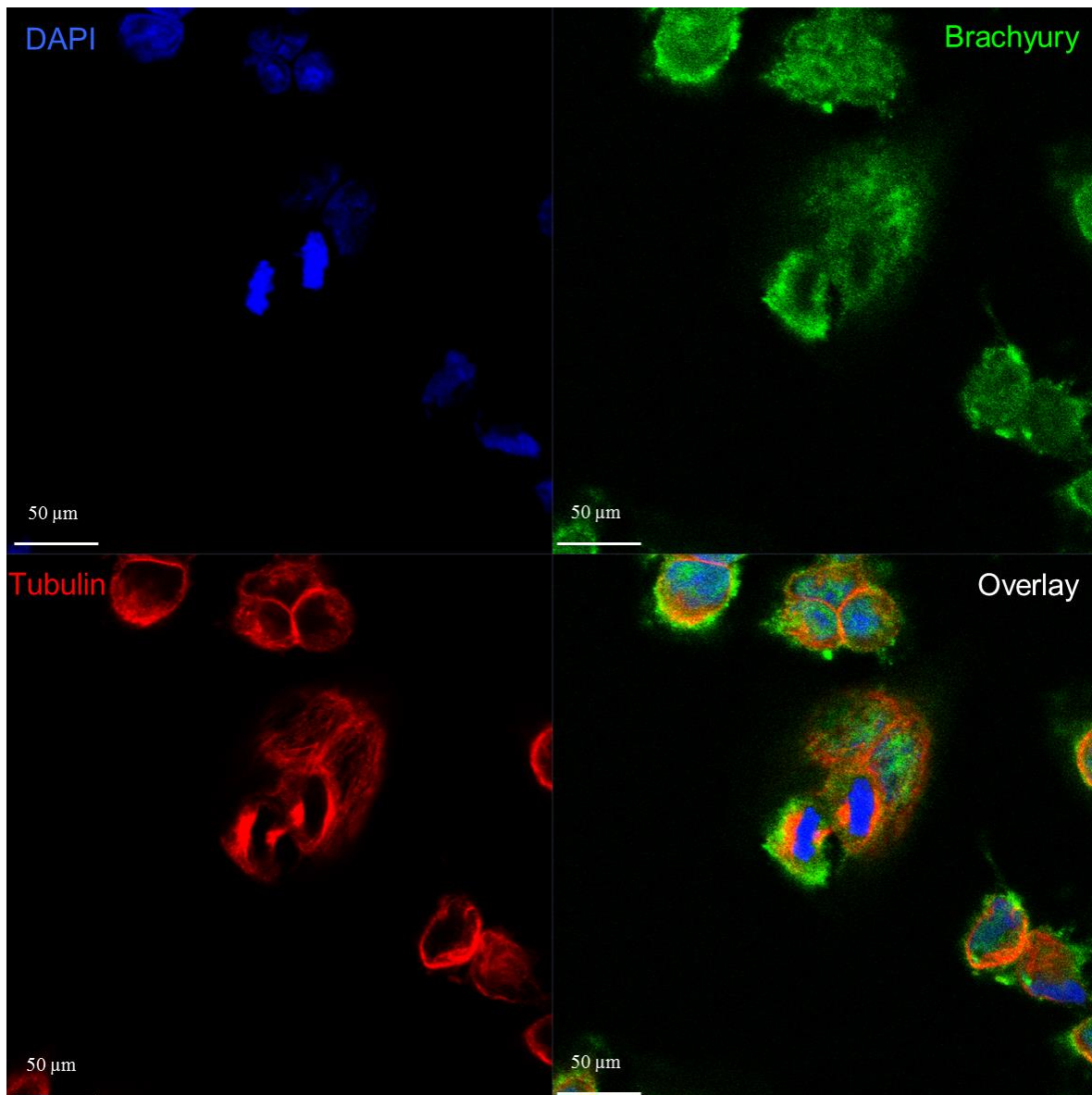
Figure 5.15 IF showing localisation of Brachyury in SW480 cells.

IF analysis carried out on SW480 cells. Brachyury (green) was detected using mouse monoclonal anti-Brachyury (Abcam, ab140661). DNA was stained with DAPI blue. Brachyury showed strong staining in cytoplasm and weak staining in nuclei. Images were acquired using a Zeiss LSM 710 confocal microscope.
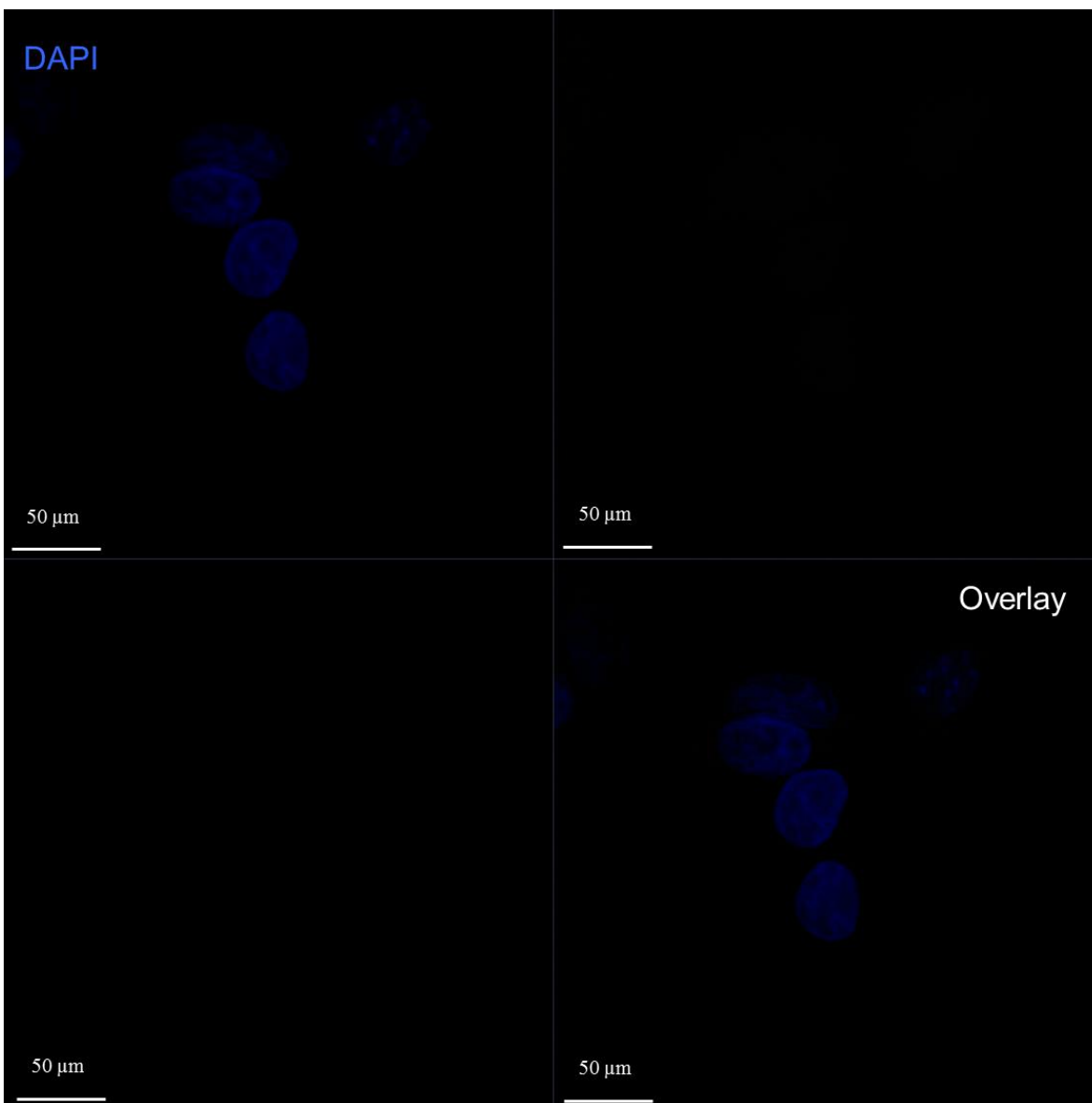
**Figure 5.16 IF negative control for SW480 sample staining.**
Top right – mouse secondary antibody (Life Technologies, A11029). Bottom left – rabbit secondary antibody (Life Technologies, A11034). Images were acquired using a Zeiss LSM 710 confocal microscope.
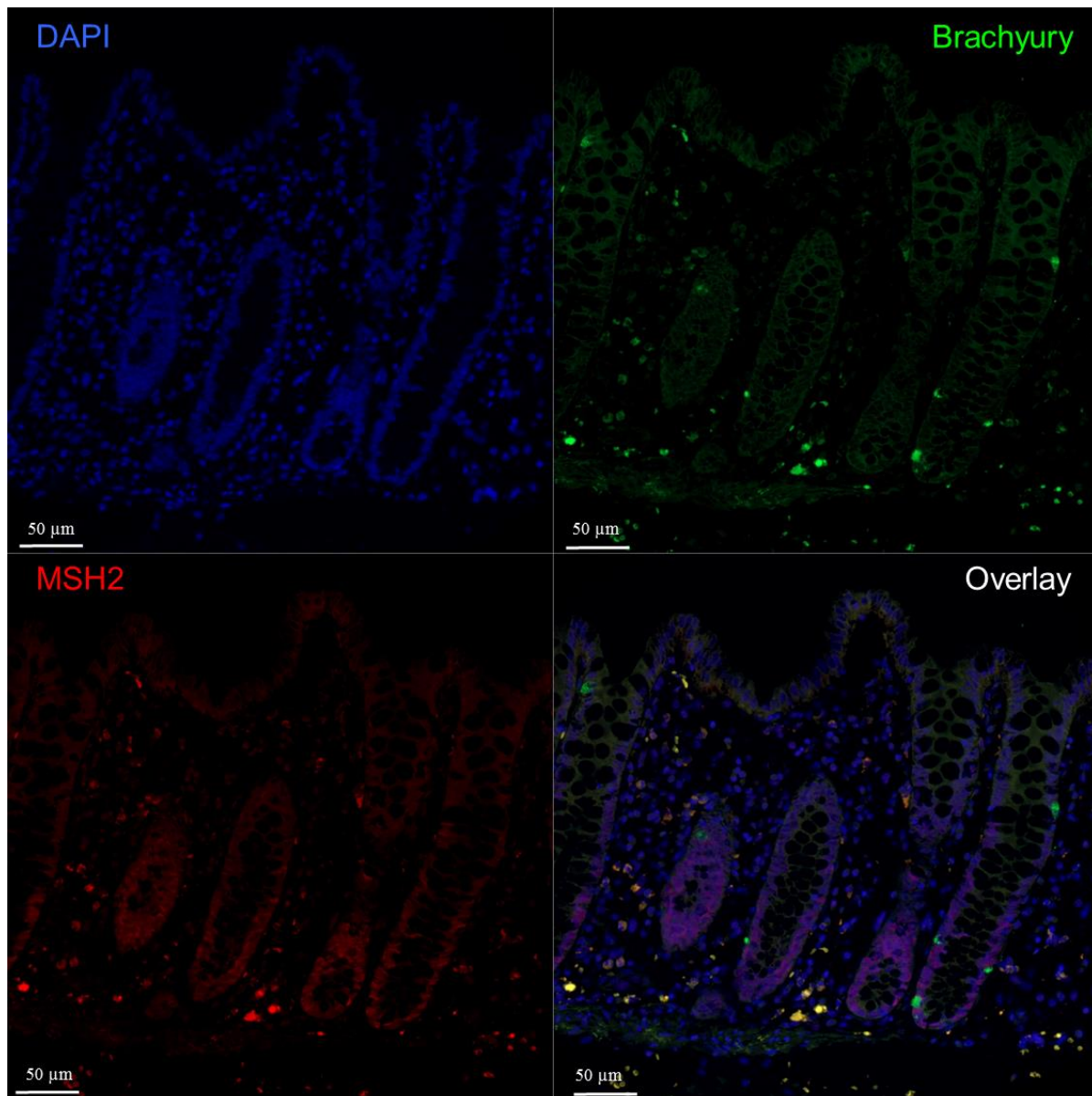
Figure 5.17 IF detection of Brachyury and MSH2 in normal human colon tissue from patient 16.
IF of Brachyury/MSH2 on normal colon crypt FFPE sections. Brachyury-positive cells are located in the cytoplasm of the EEC cells. MSH2 was detected with weak staining in the nuclei of epithelial cells. DNA was stained with DAPI blue. Brachyury staining, green/ab140661; MSH2 staining, red/2017S. Images were acquired using a Zeiss LSM 710 confocal microscope.
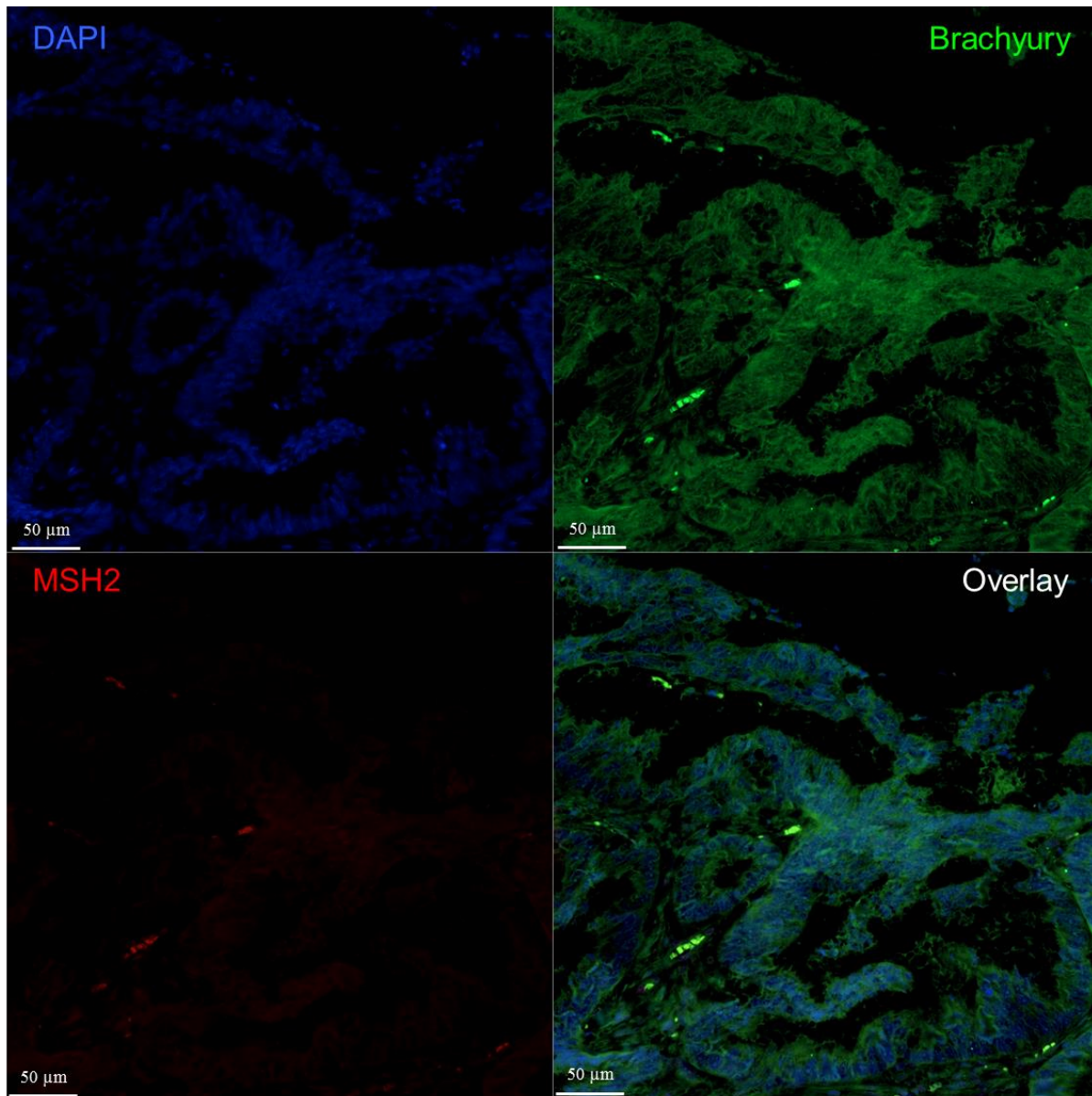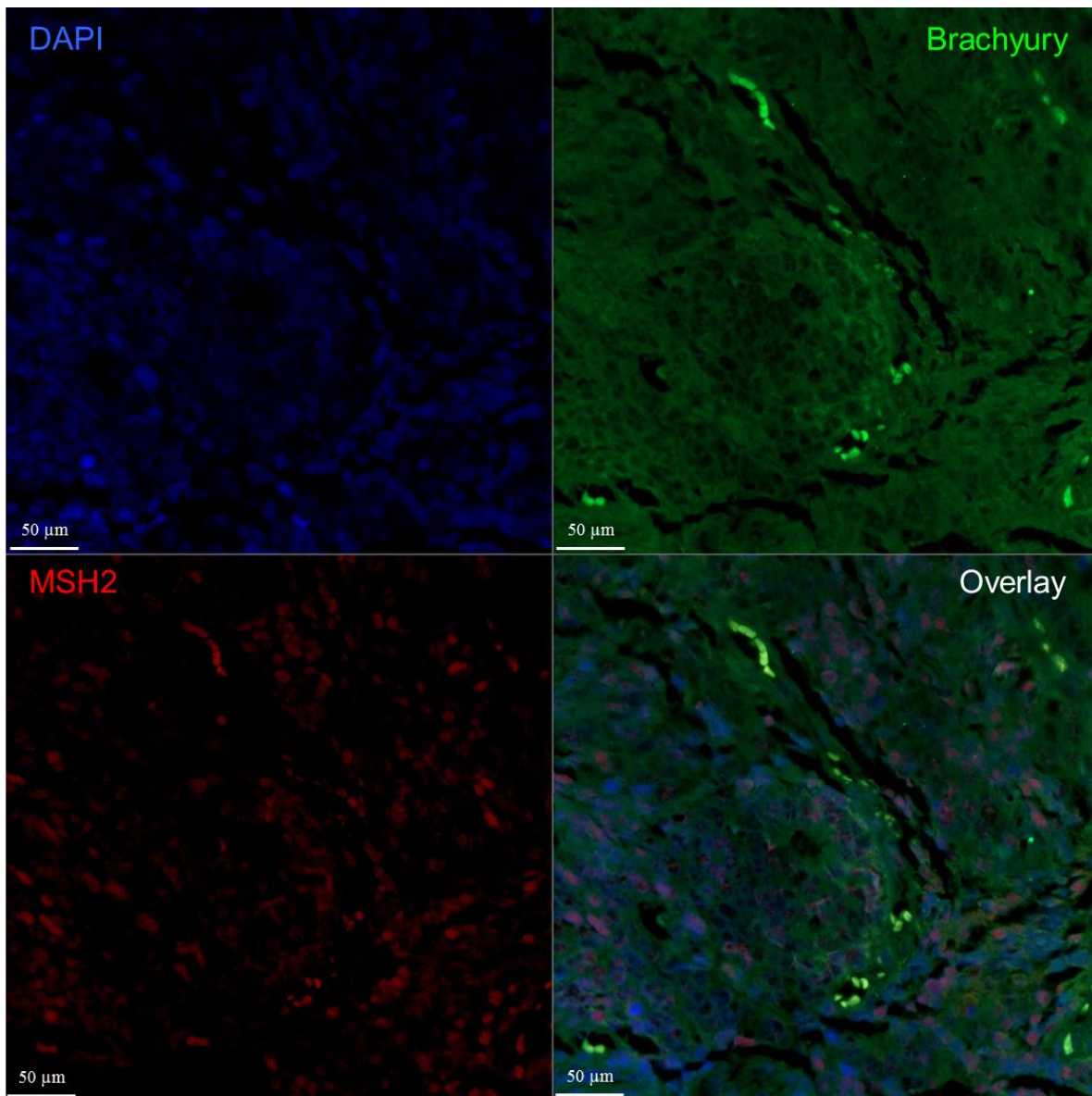
Figure 5.18 IF detection of Brachyury and MSH2 in human colon cancer tissue from patient 16.
IF of Brachyury/MSH2 on colon cancer FFPE sections. Brachyury shows strong staning in the cytoplasm; MSH2 was not detected. DNA was stained with DAPI blue. Brachyury staining, green/ab140661; MSH2 staining, red/2017S. Images were acquired using a Zeiss LSM 710 confocal microscope.
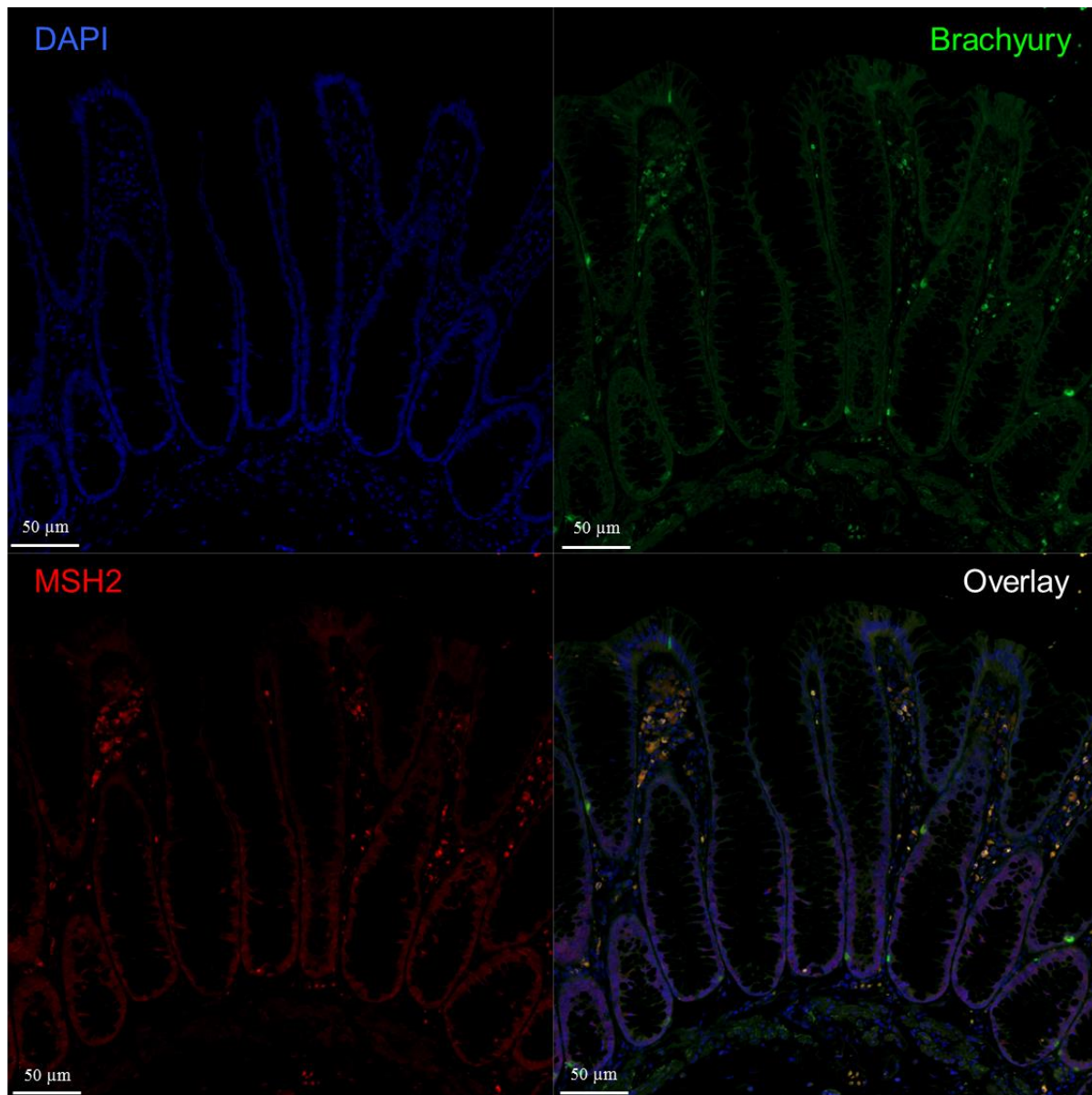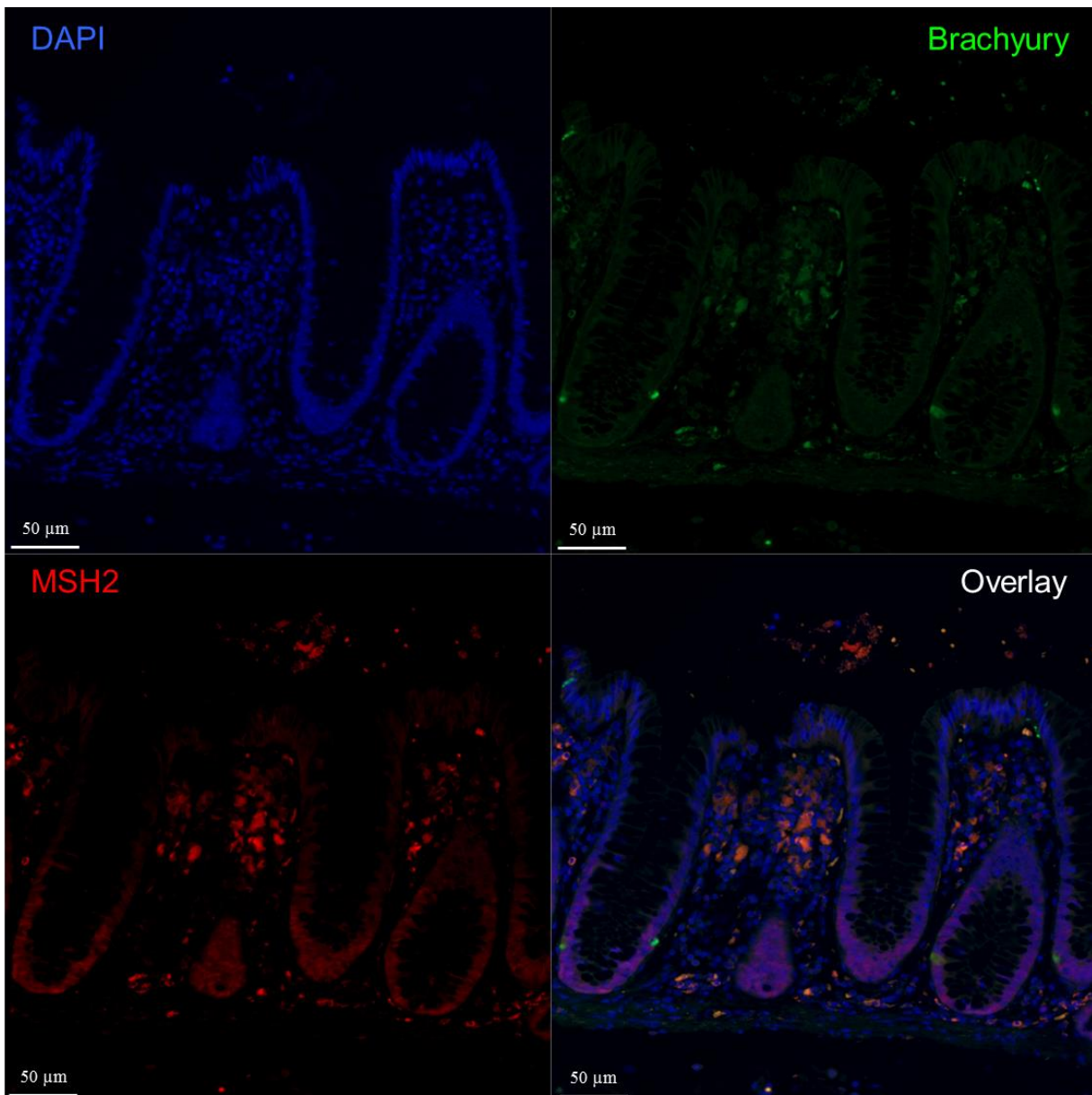
Figure 5.19 IF detection of Brachyury and MSH2 in normal human colon tissue from patient 30.
IF of Brachyury/MSH2 on normal colon crypt FFPE sections. Brachyury shows staining in the cytoplasm of EEC cells. MSH2 was detected with weak staining in the nuclei of epithelial cells. DNA was stained with DAPI blue. Brachyury staining, green/ab140661; MSH2 staining, red/2017S. Images were acquired using a Zeiss LSM 710 confocal microscope.
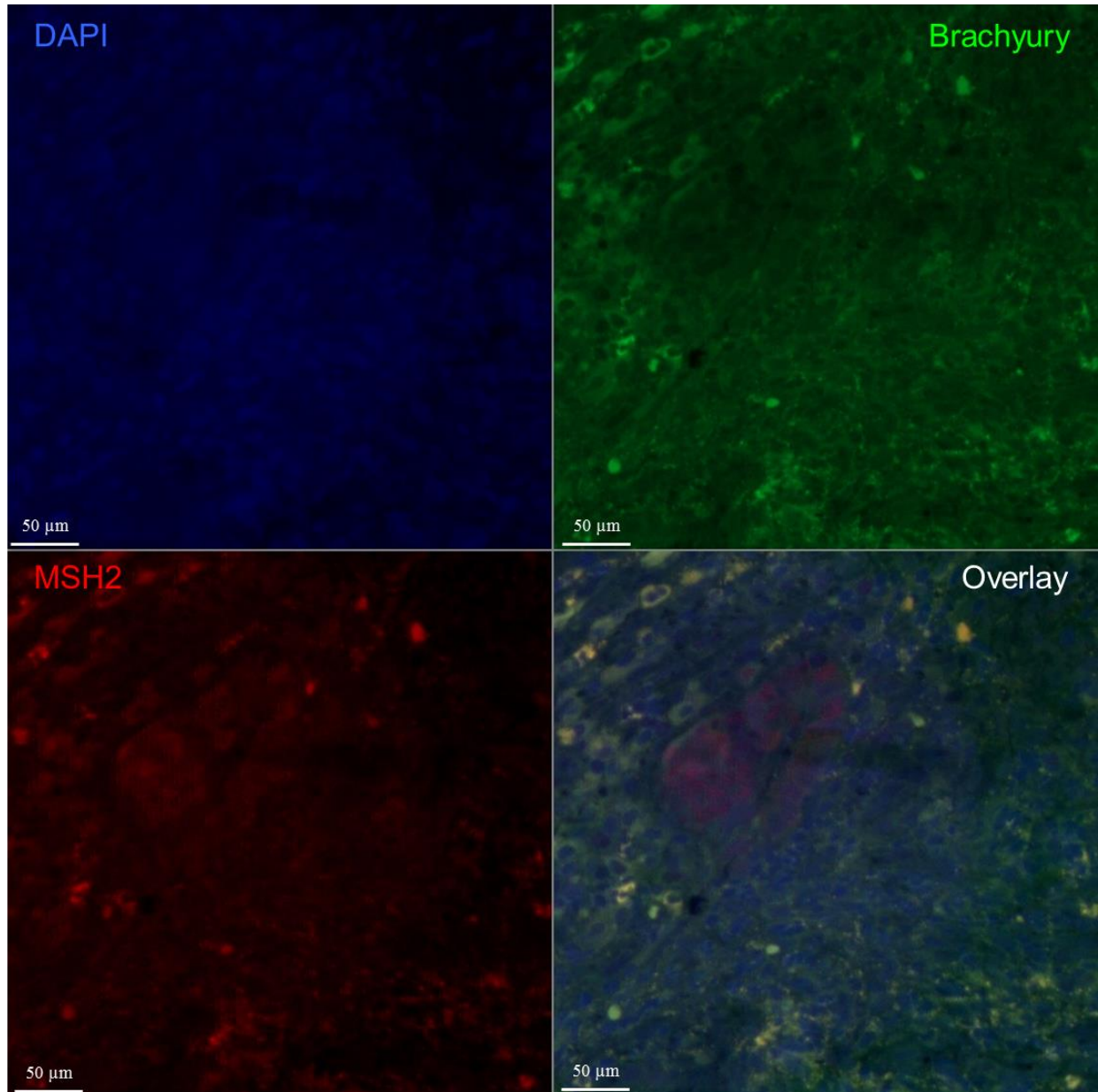
Figure 5.20 IF detection of Brachyury and MSH2 in human colon cancer tissue from patient 30.
IF of Brachyury/MSH2 on colon cancer FFPE sections. Brachyury exhibits moderate staining of the cytoplasm. MSH2 was detected with strong staining in the nuclei. DNA was stained with DAPI blue. Brachyury staining, green/ab140661; MSH2 staining, red/2017S. Images were acquired using a Zeiss LSM 710 confocal microscope.

Figure 5.21 IF detection of Brachyury and MSH2 in normal human colon tissue from patient 40.
IF of Brachyury/MSH2 on normal colon crypt FFPE sections. Brachyury shows staining in the cytoplasm of EEC cells. MSH2 was detected with weak staining in the nuclei of epithelial cells. DNA was stained with DAPI blue. Brachyury staining, green/ab140661; MSH2 staining, red/2017S. Images were acquired using a Zeiss LSM 710 confocal microscope.
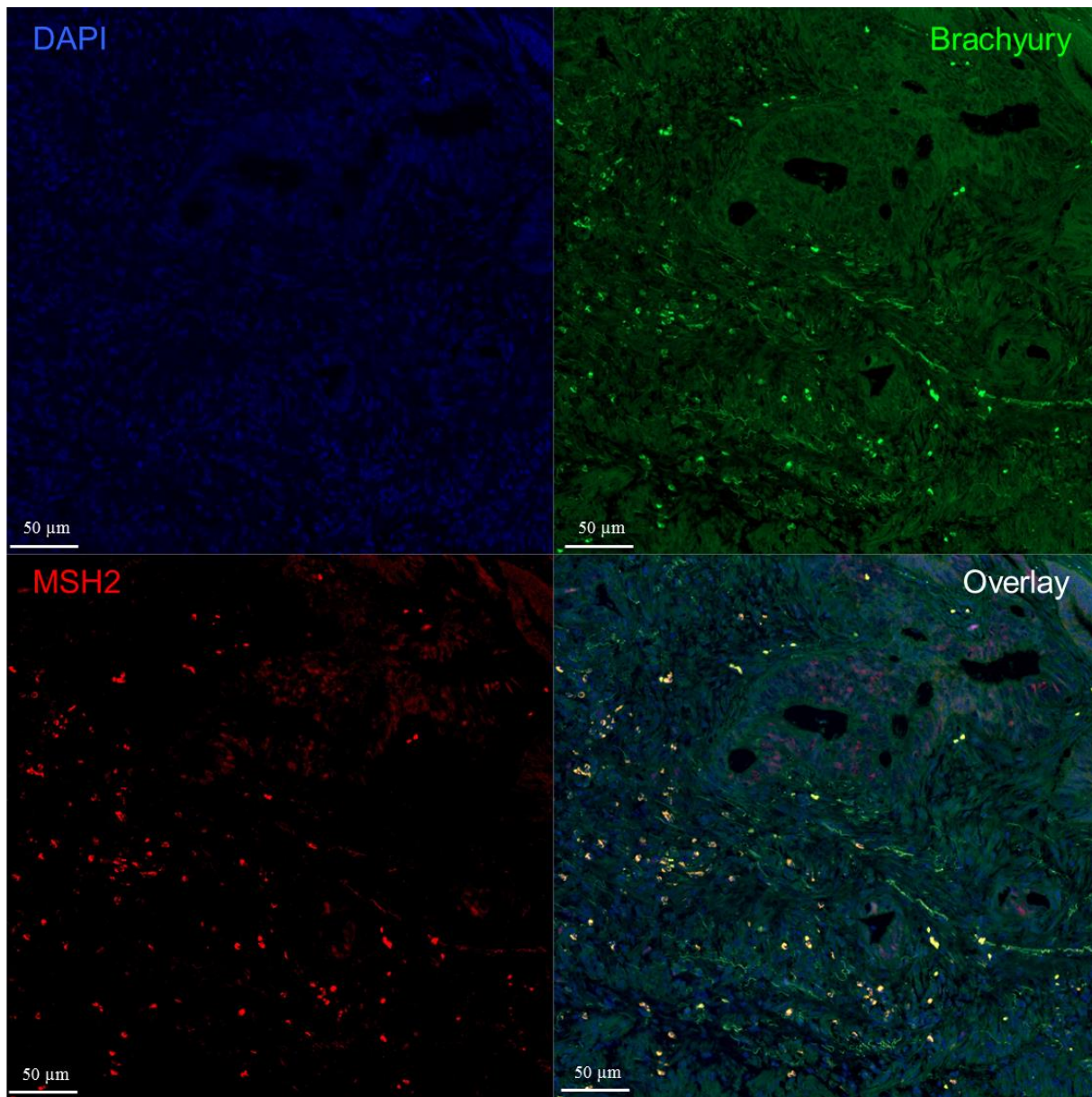
Figure 5.22 IF detection of Brachyury and MSH2 in human colon cancer tissue from patient 40.
IF of Brachyury/MSH2 on colon cancer FFPE sections. Brachyury exhibits weak staining of the cytoplasm. MSH2 was detected with weak staining in the nuclei. DNA was stained with DAPI blue. Brachyury staining, green/ab140661; MSH2 staining, red/2017S. Images were acquired using a Zeiss LSM 710 confocal microscope.
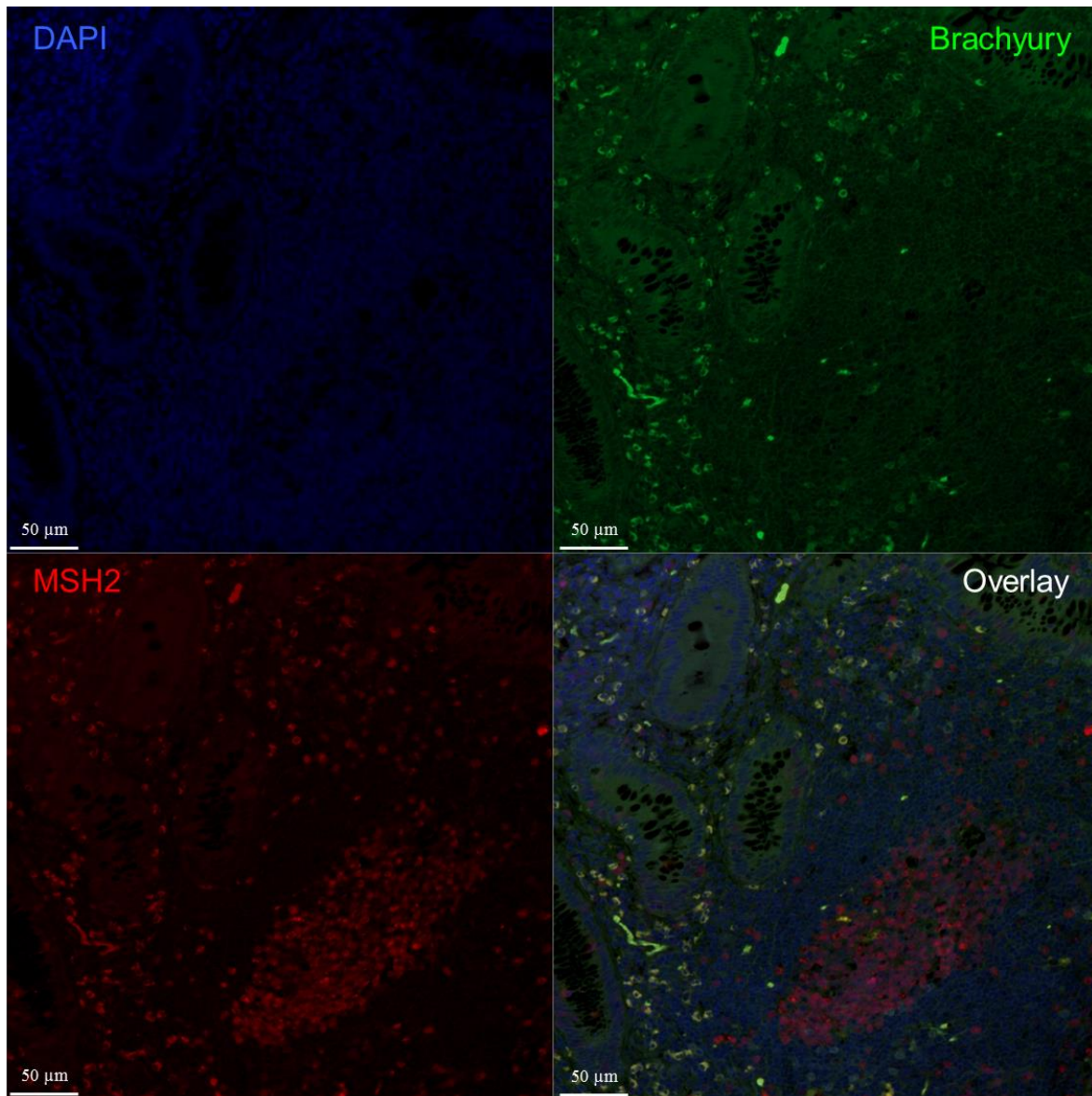
Figure 5.23 IF detection of Brachyury and MSH2 in human colon cancer tissue from patient 27.
IF of Brachyury/MSH2 on colon cancer FFPE sections. Brachyury exhibits moderate staining of the cytoplasm. MSH2 shows strong staining in the nuclei. DNA was stained with DAPI blue. Brachyury staining, green/ab140661; MSH2 staining, red/2017S. Images were acquired using a Zeiss LSM 710 confocal microscope.

Figure 5.24 IF detection of Brachyury and MSH2 in human colon cancer tissue from patient 45.
IF of Brachyury/MSH2 on colon cancer FFPE sections. Brachyury exhibits weak staining of the cytoplasm. MSH2 shows strong staining in the nuclei. DNA was stained with DAPI blue. Brachyury staining, green/ab140661; MSH2 staining, red/2017S. Images were acquired using a Zeiss LSM 710 confocal microscope.
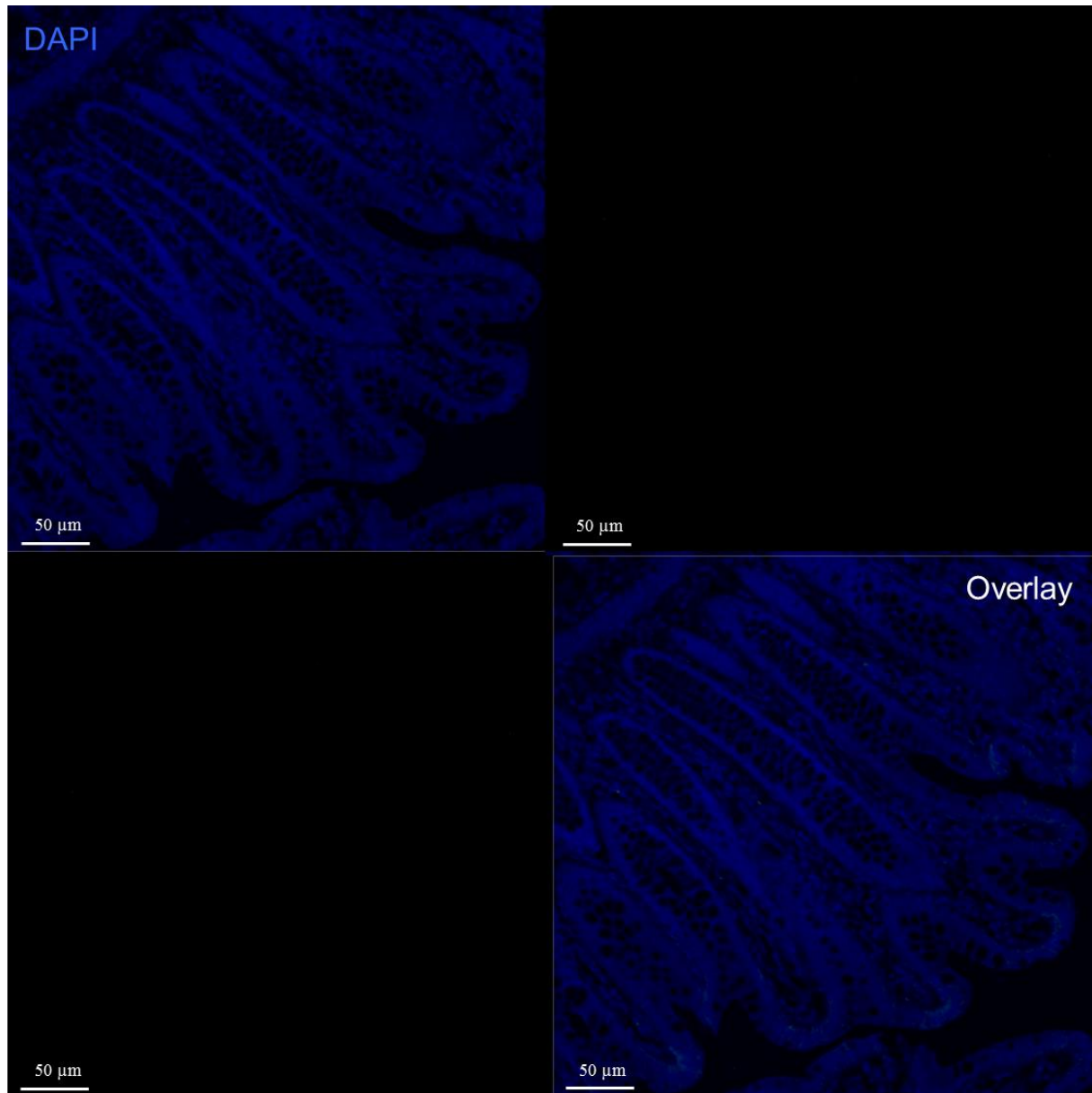
Figure 5.25 IF negative control for colon sample staining.
Top right – mouse secondary antibody (Life Technologies, A11029). Bottom left – rabbit secondary antibody (Life Technologies, A11034). Images were acquired using a Zeiss LSM 710 confocal microscope.

Table 5.2 Summary of the staining patterns of Brachyury and MSH2 in CRC samples derived from different patients.

Age	G	Case	Site	Differentiation	Duke's Stage	T	N	Positive/identified	M	EVA	Brachyury staining Normal tissue	Brachyury staining Cancer	MSH2 staining Normal tissue	MSH2 staining Cancer
64	F	C16	Ascending	Moderate	A	1	0	(0/16)	X	X	Strong cytoplasmic staining in EEC cells, weak cytoplasmic in epithelial cells	Strong cytoplasmic staining	Weak nuclear in epithelial cells	Negative
60	F	C27	Sigmoid	Moderate	B	3	0	(0/8)	X	Yes	X	Moderate cytoplasmic staining	X	Strong nuclear staining
85	M	C30	Sigmoid	Poor	C	3	1	(1/34)	X	No	Strong cytoplasmic staining in EEC cells, weak cytoplasmic in epithelial cells	Moderate cytoplasmic staining	Weak nuclear in epithelial cells	Strong nuclear staining
67	M	C40	Transverse	Moderate	B	3	0	(0/4)	X	No	Strong cytoplasmic staining in EEC cells, weak cytoplasmic in epithelial cells	Weak cytoplasmic staining	Weak nuclear in epithelial cells	Weak nuclear staining
90	M	C45	Ascending	Poor	B	3	0	(0/18)	X	No	X	Weak cytoplasmic staining	x	Strong nuclear staining

G – Gender; **T** – Tumour; **N** – Node; **M** – Metastasis; **EVA** – Extramural Vascular Invasion; **X** – denotes unknown.

5.3 Discussion

T-box transcription factors play an essential role during the development of mammals as they are involved in processes such as the formation of primary germ layers and organogenesis; their underlying mechanisms, however, are poorly understood (Naiche *et al*., 2005; Gentsch *et al*., 2013). The members of the T-box family have the capacity to act as transcriptional activators or repressors and some of these proteins can do both (Ouimette *et al*., 2010; Wansleben *et al*., 2014). The *Brachyury* (*T*) gene, a member of the T-box family, has shown overexpression in various types of tumours (Palena *et al*., 2007; Pinto *et al*., 2014; Wansleben *et al*., 2014; Shimamatsu *et al*., 2016). Furthermore, several studies have revealed the role of the *Brachyury* gene in epithelial–mesenchymal transition (EMT) during metastasis (Fernando *et al*., 2010; Chaffer and Weinberg, 2011; Imajyo *et al*., 2012; Roselli *et al*., 2012). *Brachyury* has also been classified as a CTA gene, despite some expression in normal colon (Jezkova *et al*., 2014). To improve patient outcomes, new drugs targeting various types of cancer are needed. As *Brachyury* has been implicated in tumour growth and progression and it is also associated with drug resistance in several types of tumours, it might, therefore, provide a new therapeutic target (Palena *et al*., 2014; Pinto *et al*., 2016; Huang *et al*., 2013). Moreover, a study by the Wakeman group showed that the depletion of Brachyury in CRC causes proliferation arrest (Jezkova *et al*., 2014). A phase 2 clinical trial is underway for a vaccine targeting Brachyury for the treatment of chordoma (Heery *et al*., 2015). In collaboration with the Drug Screening Platform at Cardiff University, we designed a number of small molecular inhibitors based on a crystal structure that may target the cancer-associated functions of Brachyury in cells; through this screening, we identified 19 drugs and tested their efficacies.

A qRT-PCR experiment was performed to confirm previous RNA sequencing results (Jezkova *et al*. 2014). Following Brachyury depletion in SW480 cells, a significant decrease or increase of gene expression as, measured by transcript levels, occurred. For instance, there was a significant decrease in *MFN2*, *MSH2*, *MEST*, *CCNE1* and *MTHFD2* gene transcripts, while *CROT*, *IGFBP3* and *SFRP5* demonstrated significantly increased levels of transcripts, which indicates the importance of the *Brachyury* gene's association with other genes. These results are consistent with a previous study that reported that the expression of a cohort of genes was effected through depletion of Brachyury; these 8 genes were selected from among the top 50 genes analysed by RNA-seq (Jezkova *et al*., 2014). The selected genes were observed to be involved in several

important functions in the cell cycle process and in DNA mismatch repair (for further details about the functions of these genes, see Table 5.1).

Targeting the transcription factor provides a promising strategy that may be effective in impeding the progression of cancer, as these factors have been implicated in cancer development (Konstantinopoulos and Papavassiliou, 2011). However, targeting these factors with new drugs remains challenging due to their localisation in the nucleus, which makes it difficult for therapeutic agents to access them (Yeh *et al*., 2013). Despite this problem, drugs are designed to target certain transcription factors and might affect gene functions in various ways, such as modulating their interaction with other cofactors, and they should be considered promising therapeutic targets and attractive strategies for drug discovery (Papavassiliou and Papavassiliou, 2016).

In the present study, the 19 new drugs that were design to target the transcription factor Brachyury (T) were investigated to assess whether they might affect the transcript levels of this gene. Based on qRT-PCR analysis, some drugs were observed to down-regulate the transcript level of the *Brachyury* (*T*) gene at different concentrations. Some drugs, such as drug 3, down-regulated gene transcript level at both concentrations tested. Drug 18 also affected gene transcript levels. The efficacy of some drugs, such as drugs 3 and 18 that targeted Brachyury exhibited the ability to down-regulated transcript levels of this gene, as confirmed by qRT-PCR and the measurement of viable cell numbers (Figure 5.12). Using western blot analysis, the reduction of Brachyury protein was observed in the SW480 cells following their treatment with drugs 3 and 18 (Figure 5.13). This indicates that these drugs could be considered for further research, such as the design for the analogue of these drugs, which exhibited specific effects when targeting Brachyury. The efficacy of other drugs targeting Brachyury are shown in Figure 5.26.

To test the anti-Brachyury action of these drugs we examined transcripts thought to be under Brachyury regulation following drugs treatment. The selected genes were based on the RNA-seq that was carried out previously, as the transcript levels of these genes showed down- or up-regulation following the knockdown of the Brachyury in SW480 cells (Jezkova *et al*., 2014). Analysis was conducted in order to assess whether these 19 drugs could increase or decrease the transcript level of these genes at different concentrations compared with the control. Interestingly, the transcript levels of most of these genes were down-regulated after they were treated with drug 3 at different concentrations. The qRT-PCR analysis revealed that the transcript levels of some

genes, such as *MEST*, *CCNE1* and *SFRP5*, were down-regulated with most of the drugs after treatment at both concentrations (10 µM and 100 µM). The drugs' efficacy and their effects on the transcript levels of these genes were determined by qRT-PCR (see Figure 5.26 for the drug summary and transcript level of the selected genes).

Screening the new drugs that targeted Brachyury revealed that the most effective drugs, namely drugs 3 and 18, were observed to reduce the activity of Brachyury in cancer cell lines. Therefore, among the 19 drugs targeting Brachyury, 3 and 18 were selected as potential drugs for further investigation. Also, drugs that were not observed to target Brachyury should be eliminated from further studies. Therefore, for our study, the first step was considered to be determining the drugs with the most potential and reducing the number of drugs that did not take action to inhibit the activity of this gene in cancer cells.

Western blot analysis was used to check the efficacy of these drugs at the protein level in SW480 cells; drugs 3 and 18 reduced the Brachyury protein level in the cancer cell line (Figure 5.13), which is consistent with the qRT-PCR result and the cell viability measurement of the SW480 cells following drug treatment.

RT-PCR analysis was used to investigate *Brachyury* expression in a panel of normal and cancer samples. The expression of *Brachyury* was detected in cancer samples but not in normal tissues, other than testis samples (Palena *et al*., 2007). However, in a recent study that was carried out using qRT-PCR among a panel of 16 normal tissues, the expression pattern of *Brachyury* was observed in some of these tissues, including testis, spleen, uterus, stomach and lung (Jezkova *et al*., 2016). Therefore, *Brachyury* was excluded as a CTA gene based on the stringent method that we applied. So, drug targeting this proposed CTA might not result the specificity originality aimed at.

Western blot analysis was performed to determine the presence of Brachyury in a total number of 17 cancer cell lines to investigate drug activity in cancer cell lines that exhibited the expression of Brachyury. In contrast, negative Brachyury cancer cell lines should not respond to the drug, so the presence of Brachyury-specific drugs can be determined. Based on the western blot analysis, Brachyury was detected in all the cancer cell lines tested here (Figure 5.14 A). Given this, further exploration is required to identify Brachyury negative cells, possibly primary fibroblasts. In

addition, expression of two of the *Brachyury* splice variants TV1 and TV2 were expressed with detectable levels in most cancer cell lines tested by qRT-PCR, except the expression of TV1 in some cell lines such as NTERA2 and LoVo, which were determined with a Ct valued at more than 38. However, cell lines NTERA2 and LoVo were present at protein levels.

Western blot analysis was employed to determine the localisation pattern of Brachyury in SW480 cells. Based on this analysis, Brachyury appeared as a cytoplasmic protein with low-level in the nucleus (Figure 5.14 B) this was confirmed through IF analysis (Figure 5.15). It has been observed that Brachyury in cytoplasm is associated with aggressive tumours with poor prognoses, and Brachyury has been detected in the nucleus in metastatic tumour expression (Pinto *et al*., 2014; Pinto *et al*., 2016).

MSH2 is one of the differentially expressed genes analysed by RNA-seq. It has been observed that the fundamental role of *MSH2* is encoding protein that enables the repair of mutations errors that might occur in the S phase (Lagerstedt-Robinson *et al*., 2007; Zlatanou *et al*., 2011; Martín-López and Fishel 2013; Dowty *et al*., 2013). Mutations that occur in *MSH2* have been associated with patients with hereditary nonpolyposis colorectal cancer (HNPCC) (Lagerstedt-Robinson *et al*., 2007; Martín-López and Fishel, 2013).

In this preliminary study, we set out to determine whether there is an association between Brachyury- and MSH2-positive cells in CRC patient-derived material. This may have been disrupted by the drugs' influence, which might provide another assay to investigate the action and potential of anti-Brachyury drugs. However, using IF, we did not observe a clear correlation between Brachyury and MSH2 in the small number of samples that we tested. Staining and localisation of Brachyury within tumours is heterogeneous—it appears that Brachyury staining in tumours is more diffuse than in normal tissue, suggesting broad functions of Brachyury in cancer. To determine if there are correlations between the presence of Brachyury and MSH2 within tumours and how it effects patient outcomes, a much larger sample size is needed.
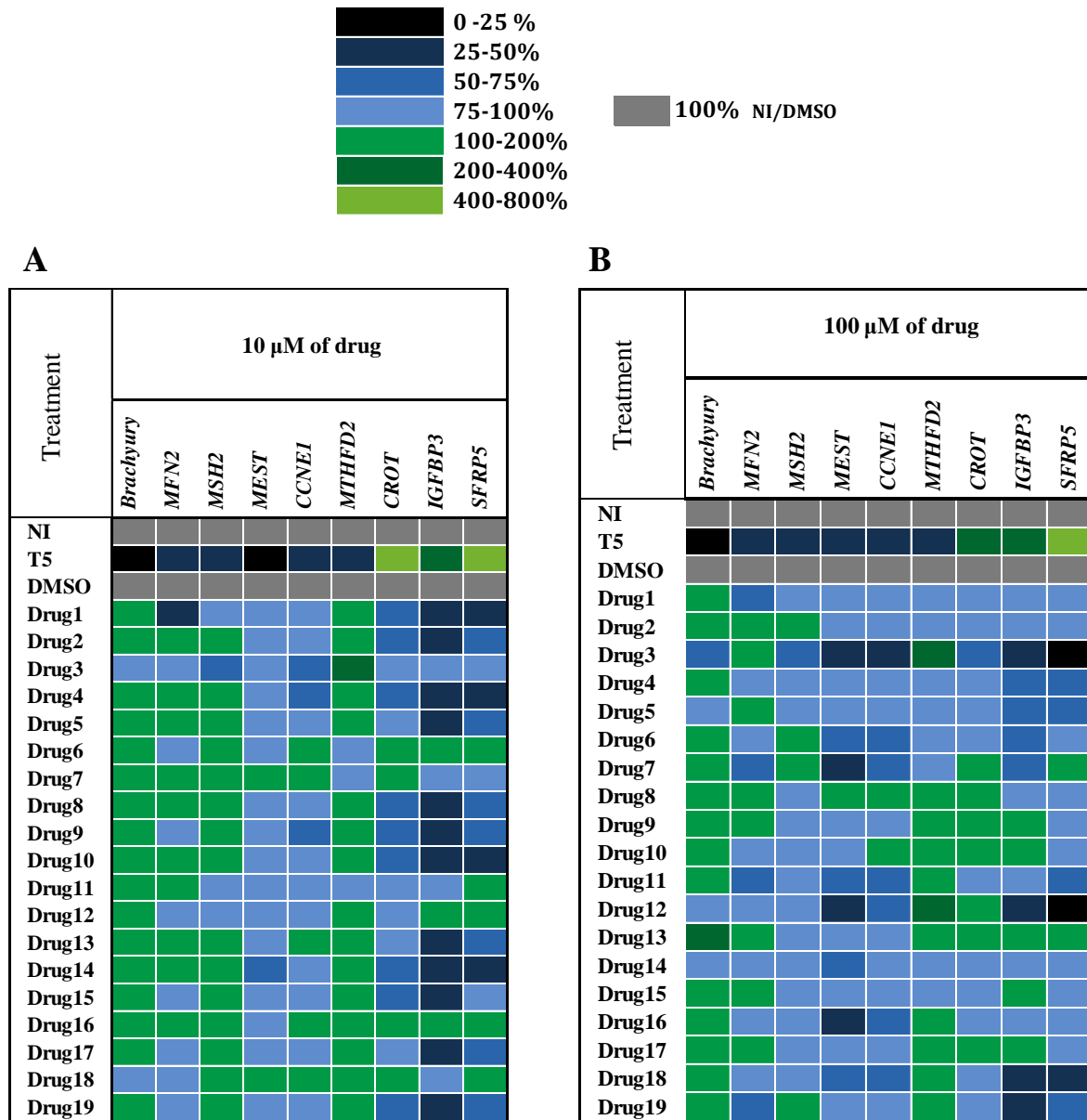
Figure 5.26 Summary of the transcript levels of the *Brachyury* and 8 other genes selected from the RNA-seq and their expression in SW480 cell line that was treated with two concentrations of the drugs.

The row represents the siRNA (NI) negative control, *Brachyury* siRNA (T5), the DMSO control and the 19 drugs that were used to treat the SW480 cells; the columns indicate the relative levels of the analysed genes. The cell colours indicate the percentages of transcripts compared to DMSO/NI. (A) Shows transcript levels in SW480 cells treated with 10 μM drug concentrations. (B) Shows transcript levels in SW480 cells treated with 100 μM drug concentrations.

5.4 Conclusion

As previously mentioned, several studies have reported the crucial role of the *Brachyury* gene in various cancer diseases. Furthermore, cohort genes that have important functions have been observed through RNA-seq to be up- or down-regulated as a result of the knockdown of the *Brachyury* gene, as confirmed in this study by qRT-PCR. The evaluation of the efficacy of 19 newly developed drugs that were designed to target the Brachyury was performed using qRT-PCR following the treatment of an SW480 cell line with two different concentrations of the drugs. Among the 50 most differentially expressed genes that were identified by RNA-seq following Brachyury knockdown, 8 genes were selected, including the *Brachyury* gene. Determination of the transcript levels of these genes in SW480 cells treated with the drugs was carried out using qRT-PCR. Interestingly, some drugs, such as drug 3, appeared to down-regulate the transcript levels of most of the genes in the SW480 cells at both concentrations; the efficacy of this drug was confirmed through western blot analysis and the viability of the SW480 cells. Other groups of drugs down-regulated gene transcript levels in the SW480 cells at the two concentrations. These new drugs require further investigation before they can be applied as anti-cancer drugs. As the Brachyury was detected in all of these cancer cell line that was used here. These drugs and their effectiveness on cell proliferation will be studied with a larger panel of cancer cell lines (see Chapter 6). Moreover, a preliminary study was carried out by IF to investigate whether there is any correlation between Brachyury and MSH2 in histological samples derived from CRC patients. Our results did not reveal a clear relationship between these genes in the samples here tested. A much larger sample size is needed to determine the exact relationship between Brachyury and MSH2 as well as possible associations with clinicopathological characteristics, such as tumour stage, site and metastasis.

Chapter 6.0 Monitoring the survival of cancer cell lines treated with potential anti-Brachyury drugs

6.1 Introduction

The mechanisms that control normal tissue growth are precisely regulated, but these are compromised in tumour cells (Hanahan and Weinberg, 2011; Feitelson *et al*., 2015). T-box genes have been reported to be involved in various cell processes, such as proliferation and maintaining the integrity of tissue and EMT. Aberrant expression of these genes has been observed in various types of cancer and may be responsible for incidences of neoplasia (Palena *et al*., 2011; Papaioannou, 2014). Loss of the function of T-box genes has been shown to be associated with human syndromes, such as DiGeorge Syndrome (DGS; *TBX1*) (Jerome and Papaioannou, 2001; Stoller and Epstein, 2005), Ulnar Mammary Syndrome (UMS, *TBX*3) (Bamshad *et al*., 1997; Bamshad *et al*., 1999), Holt-Oram Syndrome (*TBX5)* (Basson *et al*., 1997, Li *et al*., 1997), ACTH deficiency (*TBX19*) (Malpuech *et al*., 1988; Pulichino *et al*., 2003) and cleft palate with ankyloglossia (CPX), which is caused by the loss of *TBX22* (Braybrook *et al*., 2001).

The fundamental role of transcription factor Brachyury during early embryonic development, particularly in the mesoderm, has been observed. A number of studies have found that Brachyury is also associated with tumour spread (Sun *et al*., 2015; Palena *et al*., 2014). In adenoid cystic carcinoma cells (AdCC), it has been found to play a critical role in promoting tumour growth and in the formation of metastasis (Shimoda *et al*., 2012). In tumour samples and cell lines obtained from breast tissues, high levels of Brachyury have been correlated to a process leading to breast tumorigenesis, proliferation and treatment resistance (Shimoda *et al*., 2012; Palena *et al*., 2014; Pires and Aaronson, 2014; Li *et al*., 2016).

Due to the role of this transcription factor Brachyury in various types of tumours, it has been become an attractive target for the development of cancer treatments. Recently, it was demonstrated that knockdown of Brachyury in AdCC inhibits cancer metastasis (Kobayashi *et al*., 2014). In a patient with a lung tumour, expression of *Brachyury* was high in tissues with high grade II-IV and low during the early stage of lung cancer (Fernando *et al*., 2010). Another study, revealed

the potential of Brachyury in hepatocellular carcinoma (HCC) to enhance the process of metastasis by effecting the EMT via a different pathway (Du *et al*., 2014). Brachyury is an excellent target for cancer treatment because it has been implicated in several types of cancer (Palena *et al*., 2007; Kobayashi *et al*., 2014; Pinto *et al*., 2016). The expression of *Brachyury* has been reported in a wide range of human cancer samples through the use of RT-PCR (Palena *et al*., 2007). Western blot was also used to detect Brachyury at the protein level in a large number of cancer cell lines derived from different organs (see Section 5.2.4).

As mentioned above, the important role that Brachyury plays in enhancing cancer cell proliferation and metastasis makes it a promising target for cancer treatment. In this chapter, the efficacy of drugs designed in collaboration with the Drug Screening Platform at Cardiff University will be evaluated for cancer cell lines (see Section 5.2.4). By monitoring the efficacy of these new drugs, drugs that do not reduce the activity of Brachyur*y* among these cell lines can be eliminated, and drugs that effectively target cell proliferation can be determined for further study. The most effective drugs will be evaluated by applying an analysis curve, and drugs that display no effect in the cancer cell line proliferation.

6.2 Results

Cell seeding density in a 24-well plate was optimised for each type of cancer cell line that was tested and for human embryonic kidney 293 (HEK- 293; see Table 2.1). These cell lines were plated with an initial seeding density and treated with 19 drugs and DMSO at concentrations of 100 μM, except for an untreated cell line. Depending on the cell conditions, the cells were incubated for 72 h, and cell growth was checked daily. Using light microscopy, cell proliferation was monitored, and the effectiveness of each drug was compared against the DMSO-treated control and untreated cells. The human cell line used in this study is provided in Table 6.1. Cell survival was classified into four categories according to the effectiveness of the drugs affecting cell proliferation compared to the control (Figure 6.1).

Table 6.1 Cell lines used in this study and cell sources.

Source	Cell line			
Colon	SW480	HCT116	LoVo	T84
Ovary	A2780	PEO14		
Skin	G-361	COLO800		
Blood	K562	Jurkat	KBM-7	
Lung	H460			
Breast cancer	MCF-7			
Liver	HepG2			
Cervical cancer	HeLa			
Germ cell tumours	NTERA2			
Brain	1231N1			
Human embryonic kidney	HEK- 293			
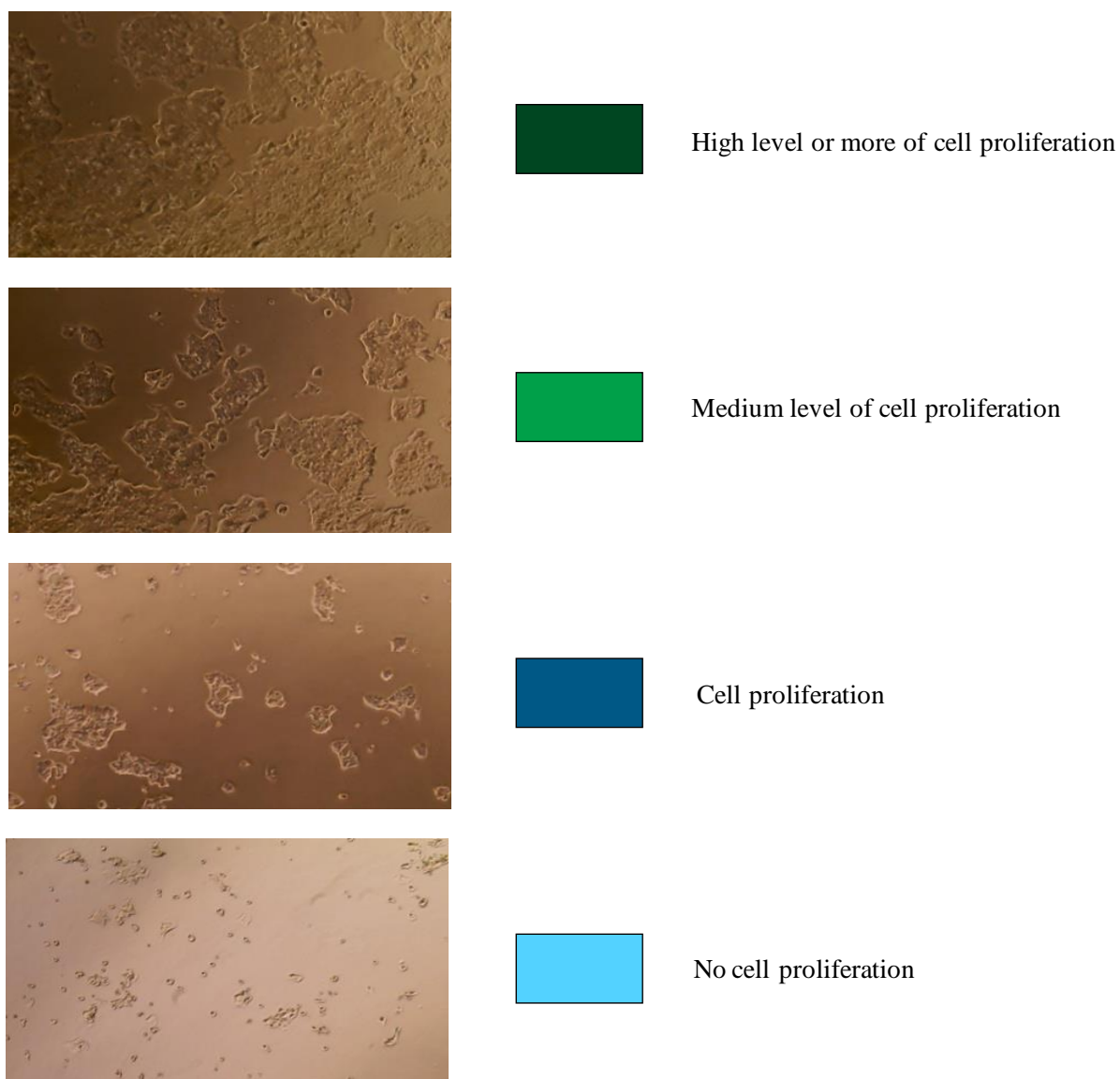
Figure 6.1 Monitoring drug efficacy for the survival of various types of cancer cell lines and HEK-293.
The effectiveness of the drugs for each cell line was tested, and cell proliferation was classified into four categories. The colours represent the four categories, which were compared to the DMSO treated control and untreated cells. Each cell line was treated with 19 drugs and DMSO at concentrations of 100 μM. Cell growth was monitor using light microscopy.

6.2.1 Monitoring proliferation of human cancer cell lines SW480 and HCT116

To assess the efficacy of the 19 new drugs for treating multiple types of cancer cells derived from various sources, each cell line was treated with a drug concentration of 100 μM. Cell proliferation was monitored using light microscopy and assessed based on four classifications for drug efficacy and cell survival (Figure 6.1). The proliferation of human CRC cell line SW480 was effected by some drugs, including 3, 6, 11 and 18 (Figure 6.2A). SW480 exhibited more sensitivity to drugs 3 and 18 compared to the control. From all the drugs tested, these two drugs effected the cell proliferation profile of SW480, which presented no cell proliferation (Figure 6.2A). Other drugs, including 6 and 11, were observed to effect the cell proliferation profile but with less efficacy. Most of the drugs, such as 1–2, 4–5and 7–10, had no effect on the cell proliferation rate and growth of this cell line, which were significantly higher compared to the control (Figure 6.2A).

Cell line HCT116 was derived from colon tissue and was used to investigate the proliferation behaviour following treatment with the study drugs. Among these drugs, some were effective for inhibiting cell proliferation. Drugs 1 and 11 had lower efficacy compared to the control, which exhibited cells with medium levels of proliferation (Figure 6.2B). Drugs 6 and 18 prevented cell proliferation and cell survival, whereas drug 19 reduced the amount of cell proliferation. According to the classifications used in this study, the efficacy of drug 19 and survival of the cancer cell line was classified as cell proliferation, which indicated that the proliferation profile of HCT116 treated with drug 19 was below a medium level (Figure 6.2B). The level of cell proliferation was monitored after treatment with other drugs and was found to increase; for example, some of the tested drugs were not effective, and cell growth increased with high levels of proliferation for drugs 2–5, 7–10 and 12–17. This indicates that most of the selected drugs increased cell proliferation (Figure 6.2B).

A   SW480
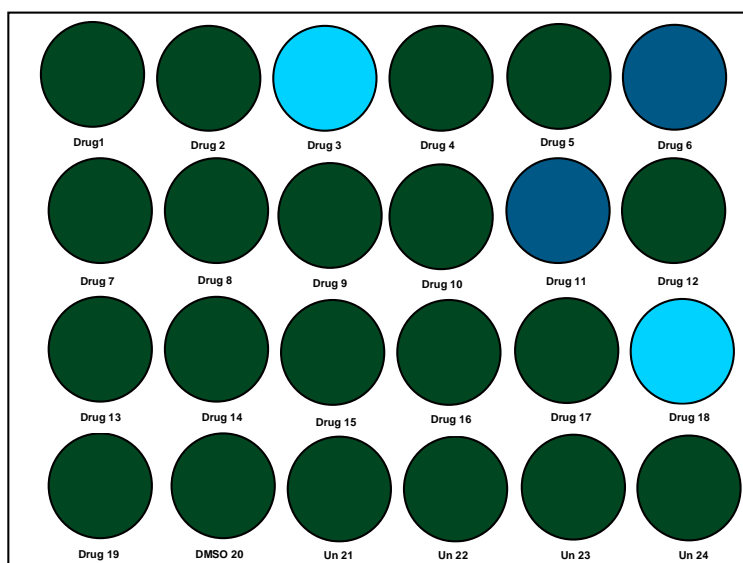
B   HCT116
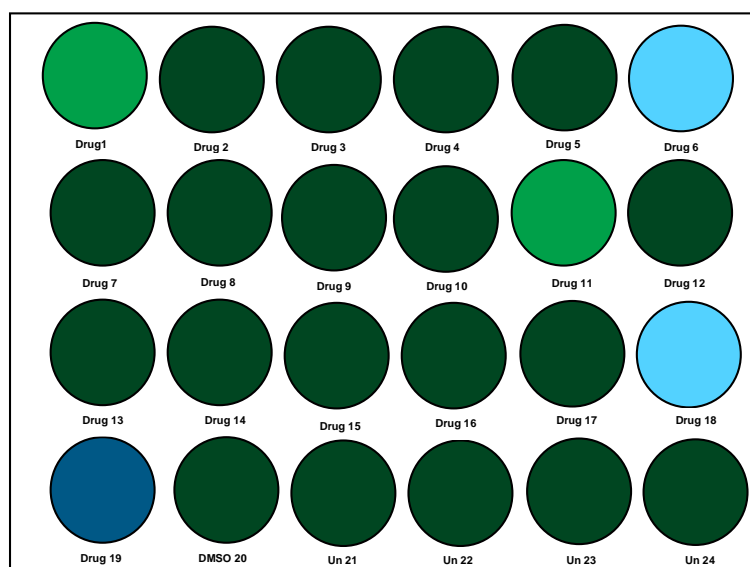
Figure 6.2 Analysis of drug efficacy, targeting Brachyury in cancer cell lines SW480 and HCT116.
Monitoring cell survival in cell lines treated with 19 new drugs and assessing the efficacy of these drugs for inhibiting cell proliferation was accomplished using light microscopy. The colours represent the four cell categories based on drug efficacy compared to the DMSO-treated and untreated cell line controls (Figure 6.1). Wells 1–19 represent cells treated with the drugs at concentrations of 100 μM, and the DMSO-treated cells are represented by well 20 and untreated cells in wells 21-24. (A) Cancer cell line SW480 was treated with drugs and DMSO. (B) Cancer cell line HCT116 that treated with drugs and DMSO.

6.2.2   Monitoring proliferation of human cancer cell lines LoVo and T84

Drug screening of cancer cell line LoVo was conducted, and the cell proliferation profile was determined using light microscopy. Some of the drugs, including 3, 11, 18 and 19, were observed to effect cell proliferation by reducing the number of cells or preventing cell proliferation. Drugs 3 and 19 were determined to effect the cells by decreasing the amount of cell proliferation compared to the control, whereas cells treated with drugs 11 and 18 were not able to survive, indicating the effect of these drugs on the survival of cells. Among the drugs that was evaluated, 15 drugs were identified by their ability to enhance the rate of cell proliferation, such as 1–2, 4–10 and 12–17. The efficacy of these drugs and cell proliferation of the LoVo cell line after treatment were classified into four category based on comparison to the DMSO-treated control (Figure 6.3A).

The growth profile of cancer cell line T84 was examined following treatment with the drugs, to eliminate the number of drugs unable to inhibit cell growth and to detect potential drugs affecting cell proliferation. The efficacy of the drugs was evaluated based on the proliferation profile of T84, which revealed that a limited number of these drugs were highly effective, In particular, drugs 7 and 11 clearly prevented cell proliferation, while drug 2 caused a medium level of proliferation and drug 18 caused a low density in the cancer cell line after treatment. The majority of these drugs had no effect on the growth rate of the cancer cell line or the level of cell proliferation, which remained high level. The following drugs should be eliminated:1, 3–6, 8–10 and 12–17 (Figure 6.3B).
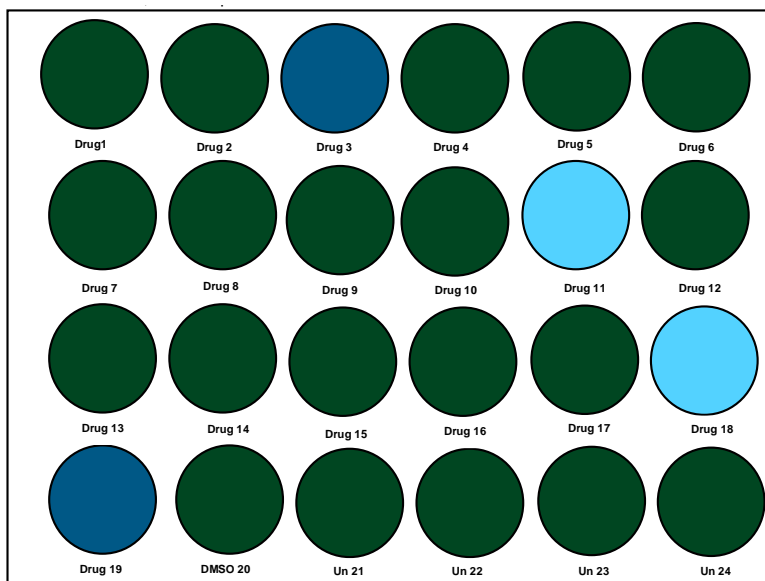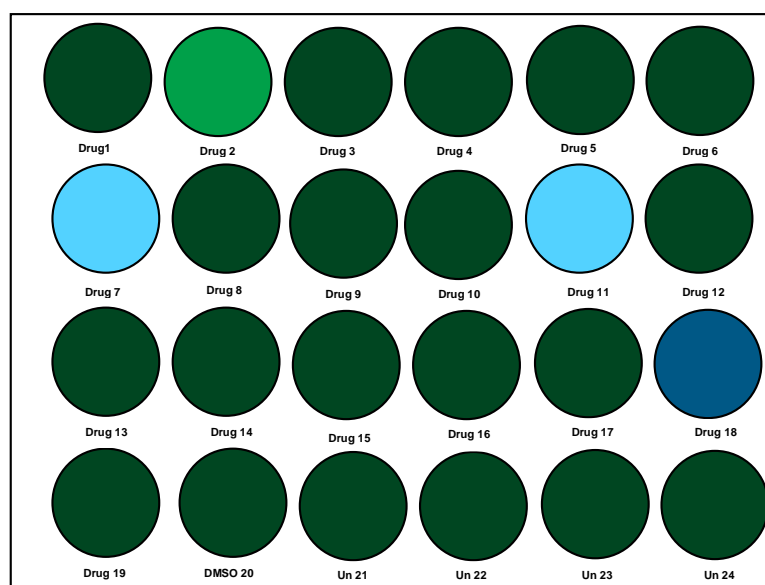
A LoVo

B T84

Figure 6.3 Analysis of drug efficacy, targeting Brachyury in cancer cell lines LoVo and T84.
Monitoring cell survival of cells treated with 19 new drugs and assessing the efficacy of these drugs for inhibiting cell proliferation was accomplished using light microscopy. The colours represent the four categories that the cells were classified into, which are based on drug efficacy compared to the DMSO-treated and untreated cell controls. Wells 1–19 represent cells treated with these drugs at concentrations of 100 μM, well 20 represents the cells treated with DMSO and untreated cells are indicated by wells 21–24. (A) Cancer cell line LoVo was treated with drugs and DMSO. (B) Cancer cell line T84 was treated with drugs and DMSO.

6.2.3   Monitoring proliferation of human cancer cell lines A2780 and PEO14

Among the selected cancer cell lines that exhibited expression of Brachyury at the protein level was the ovarian cancer cell line (A2780; see Section 5.2.4). Screening of the drugs was carried out in A2780, and cell proliferation was determined using light microscopy. The proliferation of the A2780 cell line was inhibited by drug 11, which was the most effective from the panel of drugs. Another drug that was able to inhibit growth of this cancer cell line was drug 3 but with less efficacy than drug 11. This cell line was observed to have a medium level of proliferation after treatment with drugs 9, 12, 18 and 19. High levels of cell proliferation occurred following treatment with large amounts of inhibitor, including drugs 1–2, 4–8, 10 and 13–17. Based on classification, cell proliferation for these 13 drugs caused high levels of cell proliferation (Figure 6.4A).

Ovarian cancer cell line PEO14 was also examined for cell proliferation after treatment with the 19 drugs targeting Brachyury activity. Interestingly, drug 3 was observed in both ovarian cancer cell line A2780 and PEO14 to inhibit the cell proliferation rate, significantly reducing cell proliferation or preventing it completely. Drug 7 was also observed to effect proliferation in this cell line, and cell death was observed after treatment with this inhibitor. Drug 11 was detected in both ovarian cancer cell lines to have a positive effect and reduce the amount of cell proliferation; however, it was more effective in the A2780 than the PEO14 cell line. Monitoring these drugs revealed that the PEO14 cell line was able to survive with a medium level of proliferation when treated with drugs 12 and 19. In contrast, most of these drugs did not affect the growth rate of the cancer cells, including drugs 1–2, 4–6, 8–10 and 13-17 (Figure 6.4B).

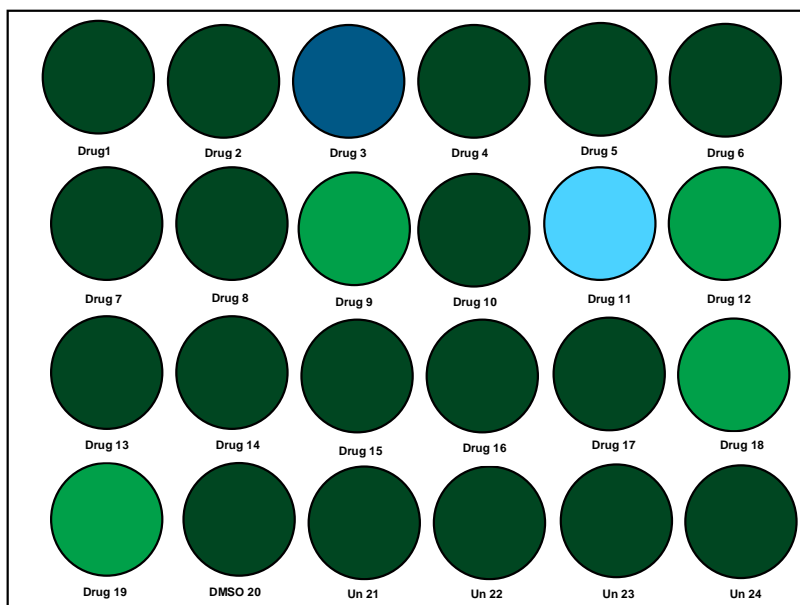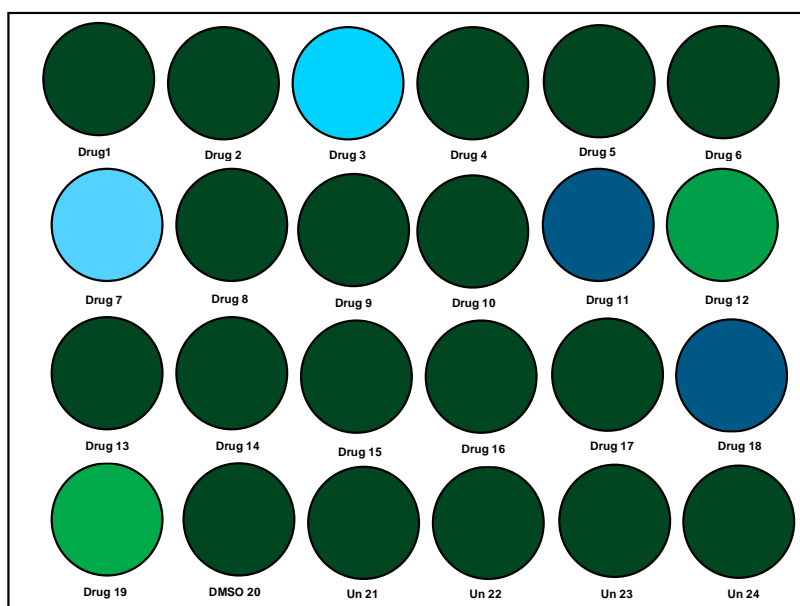**A A2780**

B PEO14

Figure 6.4 Analysis of the drug efficacy, targeting Brachyury in cancer cell lines A2780 and PEO14.
Monitoring cell survival in cell lines treated with 19 new drugs and assessing the efficacy of these drugs for inhibiting cell proliferation was accomplished using light microscopy. The colours represent the four categories that the cells were classified into, based on drug efficacy compared to the DMSO-treated and untreated cell controls. Wells 1–19 represent cells treated with the drugs at concentrations of 100 μM, well 20 represents the cells treated with DMSO and the untreated cells are represented by wells 21–24. (A) Cancer cell line A2780 was treated with drugs and DMSO. (B) Cancer cell line PEO14 was treated with drugs and DMSO.

6.2.4 Monitoring proliferation of human cancer cell lines G-361 and COLO800

This study applied four categories based on drug effectiveness and cell proliferation rate. The human malignant melanoma cell line (G-361) was examined after treatment with 19 drugs. The most effective drugs for this cancer cell line were drug 3 and 11; therefore, cells treated with these drugs were classified as having no cell proliferation. Only drugs 12 and 19 were observed to reduce the proliferation level of G-361 cells, which were classified as having a medium level of proliferation compared to the control. The proliferation of this cancer cell line after treatment with drugs 1–2, 4–0 and 13–18 was high based on the cell proliferation profile (Figure 6.5A).

Screening the efficacy of the 19 drugs for treating the COLO800 cell line revealed that some of the drugs were able to reduce cell proliferation. Drug 3 was found to affect cell growth in both of the human melanoma cell lines included here. For example, the G-361 cell line was not able to survive following treatment with drug 3, whereas the COLO800 cell line was observed to survive but with less cell growth compared to the DMSO-treated and untreated control cells. Other drugs affected cell growth specific to the COLO800 cell line, such as drugs 6, 7 and 11, which reduced COLO800 proliferation. After these 19 drugs were analysed using microscopy, only drug 18 was observed to induce cell death, and this drug was more specific to this cell line, compared to drugs 3, 6, 7 and 11. The proliferation rate of the COLO800 cell line was monitored after treatment with drugs 1–2, 4–5, 8–10 and 12–17, and a high level of proliferation indicated the most of these drug should be eliminated from further investigation (Figure 6.5B).

A G-361

B COLO800

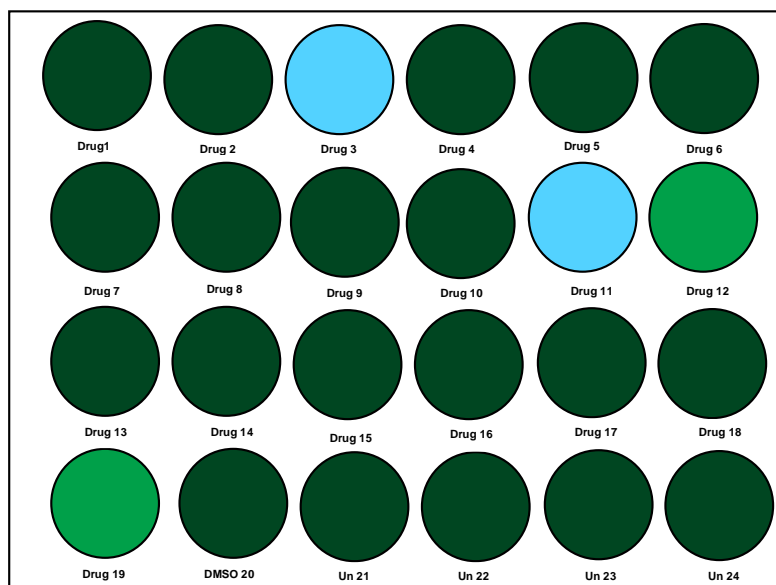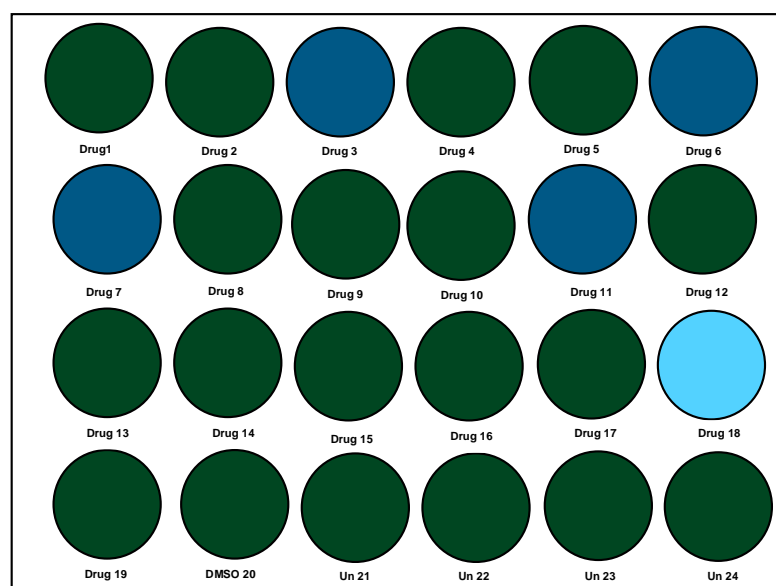**Figure 6.5 Analysis of drug efficacy, targeting Brachyury in cancer cell lines G-361 and COLO800.**
Monitoring cell survival after treatment with 19 new drugs and the efficacy of these drugs for inhibiting cell proliferation was accomplished using light microscopy. The colours represent the four categories that cells were classified into, based on drug efficacy compared to DMSO-treated and untreated control cells. Wells 1–19 represent cells treated with these drugs at concentrations of 100 μM, cells treated with DMSO are represent by well 20 and untreated cells are indicated by wells 21–24. (A) Cancer cell line G-361 was treated with drugs and DMSO. (B) Cancer cell line COLO800 was treated with drugs and DMSO.

6.2.5   Monitoring proliferation of human cancer cell lines K562 and Jurkat

Evaluation of drug efficacy was carried out in human leukaemia cell line (K562). After this cell line was plated into a 24-well plate and treated with the 19 drugs and DMSO, cell proliferation was monitored using light microscopy and cell density was compared to the DMSO-treated control. Of these 19 drugs, the most effective drug for inhibiting cell proliferation was drug 11, which indicates that this drug should be considered as potentially affecting the K562 cell line. Drugs targeting the proliferation of K562 cells, such as 3 and 18, resulted in a low cell proliferation rate, whereas drug 12 created a medium level of proliferation. Other drugs, such as 1–2, 4–10 and 13–17, can be eliminated from this panel of drugs because these created a high level of proliferation in cancer cell line K562 (Figure 6.6A).

Another human leukaemia cell line, Jurkat, was tested after Brachyury was found to be expressed in this line using western blot analysis (see Section 5.2.4). Interestingly, both leukaemia cell lines, K562 and Jurkat, were not able to survive treatment with drug 11, indicating the important role this drug plays in inducing cell death. In the present study, the Jurkat cell line was not able to survive drug 3, which acts in a similar fashion as drug 11. A medium-level proliferation rate in the Jurkat cell line when treated with drug 17 was observed, whereas reduction of cell proliferation was detected as a result of treatment with drug 7. Of the 19 drugs tested, 15 drugs did not affect proliferation of this cancer cell line, including drugs 1–2, 4–6, 8–10, 12-16 and 18-19 (Figure 6.6 B).

A K562

B Jurkat

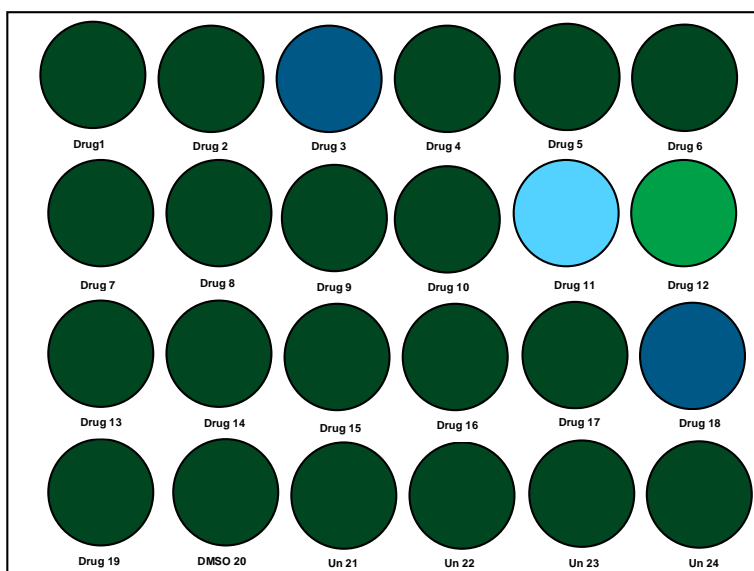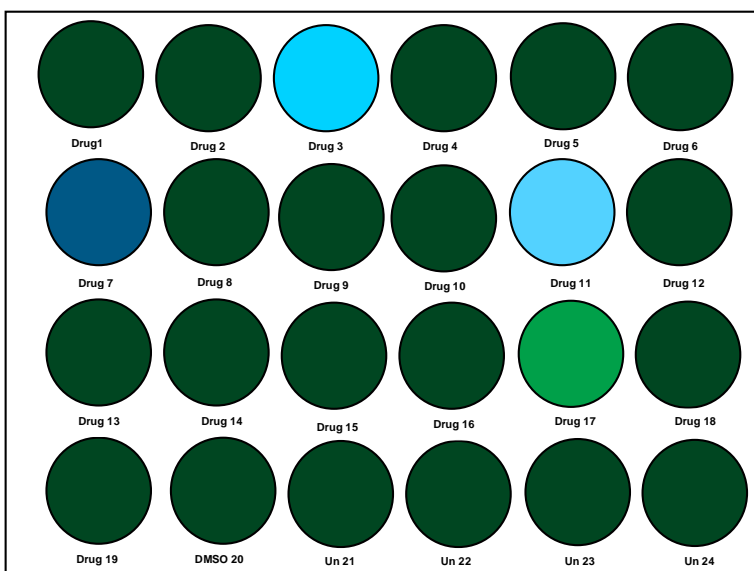**Figure 6.6 Analysis drug efficacy, targeting Brachyury in cancer cell lines K562 and Jurkat.**
Monitoring cell survival in cells treated with the 19 new drugs and the efficacy of these drugs for inhibiting cell proliferation was accomplished using light microscopy. The colours represent the four categories that cells were classified into, based on drug efficacy compared to the DMSO-treated and untreated cell controls. Wells 1–19 represent cells treated with these drugs at concentrations of 100 μM, well 20 represents cells treated with DMSO and untreated cells are indicated by wells 21–24. (A) Cancer cell line K562 was treated with drugs and DMSO. (B) Cancer cell line Jurkat was treated with drugs and DMSO**.**

6.2.6   Monitoring proliferation of human cancer cell lines KBM-7 and H460

A human myeloid leukaemia cell line, KBM-7, was among the cancer cell lines selected because Brachyury is present in this cell line (see Section 5.2.4). The proliferation of KBM-7 cells treated with the 19 drugs and DMSO was assessed. Using light microscopy techniques, the proliferation rate of the KBM-7 cell line was classified into two classes: cell proliferation with a low survival rate and a high level of cell proliferation. The first class of KBM-7 cells was observed with drugs 11, 12 and 18, while the proliferation profile revealed an increased level among KBM-7 cells treated with drugs 1–10 , 13–17 and 19 (Figure 6.7A).

Similarly, drug efficacy was investigated to determine the effectiveness of the drugs for treating human cancer cell line H460, derived from lung cancer. H460 cells were did not proliferate after being treated with drugs 11 and 18, indicating that these two drugs were the most effective among the 19 drugs tested. The cancer cell line was not able to survive after treatment with these two drugs, which were also effective for the KBM-7 cell line to a lesser degree. Because of these results, drugs 11 and 18 should be considered for further study. The activity of drug 7 was determined, and a medium rate of H460 cell line proliferation was observed, but the rate of cell survival was significantly lower with drug 3. Most of the drugs were not effective, and H460 cell line proliferation was significantly higher compared to the DMSO-treated control, including drugs 1-2, 4-6, 8-10 and 12-17 (Figure 6.7B).
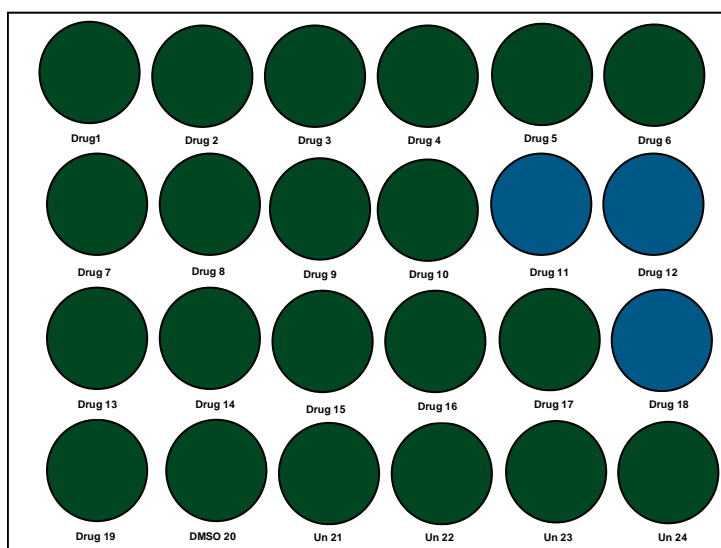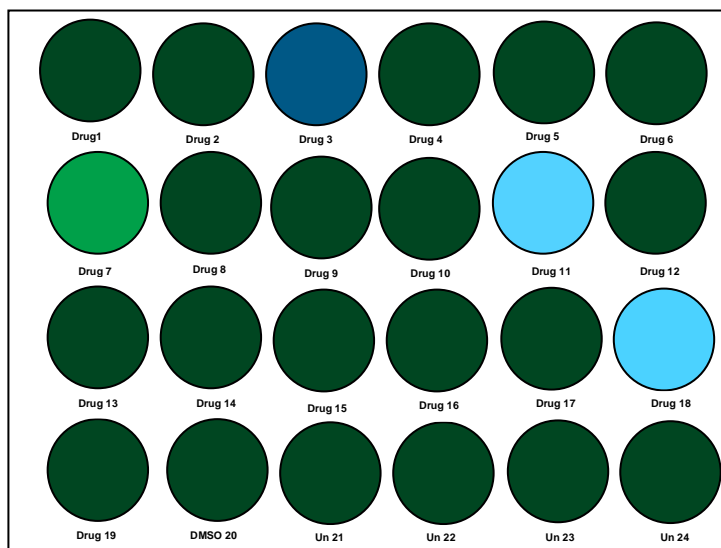
A KBM-7

B H460

Figure 6.7 Analysis of drug efficacy, targeting Brachyury in cancer cell lines KBM-7 and H460.
Monitoring survival of cells treated with 19 new drugs and the efficacy of these drugs for inhibiting cell proliferation was accomplished using light microscopy. The colours represent the four categories that the cells were classified into depending on drug efficacy compared to the DMSO-treated and untreated cell controls. Wells 1–19 represent cells treated with these drugs at concentrations of 100 μM, well 20 represented cells treated with DMSO and untreated cells are indicated by wells 21–24. (A) Cancer cell line KBM-7 was treated with drugs and DMSO. (B) Cancer cell line H460 was treated with drugs and DMSO.

6.2.7   Monitoring proliferation of human cancer cell line MCF-7 and HepG2

Of the 19 drugs screened using the human breast cancer cell line, MCF-7, only six drugs were potentially effective at targeting the cell line. The proliferation of this cancer cells treated with drug 3 was observed and classified as being a medium rate. Drugs 11 and 18 were found to be highly effective for inhibiting cell proliferation in the MCF-7 cell line. Drugs 6, 13 and 19 caused a low rate of MCF-7 cell proliferation. Most of the new drugs did not demonstrate positive effectives on this cancer cell line. MCF-7 did undergo a rapid rate of proliferation after treatment with drugs 1–2, 4–5, 7–10, 12 and 14-17; thus, only six of the 19 drugs should be selected for further investigation (Figure 6.8A).

To assess the efficacy of these new inhibitors for the human hepatoma cell line, HepG2, derived from liver, treatments were monitored using light microscopy. Interestingly, some drugs were observed to have a similar effective for both the MCF-7 and HepG2 cell lines. Drug 3 reduced the proliferation of MCF-7, whereas proliferation of HepG2 was clearly prevented. In addition, drugs 11 and 18 appeared to demonstrate positive effects in both cell lines; however, these drugs were more effective for the MCF-7 compared to the HepG2 cell line. The HepG2 cell line presented a medium level of proliferation after treatment with drug 2. The remaining drugs, including 1, 4–10 and 12–17, did not affect proliferation in the HepG2 cell line, which was significantly increased (Figure 6.8B).
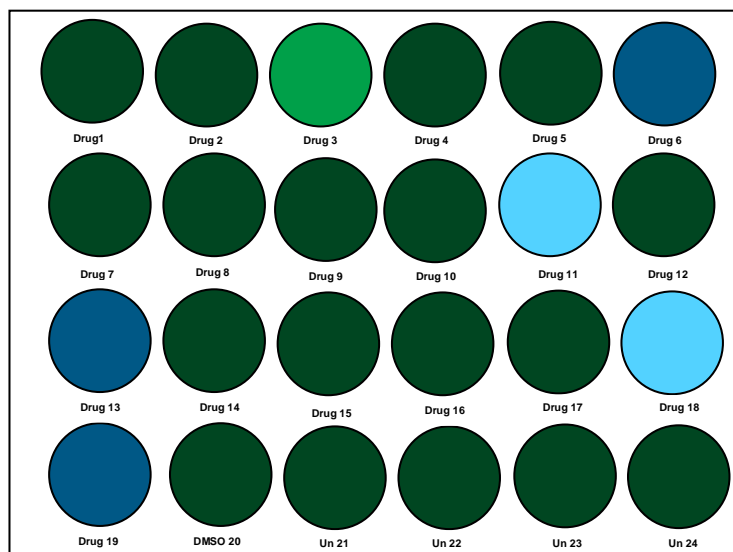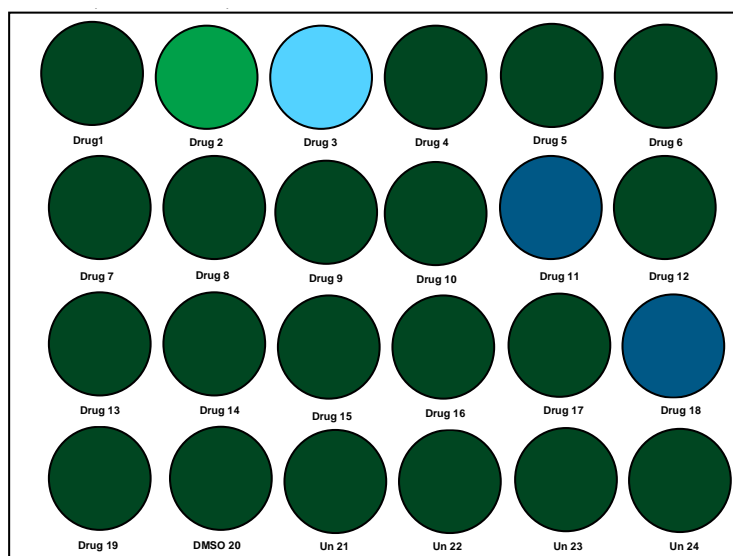
A MCF-7

B HepG2

Figure 6.8 Analysis of drug efficacy, targeting Brachyury in cancer cell line MCF-7 and HepG2.
Monitoring survival of cells treated with 19 new drugs and the efficacy of these drugs for inhibiting cell proliferation was accomplished using light microscopy. The colours represent the four categories that the cells were classified into depending on drug efficacy compared to the DMSO-treated and untreated cell controls. Wells 1–19 represent cells treated with these drugs at concentrations of 100 μM, well 20 represented cells treated with DMSO and untreated cells are indicated by wells 21–24. (A) Cancer cell line MCF-7 was treated with drugs and DMSO. (B) Cancer cell line HepG2 was treated with drugs and DMSO.

6.2.8   Monitoring proliferation of human cancer cell lines HeLa and NTERA2

New drugs have been designed *in silico* to target the function of Brachyury associated with cancer. The cervical cancer cell line, HeLa, was used to test the efficacy of these drugs in this study. Using a light microscopy technique, the survival of HeLa cell line was monitored. Only two of the 19 drugs exhibited positive effects on HeLa cell proliferation: drugs 16 and 18. After treatment with drug 16, the HeLa cell line showed no proliferation. Similarly, treatment with drug 18 caused a low level of proliferation. Based on this screening, drug 16 appears to be the most effective drug for preventing cell proliferation in this cancer cell line. The remaining 17 drugs, including drugs 1–15, 17 and 19, rapidly increased the rate of cell proliferation (Figure 6.9A).

The embryonal carcinoma, NTERA2, cell line was also used to assess drug efficacy and to determine the most effective drugs that should be considered for further investigation. The proliferation of the NTERA2 cell line was assessed after treatment with the 19 drugs and with DMSO. Among these drugs, drug 18 clearly prohibited NTERA2 cell proliferation. An analysis of the drugs and their effectiveness for preventing cell proliferation is presented, which is especially noteworthy for drugs 3 and 11; however, cell proliferation was significantly lower after treatment with drug 11 compared to drug 3 and the DMSO control. Both cancer cell lines, HeLa and NTERA2, were effected by drug 18, and the proliferation rates of these cancer cell lines were reduced, and the NTERA2 cells were not able to survive. The proliferation rate of NTERA2 was high after treatment with drugs 1–2, 4–10 and 12–17 (Figure 6.9B).

A HeLa

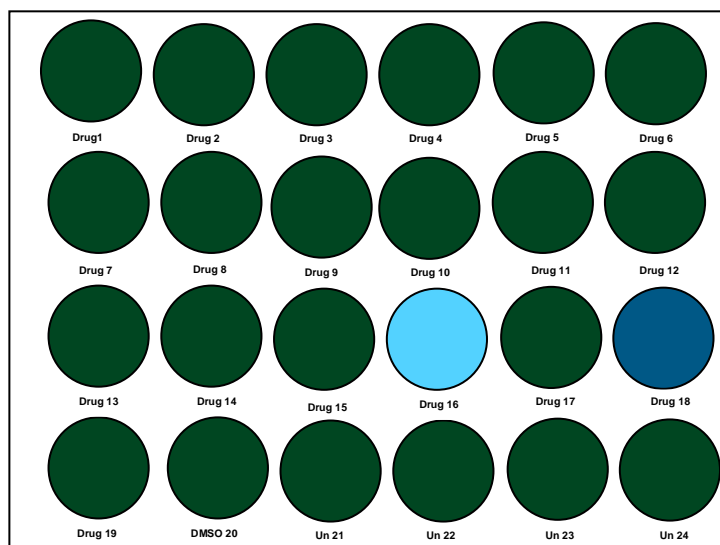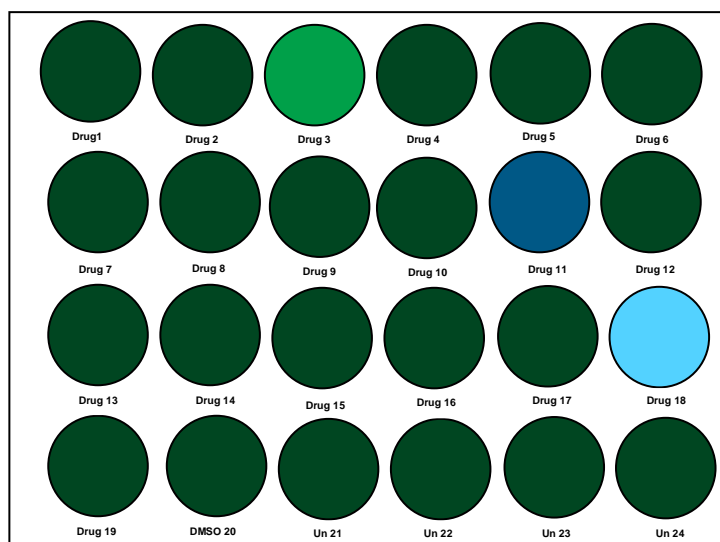## B Embryonal carcinoma (NTERA2)

Figure 6.9 Analysis of drug efficacy, targeting Brachyury in cancer cell lines HeLa and NTERA2.
Monitoring survival of cells treated with 19 new drugs and the efficacy of these drugs for inhibiting cell proliferation was accomplished using light microscopy. The colours represent the four categories that the cells were classified into depending on drug efficacy compared to the DMSO-treated and untreated cell controls. Wells 1–19 represent cells treated with these drugs at concentrations of 100 μM, well 20 represented cells treated with DMSO and untreated cells are indicated by wells 21–24. (A) Cancer cell line HeLa was treated with drugs and DMSO. (B) Cancer cell line NTERA2 was treated with drugs and DMSO.

6.2.9   Monitoring proliferation of human cancer cell lines 1231N1 and HEK-293

The human astrocytoma cell line, 1231N1, was used after the density of these cancer cells was optimised in a 24-well plate to investigate if the drugs were effective for preventing cell proliferation and to eliminate ineffective drugs that did not reduce cell proliferation or specifically target the 1231N1 cell line. Monitoring proliferation of cells from this line treated with each of the 19 drugs revealed that drug 18 inhibited proliferation of the 1231N1 cell line, which was not able to survive. The rate of proliferation decreased, and the ability of the 1231N1 cell line to survive was reduced to a medium level when treated with drug 3. The 1231N1 cell proliferation was reduced after treatment with drug 11, when compared to DMSO-treated cells. Among the drugs tested, increased proliferation was observed after treatment with drugs 1–2, 4–10, 12–17 and 19 (Figure 6.10A).

The human embryonic kidney cell line, HEK-293, was used to test drugs targeting proliferation of HEK-293. Drugs 11 and 18 were the most effective and demonstrated positive efficacy for the HEK-293 cells, which was determined by monitoring cell proliferation, which was completely prevented. Among these drugs, the cell proliferation rate was significantly reduced by drugs 3, 6–7 and 12. Thirteen drugs were not effective, and the proliferation of HEK-293 cells was clearly increased. After screening these drugs and evaluating their efficacy, most of the drugs should not be considered for further investigation (Figure 6.10B).

A 1231N1
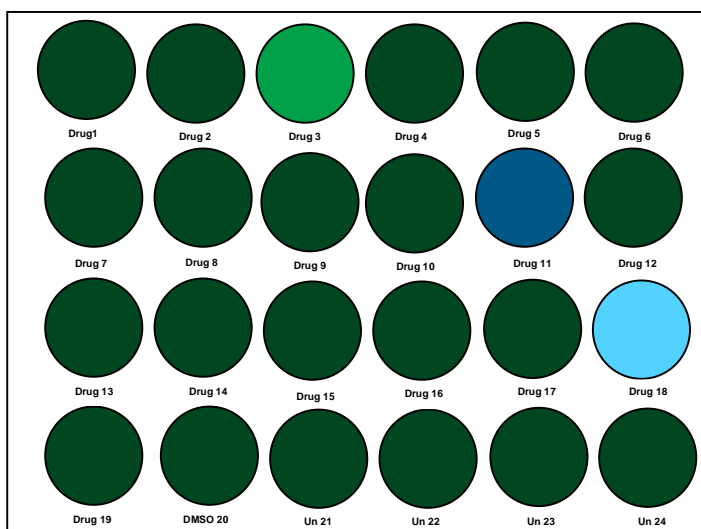
B HEK-293
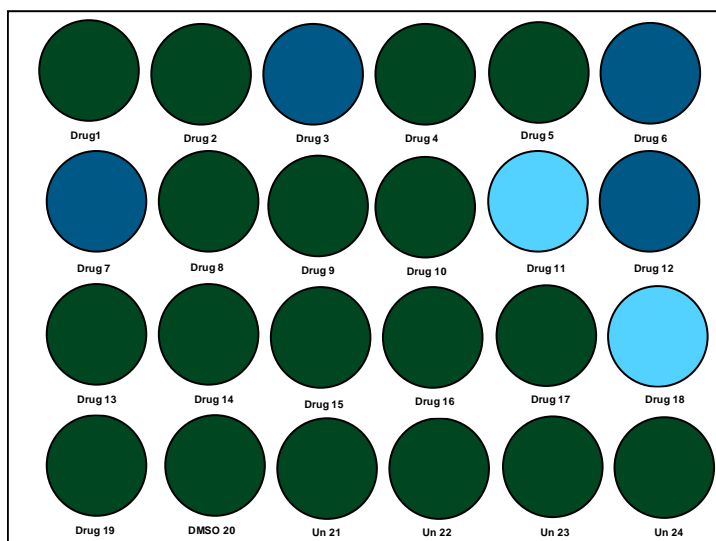
Figure 6.10 Analysis of drug efficacy, targeting Brachyury in cancer cell lines 1231N1 and HEK-293.
Monitoring survival of cells treated with 19 new drugs and the efficacy of these drugs for inhibiting cell proliferation was accomplished using light microscopy. The colours represent the four categories that the cells were classified into depending on drug efficacy compared to the DMSO-treated and untreated cell controls. Wells 1–19 represent cells treated with these drugs at concentrations of 100 μM, well 20 represented cells treated with DMSO and untreated cells are indicated by wells 21–24. (A) Cancer cell line 1231N1 was treated with drugs and DMSO. (B) Cancer cell line HEK-293 was treated with drugs and DMSO.

6.3   Evaluation the efficacy of drugs using a growth curve analysis

As mentioned previously, some drugs were able to affect the proliferation of most of these cancer cell lines, such as drugs 3, 11 and 18. Among the cancer cell lines examined in this study there were different levels of proliferation observed after treatment with the 19 drugs (see Section 6.2.1– 6.2.9). Four cancer cell lines were selected with the most effective drugs, which reduced or inhibited cell proliferation rates.

These cell lines were SW480, HCT116, H460, and HeLa, and growth curve analysis was applied. To assess whether these cancer cell lines were able to survive treatment with the drugs at a concentration of 10 μM, cells were plated in a 6-well plate and treated with the drug. The SW480 cells were treated with drugs 3, 11 and 18 because these were the most effective among the 19 drugs at 100 μM, and this cancer cell line was not able to survive after treatment with drug 3 and 18 and had low levels of survival with drug 11 (see Section 6.2.1). Therefore, these drugs were selected to investigate the behaviour of SW480 cells following treatment (Figure 6.11A). The HCT116 cells were treated with drugs 1, 6 and 18 (Figure 6.11B), and H460 cells were treated with drugs 11 and 18 (Figure 6.12A). In addition, some drugs were not effective at inhibiting the rate of proliferation in some cancer cell lines, which were used to evaluate whether these cancer cell lines were able to proliferate compared to the DMSO-treated control. For example, the HeLa cell line was selected and treated with drugs 3 and 11 because these drugs displayed no effect, and the HeLa cell line proliferated to greater numbers after treatment with these drugs (Figure 6.12B). This was consistent with the findings obtained using light microscopy (see Section 6.2.8).

The cells were counted daily by either an automatic counter or haemocytometer. Based on these cell counts, the growth curve demonstrated cell viability for each of the treated cancer cell lines. The growth curve analysis showed that the SW480 cell proliferation rate was significantly reduced compared to the DMSO-treated cells. Based on growth curve analysis, the proliferation level of HCT116 cells was also significantly reduced (Figures 6.11A and 6.11B). Additionally, the rate of proliferation was significantly decreased in H460 cells treated with drugs 11 and 18 comparing to DMSO-treated cells, whereas HeLa cells showed no significant effect and had a proliferation rate that increased rapidly (Figures 6.12A and 6.12B).

A
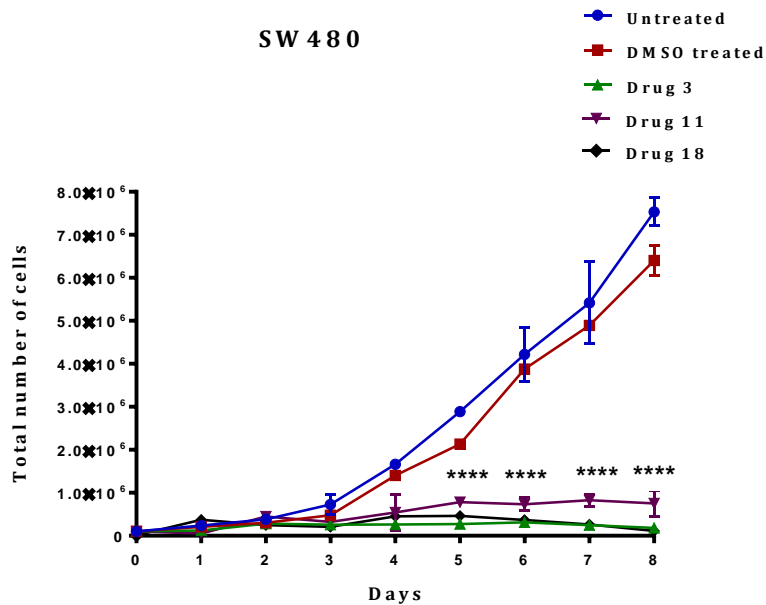
B
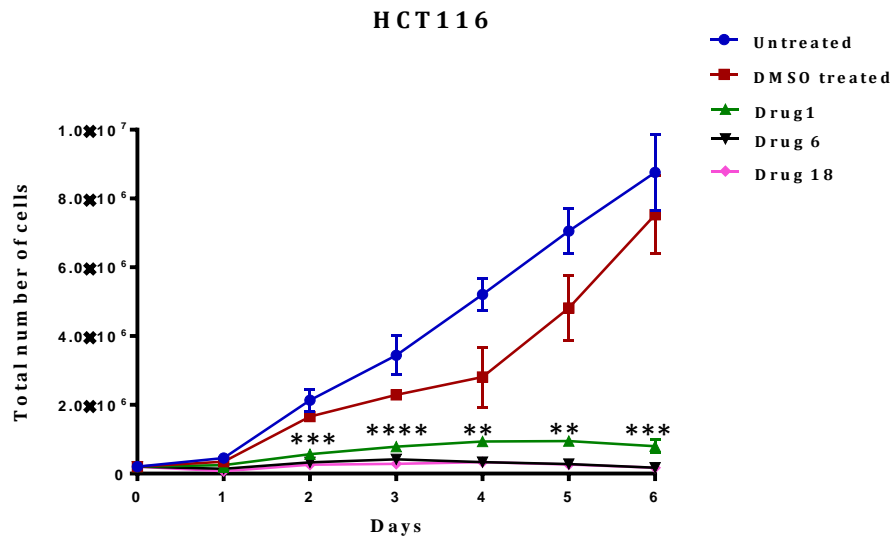
Figure 6.11 Growth curve for SW480 and HCT116 cells treated with different drugs targeting Brachyury.
(A) SW480 cells treated with drugs 3, 11 and 18 and DMSO-treated cells, and (B) HCT116 cells treated with drugs 1, 6 and 18 at a concentration of 10 μM and DMSO-treated cells. These cell line showed significant reduction in proliferation following treatment compared to the control. The error bars indicate the standard deviation (n = 3; ** $P < 0.01$, *** $P < 0.001$, **** $P < 0.0001$).

A

B
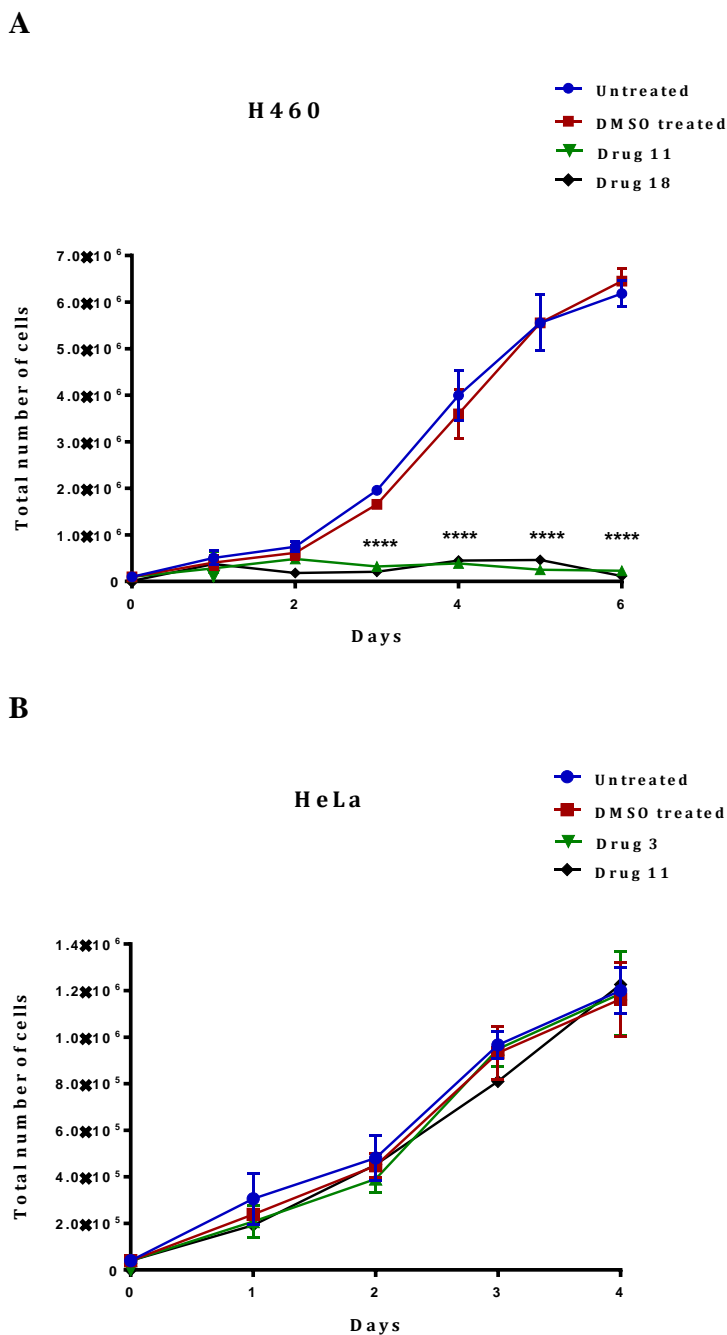
Figure 6.12 Growth curve of the H460 and HeLa cells treated with different drugs targeting Brachyury.
(A) H460 cells treated with drugs 11 and 18 and DMSO-treated cells and (B) HeLa cells treated with drugs 3 and 11 at a concentration of 10 μM and DMSO-treated cells. H460 showed significant proliferation reduction following treatment compared to the control, whereas the HeLa cells displayed no significant differences compared to the control, and proliferation was increased. The error bars indicate the standard deviation (n=3; **** $P < 0.0001$).

6.4 Discussion

Many processes occur during the development of cancer, such as proliferation and metastasis (Hanahan and Weinberg, 2011). Dysfunctional pathways play an important role in controlling cell proliferation and have been implicated in tumour growth (Mazurek, 2011; Dasgupta *et al*., 2016). Preventing aberrant proliferation of cells through some pathways, such as growth factor pathways, the transformation of normal cells to cancer cells may be inhibited (Vander *et al*., 2009). Expression of transcription factor gene *Brachyury* has been identified in various types of human cancer samples (Palena *et al*., 2007), and some studies have demonstrated that a reduced level of Brachyury in cancer cells can inhibit cell proliferation (Jezkova *et al*., 2014; Cho *et al*., 2010). Because Brachyury has been found to be involved in many types of human cancer, it could be considered to be a potential target for cancer treatment. Brachyury was detected in large numbers of human cancer cell lines, in which it is present at the protein level (see Section 5.2.4). Additionally, due to the essential role Brachyury plays in cancer proliferation, new small molecule inhibitors targeting Brachyury were designed.

In the current study, a panel of drugs was designed in collaboration with the Drug Screening Platform at Cardiff University for evaluation. Because cancer cell lines have been indicated as essential elements in the evaluation of the efficacy of new drugs (Ferreira *et al*., 2013), 17 cancer cell lines were obtained from different sources, including HEK-293, and were examined here. Brachyury was detected in these cancer cell lines using a western blot analysis (see Section 5.2.4), and these cell lines were selected for testing with 19 new drugs that target Brachyury associated with cancer.

The 19 drugs were selected from about 6 million compounds that are considered to target Brachyury in cancer cells. Evaluations of the efficacy of these drugs was conducted using a panel of 17 cancer cell lines, which revealed that some drugs were capable of affecting the proliferation rate of these cancer cell lines. In this study, a number of drugs were clearly observed to not affect the proliferation and survival rates of the cancer cells after treatment, and proliferation of cells rapidly increased, which may indicate that these drugs are not specific for inhibition of proliferation of the cancer cells lines examined here. Thus, these drugs were eliminated, and the remaining drugs exhibiting effectiveness for inhibiting or reducing the rate of cancer cell

proliferation should be selected for further studies because they could be considered for potential treatments with high efficacy.

The proliferation of SW480 cells was found to be affected by drugs 3, 6, 11 and 18 (drugs summary and classification Figure 6.14). Two of these drugs appeared to inhibit the proliferation of SW480 cells, and this cancer cell line was not able to survive after treatment with drugs 3 and 18. Because these results are consistent with other experimental results showing the drugs' effects on Brachyury, these drugs may be considered important for further investigations. Experiments were carried out in SW480 cells to evaluate the efficacy of drugs and to compare the most promising drugs. The methods employed included qRT-PCR, cell viability, light microscopy, western blot analysis, and growth curve analysis (Figure 6.13). Transcript levels of *Brachyury* were reduced by some of these drugs, including drug 3 and 18. Drug 3 down-regulated the transcript levels of genes at both concentration tested (10µM and 100 µM) (Figure 6.13 A). A cell viability assay showed that drugs 3, 7, 11, 12, 14 and 18 at concentration of 10 µM and 100 µM also affected the number of SW480 cells compared to the control (Figure 6.13B). The panel of drugs were investigated using light microscopy to assess their ability to effect the proliferation rate of this cell line, and proliferation was most notably inhibited by drugs 3, 6, 11 and 18 (Figure 6.13 C). Based on a western blot analysis, Brachyury was present in SW480 cells treated with drugs 3 and18, but there was a significant reduction in protein levels (Figure 6.13 D). Evaluation of growth curve analysis for drugs 3 and 18 was consistent with the western blot results and these drugs were confirmed to affect cell proliferation (Figure 6.13 E). In this study, the efficacy of different drugs in targeting the function of Brachyury in SW480 cells was investigated by various methods (Figure 6.13), and it is suggested that drugs 3, 11 and 18 might be more specific in their action via targeting of Brachyury function, rather than general cytotoxic affects.

Method	Concentration	Drug1	Drug2	Drug3	Drug4	Drug5	Drug6	Drug7	Drug8	Drug9	Drug10	Drug11	Drug12	Drug13	Drug14	Drug15	Drug16	Drug17	Drug18	Drug19
A qRT-PCR	10 µM of drug	G	G	B	G	G	G	G	G	G	G	G	G	G	G	G	G	G	B	G
	100 µM of drug	G	G	B	G	B	G	G	G	G	G	G	B	G	B	G	G	G	B	G
B Cell viability	10 µM of drug	G	G	B	G	G	G	B	G	G	G	B	B	G	B	G	G	G	B	G
	100 µM of drug	G	G	B	G	G	G	B	G	G	G	B	B	G	G	G	G	G	B	G
C Light microscopy	100 µM of drug	G	G	B	G	G	B	G	G	G	G	B	G	G	G	G	G	G	B	G
D Western blot	100 µM of drug			B			G					G	G				G		B	
E Growth curve	10 µM of drug			B								B							B	

Figure 6.13 Evaluation the efficacy of drugs targeting Brachyury in the cancer cell line SW480 by different methods.
(A) qRT-PCR analysis to assess different drugs concentrations and the effect on transcript levels. (B) Cell viability assay to examine the drug effect on cell number. (C) Monitoring of cell proliferation after drug treatment using light microscopy. (D) Western blot analysis after drug treatment. (E) Growth curve analysis after drug treatment. Green indicates a negative effect and blue indicates a positive effect. No colour indicates that a test was not performed.

Using the classification method applied in this study, the drugs were tested and the proliferation rates of the cancer cell lines were classified. Most of these cancer cell lines treated with the drugs showed high levels of proliferation; thus, the behaviour of these cancer cell lines and their ability to survive was assigned as being at a high level in the cell proliferation class, including cell lines tested with drugs 4, 5, 8, 10, 14 and 15 (drugs summary and classification Figure 6.14). Consequently, these inhibitors should be excluded from the 19 drugs examined here.

Only a small number of the new drugs used to treat cancer cells were able to inhibit the cell proliferation of these cancer cell lines. Among these drugs, the most effective were observed to effect the majority of cancer cell lines in this study and were drugs 3, 11 and 18. The number of cancer cells was clearly inhibited or reduced, which was determined using light microscopy to classify these cancer cells as having no rate of proliferation. For example, the positive effective of drug 3 was shown to inhibit the number of SW480, PEO14, G-361, Jurkat and HepG2 cancer cell lines (drugs summary and classification Figure 6.14). In some cancer cells treated with drug 3, the cell survival was clearly reduced and the proliferation of these cells was classified as being at a low level, such as in LoVo, A2780, COLO800, K562 and H460 cancer cell lines and HEK-293. Of the 17 cell lines, only three survived with a medium level of proliferation after treatment with drug 3: MCF-7, NTERA2 and 1231N1 cells (drugs summary and classification Figure 6.14).

The efficacy of drug 11 was evaluated using the same cancer cell lines, and the higher efficacy of drug 11 was detected in HEK-393 cells and eight cancer cell lines that displayed no ability to proliferate after treatment with this drug. These 8 cancer cell lines were LoVo, T84, A2780, G-361, K562, Jurkat, H460 and MCF-7. The proliferation rate of some cancer cell lines treated with drug 11 presented with low levels of cell survival compared to the control, and the proliferation of this group of cancer cells was classified as cell proliferation, including SW480, PEO14, COLO800, KBM-7, HepG2, NTERA2 and 1231N1 cells. The ability of HCT116 to proliferate after treatment with drug 11 was classified at a medium level of proliferation. Among the cell lines that were effected by drug 11 at different levels of efficacy, only the HeLa cell line displayed high levels of proliferation (drugs summary and classification Figure 6.14).

Drug 18 should be considered a potential drug for selection in future investigations, based on light microscopy applied in this study to compare cell proliferation to controls. Drug 18 displayed a high efficacy for inhibiting proliferation of cancer cell lines leading to the inhibition of the growth

and proliferation of these cancer cell lines. These cancer cell lines include SW480, HCT116, LoVo, COLO800, H460, MCF-7, NTERA2 and 1231N1 cells. Additionally, the proliferation of HEK-293 cells was affected. Other cancer cell lines were showed reduced rates of proliferation and cell survival following treatment with drug 18, such as T84, PEO14, K562, KBM-7, HepG2 and HeLa cells. Only the A2780 cancer cell line revealed a medium level of proliferation, whereas two cancer cell lines were not affected by drug 18, and the proliferation rates increased (G3-61 and Jurkat). These findings were observed in the majority of these cell line; thus, drug 18 should be considered a promising drug for cancer treatment that requires further study (drugs summary and classification Figure 6.14).

In this study, some drugs were sensitive and affected a limited number of cancer cell lines compared to drugs 3, 11 and 18. These drugs included drugs 6, 7, 12 and 19. The cancer cell lines that were screened with drug 6 showed that proliferation rates were affected; these cell line were SW480, HCT116, COLO800, MCF-7 and HEK-293. Cell lines that were sensitive to drug 7 included T84, PEO14, COLO800, Jurkat, H460 and HEK-293 (drugs summary and classification Figure 6.14). For drug 12, HEK-293, A2780, PEO14, G-361, K562 and KBM-7 cells displayed sensitivity.

Of the 17 cancer cell lines, only six were observed to be effected by drug 19, and their proliferation was at a medium level, such as A2780, PEO14 and G-361, or at a low level, such as HCT116, LoVo and MCF-7 (drugs summary and classification Figure 6.14). Furthermore, the growth curve analysis used four cancer cell lines to evaluate cell proliferation after treatment with these drugs and included SW480, HCT116, H460 and HeLa cells. A significant reduction in cell proliferation was observed for three of these cancer cell lines compared to the control, which were SW480, HCT116 and H460. This result is consistent with the results from the light microscopy screenings. In contrast, Hela was treated with drugs that had no effect on proliferation rate, which was consistent with light microscopy experiment results.

Legend:
- ■ High level or more of cell proliferation (dark green)
- ■ Medium level of cell proliferation (green)
- ■ Cell proliferation (blue)
- ■ , No cell proliferation (cyan)
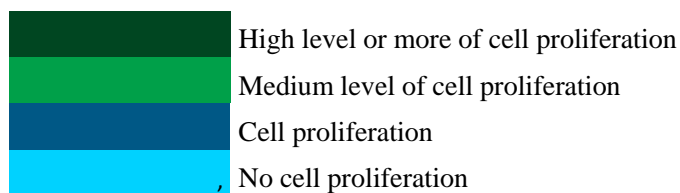
Tissue	Cell line	Drug1	Drug2	Drug3	Drug4	Drug5	Drug6	Drug7	Drug8	Drug9	Drug10	Drug11	Drug12	Drug13	Drug14	Drug15	Drug16	Drug17	Drug18	Drug19
Colon	SW480	High	High	NoProlif	High	High	Prolif	High	High	High	High	Prolif	High	High	High	High	High	High	NoProlif	High
Colon	HCT116	Medium	High	High	High	High	NoProlif	High	High	High	High	Medium	High	High	High	High	High	High	NoProlif	Prolif
Colon	LoVo	High	High	Prolif	High	High	High	High	High	High	High	NoProlif	High	High	High	High	High	High	NoProlif	High
Colon	T84	High	Medium	High	High	High	High	NoProlif	High	High	High	High	High	High	High	High	High	High	NoProlif	High
Ovary	A2780	High	High	Prolif	High	High	High	High	High	Medium	High	NoProlif	Medium	High	High	High	High	High	Medium	Medium
Ovary	PEO14	High	High	NoProlif	High	High	NoProlif	High	High	High	High	Prolif	Medium	High	High	High	High	High	Prolif	Medium
Skin	G-361	High	High	NoProlif	High	High	High	High	High	High	High	NoProlif	Medium	High	High	High	High	High	High	Medium
Skin	COLO800	High	High	Prolif	High	High	Prolif	Prolif	High	High	High	Prolif	High	High	High	High	High	High	NoProlif	High
Blood	K562	High	High	Prolif	High	High	High	High	High	High	High	Medium	High	High	High	High	High	High	Prolif	High
Blood	Jurkat	High	High	NoProlif	High	High	High	Prolif	High	High	High	NoProlif	High	High	High	High	High	Medium	High	High
Blood	KBM-7	High	High	High	High	High	High	High	High	High	High	Prolif	Prolif	High	High	High	High	High	Prolif	High
Lung	H460	High	High	Prolif	High	High	High	High	Medium	High	High	NoProlif	High	High	High	High	High	High	NoProlif	High
B.C	MCF-7	High	High	Medium	High	High	Prolif	High	High	High	High	NoProlif	High	Prolif	High	High	High	High	NoProlif	Prolif
Liver	HepG2	High	Medium	NoProlif	High	High	High	High	High	High	High	Prolif	High	High	High	High	High	High	NoProlif	High
CC	HeLa	High	High	High	High	High	High	High	High	High	High	High	High	High	High	High	NoProlif	High	Prolif	High
GCT	NTERA2	High	High	Medium	High	High	High	High	High	High	High	Prolif	High	High	High	High	High	High	NoProlif	High
Brain	1231N1	High	High	Medium	High	High	High	High	High	High	High	Prolif	High	High	High	High	High	High	NoProlif	High
HEK	HEK-293	High	High	Prolif	High	High	Prolif	Prolif	High	High	High	NoProlif	Prolif	High	High	High	High	High	NoProlif	High

Figure 6.14 Summary of the efficacy of 19 drugs targeting Brachury in cancer cell lines.
Nineteen new drugs and DMSO were used to treat various cancer cell lines and HEK-293 at concentrations of 100 μM. The proliferation rate of these cell lines after treatment was classified into four categories. Each colour represents the proliferation rate of cells compared to the control. The rows indicates cell lines tested in this study, and the column indicates the drugs that were evaluated.

6.5 Conclusion

Brachyury has been found in several types of cancer and might serve as a cancer biomarker for these types. In this preliminary study, a range of 19 drugs were designed to target the cancer-associated functions of Brachyury in cells and were evaluated with a large number of cancer cell lines to determine the efficacy of these drugs for inhibiting cell proliferation. Most of these drugs were not effective against cell proliferation for the majority of the cancer cell lines, which presented high levels of proliferation after treatment. Therefore, these drugs were eliminated from the study's 19 drug list. The minority of these drugs were able to reduce the activity of Brachyury in cancer cell lines and should be considered for further investigations.

The most promising drugs that should be targeted for further study include drugs 3, 11 and 18. Because the sensitivity of these drugs was observed in the highest number of cancer cell lines. These drugs seem to be Brachyury specific as these drugs effect most of these cell lines. However, some cancer cell lines presented a high level of proliferation after treatment with drug 3, including HCT116, T84, KBM-7 and HeLa, and the proliferation rate also increased after treatment with drug 18 in the cell lines G-361 and Jurkat. Consequently, these promising drugs may be acting specifically and their effect is not simply due to general cytotoxicity. A new analogue of these drugs needs to be designed. In the current study, we generated preliminary data showing the efficacy of these drugs, which was clearly observed in the cohort of cancer cell lines with different levels of efficacy. These drugs displayed high efficacy in cancer cell lines, and further research should be conducted to identify new drugs targeting the activity of Brachyury in different types of cancer.

Chapter 7.0 Summary and final discussion

7.1 General discussion

Detection of cancer in the early disease stage is important in order to reduce mortality and to achieve successful treatment. Cancer biomarkers have been applied in the diagnosis, prognosis and monitoring of the responses of patients to treatment (Wu and Qu, 2015; Mäbert *et al*., 2014). Therefore, the identification a new cancer biomarker is essential for successful cancer treatment (Jin *et al*., 2016). CTA genes have a specific feature and are normally expressed in human germlines and the placenta. The aberrant activation of these genes has been observed in various type of tumours, thus CTAs may serve as potential targets for cancer immunotherapy (Fratta *et al*., 2011; Whitehurst, 2014). Many studies have reported the expression of CTA genes and their association with different type of tumours, such as in lung patients with poor survival (Rousseaux *et al*., 2013), and as a cancer biomarker in breast cancer (Maine *et al*., 2016). Meiosis-specific genes may be essential and provide an additional source of CTA genes. In addition, CTAs provide excellent candidates that could be considered as potential drug targets (Whitehurst *et al*., 2007).

A cohort of CT/germlines has been identified in a large number of lung cancer patients with poor outcomes. In 293 patents with aggressive tumours, including 152 patients with early stage lung cancer, 26 genes were investigated. The expression of these 26 Testis-specific/placenta-specific (TS/PS) was not observed in non-tumour lungs, whereas the aberrant expression of these genes was detected in patients with a poor prognosis. Depending on the expression of these genes, patients were assigned into three groups which related to a positive prognosis (P1) or low survival (P3), with patients predicted intermediate survival assigned to (P2). These genes could act as a cancer biomarker in this type of aggressive tumour (Rousseaux *et al*., 2013).

The expression of these 26 was examined to investigate whether this group of genes could serve as cancer biomarkers in this type of tumour. These genes were also screened in ovarian cancer, where they could also be considered potential targets. qRT-PCR was used to assess the expression of the 26 genes in normal lung and ovarian tissues and result 10 genes were found to be expressed in both. To confirm this finding, the genes were then screened in a panel of 21 normal tissues by RT-PCR, where the expression profiles of these 10 genes was detected, including in testis tissue.

Based on these findings, these 10 genes (*BTG4*, *Hs.601545*, *LGALS14*, *EBI3*, *HIST1H3C*, *C12orf37*, *NBPF4*, *KIAA1257*, *ISM2*, and *C10orf82*) were dismissed as lung and ovarian cancer biomarkers. The expression of the remaining 16 genes was consistent with the previous study (Rousseaux *et al*., 2013), which reported that their expression was restricted to testis tissue but not found in normal lungs. Most of these promising genes showed detectable levels of expression in cancer lung tissues; however, among these candidates, *CPA5* displayed expression in normal testis tissue but not in lung cancer tissue but this may have been due to the limited number of samples examined. In addition to re-validating the expression of these 26 genes in lung tissues, the expression of these genes was assessed in normal ovarian tissues to determine whether they were good candidates in ovarian cancer. Interestingly, that genes that were dismissed as ovarian biomarkers were the same those that were excluded as potential lung cancer biomarkers including, *BTG4*, *Hs.601545*, *LGALS14*, *EBI3*, *HIST1H3C*, *C12orf37*, *NBPF4*, *KIAA1257*, *ISM2*, and *C10orf82*. Eliminating the non-candidates genes could be useful for patients' prognoses.

In this current study, the expression of a large number of CTA genes that have previously been reported as potential cancer biomarkers was investigated. The selected genes were classified based on their expression. In total, 156 genes identified by different methods were re-validated with normal tissue and normal colon tissue adjacent tumours by TLDA cards analysis. The genes studied in this project were selected from five different sources, including human orthologues of meiosis genes in mice (Feichtinger *et al*., 2012), a group of genes that restricted expression in germlines and the placenta (Rousseaux *et al*., 2013), human orthologues of germlines in *Drosophila* (Feichtinger *et al*., 2014; Janic *et al*., 2010), genes that were selected from the CT database (Almeida *et al*., 2009), and a list of identified CTA genes (Hofmann *et al*., 2008). Interestingly, re-validation of these 156 genes in normal tissues and normal colon adjacent to tumours, including testis tissue, revealed that 101 genes exhibited CTA-type expression. The remaining 55 genes, such as *ATAD2*, were excluded, as they appeared to be extensively expressed in most of the normal tissues that were tested. Based on the classification of CTAs (Hofmann *et al*., 2008; Feichtinger *et al*., 2012) these 101 genes were classified as: 67 testis-restricted genes, 9 testis/CNS-restricted genes, 11 testis-selective genes, and 14 testis-CNS-selective genes. Some of the candidates genes were not present in the cancer samples tested, including *ASB17*, *RNF17* and *BOLL,* indicating that these genes may be expressed in other samples that were not included here. According to the findings of this study, it may be worth validating the genes that are reported as

CTAs in order to identify good candidate genes that be used in cancer stratification. The explanation for the findings reported here could be the stringent settings used in the TLDA card analysis. In addition, recent studies have validated the expression of some genes known to be CTAs and suggested that these genes should be excluded from the CT database (Djureinovic *et al*., 2016). Therefore, some of the existing genes belonging to CTA group should undergo further investigations to check whether these genes could act as good candidate biomarkers in some types of cancer.

Brachyury was reported to be a member of CTA group of genes that could be utillised as a biomarker, and was only found to be expressed in testis tissue among the panel of normal tissues that was examined by RT-PCR (Palena *et al*., 2007). Recently, *Brachyury* has been reported to be expressed in a wide range of normal somatic tissues and testis tissue as assesses by qRT-PCR (Jezkova *et al*., 2016). The expression profile of *Brachyury* does not follow the stringent CTA gene classification, and consequently, this gene has been dismissed as a CTA gene. The important function of Brachyury in cancer development has been reported in various studies(for example, see Palena *et al*., 2014; Pinto *et al*., 2016; Huang *et al*., 2013) and it may provide an excellent target for immunotherapy. In addition, it has been observed that colorectal cancer depleted of Brachyury leads to the arrest of cell proliferation (Jezkova *et al*., 2014); therefore, drugs that target the function of Brachyury in cancer were designed.

The transcript levels of some genes selected from RNA-seq were altered following the depletion of Brachyury in SW480 cells, indicating the important function of Brachyury associated with these genes (Jezkova *et al*., 2014). In this study, qRT-PCR analysis was used to examine the transcript levels of these genes in SW480 cells, which were shown to be consistent with the findings of a previous study (Jezkova *et al*., 2014). Genes that demonstrated low transcript levels were *MFN2*, *MSH2*, *MEST*, *CCNE1* and *MTHFD2,* whereas *CROT*, *IGFBP3* and *SFRP5* were observed to have high transcript levels. Most of the genes affected by the depletion of Brachyury have an important function, such as *MSH2* which has a key role during the S phase as it encodes a protein that repairs errors (Lagerstedt and Robinson *et al*., 2007; Zlatanou *et al*., 2011; Martín-López and Fishel 2013; Dowty *et al*., 2013). The selected genes were screened with anti-Brachyury drugs to assess the efficacy of these drugs and to determine whether they altered the transcripts levels of these genes.

The efficacy of 19 drugs that were designed to target Brachyury, were evaluated using different methods, including qRT-PCR, cell viability, western blot analysis, growth curve analysis and the monitoring of proliferation by light microscopy. The transcript levels of *Brachyury* were measured following the treatment of SW480 cells with the 19 drugs at different concentrations. Based on the qRT-PCR analysis, the transcript level of *Brachyury* was affected by some drugs, including 3 and 18. In addition, at the protein level drugs 3 and 18 also demonstrated the down-regulation of Brachyury, together with a decrease in cell viability; drugs 11 and 12 yielded similar results but with less efficacy than drugs 3, and 18.

The presence of Brachyury in a large panel of cancer cell lines was examined by western blot analysis to determine which of the drugs were targeting Brachyury levels, and Brachyury was detected in all of the cancer cell lines tested. Therefore, it may be useful to identify cells which are negative for Brachyury. Most of the Brachyury positive cancer cell lines, including HEK-293, which had been thought to be negative for Brachyury, were treated with the 19 drugs and DMSO to evaluate their efficacy. Based on the results, the most effective drugs that were able to inhibit the proliferation rate of these cell lines were drugs 3, 11 and 18. These drugs may be more specific in their targeting of Brachyury in cancer cell lines, as they showed the ability to inhibit cell proliferation in most. Therefore, drugs 3, 11 and 18 seem to be most effective. In addition, these drugs could be considered as specific drugs for Brachyury, rather acting due to cytotoxicity, as some cell lines were not affected by these drugs. For example, the proliferation of some cancer cell lines, such as HCT116, T84 and HeLa, were not affected by drugs 3, while the proliferation rate of the HeLa cell line was increased following treatment with drug 11.

An evaluation of these new drugs was carried out using different cell lines, and most showed no effect on cell proliferation. As a result, these drugs were eliminated and only those that were able to effect the cell proliferation rate should be used in further studies. This study has generated preliminary data showing that a small number of drugs act in a Brachyury-dependent manner to reduce Brachyury activity within cancer cell lines.

7.2 Future direction

Based on the result presented in this study further investigations are suggested.

Genes that have been reported as lung cancer biomarkers should be studied at the protein level, in particular those genes that were dismissed in this study. In addition, the CTA genes that have been identified as biomarkers for different type of tumours and existing CTA genes should be re-validated, as it has been shown that some of these CTA genes are expressed in a wide range of normal tissues and clinical samples (Chapter 4). In addition, these genes could be assess as a potential CTA and should be validated against tumour samples obtained from different patients. Studying these genes at the protein level could also be useful as immunotherapy targets as they may function as new drugs targets.

The identification of a negative Brachyury cell line is required, as such a cell line could be utilised to investigative specific drugs that effect the function of Brachyury in various types of cancer. Brachyury expression was screened in 17 cancer cell lines and was detected in all of them. It would be worth examining the expression of Brachyury in primary fibroblast cells as these may represent negative Brachyury negative cells.

The drugs in this study were tested at a concentration of 100 μM in order to evaluate their efficacy in targeting the proliferation rate of different cancer cell lines and it could be useful to target cancer cells with different concentrations and to compare the resulting proliferation rates with the findings of this study. In addition, the transcript levels of *Brachyury* in these cancer cell lines following drug treatment at different concentration should be investigated. This would be provide whether these drugs can effect Brachyury activity in different cancer cell lines and would allow a comparison of the ability of these drugs to inhibit Brachyury in various types of cancer cell lines and also determine their specificity.

Out of the 19 drugs investigated, only a minority of these small molecular inhibitors should be progressed into further studies, as only these appeared to effect the function of Brachyury, including drugs 3, 11 and 18. Therefore, designing analogues for these promising anti-Brachyury drugs should be undertaken and the efficacy of these new analogues in positive and negative Brachyury cell lines needs to be examined.

Chapter 8.0 References

Abbas, T., Keaton, M.A. & Dutta, A. 2013. Genomic instability in cancer. *Cold Spring Harbor perspectives in biology.* 5 (3). pp. a012914.

Adams, M.D., Kelley, J.M., Gocayne, J.D., Dubnick, M., Polymeropoulos, M.H., Xiao, H., Merril, C.R., Wu, A., Olde, B. & Moreno, R.F. 1991. Complementary DNA sequencing: expressed sequence tags and human genome project. *Science (New York, N.Y.).* 252 (5013). pp. 1651-1656.

Agathanggelou, A., Cooper, W.N. & Latif, F. 2005. Role of the Ras-association domain family 1 tumor suppressor gene in human cancers. *Cancer research.* 65 (9). pp. 3497-3508.

Aggarwal, B.B., Vijayalekshmi, R.V. & Sung, B. 2009. Targeting inflammatory pathways for prevention and therapy of cancer: short-term friend, long-term foe. *Clinical cancer research : an official journal of the American Association for Cancer Research.* 15 (2). pp. 425-430.

Aguilera, A. & García-Muse, T. 2013. Causes of genome instability. *Annual Review of Genetics.* 47 pp. 1-32.

Ahmadivand, S., Farahmand, H., Teimoori-Toolabi, L., Mirvaghefi, A., Eagderi, S., Geerinckx, T., Shokrpoor, S. & Rahmati-Holasoo, H. 2016. Boule gene expression underpins the meiotic arrest in spermatogenesis in male rainbow trout (Oncorhynchus mykiss) exposed to DEHP and butachlor. *General and comparative endocrinology.* 225 pp. 235-241.

Akers, S.N., Odunsi, K. & Karpf, A.R. 2010. Regulation of cancer germline antigen gene expression: implications for cancer immunotherapy. *Future oncology.* 6 (5). pp. 717-732.

Akiyama, Y., Komiyama, M., Miyata, H., Yagoto, M., Ashizawa, T., Iizuka, A., Oshita, C., Kume, A., Nogami, M. & Ito, I. 2014. Novel cancer-testis antigen expression on glioma cell lines derived from high-grade glioma patients. *Oncology reports.* 31 (4). pp. 1683-1690.

Albalat, R., Marti-Solans, J. & Canestro, C. 2012. DNA methylation in amphioxus: from ancestral functions to new roles in vertebrates. *Briefings in functional genomics.* 11 (2). pp. 142-155.

Almeida, L.G., Sakabe, N.J., deOliveira, A.R., Silva, M.C., Mundstein, A.S., Cohen, T., Chen, Y.T., Chua, R., Gurung, S., Gnjatic, S., Jungbluth, A.A., Caballero, O.L., Bairoch, A., Kiesler, E., White, S.L., Simpson, A.J., Old, L.J., Camargo, A.A. & Vasconcelos, A.T. 2009. CTdatabase: a knowledge-base of high-throughput and curated data on cancer-testis antigens. *Nucleic acids research.* 37 (Database issue). pp. D816-9.

Aly, H.A. 2012. Cancer therapy and vaccination. *Journal of immunological methods.* 382 (1). pp. 1-23.

Andtbacka, R.H., Kaufman, H.L., Collichio, F., Amatruda, T., Senzer, N., Chesney, J., Delman, K.A., Spitler, L.E., Puzanov, I., Agarwala, S.S., Milhem, M., Cranmer, L., Curti, B., Lewis, K., Ross, M., Guthrie, T., Linette, G.P., Daniels, G.A., Harrington, K., Middleton, M.R., Miller, W.H.,Jr, Zager, J.S., Ye, Y., Yao, B., Li, A., Doleman, S., VanderWalde, A., Gansert, J. & Coffin, R.S. 2015. Talimogene Laherparepvec Improves Durable Response Rate in Patients With Advanced Melanoma. *Journal of clinical oncology : official journal of the American Society of Clinical Oncology.* 33 (25). pp. 2780-2788.

Aravin, A.A., Sachidanandam, R., Girard, A., Fejes-Toth, K. & Hannon, G.J. 2007. Developmentally regulated piRNA clusters implicate MILI in transposon control. *Science (New York, N.Y.).* 316 (5825). pp. 744-747.

Aris, M. & Barrio, M.M. 2015. Combining immunotherapy with oncogene-targeted therapy: a new road for melanoma treatment. *Frontiers in immunology.* 6 pp. 46.

Arya, R. White, K. 2015. Cell death in development: signaling pathways and core mechanisms. *Seminars in cell & developmental biology.* Elsevier: pp. 12.

Arzumanyan, A., Reis, H.M. & Feitelson, M.A. 2013. Pathogenic mechanisms in HBV-and HCV-associated hepatocellular carcinoma. *Nature Reviews Cancer.* 13 (2). pp. 123-135.

Auer, R.L., Starczynski, J., McElwaine, S., Bertoni, F., Newland, A.C., Fegan, C.D. & Cotter, F.E. 2005. Identification of a potential role for POU2AF1 and BTG4 in the deletion of 11q23 in chronic lymphocytic leukemia. *Genes, Chromosomes and Cancer.* 43 (1). pp. 1-10.

Bagci, O. & Kurtgöz, S. 2015. Amplification of cellular oncogenes in solid tumors. *North American journal of medical sciences.* 7 (8). pp. 341.

Bailey, A.M., Mao, Y., Zeng, J., Holla, V., Johnson, A., Brusco, L., Chen, K., Mendelsohn, J., Routbort, M.J., Mills, G.B. & Meric-Bernstam, F. 2014. Implementation of biomarker-driven cancer therapy: existing tools and remaining gaps. *Discovery medicine.* 17 (92). pp. 101-114.

Balbás-Martínez, C., Sagrera, A., Carrillo-de-Santa-Pau, E., Earl, J., Márquez, M., Vazquez, M., Lapi, E., Castro-Giner, F., Beltran, S. & Bayés, M. 2013. Recurrent inactivation of STAG2 in bladder cancer is not associated with aneuploidy. *Nature genetics.* 45 (12). pp. 1464-1469.

Baltiþ, V., Baltiþ, M., SvirĀev, Z. & JerantrPatiþ, V. 2008. microRNA expression in non-Hodgkin's lymphomas.

Bamshad, M., Le, T., Watkins, W., Dixon, M., Kramer, B., Roeder, A., Carey, J., Root, S., Schinzel, A. & Van Maldergem, L. 1999. The spectrum of mutations in TBX3: genotype/phenotype relationship in ulnar-mammary syndrome. *The American Journal of Human Genetics.* 64 (6). pp. 1550-1562.

Bamshad, M., Lin, R.C., Law, D.J., Watkins, W.S., Krakowiak, P.A., Moore, M.E., Franceschini, P., Lala, R., Holmes, L.B. & Gebuhr, T.C. 1997. Mutations in human TBX3 alter limb, apocrine and genital development in ulnar-mammary syndrome. *Nature genetics.* 16 (3). pp. 311-315.

Banerjee, R., Russo, N., Liu, M., Basrur, V., Bellile, E., Palanisamy, N., Scanlon, C.S., van Tubergen, E., Inglehart, R.C. & Metwally, T. 2014. TRIP13 promotes error-prone nonhomologous end joining and induces chemoresistance in head and neck cancer. *Nature communications.* 5.

Barnes, P.J., Adcock, I.M. & Ito, K. 2005. Histone acetylation and deacetylation: importance in inflammatory lung diseases. *The European respiratory journal.* 25 (3). pp. 552-563.

Barresi, V., Ieni, A., Branca, G. & Tuccari, G. 2014. Brachyury: a diagnostic marker for the differential diagnosis of chordoma and hemangioblastoma versus neoplastic histological mimickers. *Disease markers.* 2014 pp. 514753.

Barresi, V., Vitarelli, E., Branca, G., Antonelli, M., Giangaspero, F. & Barresi, G. 2012. Expression of brachyury in hemangioblastoma: potential use in differential diagnosis. *The American Journal of Surgical Pathology.* 36 (7). pp. 1052-1057.

Baser, E., Togrul, C., Ozgu, E., Ayhan, S., Caglar, M., Erkaya, S. & Gungor, T. 2013. Sperm-associated antigen 9 is a promising marker for early diagnosis of endometrial cancer. *Asian Pacific Journal of Cancer Prevention.* 14 (12). pp. 7635-7638.

Basson, C.T., Bachinskyz, D.R., Lin, R.C., Leviz, T., Elkinsz, I.A. & Soultsz, J. 1997. Mutations in human cause limb and cardiac malformation in Holt-Oram. *Nature genetics.* 15.

Bergers, G. & Hanahan, D. 2008. Modes of resistance to anti-angiogenic therapy. *Nature Reviews Cancer.* 8 (8). pp. 592-603.

Bettoni, F., Camargo Filho, F., Grosso, D.M., Galante, P.A., Parmigiani, R.B., Geraldo, M.V., Henrique-Silva, F., Oba-Shinjo, S.M., Marie, S.K. & Soares, F.A. 2009. Identification of FAM46D as a novel cancer/testis antigen using EST data and serological analysis. *Genomics.* 94 (3). pp. 153-160.

Bhowmick, N.A., Neilson, E.G. & Moses, H.L. 2004. Stromal fibroblasts in cancer initiation and progression. *Nature.* 432 (7015). pp. 332-337.

Bhushan, S., Wang, M., Kudipudi, P., Fijak, M. & Meinhardt, A. 2016. Testicular macrophages: Role in immune privilege and defense. *Journal of reproductive immunology.* 115 pp. 51.

Bilanges, B. & Stokoe, D. 2007. Mechanisms of translational deregulation in human tumors and therapeutic intervention strategies. *Oncogene.* 26 (41). pp. 5973-5990.

Biswas, U., Wetzker, C., Lange, J., Christodoulou, E.G., Seifert, M., Beyer, A. & Jessberger, R. 2013. Meiotic cohesin SMC1β provides prophase I centromeric cohesion and is required for multiple synapsis-associated functions. *PLoS Genet.* 9 (12). pp. e1003985.

Blank, C., Kuball, J., Voelkl, S., Wiendl, H., Becker, B., Walter, B., Majdic, O., Gajewski, T.F., Theobald, M. & Andreesen, R. 2006. Blockade of PD-L1 (B7-H1) augments human tumor-specific T cell responses in vitro. *International journal of cancer.* 119 (2). pp. 317-327.

Blasco, M.A. 2005. Telomeres and human disease: ageing, cancer and beyond. *Nature Reviews Genetics.* 6 (8). pp. 611-622.

Bode, P.K., Thielken, A., Brandt, S., Barghorn, A., Lohe, B., Knuth, A. & Moch, H. 2014. Cancer testis antigen expression in testicular germ cell tumorigenesis. *Modern Pathology.* 27 (6). pp. 899-905.

Boël, P., Wildmann, C., Sensi, M.L., Brasseur, R., Renauld, J., Coulie, P., Boon, T. & van der Bruggen, P. 1995. BAGE: a new gene encoding an antigen recognized on human melanomas by cytolytic T lymphocytes. *Immunity.* 2 (2). pp. 167-175.

Bolcun-Filas, E., Speed, R., Taggart, M., Grey, C., de Massy, B., Benavente, R. & Cooke, H.J. 2009. Mutation of the mouse Syce1 gene disrupts synapsis and suggests a link between synaptonemal complex structural components and DNA repair. *PLoS Genet.* 5 (2). pp. e1000393.

Boohaker, R.J. & Xu, B. 2014. The versatile functions of ATM kinase. *Biomedical journal.* 37 (1). pp. 3-9.

Boon, T., Coulie, P.G. & Van den Eynde, B. 1997. Tumor antigens recognized by T cells. *Immunology today.* 18 (6). pp. 267-268.

Boyerinas, B., Tucker, J.A., Poole, D.J., Jochéms, C., Palena, C., Schlom, J. & Tsang, K.Y. 2013. Generation of human T cells directed against an agonist epitope of Brachyury, a transcription factor involved in human tumor cell epithelial to mesenchymal transition (EMT). *Journal for immunotherapy of cancer.* 1 (1). pp. 1.

Braybrook, C., Doudney, K., Marçano, A.C.B., Arnason, A., Bjornsson, A., Patton, M.A., Goodfellow, P.J., Moore, G.E. & Stanier, P. 2001. The T-box transcription factor gene TBX22 is mutated in X-linked cleft palate and ankyloglossia. *Nature genetics.* 29 (2). pp. 179-183.

Brown, S., Kirkbride, P. & Marshall, E. 2015. Radiotherapy in the acute medical setting. *Clinical medicine (London, England).* 15 (4). pp. 382-387.

Bucholtz, N. & Demuth, I. 2013. DNA-repair in mild cognitive impairment and Alzheimer's disease. *DNA repair.* 12 (10). pp. 811-816.

Buckingham, K.J., McMillin, M.J., Brassil, M.M., Shively, K.M., Magnaye, K.M., Cortes, A., Weinmann, A.S., Lyons, L.A. & Bamshad, M.J. 2013. Multiple mutant T alleles cause haploinsufficiency of Brachyury and short tails in Manx cats. *Mammalian genome.* 24 (9-10). pp. 400-408.

Butterfield, L.H. 2015. Cancer vaccines. *BMJ (Clinical research ed.).* 350 pp. h988.

Caballero, O.L. & Chen, Y. 2009. Cancer/testis (CT) antigens: potential targets for immunotherapy. *Cancer science.* 100 (11). pp. 2014-2021.

Caldon, C.E. & Musgrove, E.A. 2010. Distinct and redundant functions of cyclin E1 and cyclin E2 in development and cancer. *Cell division.* 5 (1). pp. 1.

Carelle, N., Piotto, E., Bellanger, A., Germanaud, J., Thuillier, A. & Khayat, D. 2002. Changing patient perceptions of the side effects of cancer chemotherapy. *Cancer.* 95 (1). pp. 155-163.

Caron, C., Lestrat, C., Marsal, S., Escoffier, E., Curtet, S., Virolle, V., Barbry, P., Debernardi, A., Brambilla, C. & Brambilla, E. 2010. Functional characterization of ATAD2 as a new cancer/testis factor and a predictor of poor prognosis in breast and lung cancers. *Oncogene.* 29 (37). pp. 5171-5181.

Carr, A.C., Vissers, M.C. & Cook, J. 2014. Relief from cancer chemotherapy side effects with pharmacologic vitamin C. *The New Zealand Medical Journal (Online).* 127 (1388).

Carvalho, B., Postma, C., Mongera, S., Hopmans, E., Diskin, S., van de Wiel, M.A., van Criekinge, W., Thas, O., Matthai, A., Cuesta, M.A., Terhaar Sive Droste, J.S., Craanen, M., Schrock, E., Ylstra, B. & Meijer, G.A. 2009. Multiple putative oncogenes at the chromosome 20q amplicon contribute to colorectal adenoma to carcinoma progression. *Gut.* 58 (1). pp. 79-89.

Chaffer, C.L. & Weinberg, R.A. 2011. A perspective on cancer cell metastasis. *Science.* 331 (6024). pp. 1559-1564.

Chalmel, F., Rolland, A.D., Niederhauser-Wiederkehr, C., Chung, S.S., Demougin, P., Gattiker, A., Moore, J., Patard, J.J., Wolgemuth, D.J., Jegou, B. & Primig, M. 2007. The conserved transcriptome in human and rodent male gametogenesis. *Proceedings of the National Academy of Sciences of the United States of America.* 104 (20). pp. 8346-8351.

Chanvorachote, P., Chamni, S., Ninsontia, C. & Phiboonchaiyanan, P.P. 2016. Potential Anti-metastasis Natural Compounds for Lung Cancer. *Anticancer Research.* 36 (11). pp. 5707-5717.

Chapman, C., Murray, A., Chakrabarti, J., Thorpe, A., Woolston, C., Sahin, U., Barnes, A. & Robertson, J. 2007. Autoantibodies in breast cancer: their use as an aid to early diagnosis. *Annals of Oncology : Official Journal of the European Society for Medical Oncology / ESMO.* 18 (5). pp. 868-873.

Chen, H., Tsai, S. & Leone, G. 2009. Emerging roles of E2Fs in cancer: an exit from cell cycle control. *Nature Reviews Cancer.* 9 (11). pp. 785-797.

Chen, Q., Deng, T. & Han, D. 2016. Testicular immunoregulation and spermatogenesis. *Seminars in cell & developmental biology.* Elsevier: .

Chen, Y., Schlessinger, D. & Nagaraja, R. 2013. T antigen transformation reveals Tp53/RB-dependent route to PLAC1 transcription activation in primary fibroblasts. *Oncogenesis.* 2 (9). pp. e67.

Chen, Y., Hsu, M., Lee, P., Shin, S.J., Mhawech-Fauceglia, P., Odunsi, K., Altorki, N.K., Song, C., Jin, B. & Simpson, A.J. 2009. Cancer/testis antigen CT45: analysis of mRNA and protein expression in human cancer. *International Journal of Cancer.* 124 (12). pp. 2893-2898.

Chen, X., Bode, A.M., Dong, Z. & Cao, Y. 2016. The epithelial-mesenchymal transition (EMT) is regulated by oncoviruses in cancer. *FASEB journal : official publication of the Federation of American Societies for Experimental Biology.*

Chen, Y.T., Scanlan, M.J., Sahin, U., Tureci, O., Gure, A.O., Tsang, S., Williamson, B., Stockert, E., Pfreundschuh, M. & Old, L.J. 1997. A testicular antigen aberrantly expressed in human cancers detected by autologous antibody screening. *Proceedings of the National Academy of Sciences of the United States of America.* 94 (5). pp. 1914-1918.

Cheng, C.Y. & Mruk, D.D. 2012. The blood-testis barrier and its implications for male contraception. *Pharmacological reviews.* 64 (1). pp. 16-64.

Cheng, N., Chytil, A., Shyr, Y., Joly, A. & Moses, H.L. 2008. Transforming growth factor-beta signaling-deficient fibroblasts enhance hepatocyte growth factor signaling in mammary carcinoma cells to promote scattering and invasion. *Molecular cancer research : MCR.* 6 (10). pp. 1521-1533.

Chiang, C.L., Coukos, G. & Kandalaft, L.E. 2015. Whole tumor antigen vaccines: where are we? *Vaccines.* 3 (2). pp. 344-372.

Chiocca, E.A. & Rabkin, S.D. 2014. Oncolytic viruses and their application to cancer immunotherapy. *Cancer immunology research.* 2 (4). pp. 295-300.

Cho, B., Lim, Y., Lee, D., Park, S., Lee, H., Kim, W.H., Yang, H., Bang, Y. & Jeoung, D. 2002. Identification and characterization of a novel cancer/testis antigen gene CAGE. *Biochemical and biophysical research communications.* 292 (3). pp. 715-726.

Cho, M.S., Chan, I.L. & Flores, E.R. 2010. ΔNp63 transcriptionally regulates brachyury, a gene with diverse roles in limb development, tumorigenesis and metastasis. *Cell cycle.* 9 (12). pp. 2434-2441.

Choi, J. & Chang, H. 2012. The expression of MAGE and SSX, and correlation of COX2, VEGF, and survivin in colorectal cancer. *Anticancer Research.* 32 (2). pp. 559-564.

Chomez, P., De Backer, O., Bertrand, M., De Plaen, E., Boon, T. & Lucas, S. 2001. An overview of the MAGE gene family with the identification of all human members of the family. *Cancer research.* 61 (14). pp. 5544-5551.

Cilensek, Z.M., Yehiely, F., Kular, R.K. & Deiss, L.P. 2002. A member of the GAGE family of tumor antigens is an anti-apoptotic gene that confers resistance to Fas/CD95/APO-1, interferon-g, taxol and g-irradiation. *Cancer biology & therapy.* 1 (4). pp. 379-386.

Coleman, R.E. 2012. Bone cancer in 2011: Prevention and treatment of bone metastases. *Nature Reviews Clinical Oncology.* 9 (2). pp. 76-78.

Colotta, F., Allavena, P., Sica, A., Garlanda, C. & Mantovani, A. 2009. Cancer-related inflammation, the seventh hallmark of cancer: links to genetic instability. *Carcinogenesis.* 30 (7). pp. 1073-1081.

Croce, C.M. 2008. Oncogenes and cancer. *New England journal of medicine.* 358 (5). pp. 502-511.

D'Arcy, P., Maruwge, W., Wolahan, B., Ma, L. & Brodin, B. 2014. Oncogenic functions of the cancer-testis antigen SSX on the proliferation, survival, and signaling pathways of cancer cells. *PloS one.* 9 (4). pp. e95136.

da Cunha, J.P., Galante, P.A., de Souza, J.E., Pieprzyk, M., Carraro, D.M., Old, L.J., Camargo, A.A. & de Souza, S.J. 2013. The human cell surfaceome of breast tumors. *BioMed research international.* 2013 pp. 976816.

Daniel, K., Tränkner, D., Wojtasz, L., Shibuya, H., Watanabe, Y., Alsheimer, M. & Tóth, A. 2014. Mouse CCDC79 (TERB1) is a meiosis-specific telomere associated protein. *BMC cell biology.* 15 (1). pp. 1.

Dardousis, K., Voolstra, C., Roengvoraphoj, M., Sekandarzad, A., Mesghenna, S., Winkler, J., Ko, Y., Hescheler, J. & Sachinidis, A. 2007. Identification of differentially expressed genes involved in the formation of multicellular tumor spheroids by HT-29 colon carcinoma cells. *Molecular Therapy.* 15 (1). pp. 94-102.

Dasgupta, A., Paul, D. & De, R.K. 2016. A fuzzy logic controller based approach to model the switching mechanism of the mammalian central carbon metabolic pathway in normal and cancer cells. *Molecular BioSystems.* 12 (8). pp. 2490-2505.

Davalos, A., Goedeke, L., Smibert, P., Ramirez, C.M., Warrier, N.P., Andreo, U., Cirera-Salinas, D., Rayner, K., Suresh, U., Pastor-Pareja, J.C., Esplugues, E., Fisher, E.A., Penalva, L.O., Moore, K.J., Suarez, Y., Lai, E.C. & Fernandez-Hernando, C. 2011. miR-33a/b contribute to

the regulation of fatty acid metabolism and insulin signaling. *Proceedings of the National Academy of Sciences of the United States of America.* 108 (22). pp. 9232-9237.

de Anda-Jáuregui, G., Velázquez-Caldelas, T.E., Espinal-Enríquez, J. & Hernández-Lemus, E. 2016. Transcriptional Network Architecture of Breast Cancer Molecular Subtypes. *Frontiers in Physiology.* 7.

De Backer, O., Arden, K.C., Boretti, M., Vantomme, V., De Smet, C., Czekay, S., Viars, C.S., De Plaen, E., Brasseur, F., Chomez, P., Van den Eynde, B., Boon, T. & van der Bruggen, P. 1999. Characterization of the GAGE genes that are expressed in various human cancers and in normal testis. *Cancer research.* 59 (13). pp. 3157-3165.

De Brito, O.M. & Scorrano, L. 2008. Mitofusin 2: a mitochondria-shaping protein with signaling roles beyond fusion. *Antioxidants & redox signaling.* 10 (3). pp. 621-634.

de Goeij, B.E., Peipp, M., de Haij, S., van den Brink, Edward N, Kellner, C., Riedl, T., de Jong, R., Vink, T., Strumane, K. & Bleeker, W.K. 2014. HER2 monoclonal antibodies that do not interfere with receptor heterodimerization-mediated signaling induce effective internalization and represent valuable components for rational antibody-drug conjugate design. *MAbs.* Taylor & Francis: pp. 392.

De Martel, C., Ferlay, J., Franceschi, S., Vignat, J., Bray, F., Forman, D. & Plummer, M. 2012. Global burden of cancers attributable to infections in 2008: a review and synthetic analysis. *The lancet oncology.* 13 (6). pp. 607-615.

De Plaen, E., Traversari, C., Gaforio, J.J., Szikora, J., De Smet, C., Brasseur, F., van der Bruggen, P., Lethé, B., Lurquin, C. & Chomez, P. 1994. Structure, chromosomal localization, and expression of 12 genes of the MAGE family. *Immunogenetics.* 40 (5). pp. 360-369.

De Ruyck, K., Duprez, F., Ferdinande, L., Mbah, C., Rios-Velazquez, E., Hoebers, F., Praet, M., Deron, P., Bonte, K. & Speel, E. 2014. A let-7 microRNA polymorphism in the KRAS 3′-UTR is prognostic in oropharyngeal cancer. *Cancer epidemiology.* 38 (5). pp. 591-598.

De Ryck, T., Duprez, F., Bracke, M., Van de Wiele, T. & Vanhoecke, B. 2015. Dynamic shifts in the oral microbiome during radiotherapy. *CLINICAL RESEARCH IN INFECTIOUS DISEASES.* 2 (1).

De Smet, C., De Backer, O., Faraoni, I., Lurquin, C., Brasseur, F. & Boon, T. 1996. The activation of human gene MAGE-1 in tumor cells is correlated with genome-wide demethylation. *Proceedings of the National Academy of Sciences of the United States of America.* 93 (14). pp. 7149-7153.

De Smet, C., Lurquin, C., Lethe, B., Martelange, V. & Boon, T. 1999. DNA methylation is the primary silencing mechanism for a set of germ line- and tumor-specific genes with a CpG-rich promoter. *Molecular and cellular biology.* 19 (11). pp. 7327-7335.

de Vries, F.A., de Boer, E., van den Bosch, M., Baarends, W.M., Ooms, M., Yuan, L., Liu, J.G., van Zeeland, A.A., Heyting, C. & Pastink, A. 2005. Mouse Sycp1 functions in synaptonemal complex assembly, meiotic recombination, and XY body formation. *Genes & development.* 19 (11). pp. 1376-1389.

DE, E., VAN DEN, B., Knuth, A. & BOONT, T. 1991. A gene encoding an antigen recognized by cytolytic T lymphocytes on a human melanoma.

Ding, J., Miao, Z., Meng, L. & Geng, M. 2006. Emerging cancer therapeutic opportunities target DNA-repair systems. *Trends in pharmacological sciences.* 27 (6). pp. 338-344.

Djureinovic, D., Hallström, B.M., Horie, M., Mattsson, J.S.M., La Fleur, L., Fagerberg, L., Brunnström, H., Lindskog, C., Madjar, K. & Rahnenführer, J. 2016. Profiling cancer testis antigens in non–small-cell lung cancer. *JCI insight.* 1 (10).

Dobrovolskaia-Zavadskaia, N. 1927. Sur la mortification spontanee de la queue chez la souris nouveau-nee et sur l'existence d'un caractere hereditaire "non viable". *CR Soc.Biol.* 97 pp. 114-116.

Domae, S., Ono, T. & Sasaki, A. 2014. Cancer/testis antigens: A prospective reagent as diagnostic and immunotherapeutic targets for squamous cell carcinoma of the head and neck. *Japanese Dental Science Review.* 50 (4). pp. 91-99.

Dong, W., Tu, S., Xie, J., Sun, P., Wu, Y. & Wang, L. 2009. Frequent promoter hypermethylation and transcriptional downregulation of BTG4 gene in gastric cancer. *Biochemical and biophysical research communications.* 387 (1). pp. 132-138.

dos Santos, N.R., de Bruijn, D.R., Kater-Baats, E., Otte, A.P. & van Kessel, A.G. 2000. Delineation of the protein domains responsible for SYT, SSX, and SYT-SSX nuclear localization. *Experimental cell research.* 256 (1). pp. 192-202.

Dowty, J.G., Win, A.K., Buchanan, D.D., Lindor, N.M., Macrae, F.A., Clendenning, M., Antill, Y.C., Thibodeau, S.N., Casey, G. & Gallinger, S. 2013. Cancer risks for MLH1 and MSH2 mutation carriers. *Human mutation.* 34 (3). pp. 490-497.

Doyle, J.M., Gao, J., Wang, J., Yang, M. & Potts, P.R. 2010. MAGE-RING protein complexes comprise a family of E3 ubiquitin ligases. *Molecular cell.* 39 (6). pp. 963-974.

Du, R., Wu, S., Lv, X., Fang, H., Wu, S. & Kang, J. 2014. Overexpression of brachyury contributes to tumor metastasis by inducing epithelial-mesenchymal transition in hepatocellular carcinoma. *Journal of Experimental & Clinical Cancer Research.* 33 (1). pp. 105.

Dyrskjøt, L., Zieger, K., Lildal, T.K., Reinert, T., Gruselle, O., Coche, T., Borre, M. & Ørntoft, T. 2012. Expression of MAGE-A3, NY-ESO-1, LAGE-1 and PRAME in urothelial carcinoma. *British journal of cancer.* 107 (1). pp. 116-122.

Easton, D.F. 1999. How many more breast cancer predisposition genes are there? *Breast Cancer Research.* 1 (1). pp. 1.

Edwards, Y.H., Putt, W., Lekoape, K.M., Stott, D., Fox, M., Hopkinson, D.A. & Sowden, J. 1996. The human homolog T of the mouse T(Brachyury) gene; gene structure, cDNA sequence, and assignment to chromosome 6q27. *Genome research.* 6 (3). pp. 226-233.

Egydio de Carvalho, C., Tanaka, H., Iguchi, N., Ventela, S., Nojima, H. & Nishimune, Y. 2002. Molecular cloning and characterization of a complementary DNA encoding sperm tail protein SHIPPO 1. *Biology of reproduction.* 66 (3). pp. 785-795.

Ell, B. & Kang, Y. 2012. SnapShot: Bone Metastasis. *Cell.* 151 (3). pp. 690-690.e1.

Esteller, M. 2008. Epigenetics in cancer. *New England Journal of Medicine.* 358 (11). pp. 1148-1159.

Fant, M., Farina, A., Nagaraja, R. & Schlessinger, D. 2010. PLAC1 (Placenta-specific 1): a novel, X-linked gene with roles in reproductive and cancer biology. *Prenatal diagnosis.* 30 (6). pp. 497-502.

Feichtinger, J., Larcombe, L. & McFarlane, R.J. 2014. Meta-analysis of expression of l (3) mbt tumor-associated germline genes supports the model that a soma-to-germline transition is a hallmark of human cancers. *International journal of cancer.* 134 (10). pp. 2359-2365.

Feichtinger, J., Aldeailej, I., Anderson, R., Almutairi, M., Almatrafi, A., Alsiwiehri, N., Griffiths, K., Stuart, N., Wakeman, J.A., Larcombe, L. & McFarlane, R.J. 2012a. Meta-analysis of clinical data using human meiotic genes identifies a novel cohort of highly restricted cancer-specific marker genes. *Oncotarget.* 3 (8). pp. 843-853.

Feichtinger, J., McFarlane, R.J. & Larcombe, L.D. 2014. CancerEST: a web-based tool for automatic meta-analysis of public EST data. *Database : the journal of biological databases and curation.* 2014 (0). pp. bau024.

Feichtinger, J., McFarlane, R.J. & Larcombe, L.D. 2012b. CancerMA: a web-based tool for automatic meta-analysis of public cancer microarray data. *Database : the journal of biological databases and curation.* 2012 pp. bas055.

Feitelson, M.A., Arzumanyan, A., Kulathinal, R.J., Blain, S.W., Holcombe, R.F., Mahajna, J., Marino, M., Martinez-Chantar, M.L., Nawroth, R. & Sanchez-Garcia, I. 2015. Sustained

proliferation in cancer: Mechanisms and novel therapeutic targets. *Seminars in cancer biology.* Elsevier: pp. S25.

Fernando, R.I., Litzinger, M., Trono, P., Hamilton, D.H., Schlom, J. & Palena, C. 2010. The T-box transcription factor Brachyury promotes epithelial-mesenchymal transition in human tumor cells. *The Journal of clinical investigation.* 120 (2). pp. 533-544.

Ferreira, D., Adega, F. & Chaves, R. 2013. *The importance of cancer cell lines as in vitro models in cancer methylome analysis and anticancer drugs testing.* INTECH Open Access Publisher: .

Fidler, I.J. 2003. The pathogenesis of cancer metastasis: the'seed and soil'hypothesis revisited. *Nature Reviews Cancer.* 3 (6). pp. 453-458.

Firth, S.M. & Baxter, R.C. 2002. Cellular actions of the insulin-like growth factor binding proteins. *Endocrine reviews.* 23 (6). pp. 824-854.

Fok, K.L., Chung, C.M., Yi, S.Q., Jiang, X., Sun, X., Chen, H., Chen, Y.C., Kung, H.F., Tao, Q., Diao, R., Chan, H., Zhang, X.H., Chung, Y.W., Cai, Z. & Chang Chan, H. 2012. STK31 maintains the undifferentiated state of colon cancer cells. *Carcinogenesis.* 33 (11). pp. 2044-2053.

Fratta, E., Coral, S., Covre, A., Parisi, G., Colizzi, F., Danielli, R., Nicolay, H.J.M., Sigalotti, L. & Maio, M. 2011. The biology of cancer testis antigens: putative function, regulation and therapeutic potential. *Molecular oncology.* 5 (2). pp. 164-182.

Freed-Pastor, W.A., Mizuno, H., Zhao, X., Langerød, A., Moon, S., Rodriguez-Barrueco, R., Barsotti, A., Chicas, A., Li, W. & Polotskaia, A. 2012. Mutant p53 disrupts mammary tissue architecture via the mevalonate pathway. *Cell.* 148 (1). pp. 244-258.

Freidlin, B. & Korn, E.L. 2014. Biomarker enrichment strategies: matching trial design to biomarker credentials. *Nature reviews Clinical oncology.* 11 (2). pp. 81-90.

Fukunaga-Kalabis, M., Martinez, G., Nguyen, T., Kim, D., Santiago-Walker, A., Roesch, A. & Herlyn, M. 2010. Tenascin-C promotes melanoma progression by maintaining the ABCB5-positive side population. *Oncogene.* 29 (46). pp. 6115-6124.

Fukunaga-Kalabis, M., Roesch, A. & Herlyn, M. 2011. From cancer stem cells to tumor maintenance in melanoma. *Journal of Investigative Dermatology.* 131 (8). pp. 1600-1604.

Gallagher, E.J. & LeRoith, D. 2015. Obesity and Diabetes: The Increased Risk of Cancer and Cancer-Related Mortality. *Physiological Reviews.* 95 (3). pp. 727-748.

Garcia-Cruz, R., Brieno, M., Roig, I., Grossmann, M., Velilla, E., Pujol, A., Cabero, L., Pessarrodona, A., Barbero, J. & Caldes, M.G. 2010. Dynamics of cohesin proteins REC8,

STAG3, SMC1β and SMC3 are consistent with a role in sister chromatid cohesion during meiosis in human oocytes. *Human reproduction.* pp. deq180.

Garg, M., Kanojia, D., Salhan, S., Suri, S., Gupta, A., Lohiya, N.K. & Suri, A. 2009. Sperm-associated antigen 9 is a biomarker for early cervical carcinoma. *Cancer.* 115 (12). pp. 2671-2683.

Garg, M., Chaurasiya, D., Rana, R., Jagadish, N., Kanojia, D., Dudha, N., Kamran, N., Salhan, S., Bhatnagar, A., Suri, S., Gupta, A. & Suri, A. 2007. Sperm-associated antigen 9, a novel cancer testis antigen, is a potential target for immunotherapy in epithelial ovarian cancer. *Clinical cancer research : an official journal of the American Association for Cancer Research.* 13 (5). pp. 1421-1428.

Gaugler, B., Van den Eynde, B., van der Bruggen, P., Romero, P., Gaforio, J.J., De Plaen, E., Lethe, B., Brasseur, F. & Boon, T. 1994. Human gene MAGE-3 codes for an antigen recognized on a melanoma by autologous cytolytic T lymphocytes. *The Journal of experimental medicine.* 179 (3). pp. 921-930.

Gentsch, G.E., Owens, N.D., Martin, S.R., Piccinelli, P., Faial, T., Trotter, M.W., Gilchrist, M.J. & Smith, J.C. 2013. In vivo T-box transcription factor profiling reveals joint regulation of embryonic neuromesodermal bipotency. *Cell reports.* 4 (6). pp. 1185-1196.

Gerin, I., Clerbaux, L.A., Haumont, O., Lanthier, N., Das, A.K., Burant, C.F., Leclercq, I.A., MacDougald, O.A. & Bommer, G.T. 2010. Expression of miR-33 from an SREBP2 intron inhibits cholesterol export and fatty acid oxidation. *The Journal of biological chemistry.* 285 (44). pp. 33652-33661.

Ghafouri-Fard, S., Abbasi, A., Moslehi, H., Faramarzi, N., Taba Taba Vakili, S., Mobasheri, M. & Modarressi, M. 2010. Elevated expression levels of testis-specific genes TEX101 and SPATA19 in basal cell carcinoma and their correlation with clinical and pathological features. *British Journal of Dermatology.* 162 (4). pp. 772-779.

Ghafouri-Fard, S., Ghafouri-Fard, S. & Modarressi, M. 2012. Expression of splice variants of cancer-testis genes ODF3 and ODF4 in the testis of a prostate cancer patient. *Genet Mol Res.* 11 (4). pp. 3642-3648.

Giovannucci, E.L. 2015. Are Most Cancers Caused by Specific Risk Factors Acting on Tissues With High Underlying Stem Cell Divisions? *Journal of the National Cancer Institute.* 108 (3). pp. 10.1093/jnci/djv343.

Gjerstorff, M.F., Andersen, M.H. & Ditzel, H.J. 2015. Oncogenic cancer/testis antigens: prime candidates for immunotherapy. *Oncotarget.* 6 (18). pp. 15772-15787.

Gluecksohn-Schoenheimer, S. 1944. The Development of Normal and Homozygous Brachy (T/T) Mouse Embryos in the Extraembryonic Coelom of the Chick. *Proceedings of the National Academy of Sciences of the United States of America.* 30 (6). pp. 134-140.

Goldberg, E., Eddy, E.M., Duan, C. & Odet, F. 2010. LDHC: The Ultimate Testis-Specific Gene. *Journal of andrology.* 31 (1). pp. 86-94.

González, C.R., Sedó, C.A., Nodar, F., Papier, S. & Vitullo, A.D. 2016. Simultaneous expression analysis of deleted in azoospermia-family genes and CDC25A: their potential as a predictor for successful testicular sperm extraction. *Asian Journal of Andrology.* 18 pp. 1-2.

Goydos, J.S., Patel, M. & Shih, W. 2001. NY-ESO-1 and CTp11 expression may correlate with stage of progression in melanoma. *Journal of Surgical Research.* 98 (2). pp. 76-80.

Gräff, J. & Tsai, L. 2013. Histone acetylation: molecular mnemonics on the chromatin. *Nature Reviews Neuroscience.* 14 (2). pp. 97-111.

Greve, K.B., Lindgreen, J.N., Terp, M.G., Pedersen, C.B., Schmidt, S., Mollenhauer, J., Kristensen, S.B., Andersen, R.S., Relster, M.M. & Ditzel, H.J. 2015. Ectopic expression of cancer/testis antigen SSX2 induces DNA damage and promotes genomic instability. *Molecular oncology.* 9 (2). pp. 437-449.

Greve, K., Pøhl, M., Olsen, K., Nielsen, O., Ditzel, H. & Gjerstorff, M. 2014. SSX2-4 expression in early-stage non-small cell lung cancer. *Tissue antigens.* 83 (5). pp. 344-349.

Grivennikov, S.I., Greten, F.R. & Karin, M. 2010. Immunity, inflammation, and cancer. *Cell.* 140 (6). pp. 883-899.

Grzmil, M. & Hemmings, B.A. 2012. Translation regulation as a therapeutic target in cancer. *Cancer research.* 72 (16). pp. 3891-3900.

Guardia, C.M., Caramelo, J.J., Trujillo, M., Mendez-Huergo, S.P., Radi, R., Estrin, D.A. & Rabinovich, G.A. 2014. Structural basis of redox-dependent modulation of galectin-1 dynamics and function. *Glycobiology.* 24 (5). pp. 428-441.

Guleria, A. & Chandna, S. 2016. ATM kinase: Much more than a DNA damage responsive protein. *DNA repair.* 39 pp. 1-20.

Gupta, G.P. & Massagué, J. 2006. Cancer metastasis: building a framework. *Cell.* 127 (4). pp. 679-695.

Gure, A.O., Chua, R., Williamson, B., Gonen, M., Ferrera, C.A., Gnjatic, S., Ritter, G., Simpson, A.J., Chen, Y.T., Old, L.J. & Altorki, N.K. 2005. Cancer-testis genes are coordinately expressed and are markers of poor outcome in non-small cell lung cancer. *Clinical cancer*

research : an official journal of the American Association for Cancer Research. 11 (22). pp. 8055-8062.

Hackett, J.A., Reddington, J.P., Nestor, C.E., Dunican, D.S., Branco, M.R., Reichmann, J., Reik, W., Surani, M.A., Adams, I.R. & Meehan, R.R. 2012. Promoter DNA methylation couples genome-defence mechanisms to epigenetic reprogramming in the mouse germline. *Development (Cambridge, England).* 139 (19). pp. 3623-3632.

Hanahan, D. & Weinberg, R.A. 2011. Hallmarks of cancer: the next generation. *Cell.* 144 (5). pp. 646-674.

Heery, C.R., Singh, B.H., Rauckhorst, M., Marte, J.L., Donahue, R.N., Grenga, I., Rodell, T.C., Dahut, W., Arlen, P.M., Madan, R.A., Schlom, J. & Gulley, J.L. 2015. Phase I Trial of a Yeast-Based Therapeutic Cancer Vaccine (GI-6301) Targeting the Transcription Factor Brachyury. *Cancer immunology research.* 3 (11). pp. 1248-1256.

Heinzerling, L., Ott, P.A., Hodi, F.S., Husain, A.N., Tajmir-Riahi, A., Tawbi, H., Pauschinger, M., Gajewski, T.F., Lipson, E.J. & Luke, J.J. 2016. Cardiotoxicity associated with CTLA4 and PD1 blocking immunotherapy. *Journal for ImmunoTherapy of Cancer.* 4 (1). pp. 1.

Henry, N.L. & Hayes, D.F. 2012. Cancer biomarkers. *Molecular oncology.* 6 (2). pp. 140-146.

Herrero, R., González, P. & Markowitz, L.E. 2015. Present status of human papillomavirus vaccine development and implementation. *The Lancet Oncology.* 16 (5). pp. e206-e216.

Hirohashi, Y., Torigoe, T., Tsukahara, T., Kanaseki, T., Kochin, V. & Sato, N. 2016. Immune responses to human cancer stem-like cells/cancer-initiating cells. *Cancer science.* 107 (1). pp. 12-17.

Hizli, A.A., Chi, Y., Swanger, J., Carter, J.H., Liao, Y., Welcker, M., Ryazanov, A.G. & Clurman, B.E. 2013. Phosphorylation of eukaryotic elongation factor 2 (eEF2) by cyclin A-cyclin-dependent kinase 2 regulates its inhibition by eEF2 kinase. *Molecular and cellular biology.* 33 (3). pp. 596-604.

Hodi, F.S., O'Day, S.J., McDermott, D.F., Weber, R.W., Sosman, J.A., Haanen, J.B., Gonzalez, R., Robert, C., Schadendorf, D. & Hassel, J.C. 2010. Improved survival with ipilimumab in patients with metastatic melanoma. *New England Journal of Medicine.* 363 (8). pp. 711-723.

Hofmann, O., Caballero, O.L., Stevenson, B.J., Chen, Y.T., Cohen, T., Chua, R., Maher, C.A., Panji, S., Schaefer, U., Kruger, A., Lehvaslaiho, M., Carninci, P., Hayashizaki, Y., Jongeneel, C.V., Simpson, A.J., Old, L.J. & Hide, W. 2008. Genome-wide analysis of cancer/testis gene expression. *Proceedings of the National Academy of Sciences of the United States of America.* 105 (51). pp. 20422-20427.

Hormones, T.E. & Group, B.C.C. 2010. Insulin-like growth factor 1 (IGF1), IGF binding protein 3 (IGFBP3), and breast cancer risk: pooled individual data analysis of 17 prospective studies. *The lancet oncology.* 11 (6). pp. 530-542.

Hou, Y., Fan, W., Yan, L., Li, R., Lian, Y., Huang, J., Li, J., Xu, L., Tang, F. & Xie, X.S. 2013. Genome analyses of single human oocytes. *Cell.* 155 (7). pp. 1492-1506.

Hou, M., Huang, R., Song, Y., Feng, D., Jiang, Y. & Liu, M. 2016. ATAD2 overexpression is associated with progression and prognosis in colorectal cancer. *Japanese journal of clinical oncology.* 46 (3). pp. 222-227.

Hovey, A.M., Devor, E.J., Breheny, P.J., Mott, S.L., Dai, D., Thiel, K.W. & Leslie, K.K. 2015. miR-888: a novel cancer-testis antigen that targets the progesterone receptor in endometrial cancer. *Translational oncology.* 8 (2). pp. 85-96.

Hsia, E.Y., Kalashnikova, E.V., Revenko, A.S., Zou, J.X., Borowsky, A.D. & Chen, H.W. 2010. Deregulated E2F and the AAA+ coregulator ANCCA drive proto-oncogene ACTR/AIB1 overexpression in breast cancer. *Molecular cancer research : MCR.* 8 (2). pp. 183-193.

Hu, Y., Yu, H., Shaw, G., Renfree, M.B. & Pask, A.J. 2011. Differential roles of TGIF family genes in mammalian reproduction. *BMC developmental biology.* 11 (1). pp. 1.

Huang, B., Cohen, J., Fernando, R., Hamilton, D., Litzinger, M., Hodge, J. & Palena, C. 2013. The embryonic transcription factor Brachyury blocks cell cycle progression and mediates tumor resistance to conventional antitumor therapies. *Cell death & disease.* 4 (6). pp. e682.

Huang, C., Sloan, E.A. & Boerkoel, C.F. 2003. Chromatin remodeling and human disease. *Current opinion in genetics & development.* 13 (3). pp. 246-252.

Hunder, N.N., Wallen, H., Cao, J., Hendricks, D.W., Reilly, J.Z., Rodmyre, R., Jungbluth, A., Gnjatic, S., Thompson, J.A. & Yee, C. 2008. Treatment of metastatic melanoma with autologous CD4 T cells against NY-ESO-1. *New England Journal of Medicine.* 358 (25). pp. 2698-2703.

Hwang, H.C. & Clurman, B.E. 2005. Cyclin E in normal and neoplastic cell cycles. *Oncogene.* 24 (17). pp. 2776-2786.

Hwang, H.W., Ha, S.Y., Bang, H. & Park, C.K. 2015. ATAD2 as a Poor Prognostic Marker for Hepatocellular Carcinoma after Curative Resection. *Cancer research and treatment : official journal of Korean Cancer Association.* 47 (4). pp. 853-861.

Hytonen, M.K., Grall, A., Hedan, B., Dreano, S., Seguin, S.J., Delattre, D., Thomas, A., Galibert, F., Paulin, L., Lohi, H., Sainio, K. & Andre, C. 2009. Ancestral T-box mutation is present in many, but not all, short-tailed dog breeds. *The Journal of heredity.* 100 (2). pp. 236-240.

Imajyo, I., Sugiura, T., Kobayashi, Y., Shimoda, M., Ishii, K., Akimoto, N., Yoshihama, N., Kobayashi, I. & Mori, Y. 2012. T-box transcription factor Brachyury expression is correlated with epithelial-mesenchymal transition and lymph node metastasis in oral squamous cell carcinoma. *International journal of oncology.* 41 (6). pp. 1985.

Imoto, I., Pimkhaokham, A., Watanabe, T., Saito-Ohara, F., Soeda, E. & Inazawa, J. 2000. Amplification and overexpression of TGIF2, a novel homeobox gene of the TALE superclass, in ovarian cancer cell lines. *Biochemical and biophysical research communications.* 276 (1). pp. 264-270.

Inagawa, M., Nakajima, K., Makino, T., Ogawa, S., Kojima, M., Ito, S., Ikenishi, A., Hayashi, T., Schwartz, R.J. & Nakamura, K. 2013. Histone H3 lysine 9 methyltransferases, G9a and GLP are essential for cardiac morphogenesis. *Mechanisms of development.* 130 (11). pp. 519-531.

Ito, C., Yamatoya, K. & Toshimori, K. 2014. Equatorin-Related Subcellular and Molecular Events During Sperm Priming for Fertilization in Mice. In: *Sexual Reproduction in Animals and Plants.* Springer: pp. 85-95.

Jackman, S.M., Kong, X. & Fant, M.E. 2012. Plac1 (placenta-specific 1) is essential for normal placental and embryonic development. *Molecular reproduction and development.* 79 (8). pp. 564-572.

Janic, A., Mendizabal, L., Llamazares, S., Rossell, D. & Gonzalez, C. 2010. Ectopic expression of germline genes drives malignant brain tumor growth in Drosophila. *Science (New York, N.Y.).* 330 (6012). pp. 1824-1827.

Jeffery, J., Sinha, D., Srihari, S., Kalimutho, M. & Khanna, K. 2016. Beyond cytokinesis: the emerging roles of CEP55 in tumorigenesis. *Oncogene.* 35 (6). pp. 683-690.

Jerome, L.A. & Papaioannou, V.E. 2001. DiGeorge syndrome phenotype in mice mutant for the T-box gene, Tbx1. *Nature genetics.* 27 (3). pp. 286-291.

Jezkova, J., Williams, J.S., Jones-Hutchins, F., Sammut, S.J., Gollins, S., Cree, I., Coupland, S., McFarlane, R.J. & Wakeman, J.A. 2014. Brachyury regulates proliferation of cancer cells via a p27Kip1-dependent pathway. *Oncotarget.* 5 (11). pp. 3813-3822.

Jezkova, J., Williams, J.S., Pinto, F., Sammut, S.J., Williams, G.T., Gollins, S., McFarlane, R.J., Reis, R.M. & Wakeman, J.A. 2016. Brachyury identifies a class of enteroendocrine cells in normal human intestinal crypts and colorectal cancer. *Oncotarget.* 7 (10). pp. 11478-11486.

Jiang, C.L., Jin, S.G. & Pfeifer, G.P. 2004. MBD3L1 is a transcriptional repressor that interacts with methyl-CpG-binding protein 2 (MBD2) and components of the NuRD complex. *The Journal of biological chemistry.* 279 (50). pp. 52456-52464.

Jin, C., Qiu, L., Li, J., Fu, T., Zhang, X. & Tan, W. 2016. Cancer biomarker discovery using DNA aptamers. *Analyst.* 141 (2). pp. 461-466.

Jin, L., Zhou, Y., Kuang, C., Lin, L. & Chen, Y. 2005. Expression pattern of TG-interacting factor 2 during mouse development. *Gene expression patterns.* 5 (4). pp. 457-462.

Jung, H., Lee, S.K. & Jho, E. 2010. P112. MEST/Peg1 inhibits Wnt signaling via regulating maturation of LRP6. *Differentiation.* 80 pp. S54.

Kalashnikova, E.V., Revenko, A.S., Gemo, A.T., Andrews, N.P., Tepper, C.G., Zou, J.X., Cardiff, R.D., Borowsky, A.D. & Chen, H.W. 2010. ANCCA/ATAD2 overexpression identifies breast cancer patients with poor prognosis, acting to drive proliferation and survival of triple-negative cells through control of B-Myb and EZH2. *Cancer research.* 70 (22). pp. 9402-9412.

Kalejs, M. & Erenpreisa, J. 2005. Cancer/testis antigens and gametogenesis: a review and" brain-storming" session. *Cancer cell international.* 5 (1). pp. 1.

Kamei, Y., Suganami, T., Kohda, T., Ishino, F., Yasuda, K., Miura, S., Ezaki, O. & Ogawa, Y. 2007. Peg1/Mest in obese adipose tissue is expressed from the paternal allele in an isoform-specific manner. *FEBS letters.* 581 (1). pp. 91-96.

Kang, J.U., Koo, S.H., Kwon, K.C. & Park, J.W. 2010. Frequent silence of chromosome 9p, homozygous DOCK8, DMRT1 and DMRT3 deletion at 9p24. 3 in squamous cell carcinoma of the lung. *International journal of oncology.* 37 (2). pp. 327.

Kanojia, D., Garg, M., Gupta, S., Gupta, A. & Suri, A. 2009. Sperm-associated antigen 9, a novel biomarker for early detection of breast cancer. *Cancer epidemiology, biomarkers & prevention : a publication of the American Association for Cancer Research, cosponsored by the American Society of Preventive Oncology.* 18 (2). pp. 630-639.

Karahalil, B., Bohr, V.A. & Wilson, D.M.,3rd 2012. Impact of DNA polymorphisms in key DNA base excision repair proteins on cancer risk. *Human & experimental toxicology.* 31 (10). pp. 981-1005.

Karbiener, M., Glantschnig, C., Pisani, D.F., Laurencikiene, J., Dahlman, I., Herzig, S., Amri, E. & Scheideler, M. 2015. Mesoderm-specific transcript (MEST) is a negative regulator of human adipocyte differentiation. *International journal of obesity.* 39 (12). pp. 1733-1741.

Karin, M. 2006. Nuclear factor-κB in cancer development and progression. *Nature.* 441 (7092). pp. 431-436.

Karpf, A.R. 2006. A potential role for epigenetic modulatory drugs in the enhancement of cancer/germ-line antigen vaccine efficacy. *Epigenetics.* 1 (3). pp. 116-120.

Karpf, A.R., Lasek, A.W., Ririe, T.O., Hanks, A.N., Grossman, D. & Jones, D.A. 2004. Limited gene activation in tumor and normal epithelial cells treated with the DNA methyltransferase inhibitor 5-aza-2'-deoxycytidine. *Molecular pharmacology.* 65 (1). pp. 18-27.

Kasuga, C., Nakahara, Y., Ueda, S., Hawkins, C., Taylor, M.D., Smith, C.A. & Rutka, J.T. 2008. Expression of MAGE and GAGE genes in medulloblastoma and modulation of resistance to chemotherapy.

Kaur, G., Thompson, L.A. & Dufour, J.M. 2014. Sertoli cells–Immunological sentinels of spermatogenesis. *Seminars in cell & developmental biology.* Elsevier: pp. 36.

Kawamura, M., Taki, T., Kaku, H., Ohki, K. & Hayashi, Y. 2015. Identification of SPAG9 as a novel JAK2 fusion partner gene in pediatric acute lymphoblastic leukemia with t (9; 17)(p24; q21). *Genes, Chromosomes and Cancer.* 54 (7). pp. 401-408.

Khlifi, R., Rebai, A. & Hamza-Chaffai, A. 2012. Polymorphisms in human DNA repair genes and head and neck squamous cell carcinoma. *Journal of genetics.* 91 (3). pp. 375-384.

Kierszenbaum, A.L. 2002. Keratins: unraveling the coordinated construction of scaffolds in spermatogenic cells. *Molecular reproduction and development.* 61 (1). pp. 1-2.

Kilic, N., Feldhaus, S., Kilic, E., Tennstedt, P., Wicklein, D., von Wasielewski, R., Viebahn, C., Kreipe, H. & Schumacher, U. 2011. Brachyury expression predicts poor prognosis at early stages of colorectal cancer. *European journal of cancer.* 47 (7). pp. 1080-1085.

Kim, R., Kulkarni, P. & Hannenhalli, S. 2013. Derepression of Cancer/testis antigens in cancer is associated with distinct patterns of DNA hypomethylation. *BMC cancer.* 13 (1). pp. 1.

Kim, B., Lee, H.J., Choi, H.Y., Shin, Y., Nam, S., Seo, G., Son, D.S., Jo, J., Kim, J., Lee, J., Kim, J., Kim, K. & Lee, S. 2007. Clinical validity of the lung cancer biomarkers identified by bioinformatics analysis of public expression data. *Cancer research.* 67 (15). pp. 7431-7438.

Kim, Y., Park, D., Kim, H., Choi, M., Lee, H., Lee, Y.S., Choe, J., Kim, Y.M. & Jeoung, D. 2013. miR-200b and cancer/testis antigen CAGE form a feedback loop to regulate the invasion and tumorigenic and angiogenic responses of a cancer cell line to microtubule-targeting drugs. *The Journal of biological chemistry.* 288 (51). pp. 36502-36518.

Kispert, A. & Herrmann, B.G. 1993. The Brachyury gene encodes a novel DNA binding protein. *The EMBO journal.* 12 (8). pp. 3211-3220.

Kobayashi, Y., Sugiura, T., Imajyo, I., Shimoda, M., Ishii, K., Akimoto, N., Yoshihama, N. & Mori, Y. 2014. Knockdown of the T-box transcription factor Brachyury increases sensitivity of adenoid cystic carcinoma cells to chemotherapy and radiation in vitro: Implications for a new therapeutic principle. *International journal of oncology.* 44 (4). pp. 1107-1117.

Kober, K.M., Cooper, B.A., Paul, S.M., Dunn, L.B., Levine, J.D., Wright, F., Hammer, M.J., Mastick, J., Venook, A. & Aouizerat, B.E. 2016. Subgroups of chemotherapy patients with distinct morning and evening fatigue trajectories. *Supportive Care in Cancer.* 24 (4). pp. 1473-1485.

Koch, J., Dübel, S., Usener, D., Schadendorf, D. & Eichmüller, S. 2003. cTAGE: a cutaneous T cell lymphoma associated antigen family with tumor-specific splicing. *Journal of investigative dermatology.* 121 (1). pp. 198-206.

Koebel, C.M., Vermi, W., Swann, J.B., Zerafa, N., Rodig, S.J., Old, L.J., Smyth, M.J. & Schreiber, R.D. 2007. Adaptive immunity maintains occult cancer in an equilibrium state. *Nature.* 450 (7171). pp. 903-907.

Konstantinopoulos, P.A. & Papavassiliou, A.G. 2011. Seeing the future of cancer-associated transcription factor drug targets. *Jama.* 305 (22). pp. 2349-2350.

Kouzarides, T. 2007. Chromatin modifications and their function. *Cell.* 128 (4). pp. 693-705.

Krishnadas, D.K., Shusterman, S., Bai, F., Diller, L., Sullivan, J.E., Cheerva, A.C., George, R.E. & Lucas, K.G. 2015. A phase I trial combining decitabine/dendritic cell vaccine targeting MAGE-A1, MAGE-A3 and NY-ESO-1 for children with relapsed or therapy-refractory neuroblastoma and sarcoma. *Cancer Immunology, Immunotherapy.* 64 (10). pp. 1251-1260.

Krishnadas, D.K., Bai, F. & Lucas, K. 2013. Cancer testis antigen and immunotherapy. *ImmunoTargets and Therapy.* 2 pp. 11-19.

Kromik, A., Ulrich, R., Kusenda, M., Tipold, A., Stein, V.M., Hellige, M., Dziallas, P., Hadlich, F., Widmann, P., Goldammer, T., Baumgartner, W., Rehage, J., Segelke, D., Weikard, R. & Kuhn, C. 2015. The mammalian cervical vertebrae blueprint depends on the T (brachyury) gene. *Genetics.* 199 (3). pp. 873-883.

Kumara, H.S., Grieco, M.J., Caballero, O.L., Su, T., Ahmed, A., Ritter, E., Gnjatic, S., Cekic, V., Old, L.J. & Simpson, A.J. 2012. MAGE-A3 is highly expressed in a subset of colorectal cancer patients. *Cancer Immunity Archive.* 12 (2). pp. 16.

Kunkel, J., Peng, Y., Tao, Y., Krigman, H. & Cao, D. 2012. Presence of a sarcomatous component outside the ovary is an adverse prognostic factor for primary ovarian malignant mixed mesodermal/mullerian tumors: a clinicopathologic study of 47 cases. *The American Journal of Surgical Pathology.* 36 (6). pp. 831-837.

Kuo, P., Huang, Y., Hsieh, C.C., Lee, J., Lin, B. & Hung, L. 2014. STK31 is a cell-cycle regulated protein that contributes to the tumorigenicity of epithelial cancer cells. *PloS one.* 9 (3). pp. e93303.

Kuramochi-Miyagawa, S., Kimura, T., Ijiri, T.W., Isobe, T., Asada, N., Fujita, Y., Ikawa, M., Iwai, N., Okabe, M., Deng, W., Lin, H., Matsuda, Y. & Nakano, T. 2004. Mili, a mammalian member of piwi family gene, is essential for spermatogenesis. *Development (Cambridge, England).* 131 (4). pp. 839-849.

Kurashige, T., Noguchi, Y., Saika, T., Ono, T., Nagata, Y., Jungbluth, A., Ritter, G., Chen, Y.T., Stockert, E., Tsushima, T., Kumon, H., Old, L.J. & Nakayama, E. 2001. Ny-ESO-1 expression and immunogenicity associated with transitional cell carcinoma: correlation with tumor grade. *Cancer research.* 61 (12). pp. 4671-4674.

Laban, S., Atanackovic, D., Luetkens, T., Knecht, R., Busch, C., Freytag, M., Spagnoli, G., Ritter, G., Hoffmann, T.K. & Knuth, A. 2014. Simultaneous cytoplasmic and nuclear protein expression of melanoma antigen-A family and NY-ESO-1 cancer-testis antigens represents an independent marker for poor survival in head and neck cancer. *International Journal of Cancer.* 135 (5). pp. 1142-1152.

Lagerstedt Robinson, K., Liu, T., Vandrovcova, J., Halvarsson, B., Clendenning, M., Frebourg, T., Papadopoulos, N., Kinzler, K.W., Vogelstein, B., Peltomaki, P., Kolodner, R.D., Nilbert, M. & Lindblom, A. 2007. Lynch syndrome (hereditary nonpolyposis colorectal cancer) diagnostics. *Journal of the National Cancer Institute.* 99 (4). pp. 291-299.

Lange, J., Pan, J., Cole, F., Thelen, M.P., Jasin, M. & Keeney, S. 2011. ATM controls meiotic double-strand-break formation. *Nature.* 479 (7372). pp. 237-240.

Larkin, S., Holmes, S., Cree, I., Walker, T., Basketter, V., Bickers, B., Harris, S., Garbis, S.D., Townsend, P. & Aukim-Hastie, C. 2012. Identification of markers of prostate cancer progression using candidate gene expression. *British journal of cancer.* 106 (1). pp. 157-165.

Le Borgne, F., Mohamed, A.B., Logerot, M., Garnier, E. & Demarquoy, J. 2011. Changes in carnitine octanoyltransferase activity induce alteration in fatty acid metabolism. *Biochemical and biophysical research communications.* 409 (4). pp. 699-704.

Leary, R.J., Lin, J.C., Cummins, J., Boca, S., Wood, L.D., Parsons, D.W., Jones, S., Sjoblom, T., Park, B.H., Parsons, R., Willis, J., Dawson, D., Willson, J.K., Nikolskaya, T., Nikolsky, Y., Kopelovich, L., Papadopoulos, N., Pennacchio, L.A., Wang, T.L., Markowitz, S.D., Parmigiani, G., Kinzler, K.W., Vogelstein, B. & Velculescu, V.E. 2008. Integrated analysis of homozygous deletions, focal amplifications, and sequence alterations in breast and colorectal cancers. *Proceedings of the National Academy of Sciences of the United States of America.* 105 (42). pp. 16224-16229.

LeBeau, A.M., Singh, P., Isaacs, J.T. & Denmeade, S.R. 2009. Prostate-Specific Antigen Is a "Chymotrypsin-like" Serine Protease with Unique P1 Substrate Specificity†. *Biochemistry.* 48 (15). pp. 3490-3496.

Legros, F., Lombes, A., Frachon, P. & Rojo, M. 2002. Mitochondrial fusion in human cells is efficient, requires the inner membrane potential, and is mediated by mitofusins. *Molecular biology of the cell.* 13 (12). pp. 4343-4354.

Lehtinen, M. & Dillner, J. 2013. Clinical trials of human papillomavirus vaccines and beyond. *Nature reviews Clinical oncology.* 10 (7). pp. 400-410.

Lethé, B., Lucas, S., Michaux, L., De Smet, C., Godelaine, D., Serrano, A., De Plaen, E. & Boon, T. 1998. LAGE-1, a new gene with tumor specificity. *International journal of cancer.* 76 (6). pp. 903-908.

Li, H., Peng, Y., Niu, H., Wu, B., Zhang, Y., Zhang, Y., Bai, X. & He, P. 2014. SPAG9 is overexpressed in human prostate cancer and promotes cancer cell proliferation. *Tumor Biology.* 35 (7). pp. 6949-6954.

Li, K., Ying, M., Feng, D., Chen, Y., Wang, J. & Wang, Y. 2016. SMC1 promotes epithelial-mesenchymal transition in triple-negative breast cancer through upregulating Brachyury. *Oncology reports.* 35 (4). pp. 2405-2412.

Li, Q.Y., Newbury-Ecob, R.A., Terrett, J.A., Wilson, D.I., Curtis, A.R., Yi, C.H., Gebuhr, T., Bullen, P.J., Robson, S.C. & Strachan, T. 1997. Holt-Oram syndrome is caused by mutations in TBX5, a member of the Brachyury (T) gene family. *Nature genetics.* 15 (1). pp. 21-29.

Li, Y., Hu, X., Zhang, K., Guo, J., Hu, Z., Tao, S., Xiao, L., Wang, Q., Han, C. & Liu, Y. 2006. Afaf, a novel vesicle membrane protein, is related to acrosome formation in murine testis. *FEBS letters.* 580 (17). pp. 4266-4273.

Li, M., Yuan, Y.H., Han, Y., Liu, Y.X., Yan, L., Wang, Y. & Gu, J. 2005. Expression profile of cancer-testis genes in 121 human colorectal cancer tissue and adjacent normal tissue. *Clinical cancer research : an official journal of the American Association for Cancer Research.* 11 (5). pp. 1809-1814.

Li, N., Tang, E.I. & Cheng, C.Y. 2016. Regulation of blood-testis barrier by actin binding proteins and protein kinases. *Reproduction (Cambridge, England).* 151 (3). pp. R29-41.

Lifantseva, N., Koltsova, A., Krylova, T., Yakovleva, T., Poljanskaya, G. & Gordeeva, O. 2011. Expression patterns of cancer-testis antigens in human embryonic stem cells and their cell derivatives indicate lineage tracks. *Stem cells international.* 2011 pp. 795239.

Liggins, A., Brown, P., Asker, K., Pulford, K. & Banham, A. 2004. A novel diffuse large B-cell lymphoma-associated cancer testis antigen encoding a PAS domain protein. *British journal of cancer.* 91 (1). pp. 141-149.

Liggins, A.P., Lim, S.H., Soilleux, E.J., Pulford, K. & Banham, A.H. 2010. A panel of cancer-testis genes exhibiting broad-spectrum expression in haematological malignancies. *Cancer immunity.* 10 pp. 8.

Lim, S.L., Ricciardelli, C., Oehler, M.K., Tan, Izza MD De Arao, Russell, D. & Grützner, F. 2014. Overexpression of piRNA pathway genes in epithelial ovarian cancer. *PLoS One.* 9 (6). pp. e99687.

Lin, Y. & Page, D.C. 2005. Dazl deficiency leads to embryonic arrest of germ cell development in XY C57BL/6 mice. *Developmental biology.* 288 (2). pp. 309-316.

Lin, Y., Lin, Y., Teng, Y., Hsieh, T.T., Lin, Y. & Kuo, P. 2006. Identification of ten novel genes involved in human spermatogenesis by microarray analysis of testicular tissue. *Fertility and sterility.* 86 (6). pp. 1650-1658.

Lindblom, A. & Liljegren, A. 2000. Tumour markers in malignancies. *British medical journal.* 320 (7232). pp. 424.

Lindemann, C.B. & Lesich, K.A. 2016. Functional anatomy of the mammalian sperm flagellum. *Cytoskeleton.*

Lingel, A. & Sattler, M. 2005. Novel modes of protein–RNA recognition in the RNAi pathway. *Current opinion in structural biology.* 15 (1). pp. 107-115.

Link, P.A., Gangisetty, O., James, S.R., Woloszynska-Read, A., Tachibana, M., Shinkai, Y. & Karpf, A.R. 2009. Distinct roles for histone methyltransferases G9a and GLP in cancer germ-line antigen gene regulation in human cancer cells and murine embryonic stem cells. *Molecular cancer research : MCR.* 7 (6). pp. 851-862.

Lips, E.H., van Eijk, R., de Graaf, E.J., Oosting, J., de Miranda, N.F., Karsten, T., van de Velde, Cornelis J, Eilers, P.H., Tollenaar, R.A. & van Wezel, T. 2008. Integrating chromosomal aberrations and gene expression profiles to dissect rectal tumorigenesis. *BMC cancer.* 8 (1). pp. 1.

Litvinov, I.V., Cordeiro, B., Huang, Y., Zargham, H., Pehr, K., Dore, M.A., Gilbert, M., Zhou, Y., Kupper, T.S. & Sasseville, D. 2014. Ectopic expression of cancer-testis antigens in cutaneous T-cell lymphoma patients. *Clinical cancer research : an official journal of the American Association for Cancer Research.* 20 (14). pp. 3799-3808.

Liu, C., Yang, H., Zhang, R., Zhao, J. & Hao, D. 2016. Tumour-associated antigens and their anti-cancer applications. *European journal of cancer care.*

Liu, F., Zhang, H., Shen, D., Wang, S., Ye, Y., Chen, H., Pang, X., Song, Q. & He, P. 2014. Identification of two new HLA-A* 0201-restricted cytotoxic T lymphocyte epitopes from

colorectal carcinoma-associated antigen PLAC1/CP1. *Journal of gastroenterology.* 49 (3). pp. 419-426.

Liu, J., Zhang, C., Hu, W. & Feng, Z. 2015. Tumor suppressor p53 and its mutants in cancer metabolism. *Cancer letters.* 356 (2). pp. 197-203.

Liu, W., Zhai, M., Wu, Z., Qi, Y., Wu, Y., Dai, C., Sun, M., Li, L. & Gao, Y. 2012. Identification of a novel HLA-A2-restricted cytotoxic T lymphocyte epitope from cancer-testis antigen PLAC1 in breast cancer. *Amino acids.* 42 (6). pp. 2257-2265.

Liu, W., Jiang, X. & Zhang, Z. 2010. Expression of PSCA, PIWIL1 and TBX2 and its correlation with HPV16 infection in formalin-fixed, paraffin-embedded cervical squamous cell carcinoma specimens. *Archives of Virology.* 155 (5). pp. 657-663.

Long, J., Zhang, X., Wen, M., Kong, Q., Lv, Z., An, Y. & Wei, X. 2013. IL-35 over-expression increases apoptosis sensitivity and suppresses cell growth in human cancer cells. *Biochemical and biophysical research communications.* 430 (1). pp. 364-369.

Loughery, J. & Meek, D. 2013. Switching on p53: an essential role for protein phosphorylation? *BioDiscovery.* 8.

Lu, Y., Zhang, K., Li, C., Yao, Y., Tao, D., Liu, Y., Zhang, S. & Ma, Y. 2012. Piwil2 suppresses p53 by inducing phosphorylation of signal transducer and activator of transcription 3 in tumor cells. *PLoS One.* 7 (1). pp. e30999.

Lucas, S., De Plaen, E. & Boon, T. 2000. MAGE-B5, MAGE-B6, MAGE-C2, and MAGE-C3: four new members of the MAGE family with tumor-specific expression. *International journal of cancer.* 87 (1). pp. 55-60.

Luetjens, C.M., Xu, E.Y., Rejo Pera, R.A., Kamischke, A., Nieschlag, E. & Gromoll, J. 2004. Association of meiotic arrest with lack of BOULE protein expression in infertile men. *The Journal of Clinical Endocrinology & Metabolism.* 89 (4). pp. 1926-1933.

Luo, J., Solimini, N.L. & Elledge, S.J. 2009. Principles of cancer therapy: oncogene and non-oncogene addiction. *Cell.* 136 (5). pp. 823-837.

Luo, Y., Ye, G.Y., Qin, S.L., Yu, M.H., Mu, Y.F. & Zhong, M. 2015. ATAD2 Overexpression Identifies Colorectal Cancer Patients with Poor Prognosis and Drives Proliferation of Cancer Cells. *Gastroenterology research and practice.* 2015 pp. 936564.

Mäbert, K., Cojoc, M., Peitzsch, C., Kurth, I., Souchelnytskyi, S. & Dubrovska, A. 2014. Cancer biomarker discovery: current status and future perspectives. *International journal of radiation biology.* 90 (8). pp. 659-677.

Macheret, M. & Halazonetis, T.D. 2015. DNA replication stress as a hallmark of cancer. *Annual Review of Pathology: Mechanisms of Disease.* 10 pp. 425-448.

Maine, E.A., Westcott, J.M., Prechtl, A.M., Dang, T.T., Whitehurst, A.W. & Pearson, G.W. 2016. The cancer-testis antigens SPANX-A/C/D and CTAG2 promote breast cancer invasion. *Oncotarget.* 7 (12). pp. 14708-14726.

Maio, M., Coral, S., Sigalotti, L., Elisei, R., Romei, C., Rossi, G., Cortini, E., Colizzi, F., Fenzi, G. & Altomonte, M. 2003. Analysis of cancer/testis antigens in sporadic medullary thyroid carcinoma: expression and humoral response to NY-ESO-1. *The Journal of Clinical Endocrinology & Metabolism.* 88 (2). pp. 748-754.

Makise, N., Morikawa, T., Nakagawa, T., Ichimura, T., Kawai, T., Matsushita, H., Kakimi, K., Kume, H., Homma, Y. & Fukayama, M. 2016. MAGE-A expression, immune microenvironment, and prognosis in upper urinary tract carcinoma. *Human pathology.* 50 pp. 62-69.

Malpuech, G., Vanlieferinghen, P., Dechelotte, P., Gaulme, J., Labbé, A., Guiot, F., Optiz, J.M. & Reynolds, J.F. 1988. Isolated familial adrenocorticotropin deficiency: prenatal diagnosis by maternal plasma estriol assay. *American Journal of Medical Genetics Part A.* 29 (1). pp. 125-130.

Mannini, L., Cucco, F., Quarantotti, V., Amato, C., Tinti, M., Tana, L., Frattini, A., Delia, D., Krantz, I.D., Jessberger, R. & Musio, A. 2015. SMC1B is present in mammalian somatic cells and interacts with mitotic cohesin proteins. *Scientific reports.* 5 pp. 18472.

Mantovani, A., Allavena, P., Sica, A. & Balkwill, F. 2008. Cancer-related inflammation. *Nature.* 454 (7203). pp. 436-444.

Marchand, M., Van Baren, N., Weynants, P., Brichard, V., Dréno, B., Tessier, M., Rankin, E., Parmiani, G., Arienti, F. & Humblet, Y. 1999. Tumor regressions observed in patients with metastatic melanoma treated with an antigenic peptide encoded by gene MAGE-3 and presented by HLA-A1. *International Journal of Cancer.* 80 (2). pp. 219-230.

Marchand, M., Punt, C., Aamdal, S., Escudier, B., Kruit, W., Keilholz, U., Håkansson, L., van Baren, N., Humblet, Y. & Mulders, P. 2003. Immunisation of metastatic cancer patients with MAGE-3 protein combined with adjuvant SBAS-2: a clinical report. *European journal of cancer.* 39 (1). pp. 70-77.

Martín-López, J.V. & Fishel, R. 2013. The mechanism of mismatch repair and the functional analysis of mismatch repair defects in Lynch syndrome. *Familial cancer.* 12 (2). pp. 159-168.

Massagué, J. & Obenauf, A.C. 2016. Metastatic colonization by circulating tumour cells. *Nature.* 529 (7586). pp. 298-306.

Mazurek, S. 2011. Pyruvate kinase type M2: a key regulator of the metabolic budget system in tumor cells. *The international journal of biochemistry & cell biology.* 43 (7). pp. 969-980.

McFadden, K. & Luftig, M.A. 2013. Interplay between DNA tumor viruses and the host DNA damage response. In: *Intrinsic Immunity.* Springer: pp. 229-257.

McFarlane, R.J., Feichtinger, J. & Larcombe, L. 2015. Germline/meiotic genes in cancer: new dimensions. *Cell cycle (Georgetown, Tex.).* 14 (6). pp. 791-792.

McGuire, A., Brown, J.A. & Kerin, M.J. 2015. Metastatic breast cancer: the potential of miRNA for diagnosis and treatment monitoring. *Cancer and metastasis reviews.* 34 (1). pp. 145-155.

Melero, I., Gaudernack, G., Gerritsen, W., Huber, C., Parmiani, G., Scholl, S., Thatcher, N., Wagstaff, J., Zielinski, C. & Faulkner, I. 2014. Therapeutic vaccines for cancer: an overview of clinical trials. *Nature reviews Clinical oncology.* 11 (9). pp. 509-524.

Menendez, L., Walker, D., Matyunina, L.V., Dickerson, E.B., Bowen, N.J., Polavarapu, N., Benigno, B.B. & McDonald, J.F. 2007. Identification of candidate methylation-responsive genes in ovarian cancer. *Molecular cancer.* 6 (1). pp. 1.

Menez-Jamet, J., Gallou, C., Rougeot, A. & Kosmatopoulos, K. 2016. Optimized tumor cryptic peptides: the basis for universal neo-antigen-like tumor vaccines. *Annals of Translational Medicine.*

Mesri, E.A., Feitelson, M.A. & Munger, K. 2014. Human viral oncogenesis: a cancer hallmarks analysis. *Cell host & microbe.* 15 (3). pp. 266-282.

Messerschmidt, D.M., Knowles, B.B. & Solter, D. 2014. DNA methylation dynamics during epigenetic reprogramming in the germline and preimplantation embryos. *Genes & development.* 28 (8). pp. 812-828.

Mikelsaar, R., Nelis, M., Kurg, A., Žilina, O., Korrovits, P., Rätsep, R. & Väli, M. 2012. Balanced reciprocal translocation t (5; 13)(q33; q12) and 9q31. 1 microduplication in a man suffering from infertility and pollinosis. *Journal of Applied Genetics.* 53 (1). pp. 93-97.

Mittal, D., Gubin, M.M., Schreiber, R.D. & Smyth, M.J. 2014. New insights into cancer immunoediting and its three component phases—elimination, equilibrium and escape. *Current opinion in immunology.* 27 pp. 16-25.

Miyamoto, T., Sengoku, K., Hasuike, S., Takuma, N., Hayashi, H., Yamashita, T. & Ishikawa, M. 2003. Isolation and expression analysis of the human testis-specific gene, SPERGEN-1, a spermatogenic cell-specific gene-1. *Journal of assisted reproduction and genetics.* 20 (2). pp. 101-104.

Mobasheri, M.B., Shirkoohi, R., Zendehdel, K., Jahanzad, I., Talebi, S., Afsharpad, M. & Modarressi, M.H. 2015. Transcriptome analysis of the cancer/testis genes, DAZ1, AURKC, and TEX101, in breast tumors and six breast cancer cell lines. *Tumor Biology.* 36 (10). pp. 8201-8206.

Mohan, S. & Baylink, D.J. 2002. IGF-binding proteins are multifunctional and act via IGF-dependent and -independent mechanisms. *The Journal of endocrinology.* 175 (1). pp. 19-31.

Molania, R., Mahjoubi, F., Mirzaei, R., Khatami, S. & Mahjoubi, B. 2014. A Panel of Cancer Testis Antigens and Clinical Risk Factors to Predict Metastasis in Colorectal Cancer. *Journal of biomarkers.* 2014.

Morgan, R.A., Chinnasamy, N., Abate-Daga, D., Gros, A., Robbins, P.F., Zheng, Z., Dudley, M.E., Feldman, S.A., Yang, J.C., Sherry, R.M., Phan, G.Q., Hughes, M.S., Kammula, U.S., Miller, A.D., Hessman, C.J., Stewart, A.A., Restifo, N.P., Quezado, M.M., Alimchandani, M., Rosenberg, A.Z., Nath, A., Wang, T., Bielekova, B., Wuest, S.C., Akula, N., McMahon, F.J., Wilde, S., Mosetter, B., Schendel, D.J., Laurencot, C.M. & Rosenberg, S.A. 2013. Cancer regression and neurological toxicity following anti-MAGE-A3 TCR gene therapy. *Journal of immunotherapy (Hagerstown, Md.: 1997).* 36 (2). pp. 133-151.

Mueller, J.L., Mahadevaiah, S.K., Park, P.J., Warburton, P.E., Page, D.C. & Turner, J.M. 2008. The mouse X chromosome is enriched for multicopy testis genes showing postmeiotic expression. *Nature genetics.* 40 (6). pp. 794-799.

Muller, P.A., Vousden, K.H. & Norman, J.C. 2011. P53 and its Mutants in Tumor Cell Migration and Invasion. *The Journal of cell biology.* 192 (2). pp. 209-218.

Muto, M., Fujihara, Y., Tobita, T., Kiyozumi, D. & Ikawa, M. 2016. Lentiviral Vector-Mediated Complementation Restored Fetal Viability but Not Placental Hyperplasia in Plac1-Deficient Mice. *Biology of reproduction.* 94 (1). pp. 6.

Naiche, L., Harrelson, Z., Kelly, R.G. & Papaioannou, V.E. 2005. T-box genes in vertebrate development. *Annu.Rev.Genet.* 39 pp. 219-239.

Naiche, L., Harrelson, Z., Kelly, R.G. & Papaioannou, V.E. 2005b. T-box genes in vertebrate development. *Annu.Rev.Genet.* 39 pp. 219-239.

Navarro, A., Tejero, R., Vinolas, N., Cordeiro, A., Marrades, R.M., Fuster, D., Caritg, O., Moises, J., Munoz, C., Molins, L., Ramirez, J. & Monzo, M. 2015. The significance of PIWI family expression in human lung embryogenesis and non-small cell lung cancer. *Oncotarget.* 6 (31). pp. 31544-31556.

Negrini, S., Gorgoulis, V.G. & Halazonetis, T.D. 2010. Genomic instability—an evolving hallmark of cancer. *Nature reviews Molecular cell biology.* 11 (3). pp. 220-228.

Nesrua, F.O., Atuaolcl, S., GILLIE, M., SUNZ, Y. & Gimasr, S. 1998. Vaccination of melanoma patients with peptide-or tumor lysate-pulsed dendritic cells. *Peptides.* 1 pp. A2.

Newick, K., Moon, E. & Albelda, S.M. 2016. Chimeric antigen receptor T-cell therapy for solid tumors. *Molecular therapy oncolytics.* 3 pp. 16006.

Nibu, Y., Jose-Edwards, D.S. & Di Gregorio, A. 2013. From notochord formation to hereditary chordoma: the many roles of Brachyury. *BioMed research international.* 2013 pp. 826435.

Nielsen, A.Y. & Gjerstorff, M.F. 2016. Ectopic Expression of Testis Germ Cell Proteins in Cancer and Its Potential Role in Genomic Instability. *International Journal of Molecular Sciences.* 17 (6). pp. 890.

Nikonova, L., Koza, R.A., Mendoza, T., Chao, P.M., Curley, J.P. & Kozak, L.P. 2008. Mesoderm-specific transcript is associated with fat mass expansion in response to a positive energy balance. *FASEB journal : official publication of the Federation of American Societies for Experimental Biology.* 22 (11). pp. 3925-3937.

Nilsson, R., Jain, M., Madhusudhan, N., Sheppard, N.G., Strittmatter, L., Kampf, C., Huang, J., Asplund, A. & Mootha, V.K. 2014. Metabolic enzyme expression highlights a key role for MTHFD2 and the mitochondrial folate pathway in cancer. *Nature communications.* 5.

Nishimura, H., Kim, E., Nakanishi, T. & Baba, T. 2004. Possible function of the ADAM1a/ADAM2 Fertilin complex in the appearance of ADAM3 on the sperm surface. *The Journal of biological chemistry.* 279 (33). pp. 34957-34962.

Nishino, R., Takano, A., Oshita, H., Ishikawa, N., Akiyama, H., Ito, H., Nakayama, H., Miyagi, Y., Tsuchiya, E., Kohno, N., Nakamura, Y. & Daigo, Y. 2011. Identification of Epstein-Barr virus-induced gene 3 as a novel serum and tissue biomarker and a therapeutic target for lung cancer. *Clinical cancer research : an official journal of the American Association for Cancer Research.* 17 (19). pp. 6272-6286.

Nourashrafeddin, S., Ebrahimzadeh-Vesal, R., Miryounesi, M., Aarabi, M., Zarghami, N., Modarressi, M.H. & Nouri, M. 2014a. Analysis of SPATA19 gene expression during male germ cells development, lessons from in vivo and in vitro study. *Cell biology international reports.* 21 (1). pp. 1-7.

Nourashrafeddin, S., Ebrahimzadeh-Vesal, R., Modarressi, M.H., Zekri, A. & Nouri, M. 2014b. Identification of Spata-19 new variant with expression beyond meiotic phase of mouse testis development. *Reports of biochemistry & molecular biology.* 2 (2). pp. 89.

Oji, Y., Tatsumi, N., Fukuda, M., Nakatsuka, S., Aoyagi, S., Hirata, E., Nanchi, I., Fujiki, F., Nakajima, H. & Yamamoto, Y. 2014. The translation elongation factor eEF2 is a novel

tumor-associated antigen overexpressed in various types of cancers. *International journal of oncology.* 44 (5). pp. 1461-1469.

Old, L.J. 2008. Cancer vaccines: an overview. *Cancer immunity.* 8 Suppl 1 pp. 1.

Ordóñez-Mena, J.M., Schöttker, B., Mons, U., Jenab, M., Freisling, H., Bueno-de-Mesquita, B., O'Doherty, M.G., Scott, A., Kee, F. & Stricker, B.H. 2016. Quantification of the smoking-associated cancer risk with rate advancement periods: meta-analysis of individual participant data from cohorts of the CHANCES consortium. *BMC medicine.* 14 (1). pp. 1.

Ouchi, N., Higuchi, A., Ohashi, K., Oshima, Y., Gokce, N., Shibata, R., Akasaki, Y., Shimono, A. & Walsh, K. 2010. Sfrp5 is an anti-inflammatory adipokine that modulates metabolic dysfunction in obesity. *Science (New York, N.Y.).* 329 (5990). pp. 454-457.

Ouimette, J., Jolin, M.L., L'honoré, A., Gifuni, A. & Drouin, J. 2010. Divergent transcriptional activities determine limb identity. *Nature communications.* 1 pp. 35.

Page, D.B., Bourla, A.B., Daniyan, A., Naidoo, J., Smith, E., Smith, M., Friedman, C., Khalil, D.N., Funt, S. & Shoushtari, A.N. 2015. Tumor immunology and cancer immunotherapy: summary of the 2014 SITC primer. *Journal for immunotherapy of cancer.* 3 (1). pp. 1.

Palena, C., Fernando, R.I., Litzinger, M.T., Hamilton, D.H., Huang, B. & Schlom, J. 2011. Strategies to target molecules that control the acquisition of a mesenchymal-like phenotype by carcinoma cells. *Experimental biology and medicine (Maywood, N.J.).* 236 (5). pp. 537-545.

Palena, C., Polev, D.E., Tsang, K.Y., Fernando, R.I., Litzinger, M., Krukovskaya, L.L., Baranova, A.V., Kozlov, A.P. & Schlom, J. 2007. The human T-box mesodermal transcription factor Brachyury is a candidate target for T-cell-mediated cancer immunotherapy. *Clinical cancer research : an official journal of the American Association for Cancer Research.* 13 (8). pp. 2471-2478.

Palena, C., Roselli, M., Litzinger, M.T., Ferroni, P., Costarelli, L., Spila, A., Cavaliere, F., Huang, B., Fernando, R.I., Hamilton, D.H., Jochems, C., Tsang, K.Y., Cheng, Q., Lyerly, H.K., Schlom, J. & Guadagni, F. 2014. Overexpression of the EMT driver brachyury in breast carcinomas: association with poor prognosis. *Journal of the National Cancer Institute.* 106 (5). pp. 10.1093/jnci/dju054.

Palucka, K. & Banchereau, J. 2013. Human dendritic cell subsets in vaccination. *Current opinion in immunology.* 25 (3). pp. 396-402.

Panula, S., Reda, A., Stukenborg, J., Ramathal, C., Sukhwani, M., Albalushi, H., Edsgärd, D., Nakamura, M., Söder, O. & Orwig, K.E. 2016. Over Expression of NANOS3 and DAZL in Human Embryonic Stem Cells. *PloS one.* 11 (10). pp. e0165268.

Papaioannou, V.E. 2001. T-box genes in development: from hydra to humans. *International review of cytology.* 207 pp. 1-70.

Papaioannou, V.E. 2014. The T-box gene family: emerging roles in development, stem cells and cancer. *Development (Cambridge, England).* 141 (20). pp. 3819-3833.

Papavassiliou, K.A. & Papavassiliou, A.G. 2016. Transcription Factor Drug Targets. *Journal of cellular biochemistry.*

Pardoll, D. 2003. Does the immune system see tumors as foreign or self? *Annual Review of Immunology.* 21 (1). pp. 807-839.

Pardoll, D.M. 2012. The blockade of immune checkpoints in cancer immunotherapy. *Nature Reviews Cancer.* 12 (4). pp. 252-264.

Parkin, D. 2011. 2. Tobacco-attributable cancer burden in the UK in 2010. *British journal of cancer.* 105 pp. S6-S13.

Partheen, K., Levan, K., Österberg, L., Claesson, I., Fallenius, G., Sundfeldt, K. & Horvath, G. 2008. Four potential biomarkers as prognostic factors in stage III serous ovarian adenocarcinomas. *International Journal of Cancer.* 123 (9). pp. 2130-2137.

Patel, S. & Ahmed, S. 2015. Emerging field of metabolomics: big promise for cancer biomarker identification and drug discovery. *Journal of pharmaceutical and biomedical analysis.* 107 pp. 63-74.

Paull, T.T. 2015. Mechanisms of ATM activation. *Annual Review of Biochemistry.* 84 pp. 711-738.

Peggs, K.S., Quezada, S.A., Korman, A.J. & Allison, J.P. 2006. Principles and use of anti-CTLA4 antibody in human cancer immunotherapy. *Current opinion in immunology.* 18 (2). pp. 206-213.

Peggs, K.S., Quezada, S.A., Chambers, C.A., Korman, A.J. & Allison, J.P. 2009. Blockade of CTLA-4 on both effector and regulatory T cell compartments contributes to the antitumor activity of anti-CTLA-4 antibodies. *The Journal of experimental medicine.* 206 (8). pp. 1717-1725.

Pennimpede, T., Proske, J., König, A., Vidigal, J.A., Morkel, M., Bramsen, J.B., Herrmann, B.G. & Wittler, L. 2012. In vivo knockdown of Brachyury results in skeletal defects and urorectal malformations resembling caudal regression syndrome. *Developmental biology.* 372 (1). pp. 55-67.

Perez-Moreno, P., Brambilla, E., Thomas, R. & Soria, J.C. 2012. Squamous cell carcinoma of the lung: molecular subtypes and therapeutic opportunities. *Clinical cancer research : an official journal of the American Association for Cancer Research.* 18 (9). pp. 2443-2451.

Perfézou, M., Turner, A. & Merkoçi, A. 2012. Cancer detection using nanoparticle-based sensors. *Chemical Society Reviews.* 41 (7). pp. 2606-2622.

Pichiorri, F., Suh, S., Rocci, A., De Luca, L., Taccioli, C., Santhanam, R., Zhou, W., Benson, D.M., Hofmainster, C. & Alder, H. 2010. Downregulation of p53-inducible microRNAs 192, 194, and 215 impairs the p53/MDM2 autoregulatory loop in multiple myeloma development. *Cancer cell.* 18 (4). pp. 367-381.

Pierce, A., Barron, N., Linehan, R., Ryan, E., O'Driscoll, L., Daly, C. & Clynes, M. 2008. Identification of a novel, functional role for S100A13 in invasive lung cancer cell lines. *European journal of cancer.* 44 (1). pp. 151-159.

Pike, S.T., Rajendra, R., Artzt, K. & Appling, D.R. 2010. Mitochondrial C1-tetrahydrofolate synthase (MTHFD1L) supports the flow of mitochondrial one-carbon units into the methyl cycle in embryos. *The Journal of biological chemistry.* 285 (7). pp. 4612-4620.

Pillay, N., Plagnol, V., Tarpey, P.S., Lobo, S.B., Presneau, N., Szuhai, K., Halai, D., Berisha, F., Cannon, S.R. & Mead, S. 2012. A common single-nucleotide variant in T is strongly associated with chordoma. *Nature genetics.* 44 (11). pp. 1185-1187.

Pinto, F., Campanella, N.C., Abrahao-Machado, L.F., Scapulatempo-Neto, C., de Oliveira, A.T., Brito, M.J., Andrade, R.P., Guimaraes, D.P. & Reis, R.M. 2016a. The embryonic Brachyury transcription factor is a novel biomarker of GIST aggressiveness and poor survival. *Gastric Cancer.* 19 (2). pp. 651-659.

Pinto, F., Pertega-Gomes, N., Pereira, M.S., Vizcaino, J.R., Monteiro, P., Henrique, R.M., Baltazar, F., Andrade, R.P. & Reis, R.M. 2014. T-box transcription factor brachyury is associated with prostate cancer progression and aggressiveness. *Clinical cancer research : an official journal of the American Association for Cancer Research.* 20 (18). pp. 4949-4961.

Pinto, F., Pertega-Gomes, N., Vizcaino, J.R., Andrade, R.P., Carcano, F.M. & Reis, R.M. 2016b. Brachyury as a potential modulator of androgen receptor activity and a key player in therapy resistance in prostate cancer. *Oncotarget.* 7 (20). pp. 28891-28902.

Pires, M.M. & Aaronson, S.A. 2014. Brachyury: a new player in promoting breast cancer aggressiveness. *Journal of the National Cancer Institute.* 106 (5). pp. 10.1093/jnci/dju094.

Polverini, P.J. 1995. The pathophysiology of angiogenesis. *Critical reviews in oral biology and medicine : an official publication of the American Association of Oral Biologists.* 6 (3). pp. 230-247.

Por, E., Byun, H.J., Lee, E.J., Lim, J.H., Jung, S.Y., Park, I., Kim, Y.M., Jeoung, D.I. & Lee, H. 2010. The cancer/testis antigen CAGE with oncogenic potential stimulates cell proliferation by up-regulating cyclins D1 and E in an AP-1- and E2F-dependent manner. *The Journal of biological chemistry.* 285 (19). pp. 14475-14485.

Posey, A.D., Schwab, R.D., Boesteanu, A.C., Steentoft, C., Mandel, U., Engels, B., Stone, J.D., Madsen, T.D., Schreiber, K. & Haines, K.M. 2016. Engineered CAR T Cells targeting the cancer-associated Tn-glycoform of the membrane mucin MUC1 control adenocarcinoma. *Immunity.* 44 (6). pp. 1444-1454.

Pulichino, A.M., Vallette-Kasic, S., Couture, C., Gauthier, Y., Brue, T., David, M., Malpuech, G., Deal, C., Van Vliet, G., De Vroede, M., Riepe, F.G., Partsch, C.J., Sippell, W.G., Berberoglu, M., Atasay, B. & Drouin, J. 2003. Human and mouse TPIT gene mutations cause early onset pituitary ACTH deficiency. *Genes & development.* 17 (6). pp. 711-716.

Qin, X., Zhang, W., Zou, L., Huang, P. & Sun, B. 2016. Identification potential biomarkers in pulmonary tuberculosis and latent infection based on bioinformatics analysis. *BMC Infectious Diseases.* 16 (1). pp. 500.

Rajagopalan, K., Mooney, S.M., Parekh, N., Getzenberg, R.H. & Kulkarni, P. 2011. A majority of the cancer/testis antigens are intrinsically disordered proteins. *Journal of cellular biochemistry.* 112 (11). pp. 3256-3267.

Ranzani, M., Annunziato, S., Adams, D.J. & Montini, E. 2013. Cancer gene discovery: exploiting insertional mutagenesis. *Molecular cancer research : MCR.* 11 (10). pp. 1141-1158.

Rashvand, Z., Heidari, M., Raoofian, R., Modarresi, M.H. & Shirkoohi, R. 2013. Induction of Apoptosis and Growth Suppression by Homeobox Gene TGIFLX in Prostate Cancer Cell Line Lncap. *Iranian journal of public health.* 42 (11). pp. 1242.

Rauch, T. & Pfeifer, G.P. 2005. Methylated-CpG island recovery assay: a new technique for the rapid detection of methylated-CpG islands in cancer. *Laboratory Investigation.* 85 (9). pp. 1172-1180.

Rauch, T., Li, H., Wu, X. & Pfeifer, G.P. 2006. MIRA-assisted microarray analysis, a new technology for the determination of DNA methylation patterns, identifies frequent methylation of homeodomain-containing genes in lung cancer cells. *Cancer research.* 66 (16). pp. 7939-7947.

Ren, B., Wei, X., Zou, G., He, J., Xu, G., Xu, F., Huang, Y., Zhu, H., Li, Y. & Ma, G. 2016. Cancer testis antigen SPAG9 is a promising marker for the diagnosis and treatment of lung cancer. *Oncology reports.* 35 (5). pp. 2599-2605.

Riebler, A., Menigatti, M., Song, J.Z., Statham, A.L., Stirzaker, C., Mahmud, N., Mein, C.A., Clark, S.J. & Robinson, M.D. 2014. BayMeth: improved DNA methylation quantification for affinity capture sequencing data using a flexible Bayesian approach. *Genome biology.* 15 (2). pp. 1.

Rivera, E. & Gomez, H. 2010. Chemotherapy resistance in metastatic breast cancer: the evolving role of ixabepilone. *Breast Cancer Research.* 12 (2). pp. 1.

Rosa, A.M., Dabas, N., Byrnes, D.M., Eller, M.S. & Grichnik, J.M. 2012. Germ cell proteins in melanoma: prognosis, diagnosis, treatment, and theories on expression. *Journal of skin cancer.* 2012 pp. 621968.

Roselli, M., Fernando, R.I., Guadagni, F., Spila, A., Alessandroni, J., Palmirotta, R., Costarelli, L., Litzinger, M., Hamilton, D., Huang, B., Tucker, J., Tsang, K.Y., Schlom, J. & Palena, C. 2012. Brachyury, a driver of the epithelial-mesenchymal transition, is overexpressed in human lung tumors: an opportunity for novel interventions against lung cancer. *Clinical cancer research : an official journal of the American Association for Cancer Research.* 18 (14). pp. 3868-3879.

Rosenberg, S.A. & Restifo, N.P. 2015. Adoptive cell transfer as personalized immunotherapy for human cancer. *Science (New York, N.Y.).* 348 (6230). pp. 62-68.

Ross, M.T., Grafham, D.V., Coffey, A.J., Scherer, S., McLay, K., Muzny, D., Platzer, M., Howell, G.R., Burrows, C. & Bird, C.P. 2005. The DNA sequence of the human X chromosome. *Nature.* 434 (7031). pp. 325-337.

Rousseaux, S., Debernardi, A., Jacquiau, B., Vitte, A.L., Vesin, A., Nagy-Mignotte, H., Moro-Sibilot, D., Brichon, P.Y., Lantuejoul, S., Hainaut, P., Laffaire, J., de Reynies, A., Beer, D.G., Timsit, J.F., Brambilla, C., Brambilla, E. & Khochbin, S. 2013. Ectopic activation of germline and placental genes identifies aggressive metastasis-prone lung cancers. *Science translational medicine.* 5 (186). pp. 186ra66.

RUGGIU, M., SAUNDERS, P.T. & COOKE, H.J. 2000. Dynamic subcellular distribution of the DAZL protein is confined to primate male germ cells. *Journal of andrology.* 21 (3). pp. 470-477.

Ruiz, A., Pujana, M.A. & Estivill, X. 2000. Isolation and characterisation of a novel human gene (C9orf11) on chromosome 9p21, a region frequently deleted in human cancer. *Biochimica et Biophysica Acta (BBA)-Gene Structure and Expression.* 1517 (1). pp. 128-134.

Sahin, U., Tureci, O., Schmitt, H., Cochlovius, B., Johannes, T., Schmits, R., Stenner, F., Luo, G., Schobert, I. & Pfreundschuh, M. 1995. Human neoplasms elicit multiple specific immune responses in the autologous host. *Proceedings of the National Academy of Sciences of the United States of America.* 92 (25). pp. 11810-11813.

Sakai, M., Shimokawa, T., Kobayashi, T., Matsushima, S., Yamada, Y., Nakamura, Y. & Furukawa, Y. 2006. Elevated expression of C10orf3 (chromosome 10 open reading frame 3) is involved in the growth of human colon tumor. *Oncogene.* 25 (3). pp. 480-486.

Sammut, S.J., Feichtinger, J., Stuart, N., Wakeman, J.A., Larcombe, L. & McFarlane, R.J. 2014. A novel cohort of cancer-testis biomarker genes revealed through meta-analysis of clinical data sets. *Oncoscience.* 1 (5). pp. 349-359.

Sandoval, J. & Esteller, M. 2012. Cancer epigenomics: beyond genomics. *Current opinion in genetics & development.* 22 (1). pp. 50-55.

Santel, A. & Fuller, M.T. 2001. Control of mitochondrial morphology by a human mitofusin. *Journal of cell science.* 114 (Pt 5). pp. 867-874.

Satoh, N., Tagawa, K. & Takahashi, H. 2012. How was the notochord born? *Evolution & development.* 14 (1). pp. 56-75.

Satyanarayana, A. & Kaldis, P. 2009. Mammalian cell-cycle regulation: several Cdks, numerous cyclins and diverse compensatory mechanisms. *Oncogene.* 28 (33). pp. 2925-2939.

Scanlan, M.J., Gout, I., Gordon, C.M., Williamson, B., Stockert, E., Gure, A.O., Jäger, D., Chen, Y., Mackay, A. & O'Hare, M.J. 2001. Humoral immunity to human breast cancer: antigen definition and quantitative analysis of mRNA expression. *Cancer Immunity Archive.* 1 (1). pp. 4.

Scanlan, M.J., Simpson, A.J. & Old, L.J. 2004. The cancer/testis genes: review, standardization, and commentary. *Cancer Immunity Archive.* 4 (1). pp. 1.

Scanlan, M.J., Gure, A.O., Jungbluth, A.A., Old, L.J. & Chen, Y.T. 2002. Cancer/testis antigens: an expanding family of targets for cancer immunotherapy. *Immunological reviews.* 188 pp. 22-32.

Schrans-Stassen, B.H., Saunders, P.T., Cooke, H.J. & de Rooij, D.G. 2001. Nature of the spermatogenic arrest in Dazl -/- mice. *Biology of reproduction.* 65 (3). pp. 771-776.

Secretan, B., Straif, K., Baan, R., Grosse, Y., El Ghissassi, F., Bouvard, V., Benbrahim-Tallaa, L., Guha, N., Freeman, C. & Galichet, L. 2009. A review of human carcinogens—Part E: tobacco, areca nut, alcohol, coal smoke, and salted fish. *The lancet oncology.* 10 (11). pp. 1033-1034.

Seguin, L., Desgrosellier, J.S., Weis, S.M. & Cheresh, D.A. 2015. Integrins and cancer: regulators of cancer stemness, metastasis, and drug resistance. *Trends in cell biology.* 25 (4). pp. 234-240.

Sharma, P., Gnjatic, S., Jungbluth, A.A., Williamson, B., Herr, H., Stockert, E., Dalbagni, G., Donat, S.M., Reuter, V.E. & Santiago, D. 2003. Frequency of NY-ESO-1 and LAGE-1

expression in bladder cancer and evidence of a new NY-ESO-1 T-cell epitope in a patient with bladder cancer. *Cancer Immunity Archive.* 3 (1). pp. 19.

Sharma, S., Kelly, T.K. & Jones, P.A. 2010. Epigenetics in cancer. *Carcinogenesis.* 31 (1). pp. 27-36.

Shay, J.W. & Wright, W.E. 2000. Hayflick, his limit, and cellular ageing. *Nature reviews Molecular cell biology.* 1 (1). pp. 72-76.

Shen, H. & Laird, P.W. 2013. Interplay between the cancer genome and epigenome. *Cell.* 153 (1). pp. 38-55.

Shenoy, N., Vallumsetla, N., Zou, Y., Galeas, J.N., Shrivastava, M., Hu, C., Susztak, K. & Verma, A. 2015. Role of DNA methylation in renal cell carcinoma. *Journal of hematology & oncology.* 8 (1). pp. 1.

Shi, Y., Zhang, L., Song, S., Teves, M., Li, H., Wang, Z., Hess, R., Jiang, G. & Zhang, Z. 2013. The mouse transcription factor-like 5 gene encodes a protein localized in the manchette and centriole of the elongating spermatid. *Andrology.* 1 (3). pp. 431-439.

Shiloh, Y. 2014. ATM: Expanding roles as a chief guardian of genome stability. *Experimental cell research.* 329 (1). pp. 154-161.

Shiloh, Y. & Ziv, Y. 2013. The ATM protein kinase: regulating the cellular response to genotoxic stress, and more. *Nature reviews Molecular cell biology.* 14 (4). pp. 197-210.

Shimamatsu, S., Okamoto, T., Haro, A., Kitahara, H., Kohno, M., Morodomi, Y., Tagawa, T., Okano, S., Oda, Y. & Maehara, Y. 2016. Prognostic Significance of Expression of the Epithelial-Mesenchymal Transition-Related Factor Brachyury in Intrathoracic Lymphatic Spread of Non-Small Cell Lung Cancer. *Annals of surgical oncology.* 23 (5). pp. 1012-1020.

Shimoda, M., Sugiura, T., Imajyo, I., Ishii, K., Chigita, S., Seki, K., Kobayashi, Y. & Shirasuna, K. 2012. The T-box transcription factor Brachyury regulates epithelial–mesenchymal transition in association with cancer stem-like cells in adenoid cystic carcinoma cells. *BMC cancer.* 12 (1). pp. 377.

Shiraishi, T., Terada, N., Zeng, Y., Suyama, T., Luo, J., Trock, B., Kulkarni, P. & Getzenberg, R.H. 2011. Cancer/testis antigens as potential predictors of biochemical recurrence of prostate cancer following radical prostatectomy. *Journal of translational medicine.* 9 (1). pp. 1.

Showell, C., Binder, O. & Conlon, F.L. 2004. T-box genes in early embryogenesis. *Developmental Dynamics.* 229 (1). pp. 201-218.

Siegel, R.L., Miller, K.D. & Jemal, A. 2016. Cancer statistics, 2016. *CA: a cancer journal for clinicians.* 66 (1). pp. 7-30.

Siep, M., Sleddens-Linkels, E., Mulders, S., van Eenennaam, H., Wassenaar, E., Van Cappellen, W.A., Hoogerbrugge, J., Grootegoed, J.A. & Baarends, W.M. 2004. Basic helix-loop-helix transcription factor Tcfl5 interacts with the Calmegin gene promoter in mouse spermatogenesis. *Nucleic acids research.* 32 (21). pp. 6425-6436.

Sigalotti, L., Coral, S., Altomonte, M., Natali, L., Gaudino, G., Cacciotti, P., Libener, R., Colizzi, F., Vianale, G. & Martini, F. 2002. Cancer testis antigens expression in mesothelioma: role of DNA methylation and bioimmunotherapeutic implications. *British journal of cancer.* 86 (6). pp. 979-982.

Sigalotti, L., Fratta, E., Coral, S., Cortini, E., Covre, A., Nicolay, H.J., Anzalone, L., Pezzani, L., Di Giacomo, A.M. & Fonsatti, E. 2007. Epigenetic drugs as pleiotropic agents in cancer treatment: biomolecular aspects and clinical applications. *Journal of cellular physiology.* 212 (2). pp. 330-344.

Silva, W.A.,Jr, Gnjatic, S., Ritter, E., Chua, R., Cohen, T., Hsu, M., Jungbluth, A.A., Altorki, N.K., Chen, Y.T., Old, L.J., Simpson, A.J. & Caballero, O.L. 2007. PLAC1, a trophoblast-specific cell surface protein, is expressed in a range of human tumors and elicits spontaneous antibody responses. *Cancer immunity.* 7 pp. 18.

Silveira, V.S., Scrideli, C.A., Moreno, D.A., Yunes, J.A., Queiroz, R.G., Toledo, S.C., Lee, M.L.M., Petrilli, A.S., Brandalise, S.R. & Tone, L.G. 2013. Gene expression pattern contributing to prognostic factors in childhood acute lymphoblastic leukemia. *Leukemia & lymphoma.* 54 (2). pp. 310-314.

Simpson, A.J., Caballero, O.L., Jungbluth, A., Chen, Y. & Old, L.J. 2005. Cancer/testis antigens, gametogenesis and cancer. *Nature Reviews Cancer.* 5 (8). pp. 615-625.

Smorag, L., Xu, X., Engel, W. & Pantakani, D. 2014. The roles of DAZL in RNA biology and development. *Wiley Interdisciplinary Reviews: RNA.* 5 (4). pp. 527-535.

Smyth, M.J., Yagita, H. & McArthur, G.A. 2016. Combination Anti-CTLA-4 and Anti-RANKL in Metastatic Melanoma. *Journal of clinical oncology : official journal of the American Society of Clinical Oncology.* 34 (12). pp. e104-6.

Sousa, F.G., Matuo, R., Tang, S., Rajapakse, V.N., Luna, A., Sander, C., Varma, S., Simon, P.H., Doroshow, J.H. & Reinhold, W.C. 2015. Alterations of DNA repair genes in the NCI-60 cell lines and their predictive value for anticancer drug activity. *DNA repair.* 28 pp. 107-115.

Stanton, P.G. 2016. Regulation of the blood-testis barrier. *Seminars in Cell & Developmental Biology.* Elsevier: .

Stockert, E., Jager, E., Chen, Y.T., Scanlan, M.J., Gout, I., Karbach, J., Arand, M., Knuth, A. & Old, L.J. 1998. A survey of the humoral immune response of cancer patients to a panel of human tumor antigens. *The Journal of experimental medicine.* 187 (8). pp. 1349-1354.

Stoller, J.Z. & Epstein, J.A. 2005. Identification of a novel nuclear localization signal in Tbx1 that is deleted in DiGeorge syndrome patients harboring the 1223delC mutation. *Human molecular genetics.* 14 (7). pp. 885-892.

Strahl, B.D. & Allis, C.D. 2000. The language of covalent histone modifications. *Nature.* 403 (6765). pp. 41-45.

Strunnikov, A. 2013. Cohesin complexes with a potential to link mammalian meiosis to cancer. *Cell Regeneration.* 2 (1). pp. 1.

Sugimoto, K., Kage, H., Aki, N., Sano, A., Kitagawa, H., Nagase, T., Yatomi, Y., Ohishi, N. & Takai, D. 2007. The induction of H3K9 methylation by PIWIL4 at the p16 Ink4a locus. *Biochemical and biophysical research communications.* 359 (3). pp. 497-502.

Sun, X., Hornicek, F. & Schwab, J.H. 2015. Chordoma: an update on the pathophysiology and molecular mechanisms. *Current reviews in musculoskeletal medicine.* 8 (4). pp. 344-352.

Suri, A. 2006. Cancer testis antigens–their importance in immunotherapy and in the early detection of cancer. *Expert opinion on biological therapy.* 6 (4). pp. 379-389.

Suri, A., Jagadish, N., Saini, S. & Gupta, N. 2015. Targeting cancer testis antigens for biomarkers and immunotherapy in colorectal cancer: Current status and challenges. *World journal of gastrointestinal oncology.* 7 (12). pp. 492.

Suzuki-Toyota, F., Ito, C., Toyama, Y., Maekawa, M., Yao, R., Noda, T., Iida, H. & Toshimori, K. 2007. Factors maintaining normal sperm tail structure during epididymal maturation studied in Gopc-/- mice. *Biology of reproduction.* 77 (1). pp. 71-82.

Tachibana, M., Sugimoto, K., Nozaki, M., Ueda, J., Ohta, T., Ohki, M., Fukuda, M., Takeda, N., Niida, H., Kato, H. & Shinkai, Y. 2002. G9a histone methyltransferase plays a dominant role in euchromatic histone H3 lysine 9 methylation and is essential for early embryogenesis. *Genes & development.* 16 (14). pp. 1779-1791.

Tachibana, M., Ueda, J., Fukuda, M., Takeda, N., Ohta, T., Iwanari, H., Sakihama, T., Kodama, T., Hamakubo, T. & Shinkai, Y. 2005. Histone methyltransferases G9a and GLP form heteromeric complexes and are both crucial for methylation of euchromatin at H3-K9. *Genes & development.* 19 (7). pp. 815-826.

Tagliamonte, M., Petrizzo, A., Tornesello, M.L., Buonaguro, F.M. & Buonaguro, L. 2014. Antigen-specific vaccines for cancer treatment. *Human vaccines & immunotherapeutics.* 10 (11). pp. 3332-3346.

Takahashi, M., Kamei, Y. & Ezaki, O. 2005. Mest/Peg1 imprinted gene enlarges adipocytes and is a marker of adipocyte size. *American journal of physiology.Endocrinology and metabolism.* 288 (1). pp. E117-24.

Tao, J., Zhi, X., Tian, Y., Li, Z., Zhu, Y., Wang, W., Xie, K., Tang, J., Zhang, X. & Wang, L. 2014. CEP55 contributes to human gastric carcinoma by regulating cell proliferation. *Tumor Biology.* 35 (5). pp. 4389-4399.

Tarnowski, M., Czerewaty, M., Deskur, A., Safranow, K., Marlicz, W., Urasińska, E., Ratajczak, M.Z. & Starzyńska, T. 2016. Expression of Cancer Testis Antigens in Colorectal Cancer: New Prognostic and Therapeutic Implications. *Disease markers.* 2016.

Tchabo, N.E., Mhawech-Fauceglia, P., Caballero, O.L., Villella, J., Beck, A.F., Miliotto, A.J., Liao, J., Andrews, C., Lele, S., Old, L.J. & Odunsi, K. 2009. Expression and serum immunoreactivity of developmentally restricted differentiation antigens in epithelial ovarian cancer. *Cancer immunity.* 9 pp. 6.

Thoma, C.R., Toso, A., Meraldi, P. & Krek, W. 2011. Mechanisms of aneuploidy and its suppression by tumour suppressor proteins. *Swiss medical weekly.* 141 pp. w13170.

thor Straten, P. & Garrido, F. 2016. Targetless T cells in cancer immunotherapy. *Journal for immunotherapy of cancer.* 4 (1). pp. 1.

Topalian, S.L. & Sharpe, A.H. 2014. Balance and imbalance in the immune system: life on the edge. *Immunity.* 41 (5). pp. 682-684.

Torre, L.A., Bray, F., Siegel, R.L., Ferlay, J., Lortet-Tieulent, J. & Jemal, A. 2015. Global cancer statistics, 2012. *CA: a cancer journal for clinicians.* 65 (2). pp. 87-108.

Tsai, J., Chong, I., Chen, Y., Yang, M., Sheu, C., Chang, H., Hwang, J., Hung, J. & Lin, S. 2007. Differential expression profile of MAGE family in non-small-cell lung cancer. *Lung Cancer.* 56 (2). pp. 185-192.

Tureci, O., Sahin, U., Koslowski, M., Buss, B., Bell, C., Ballweber, P., Zwick, C., Eberle, T., Zuber, M. & Villena-Heinsen, C. 2002. A novel tumour associated leucine zipper protein targeting to sites of gene transcription and splicing. *ONCOGENE-BASINGSTOKE-.* 21 pp. 3879-3888.

TUreci, O., Chen, Y., Sahin, U., GUre, A.O., Zwick, C., Villena, C., Tsang, S., Seitz, G., Old, L. & Pfreundschuh, M. 1998. Expression of SSX genes in human tumors. *International Journal of Cancer.* 77 (1). pp. 19-23.

Valastyan, S. & Weinberg, R.A. 2011. Tumor metastasis: molecular insights and evolving paradigms. *Cell.* 147 (2). pp. 275-292.

Vander Heiden, M.G., Cantley, L.C. & Thompson, C.B. 2009. Understanding the Warburg effect: the metabolic requirements of cell proliferation. *Science (New York, N.Y.).* 324 (5930). pp. 1029-1033.

Varela-Rohena, A., Carpenito, C., Perez, E.E., Richardson, M., Parry, R.V., Milone, M., Scholler, J., Hao, X., Mexas, A. & Carroll, R.G. 2008. Genetic engineering of T cells for adoptive immunotherapy. *Immunologic research.* 42 (1-3). pp. 166-181.

Veeck, J., Geisler, C., Noetzel, E., Alkaya, S., Hartmann, A., Knuchel, R. & Dahl, E. 2008. Epigenetic inactivation of the secreted frizzled-related protein-5 (SFRP5) gene in human breast cancer is associated with unfavorable prognosis. *Carcinogenesis.* 29 (5). pp. 991-998.

Vigneron, N. 2015. Human tumor antigens and cancer immunotherapy. *BioMed research international.* 2015.

Viphakone, N., Cumberbatch, M.G., Livingstone, M.J., Heath, P.R., Dickman, M.J., Catto, J.W. & Wilson, S.A. 2015. Luzp4 defines a new mRNA export pathway in cancer cells. *Nucleic acids research.* 43 (4). pp. 2353-2366.

Vogelstein, B., Papadopoulos, N., Velculescu, V.E., Zhou, S., Diaz, L.A.,Jr & Kinzler, K.W. 2013. Cancer genome landscapes. *Science (New York, N.Y.).* 339 (6127). pp. 1546-1558.

Wang, D., Wang, Z., Wang, L., Song, Y. & Zhang, G. 2013. Overexpression of hiwi promotes growth of human breast cancer cells. *Asian Pacific journal of cancer prevention: APJCP.* 15 (18). pp. 7553-7558.

Wang, J.Y., Lan, J., Zhao, J., Chen, L. & Liu, Y. 2012. Molecular characterization, polymorphism and association of porcine SPATA19 gene. *Molecular biology reports.* 39 (10). pp. 9741-9746.

Wang, X., Baddoo, M.C. & Yin, Q. 2014. The placental specific gene, PLAC1, is induced by the Epstein-Barr virus and is expressed in human tumor cells. *Virology journal.* 11 (1). pp. 1.

Wang, X., Tong, X., Gao, H., Yan, X., Xu, X., Sun, S., Wang, Q. & Wang, J. 2014a. Silencing HIWI suppresses the growth, invasion and migration of glioma cells. *International journal of oncology.* 45 (6). pp. 2385-2392.

Wang, Y., Jin, T., Dai, X. & Xu, J. 2016. Lentivirus-mediated knockdown of CEP55 suppresses cell proliferation of breast cancer cells. *Bioscience trends.* (0).

Wang, C., Thudium, K.B., Han, M., Wang, X.T., Huang, H., Feingersh, D., Garcia, C., Wu, Y., Kuhne, M., Srinivasan, M., Singh, S., Wong, S., Garner, N., Leblanc, H., Bunch, R.T., Blanset, D., Selby, M.J. & Korman, A.J. 2014b. In vitro characterization of the anti-PD-1 antibody nivolumab, BMS-936558, and in vivo toxicology in non-human primates. *Cancer immunology research.* 2 (9). pp. 846-856.

Wang, K., Sturt-Gillespie, B., Hittle, J.C., Macdonald, D., Chan, G.K., Yen, T.J. & Liu, S.T. 2014c. Thyroid hormone receptor interacting protein 13 (TRIP13) AAA-ATPase is a novel mitotic checkpoint-silencing protein. *The Journal of biological chemistry.* 289 (34). pp. 23928-23937.

Wansleben, S., Peres, J., Hare, S., Goding, C.R. & Prince, S. 2014. T-box transcription factors in cancer biology. *Biochimica et Biophysica Acta (BBA)-Reviews on Cancer.* 1846 (2). pp. 380-391.

Warfel, N.A. & El-Deiry, W.S. 2013. p21WAF1 and tumourigenesis: 20 years after. *Current opinion in oncology.* 25 (1). pp. 52-58.

Weber, J., Salgaller, M., Samid, D., Johnson, B., Herlyn, M., Lassam, N., Treisman, J. & Rosenberg, S.A. 1994. Expression of the MAGE-1 tumor antigen is up-regulated by the demethylating agent 5-aza-2'-deoxycytidine. *Cancer research.* 54 (7). pp. 1766-1771.

Weiner, G.J. 2015. Building better monoclonal antibody-based therapeutics. *Nature Reviews Cancer.* 15 (6). pp. 361-370.

Weitzman, M.D. & Weitzman, J.B. 2014. What's the damage? The impact of pathogens on pathways that maintain host genome integrity. *Cell host & microbe.* 15 (3). pp. 283-294.

Wen, J., Li, H., Tao, W., Savoldo, B., Foglesong, J.A., King, L.C., Zu, Y. & Chang, C. 2014. High throughput quantitative reverse transcription PCR assays revealing over-expression of cancer testis antigen genes in multiple myeloma stem cell-like side population cells. *British journal of haematology.* 166 (5). pp. 711-719.

Weon, J.L. & Potts, P.R. 2015. The MAGE protein family and cancer. *Current opinion in cell biology.* 37 pp. 1-8.

Whitehurst, A.W. 2014. Cause and consequence of cancer/testis antigen activation in cancer. *Annual Review of Pharmacology and Toxicology.* 54 pp. 251-272.

Whitehurst, A.W., Bodemann, B.O., Cardenas, J., Ferguson, D., Girard, L., Peyton, M., Minna, J.D., Michnoff, C., Hao, W. & Roth, M.G. 2007. Synthetic lethal screen identification of chemosensitizer loci in cancer cells. *Nature.* 446 (7137). pp. 815-819.

Wilson, V. & Conlon, F.L. 2002. The T-box family. *Genome biology.* 3 (6). pp. 1.

Winkler, G.S. 2010. The mammalian anti-proliferative BTG/Tob protein family. *Journal of cellular physiology.* 222 (1). pp. 66-72.

Wischnewski, F., Pantel, K. & Schwarzenbach, H. 2006. Promoter demethylation and histone acetylation mediate gene expression of MAGE-A1, -A2, -A3, and -A12 in human cancer cells. *Molecular cancer research : MCR.* 4 (5). pp. 339-349.

Wu, G., Liu, H., He, H., Wang, Y., Lu, X., Yu, Y., Xia, S., Meng, X. & Liu, Y. 2014a. miR-372 down-regulates the oncogene ATAD2 to influence hepatocellular carcinoma proliferation and metastasis. *BMC cancer.* 14 (1). pp. 1.

Wu, G., Lu, X., Wang, Y., He, H., Meng, X., Xia, S., Zhen, K. & Liu, Y. 2014b. Epigenetic high regulation of ATAD2 regulates the Hh pathway in human hepatocellular carcinoma. *International journal of oncology.* 45 (1). pp. 351-361.

Wu, L. & Qu, X. 2015. Cancer biomarker detection: recent achievements and challenges. *Chemical Society Reviews.* 44 (10). pp. 2963-2997.

Xia, J., Jia, P., Hutchinson, K.E., Dahlman, K.B., Johnson, D., Sosman, J., Pao, W. & Zhao, Z. 2014. A meta-analysis of somatic mutations from next generation sequencing of 241 melanomas: a road map for the study of genes with potential clinical relevance. *Molecular cancer therapeutics.* 13 (7). pp. 1918-1928.

Xie, C., Fu, L., Liu, N. & Li, Q. 2014. Overexpression of SPAG9 correlates with poor prognosis and tumor progression in hepatocellular carcinoma. *Tumor Biology.* 35 (8). pp. 7685-7691.

Xue, Y., Hou, S., Ji, H. & Han, X. 2016. Evolution from genetics to phenotype: reinterpretation of NSCLC plasticity, heterogeneity, and drug resistance. *Protein & Cell.* pp. 1-13.

Yang, Q., Ying, K., Yuan, H., Chen, J., Meng, X., Wang, Z., Xie, Y. & Mao, Y. 2002. Cloning and expression of a novel human galectin cDNA, predominantly expressed in placenta. *Biochimica et Biophysica Acta (BBA)-Gene Structure and Expression.* 1574 (3). pp. 407-411.

Yang, X.R., Ng, D., Alcorta, D.A., Liebsch, N.J., Sheridan, E., Li, S., Goldstein, A.M., Parry, D.M. & Kelley, M.J. 2009. T (brachyury) gene duplication confers major susceptibility to familial chordoma. *Nature genetics.* 41 (11). pp. 1176-1178.

Yang, B., O'Herrin, S.M., Wu, J., Reagan-Shaw, S., Ma, Y., Bhat, K.M., Gravekamp, C., Setaluri, V., Peters, N., Hoffmann, F.M., Peng, H., Ivanov, A.V., Simpson, A.J. & Longley, B.J. 2007. MAGE-A, mMage-b, and MAGE-C proteins form complexes with KAP1 and suppress p53-dependent apoptosis in MAGE-positive cell lines. *Cancer research.* 67 (20). pp. 9954-9962.

Yeh, J.E., Toniolo, P.A. & Frank, D.A. 2013. Targeting transcription factors: promising new strategies for cancer therapy. *Current opinion in oncology.* 25 (6). pp. 652-658.

Yen, P.H., Chai, N.N. & Salido, E.C. 1996. The human autosomal gene DAZLA: testis specificity and a candidate for male infertility. *Human molecular genetics.* 5 (12). pp. 2013-2017.

Yin, M., Yan, J., Martinez-Balibrea, E., Graziano, F., Lenz, H.J., Kim, H.J., Robert, J., Im, S.A., Wang, W.S., Etienne-Grimaldi, M.C. & Wei, Q. 2011. ERCC1 and ERCC2 polymorphisms predict clinical outcomes of oxaliplatin-based chemotherapies in gastric and colorectal

cancer: a systemic review and meta-analysis. *Clinical cancer research : an official journal of the American Association for Cancer Research.* 17 (6). pp. 1632-1640.

Yu, C., Ji, S., Sha, Q., Dang, Y., Zhou, J., Zhang, Y., Liu, Y., Wang, Z., Hu, B. & Sun, Q. 2016. BTG4 is a meiotic cell cycle-coupled maternal-zygotic-transition licensing factor in oocytes. *Nature structural & molecular biology.* 23 (5). pp. 387-394.

Yuan, H., Glazer, R., Wang, X., Jin, L., Li, J., Vijayendra, N., Doodala, V. & Weiss, S. 2015. Placental protein-1 (plac1) modulates immune tolerance in mammary tumor cells. *Journal for immunotherapy of cancer.* 3 (2). pp. 1.

Zendman, A.J., Ruiter, D.J. & Van Muijen, G.N. 2003. Cancer/testis-associated genes: identification, expression profile, and putative function. *Journal of cellular physiology.* 194 (3). pp. 272-288.

Zeng, Y., He, Y., Yang, F., Mooney, S.M., Getzenberg, R.H., Orban, J. & Kulkarni, P. 2011. The cancer/testis antigen prostate-associated gene 4 (PAGE4) is a highly intrinsically disordered protein. *The Journal of biological chemistry.* 286 (16). pp. 13985-13994.

Zhang, J., Tripathi, D.N., Jing, J., Alexander, A., Kim, J., Powell, R.T., Dere, R., Tait-Mulder, J., Lee, J. & Paull, T.T. 2015a. ATM functions at the peroxisome to induce pexophagy in response to ROS. *Nature cell biology.* 17 (10). pp. 1259-1269.

Zhang, M., Zhang, C., Du, W., Yang, X. & Chen, Z. 2015b. ATAD2 is overexpressed in gastric cancer and serves as an independent poor prognostic biomarker. *Clinical and Translational Oncology.* pp. 1-6.

Zhang, Z., Xuan, Y., Jin, X., Tian, X. & Wu, R. 2013. Meta-analysis demonstrates association of XRCC1 genetic polymorphism Arg399Gln with esophageal cancer risk in the Chinese population. *Genetics Mol Res.* 12.

Zhang, X., Yang, H., Lee, J.J., Kim, E., Lippman, S.M., Khuri, F.R., Spitz, M.R., Lotan, R., Hong, W.K. & Wu, X. 2010. MicroRNA-related genetic variations as predictors for risk of second primary tumor and/or recurrence in patients with early-stage head and neck cancer. *Carcinogenesis.* 31 (12). pp. 2118-2123.

Zlatanou, A., Despras, E., Braz-Petta, T., Boubakour-Azzouz, I., Pouvelle, C., Stewart, G.S., Nakajima, S., Yasui, A., Ishchenko, A.A. & Kannouche, P.L. 2011. The hMsh2-hMsh6 complex acts in concert with monoubiquitinated PCNA and Pol η in response to oxidative DNA damage in human cells. *Molecular cell.* 43 (4). pp. 649-662.